Antimicrobial Polymers for Catheter Coatings

Andersen, Christian

Publication date:
2019

Document Version
Publisher's PDF, also known as Version of record

Antimicrobial Polymers for Catheter Coatings

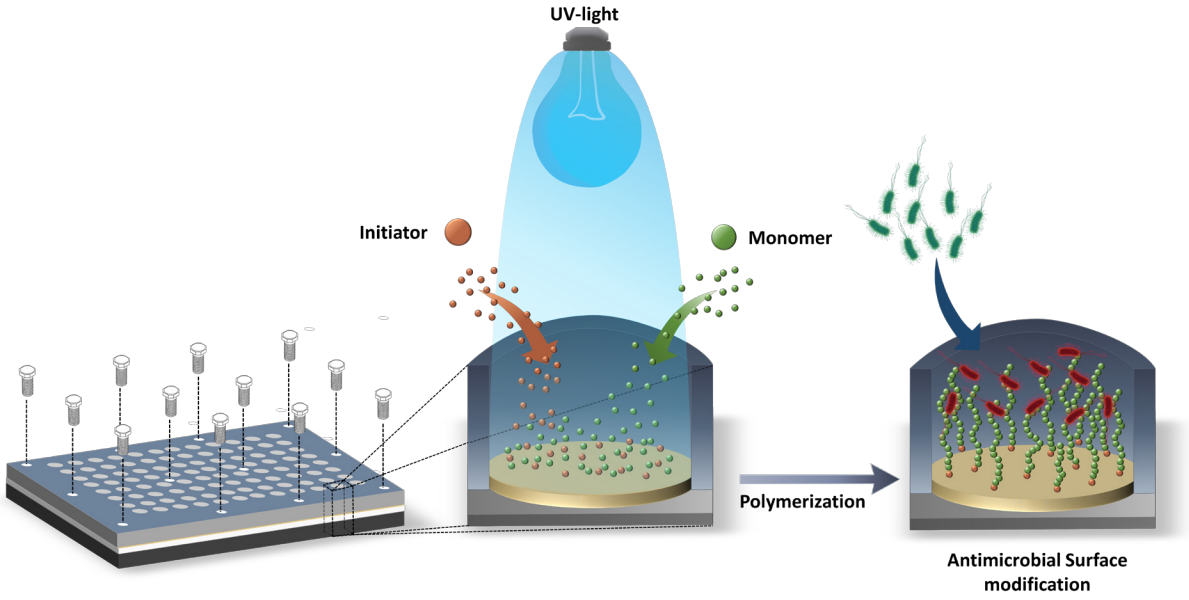

Christian Andersen
Ph.D. Thesis
December 2019
DTU Chemical Engineering
Department of Chemical and Biochemical Engineering

Preface

This thesis is the result of my Ph.D. project conducted both at Coloplast A/S and the Danish Polymer Centre (DPC), Department of Chemical and Biochemical Engineering, Technical University of Denmark, from January 2017 to December 2019 under the supervision of Associate Professor Anders E. Daugaard and company co-supervisor Niels Jørgen Madsen. The project was funded by Coloplast A/S and Innovationsfonden.

Christian Andersen

Christian Andersen

Kongens Lyngby 2019

Abstract

People suffering from urinary tract disorders often rely on urinary catheters for proper voiding of their bladder. However, the use of such medical devices are connected with an increased risk of contracting urinary tract infections (UTI). Administration of antibiotics are used in the treatment of such patients but the repeated use of these medications have shown to be leading to antibiotic resistant bacteria. The painful and reoccurring infections is a severe limitation in their everyday life and measures to prevent this have revolved around antimicrobial coatings that releases antibiotics or repel adhesion of bacteria but have shown limited effect. Cationic polymer surfaces have emerged as an alternative solution able to kill bacteria in direct contact and thereby avoids depletion by release of an active compound. Especially quaternary ammonium polymer coatings have been exploited for their antimicrobial activity and investigation and application of such systems in relation to urinary catheter coatings to reduce or prevent catheter associated urinary tract infections (CAUTI), is the focus of this dissertation.

Initially, a screening platform able to conduct surface modification directly onto polyurethane (PU) catheter material, was developed to investigate grafting conditions of monomers via an industrially relevant process. Here, the combination and concentration of monomers proved to be important parameters for the outcome of the polymerization. The design of the device also allowed for detailed chemical analysis and characterization of the surface by both water contact angle analysis (WCA), x-ray photoelectron spectroscopy (XPS), Fourier-transform infrared spectroscopy (FT-IR) and UV-vis spectroscopy. The platform thereby proved to be a suitable tool for exploring large variations in grafted polymer coatings.

In the next step, the platform was utilized for the preparation of a series of quaternary ammonium based coatings on PU and was used to establish a suitable bacteriological methodology for the evaluation of the antimicrobial activity. A long range of different assays were applied but the chemical nature of PU as well as diffusion of process aids lead to inconclusive results. A method for conducting high throughput screening of quaternary ammonium modified PU was therefore, in this case, not possible using conventional methods.

Alternatively, polydimethylsiloxane (PDMS) was chosen as a more inert catheter substrate and used for the development of a controlled surface initiated supplemental activation reducing agent atom transfer radical polymerization (SI-SARA-ATRP) technique. This method was applied to gain a more fundamental understanding of the structure-property relationship relating to the antimicrobial activity of quaternized 2-(dimethylamino)ethyl methacrylate (DMAEMA) polymer systems. The effect of brush length and choice of alkylation agent showed that charge density, mobility and amphiphilicity were pivotal for achieving highest possible antimicrobial effect.

As a final part of the thesis, quaternary ammonium polymers were implemented as an additive in existing Coloplast coating formulations to evaluate their applicability in production of antimicrobial urinary catheters. Initial investigations were made on flat polymer substrates, which showed that antimicrobial activity increased with increasing content of the quaternary ammonium polymer and retained activity even after exposure to E-beam sterilization treatment. Applying the coating directly onto urinary catheters gave both smooth low friction surfaces and an evenly distributed polymer layer. This proved that quaternary ammonium polymers could be incorporated in an industrial process for production of

smooth hydrophilic catheter coatings. However, in disagreement with previous results, reduced antimicrobial activity was seen for quaternary ammonium containing coatings. The lack of antimicrobial activity for quaternary ammonium polymers in combination with hydrophilic coatings, was attributed to high water uptake and swelling of the system. This could dilute the charge density resulting in diminished effect. This is, however, a subject for further investigation to clarify the precise cause for the observed trend.

Resumé

Personer med urinvejslidelser er ofte afhængige af at bruge urinvejskatetre for at udføre regelmæssig vandladning, men dette er imidlertid også forbundet med en øget risiko for at få urinvejsinfektioner (UTI). Samtidig er der stor risiko for tilbagevendende infektioner, som kræver gentagende behandlinger med antibiotika, hvilket har vist sig at lede til udvikling af antibiotikaresistente bakterier. De smertefulde og hyppigt forekomne infektioner forringer livskvaliteten for disse personer og er til stor gene i deres hverdag. Metoder til at løse dette problem har fokuseret på udvikling af antimikrobielle overflademodificeringer af katetre og har involveret bl.a. frigivelse af antibiotika og afvisende overflader, som beskytter mod adhæsion af bakterier, men har indtil videre haft relativt lille effekt. Kationiske polymeroverflader har i mellemtiden vist sig som en alternativ metode, som er i stand til at dræbe bakterier ved direkte kontakt og derved undgå frigivelse af fx antibiotika, som forsvinder over tid. Specielt brugen af kvaternær ammonium polymere har udvist høj antimikrobiel effekt mod en lang række af bakterier. Formålet for denne afhandling er derfor at undersøge anvendelsen af sådanne systemer i katetercoatninger til at forhindre kateterrelaterede urinvejsinfektioner (CAUTI).

Indledningsvist blev en screeningplatform udviklet og anvendt til at udføre overflademodifikationer på polyurethan (PU) katetermateriale. Dette havde til hensigt at undersøge indflydelsen af forskellige reaktionsbetingelser ved brug af monomere i en industriel relevant proces og viste, at både kombinationen og koncentrationen af monomer, havde stor indflydelse for resultatet af polymerisationen. Designet af platformen tillod endvidere brugen af kontaktvinkel måling (WCA), x-ray photoelctron spektroskopi (XPS), FT infrarød spektroskopi (FT-IR) og UV-vis spektroskopi til at opnå en detaljeret kemisk analyse og karakterisering af overfladen. Platformen viste sig dermed at være et værdifuldt værktøj til screening af overflademodifikationer på polymeroverflader.

Derefter, blev platformen benyttet til forberedelse af en serie af kvarternære ammoniumbaserede overflademodificeringer på PU og til at etablere en retvisende bakteriologisk metodologi til evaluering af antimikrobiel aktivitet. En lang række forskellige biologiske metoder blev undersøgt, men grundet den kemiske sammensætning af PUen samt diffusion af procesmidler fra substratet, gav det tvetydige resultater. Det var derfor i dette tilfælde ikke muligt at anvende screeningplatformen i kombination med konventionelle testmetoder til evaluering af antimikrobielle egenskaber for overflademodifikation af PU.

Polydimethylsiloxan (PDMS) blev valgt som et alternativt katetermateriale grundet dets mere inerte kemi og blev anvendt til at udvikle en metode til at udføre kontrolleret overfladeinitieret polymerisation via SARA-ATRP. Denne metode blev benyttet til at opnå en bedre forståelse for sammenhængen mellem den kemiske overfladestruktur af kvarternære 2-(dimethylamino)ethyl methacrylate (DMAEMA) polymer systemer og deres antimikrobielle egenskaber. Længden af polymerkæderne samt valg af alkyleringsagent viste at ladningsdensitet, mobilitet og amfifilicitet var afgørende parametre for at opnå den højest mulige antimikrobielle aktivitet.

Som en sidste del af afhandlingen, blev kvarternære ammonium polymere inkorporeret i eksisterende Coloplast coatingformuleringer for at evaluere deres anvendelse i produktion af antimikrobielle urinvejskatetre. I et indledende studie udført på flade polymersubstrater viste det sig, at den antimikrobielle aktivitet steg med øget indhold af en kvarternær ammonium polymer og at coatningerne var i stand til at bibeholde det antimikrobielle niveau selv efter E-beam sterilisation. Anvendelse af

coatningerne på urinvejskatetre gav glatte overflader med lav friktion, samt et jævnt fordelt coatninglag. Dette beviste at kvarternære ammonium polymere kunne implementeres i en industriel produktion af glatte hydrofile katetercoatninger. Ved anvendelse på kateteroverflader, viste coatningerne sig imidlertid, at have en reduceret antimikrobiel effekt, hvilket var i modstrid med tidligere resultater. Den nedsatte aktivitet for kvarternære ammonium polymere i kombination med hydrofile coatninger kunne tilskrives det høje vandoptag og kvældning af systemet. Dette kunne medføre en fortynding af ladningsdensiteten og resultere i en mindsket effekt. En videre undersøgelse er dog nødvendig for at kunne klarlægge den præcise baggrund for dette fænomen.

Acknowledgements

First and foremost, I wish to express my sincere appreciation to my supervisor Associate Professor Anders Egede Daugaard for your persistent support and encouragement. I am also grateful for your invaluable guidance, which have helped me to stay on the right track throughout this project. Your door was always open and you were never too busy for a discussion, whenever I stopped by your office. Your extensive knowledge and skills as a supervisor have taught me many great things, which I will make sure to carry with me in my future carrier.

Next, I would like to thank my co-supervisor Niels Jørgen Madsen for introducing me to the workplace at Coloplast and making me feel welcome here. Apart from contributing with your vast know-how within the industrial field you have also always ensured that nothing was missing in my project. Whatever I needed, being everything from chemicals, materials or contacting people to help me with various tasks you made sure to make it happen.

Additionally, I would also like to show my appreciation to my Coloplast colleagues, Tina Sortberg, Carsten Høj, Mads Hjælmsø Hansen and Thomas Hansen who helped me around the laboratories and facilities and also made sure that I was part of the team. A special thanks goes out to Lotte Stoklund Jensen who have been responsible for almost all biological testing conducted in this thesis and for taking the time to answer my endless questions regarding biology, which only a chemist could ask.

From DTU Chemistry, I would like to thank Koosha Ehtiati for assisting with your skills in handling silicon wafers and carrying out ellipsometry, which undoubtedly provided valuable insight for the chemistry used in chapter 5 of this thesis.

At DTU National Food Institute, I would like to show my gratitude to both Hanne Mordhorst and Sünje Johanna Pamp for helping me with carrying out biological testing, which I under no circumstances would have managed on my own. I highly appreciate that you agreed to take up this task with such a short notice towards the end of my Ph.D. and the work you have done, truly helped clarify important aspects of my project.

I am also grateful for all of my colleagues at the Danish Polymer Centre that I have had the pleasure to work alongside during my stay. I have enjoyed spending my time in your presence whether it being at or outside DTU and hope to continue to do so.

Finally, I would like to thank my family for your great support and for enduring my long, complicated explanations whenever you dared to ask me, what I was working with. A special thanks goes to my girlfriend Alena for always being there for me and for taking me on so many great adventures around the world.

Abbreviations

AA	Acrylic acid
A. acidoterrestris	Alicyclobacillus acidoterrestris
A. baumannii	Acinetobacter baumannii
ANOVA	Analysis of variance
APTES	(3-Aminopropyl)-triethoxysilan
ARGET-ATRP	Activators regenerated by electron transfer atom transfer radical polymerization
BBOx	3-((4-Bromobutoxy)methyl)-3-methyloxetane
B. cereus	Bacillus cereus
BIBB	2-bromoisobutyryl bromide
Bpy	2,2'-Bipyridine
BSA	Bovine serum albumin
C. albicans	Candida albicans
CAUTI	Catheter associated urinary tract infection
CFU	Colony forming units
CRP	Controlled radical polymerization
DABCO	1,4-Diazabicyclo[2.2.2]octane
DMAEMA	2-(Dimethylamino)ethyl methacrylate
DMBQPEI	N,N-Dodecyl methyl-co-N,N- methylbenzophenone methyl quaternary polyethyleneimine
E. aerogenes	Enterobacter aerogenes
E. cloacae	Enterobacter cloacae
FBG	Fibrinogen
FRP	Free radical polymerization
FT-IR	Fourier-transform infrared
HEMA	2-Hydroxyethyl methacrylate
HMDI	4,4-Methylenebis(cyclohexyl isocyanate)
HMTETA	1,1,4,7,10,10-Hexamethyltriethylene tetramine
HAS	Human serum albumin
iPrOH	Isopropanol
K. pneumonia	Klebsiella pneumonia
LbL	Layer-by-layer
LCST	Lower critical solution temperature
L. monocytogens	Listeria monocytogens
MAA	Methacrylic acid
MDEGMA	Di(ethylene glycol) methyl ether methacrylate
ME2Ox	3-((2-(2-Methoxyethoxy)ethoxy)methyl)-3-methyloxetane
MeOH	Methanol
MIC	Minimum inhibitory concentration
M. luteus	Micrococcus luteus
MPC	2-Methacryloyloxyethyl phosphorylcholine
MPEGMA	Poly(ethylene glycol) methyl ether methacrylate
MPTMS	Mercaptopropyltrimethoxysilane
MRSA	Methicillin-resistant staphylococcus aureus
MRSE	Methicillin-resistant staphylococcus epidermidis
MSC	Human mesenchymal stem cells
MW	Molecular weight
NIPAAm	N-isopropylacrylamide
NMR	Nuclear magnetic resonance
OD	Optical density
PAA	Poly(acrylic acid)
PBS	Phosphate-buffered saline
PCBMA	Poly(carboxybetaine methacrylate)

PCL	Polycaprolactone
Đ	Dipsersity
PDMS	Polydimethylsiloxane
PE	Polyethylene
PEG	Poly(ethylene glycol)
PEGMA	Poly(ethylene glycol) methacrylate
PEI	Polyethyleneimine
PET	Polyethylene terephthalate
PHMB	Polyhexamethylene biguanide
PHMG	Poly(hexamethylenediamine guanidinium chloride)
PI	Photoinitiator
PMDETA	N,N,N′,N′′,N′′-Pentamethyldiethylenetriamine
PP	Polypropylene
PSf	Polysulfone
PTFE	Polytetrafluoroethylene
PTMO	Poly(tetramethylene oxide)
PU	Polyurethane
PVA	Polyvinylalcohol
PVC	Polyvinylchloride
PVDF	Polyvinylidene fluoride
PVP	Polyvinylpyrrolidone
P. vulgaris	Proteus vulgaris
SBMA	Sulfobetaine methacrylate
SEC	Size exclusion chromatography
S. enterica sv.	Salmonella enterica
S. epidermidis	Staphylococcus epidermidis
SI-ATRP	Surface initiated atom transfer radical polymerization
SI-SARA-ATRP	Surface initiated supplemental activation reducing agent atom transfer radical polymerization
S. saprophyticus	Staphylococcus saprophyticus
TBEC	Tert-butylperoxy 2-ethylhexyl carbonate
THF	Tetrahydrofuran
T_m	Melting temperature
TrFEMA	2,2,2-Trifluoroethyl methacrylate
UTI	Urinary tract infection
UV-vis	Ultraviolet–visible spectroscopy
VI	1-Vinylimidazole
WCA	Water contact angle
XPS	X-ray photoelectron spectroscopy
ZOI	Zone of inhibition

Contents

1. Objective and Outline

People with urinary incontinence, urinary retention and many cases of spinal cord injury, suffer from lack of bladder control, also commonly referred to as neurogenic bladder disease. This makes them unable to efficiently drain the content of their bladder on their own and they have to insert a urinary catheter to allow drainage. However, use of urinary catheters are also associated with an increased risk of contracting urinary tract infections (UTI) from either daily (intermittent) or long-term (indwelling) use. Treatments often involves the use of strong antibiotics to knock down infections, but it is not always capable to completely eradicate the pathogens. Surviving bacteria are thereby able to start new infections and reoccurring incidences are therefore a prominent issue. The frequent and painful infections, along with repeated need for medication, greatly reduces the quality of life for these people. In addition, the repeated use of antibiotics can eventually lead to the development of antibiotic resistant strains making treatment even more difficult.
The main cause for the formation of catheter associated urinary tract infections (CAUTI) is believed to be from bacteria being transported from the catheter through the urethra and into the bladder and irritation of the mucosal layer during insertion. Despite repeated efforts to apply different strategies to either prevent or kill bacteria entering the bladder, the initiatives have not yet lead to any significant improvements.

The overarching objective for this project was therefore to establish a hydrophilic antimicrobial coating able to prevent or reduce the number of UTIs without the use of leaching antimicrobial agents.
This was to be achieved through initially conducting a state-of-the art literature study of antimicrobial polymer surfaces. Based on the survey, synthesis and screening of appropriate antimicrobial candidates applicable for coating on polyurethane based catheter material should be investigated. These coatings should then be applied by the use of an industrially feasible procedure and undergo bacteriological testing against relevant pathogens, such as E. coli, to confirm their antimicrobial activity. Ultimately, an antimicrobial urinary catheter having a smooth surface, no leachable compounds, good binding stability and be able to endure sterilization should be achieved by implementation of the best candidates in a hydrophilic catheter coating formulation.

Relevant aspects of the pathogenesis of UTI and the pathogens involved are described in **Chapter 2**, followed by an overview of some of the various strategies investigated in relation to prevention of microbial colonization of polymer surfaces. Special attention was made with respect to contact active antimicrobial surfaces based polymeric quaternary ammonium systems. A more comprehensive summary of antimicrobial surfaces can be found in the literature study, which have been provided in **Appendix 2**.
Chapter 3 comprises the development of a screening platform to investigate grafting of various monomer systems onto polyurethane (PU). The effect of monomer concentration and oxygen tolerance during polymerization was studied in order to achieve optimal grafting conditions.
In **Chapter 4**, the platform was utilized for grafting of antimicrobial quaternary ammonium candidates, which were chosen based on the literature survey. The focus of this chapter, was to evaluate the antimicrobial activity of said modified PU substrates against relevant pathogens and to find a suitable biological methodology for antimicrobial testing.
The broad applicability of the screening platform was further investigated in combination with a controlled radical polymerization technique. Through this new method, the identification of important

structure-property relationships for high antimicrobial activity with respect to brush length of the polymer chain, as well as choice of N-alkylation agents was investigated, which is described in **Chapter 5**.
The implementation of identified candidates, based on previous chapters, within urinary catheter coatings were the scope of **Chapter 6**. Here, the influence of the polymer additive on chemical stability towards E-beam sterilization, binding of coating to polymer substrate, smoothness and antimicrobial activity was investigated.
The overall conclusion and outlook can be found in **Chapter 7** and **8** followed by the procedures of unpublished experimental work in **Chapter 9**.

The dissertation is based on the following publications and presentations at international conferences, which are listed below:

Publications

Andersen C.; Madsen, N. J.; Daugaard, A. E. Screening Platform for Identification of Suitable Monomer Mixtures Able To Form Thin-Film Coatings on Polyurethanes by UV-Initiated Free Radical Polymerization, *ACS Applied Polymer Materials*, 2020, DOI: 10.1021/acsapm.9b00744 (see **Appendix 1.1** and supporting information in **Appendix 1.2**)

Literature report: An internal report on antimicrobial polymer surfaces were made for Coloplast A/S. (see **Appendix 2**)

Conferences and Seminars

Andersen C.; Madsen, N. J.; Daugaard, A. E. "Anti-Microbial Coatings for Polymer Surfaces ", *Annual Polymer Day*, Kgs. Lyngby, Denmark, November 2017 (oral presentation)

Andersen C.; Madsen, N. J.; Daugaard, A. E. "Screenings Platform for Easy Surface Modification of Polymers", *Nordic Polymer Days*, Copenhagen, Denmark, May 2018 (oral presentation)

Andersen C.; Madsen, J. E.; Daugaard, A. E. "Anti-microbial Polymers for Catheter Coating ", *Knowledge Sharing Day*, Humlebæk, Denmark, March 2019 (oral presentation)

Andersen C.; Madsen, J. E.; Daugaard, A. E. "Method of Making Polymer Surface Modifications Through the use of Screening Platforms ", *Nordic Polymer Days*, Trondheim, Norway, June 2019 (oral presentation)

Andersen C.; Madsen, J. E.; Daugaard, A. E. "Screening of grafting methods for modification of polymer surfaces ", *Annual Polymer Day*, Humlebæk, Denmark, November 2019 (oral presentation)

Project Supervision

Beate Ramshøj Knudsen, BSc project "Synthesis of Antimicrobial Polymers and Anchoring on Surfaces", September-March 2017-2018. (15 ECTS)

Thea Louise Hansen, BSc project "Preparation of antimicrobial polymer surfaces", January-June 2018. (20 ECTS).

2. Background

Cather associated urinary tract infection (CAUTI) is one of the most frequent types of infections related to medical devices. It is responsible for app. 40% of all hospital acquired infections and prolongs the mean bed time for patients by up to 2.4 days estimated at a total of 900.000 additional hospital days/year in the US alone[1–3]. The high infection rate also relates to the frequent use of catheters in hospital settings, where around 25% of all patients will need a urinary catheter during their stay[2]. Current strategies to prevent CAUTI have mainly evolved around implementing antimicrobial coatings on catheters. Hydrophilic surfaces have been made in an attempt to avoid attachment or by adsorption of antibiotics or silver to be released and kill bacteria during insertion, but so far these approaches have shown minimal effect[4]. Finding ways to prevent or reduce the occurrence of UTI would reduce both cost and time associated with these events, but more importantly also significantly improve the quality of life for the patients. In doing so, a deeper understanding for the way bacterial infection occurs is needed to be able to take proper initiatives towards a solution.

The following chapter comprises theoretical background on the pathogenesis of UTI and summarizes the main findings of state of the art literature on antimicrobial surfaces tested in relation to prevention of bacterial colonization.

2.1. Pathogenesis of UTI

One of the main causes for CAUTI is the introduction of bacteria into the bladder during insertion of the catheter[3,5]. The catheter is inserted through the urethra and bacteria from the urethra, surrounding skin or rectum can adhere onto the catheter surface and thereby be transported into the bladder and start multiplying (see **Figure 1**). Many other factors affects the chance of contracting UTI such as incomplete voiding leaving behind residual urine containing bacteria[6], the female gender have a higher prevalence due to the shorter anatomy of the urethra and the type of catheterization used. Indwelling catheters have a much higher chance, compared to intermittent catheters, to develop UTI with a 5-10% incidence risk per day of catheterization[7].

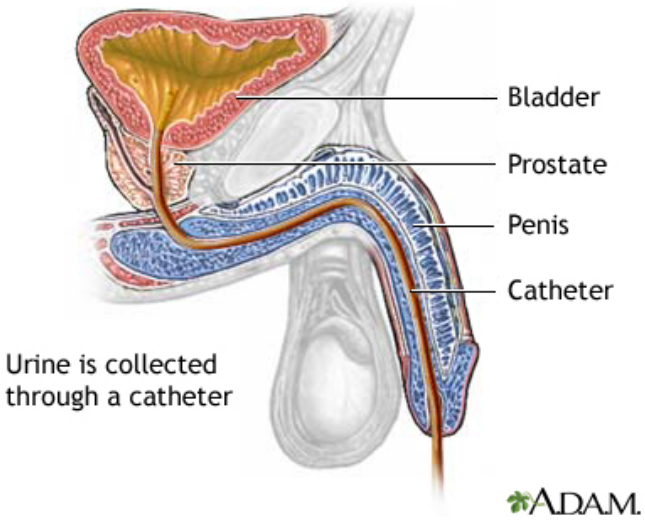

Figure 1 Insertion of urinary catheter in male. Reprinted with permission from A.D.A.M. Images.

Bacteria and fungi have developed an efficient way to protect themselves against threats from the surrounding environment, by being able to adhere to both biotic and abiotic surfaces. The presence of an

indwelling catheter in combination with longer insertion times allows bacteria to settle and colonize on the surface. The bacteria then forms a conditioning film, called biofilm, which consists of various biomolecules, such as proteins, polysaccharides, extracellular DNA and lipids and serves to protect against the outside environment[8]. The way that biofilm is formed, can be divided into 5 steps; 1) Reversible association with the surface 2) Irreversible attachment 3) Growth and proliferation 4) Maturation and 5) Dispersion (see **Figure 2**).

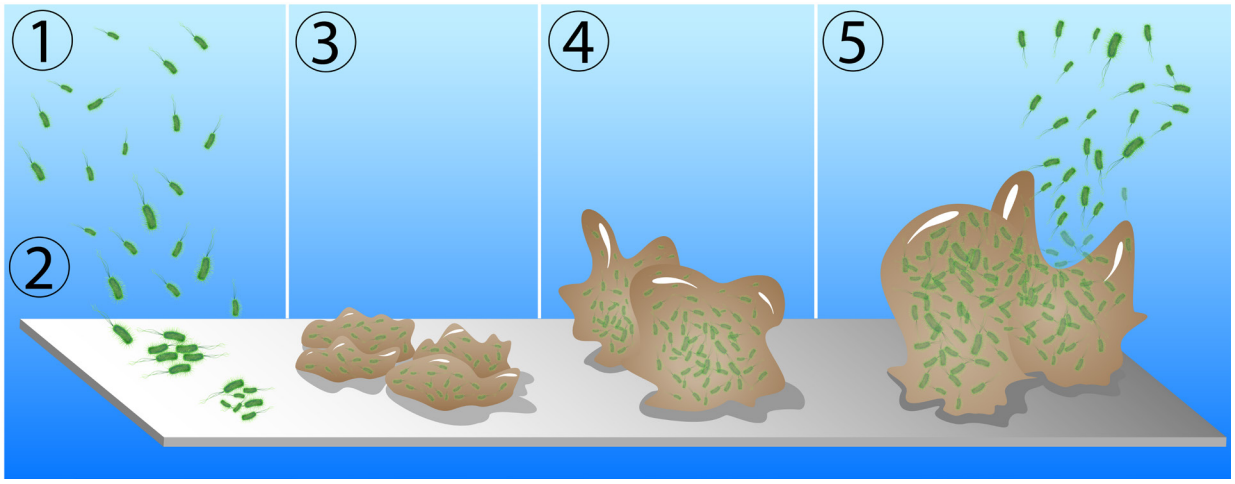

Figure 2 Schematic representation of the steps involved in biofilm formation 1) Reversible association with surface 2) Irreversible attachment 3) Growth and proliferation 4) Maturation and 5) Dispersion.

Initially, free planktonic bacteria are able to move into close approximation of the surface by the use of tail/hair-like appendages known as flagella or pili located on the exterior of cell. They are able to create a spinning motion that propel the bacteria forward or backwards[9]. This type of bacterial movement is called locomotion and is important for seeking out nutrients or escape toxic chemicals[10]. The adsorption is mainly loosely formed at first and the strength of the association is predominantly derived from van der Waals forces, electrostatic and steric interactions[11]. Bacterial appendages are, in addition, able to assist in this first level of binding. Secondly, some of the bacteria settle down on the surface and commit to adhering themselves, becoming irreversibly attached. Here the repulsive forces, such as electrostatic repulsion from the cell bilayer membrane, have been overcome by flagella or pili and turn into sessile bacteria. Appendages have also been proven to be able to promote chemical oxidation and hydration of the bulk substrate, further reinforcing the adhesion[12]. In the third step, quorum sensing molecules are released, signaling and activating a cascade of different biological pathways for production of biofilm when high enough concentrations are met[13,14]. A conditioning film appears rather quickly (within hours) and grows both horizontally and vertically and can in this stage reach around 10 µm in height[8]. Typically, various types of polysaccharides are secreted from the sessile bacteria, but molecules from the surrounding environment can also be captured and used to reinforce the matrix. For the fourth step, maturation and growth of the biofilm continues and fully mature biofilm cultures can be almost up to 100 µm tall. Restrictions to diffusion of nutrients and water increases as biofilm grows. Certain cultures of bacteria, such as P. aeruginosa[15], have developed distinctive structural growth patterns for their biofilm to resolve this limitation. They form what is described as a mushroom-shape and allows for nutrient flow in-between and below the stem of the mushroom-head. The final step in the cycle of biofilm is dispersion. This involves the bacteria releasing itself from the biofilm matrix and return to their planktonic state to find new surfaces to colonize. The bacteria initiates this process by breaking down the biofilm through the

production of specific enzymes, that cleaves stabilizing bonds within the matrix molecules[11,16]. The type of produced enzymes depends on the bacterial species due to differences in biofilm composition. An upregulation in flagella producing genes are also seen, making the bacteria ready to become motile again. Different factors can induce this kind of behavior such as nutrient and oxygen deficiency, increase in toxic products and accumulated cell death[16,17]. Simple shedding from shear stress can also release bacteria from their sessile state.

The reason that most bacteria are found as sessile and not in their free planktonic state, is because biofilm offers several layers of protection against many sorts of threats. For example, host immune systems in most cases fail to deal with biofilm as diffusion of toxic compounds from leukocytes are limited and the size of the film can become too large for macrophages to engulf them, leading to frustrated phagocytosis[18]. Antibiotics also struggle against biofilm since bacteria, depending on nutrient and oxygen availability, show different gene expression[16]. Despite the bacteria being genetically identical, various metabolic states may render antibiotics inefficient since they aim at specific biological targets, which may not be present or active due to downregulation[16,19]. The restricted diffusion also creates areas with sub-inhibitory concentrations, leading to the creation of antibiotic resistant bacterial strains[8,20,21]. In addition, biofilm colonies do often not only consist of a single organism but rather a combination of species. The colonies exists in a symbiotic state and provide nutrients and mutual protection for each other. The close approximation of bacteria also promotes rapid gene transfer, which helps to spread virulent strains[8,22,23]. Similarly, this is also the case for UTI and a large variety of bacteria have been associated with these types of infections (see **Figure 3**).

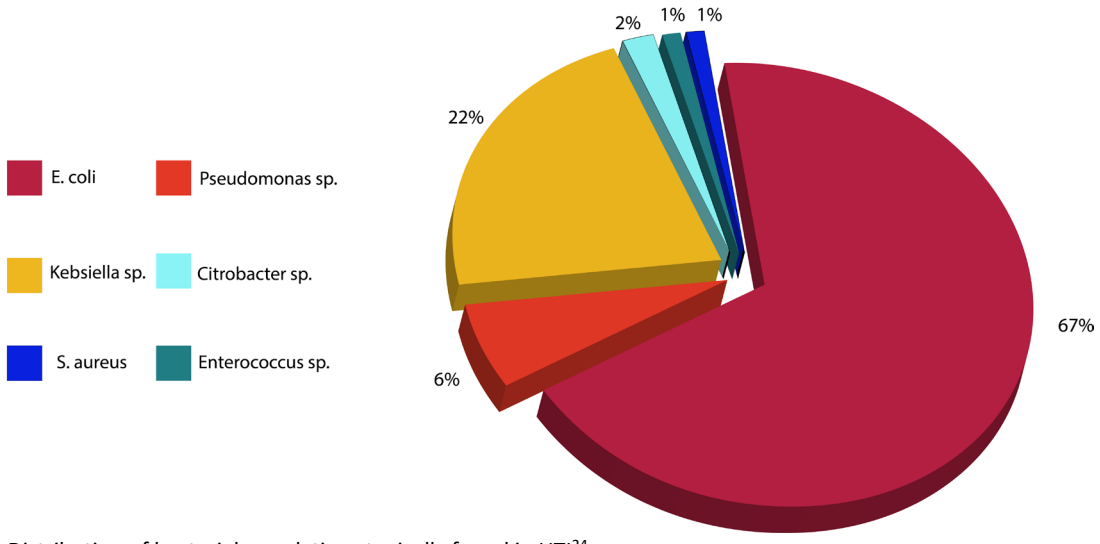

Figure 3 Distribution of bacterial populations typically found in UTI[24].

The primary pathogens found are gram negative (g-) bacteria, such as Escherichia coli (E. coli) and Klebsiella species, specifically Klebsiella pneumonia (K. pneumonia.)[25], which represents around 67 and 22% of the bacterial population respectively. Other types of bacteria such as (g-) Pseudomonas, (g-) Citrobacter, gram positive (g+) Enterococcus and (g+) Staphylococcus aureus (S. aureus) are also found[24].

The combination of heterogeneous bacterial colonies and resilient biofilm makes for persistent infections and high reoccurrence rate have been observed[26]. The best way to protect against CAUTI is therefore to prevent infection occurring in the first place. Besides CAUTI, the medical field is in general dealing with a high number of nosocomial infections originating from contaminated equipment and implants.

Since polymer surfaces are often used in this relation, several studies on antimicrobial polymer coatings have been conducted in the search of a constant sterile surface. Having a catheter surface capable of killing or repel microorganisms, would most likely be able to prevent the introduction of bacteria to the bladder during insertion and thereby UTI.

2.2. Antimicrobial Polymer Surfaces

Different approaches have been utilized in developing antimicrobial polymer surfaces and can overall be divided into three categories; 1) release of antimicrobial compounds; 2) repelling and; 3) contact active systems. In relation to release based systems, compounds such as antibiotics and silver have been investigated (see **Table 1**). Impregnation of polymeric substrates (polyurethane (PU), polytetrafluoroethylene (PTFE) and polydimethylsiloxane (PDMS)) with antibiotics such as Nitrofurazone, Flucloxacillin and Ciprofloxacin have shown good effect in preventing colonization in *in-vitro* experiments[4,27,28] (see **Table 1**). However, for reasons discussed previously, the repeated use of especially intermittent catheters, would eventually lead to development of antibiotic resistant strains and would not be viable as a long-term strategy. Triclosan have, similarly to antibiotics, been effective *in vitro* but also encounters issues with respect to resistance and are also under ongoing investigations for hormonal disruption[29].

Table 1 Compounds used for release based antimicrobial coatings of polymer surfaces.

Compound	Ref.	Compound	Ref.
Ciprofloxacin 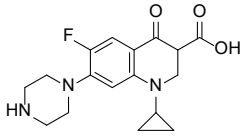	27	Silver Ag	4,30
Flucloxacillin 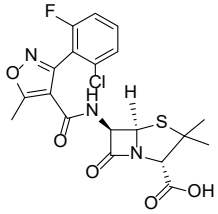	27	Silver alloy Au, Ag, Pd	32
Nitrofurazone 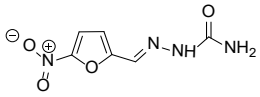	4,28	Silver nanoparticles 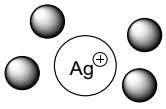	31
Triclosan 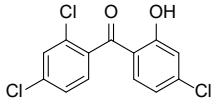	29		

Silver and silver alloy catheters have gained a lot of attentions due to their broad spectrum antimicrobial activity and low tendency for bacteria to develop resistance towards these kinds of compounds. However, clinical trials have shown that the effect is less than what is considered clinically important and does therefore, not offer sufficient protection against CAUTI[4,30,32]. New strategies in the impregnation method of catheters have, in the meantime, been able to raise the concentration of silver at the surface by the

use of nanoparticles[31]. This also increased the total load capacity and thereby increased and prolonged antimicrobial activity. The use of silver in nanoparticles does, on the other hand, pose implications related to the environment. It has been shown that these compounds have the ability to accumulate in soil and aquatic environment and are damaging for wastewater treatment facilities[33]. Although the wastewater is initially filtered, the small size of the particles makes it difficult to reliably remove them and therefore, end up in the wastewater sludge. A part of the wastewater treatment process relies on certain bacteria to break down organic matter, but they are killed due to the presence of antimicrobial nanosilver.

Though release based systems may be attractive for their high efficacy, the long-term consequences of antimicrobial resistance and environmental burden, makes them less appealing solutions in combating CAUTI.

Surfaces that offer antimicrobial activity without diffusion of an active substance are often repellent or antifouling coatings. These types of surfaces rely on being able to prevent initial attachment of cells or molecules that can serve as anchor points for adhesion. The following part includes a discussion regarding the synthesis and effectiveness of such coatings on polymeric materials. **Table 2** provides an overview of selected antifouling coatings, which have been tested by biologically relevant methods along with their fouling reduction against various microorganisms and molecules.

Table 2 Antifouling surface coatings on polymer substrates. A wavy structure (~) symbolizes a non-covalently attached coating.

Polymer substrate	Structure	Fouling reduction	Comments	Ref.
PET	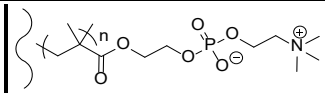	**g(+)** S. aureus: significant, S. mutans: significant. **g(-)** P. aeruginosa: significant. **Yeast** C. albicans: significant.		34
	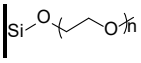	**g(+)** L. monocytogenes: 96.1%, S. enterica sv.: 99.8%	Best result obtained with PEG chains of 2000 g/mol.	35
PVDF	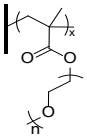	**Protein** HSA: >80%, γ-globulin: >80%, FBG: >80%	Good hemocompatibility.	36
	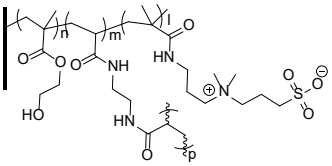	**Protein** BSA: 100%, Lysozyme: 100%		37
PSf	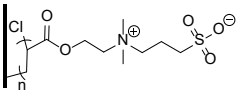	**Protein** BSA: Significant, FBG: Significant, Platelet: 100%	Non-cytotoxic and good biocompatibility.	38
PDMS	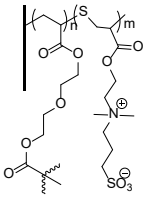	**g(+)** S. aureus: ca. 93%, S. epidermidis: >90%. **g(-)** E. coli: >99% **Cells** 3T3 fibroblast:>90% **Protein** FBG: 92%, BSA: 90%	Negligible cytotoxicity. Good hemocompatibility	39
	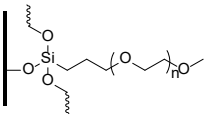	**Protein** FBG: 90%, BSA: 85%, lysozyme: 88%.		40

	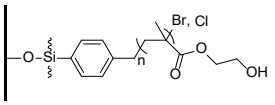	**Protein** FBG: Significant		41
	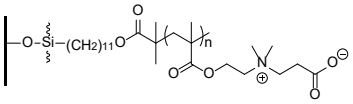	**Protein** FBG: >98%, BSA: 100%	Maintained antifouling properties after storage for >74 days under wet conditions.	42
	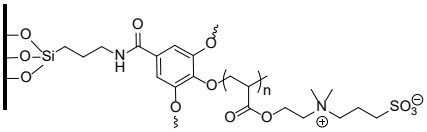	**g(+)** S. aureus: 58%, **g(-)** P. aeruginosa: 65%. **Protein** BSA: significant reduction	Good biocompatibility	43
PU	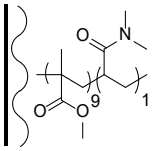	**g(+)** S. saprophyticus: 96-98%, S. aureus: 96-98%, S. mutans: ≥ 98% **g(-)** K. pneumonia: ≥ 96%, E. faecalis: ≥ 98%.	Part of screening library of 381 polyacrylate /acrylamides. Mixtures of bacteria was used instead of homogenous culture.	44
	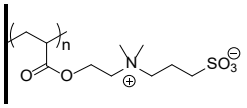	**g(+)** S. epidermidis: 97-99.9%, MRSA: 97-99.9%, S. aureus: 97-99.9%. **g(-)** A. baumannii: 97-99.9%, E. Coli: 97-99.9%. **Yeast** C. albicans: 97-99.9% **Cells** human platelets: >98%, polymorphonuclear leukocytes: >98%, monocytes: >98%, lymphocytes: >98%.	*In vivo* experiment in both canine and rabbits showed excellent reduction in thrombus accumulation and inflammation.	45
	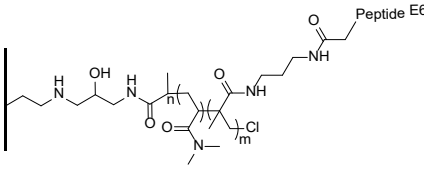	**g(+)** S. aureus: 98.4%, S. saprophyticus: 96.6%. **g(-)** P. aeruginosa: 93.2%		46

Here it can be seen that hydrogels, hydrophilic brushes and zwitterions have been extensively studied for their low fouling abilities against both bacteria and proteins. The strong hydrophilicity of these coatings generates a hydration layer of tightly bound water, creating a physical barrier that prevents direct contact and thereby adhesion[47,48]. For brush coatings of e.g. polyethylene glycol (PEG), steric repulsion from chain compression, resulting in unfavorable decrease in entropy, have also been shown to play an important role for non-specific protein adsorption[49]. However, a common criteria to efficiently protect against fouling is the surface coverage and/or grafting density of the coating[47–49].

Chang et al.[36] synthesized antifouling brush-like PEG layers on polyvinylidene fluoride (PVDF) membranes via a simple plasma treatment method. The membranes were first incubated with an isopropanol (iPrOH) solution of poly(ethylene glycol) methacrylate (PEGMA) (M_n = 500 g/mol) and dried for 24 h., before undergoing atmospheric plasma treatment (60 min.). The membranes showed significant reduction for both human serum albumin (HSA) >80%, γ-globulin > 80% and fibrinogen (FBG) >80%. Chang et al. claim that the architecture of the formed polymer layer can be controlled by the type of plasma used. Atmospheric plasma resulted in a brush-like coating, whereas low pressure plasma gave a crosslinked network instead. A comparison between the two methods showed that the brush-like structure had slightly superior protein repellency. It was also shown that higher hydration capabilities was achieved for the brush-like structure and thereby, stronger bonding of water. Good hemocompatibility of the

membrane was also shown with respect to human platelet adhesion and plasma clotting time. The membrane showed no observable adhesion of platelets and had excellent anticoagulant activity.
Dong et al.[35] made PEG brush coatings of various molecular weight (MW) onto polyethylene terephthalate (PET). The coatings were synthesized via a "grafting to" approach and substrates were initially functionalized with silicon tetrachloride ($SiCl_4$) plasma. This was followed by grafting of PEG having a MW of 200, 400, 600, 2000 or 4000 g/mol (2 h.). The resistance to colonization was in this case evaluated against g(+) pathogens of Salmonella enterica sv. Typhimurium (S. enterica sv.) and (g+) Listeria monocytogens (L. monocytogens). Here, it was found that an upper limit of 2000 g/mol PEG chain resulted in the best antifouling properties with a reduction of L. monocytogenes and S. enterica sv. of 96.1% and 99.8% respectively. PEG have in general been used for a broad range of biomedical application and possess good biocompatibility and is FDA approved[50]. As such, PEG based coatings may be good candidates for creating non-fouling surfaces and urinary catheter coatings based on hydrophilic PEG and polyvinylpyrrolidone (PVP) already exists[51]. They serve, in addition to the antifouling properties, to create a smooth surface and reduces both discomfort during insertion and minimizes potential damage to the mucosal layer of the urethra. Despite the use of such antifouling coatings, the issue of CAUTI still persists.

Zwitterionic coatings are comprised of both positive and negative charges with an overall net charge of zero. They have shown to bind water even more tightly than polyhydrophilic coatings due strong ionic solvation [48]. PET was coated with 2-methacryloyloxyethyl phosphorylcholine (MPC) via a simple solvent cast method by Hirota et al.[34]. The coating showed significant reduction against both g(+) S. aureus, g(-) P. aeruginosa and yeast Candida albicans (C. albicans). Although, the coating was effective against a broad range of different pathogens, one could question whether a solvent cast method can be a sufficient way to secure durable long-term binding of the coating to the substrate. Since MPC is very hydrophilic and water soluble one could imagine a steady degradation of the surface over time. This method is also used within coatings of ships, which slowly removes layers of paint along with any attached marine fouling[52].
An example of a covalently attached zwitterion was made by Yue et al.[38]. Here, grafting of sulfobetaine methacrylate (SBMA) was done via surface initiated atom transfer radical polymerization (SI-ATRP) from polysulfone (PSf) membranes. Anchoring of the ATRP initiator was done through chloromethylation and subsequent SI-ATRP of SBMA was conducted using Cu(I)Cl as catalyst and N,N,N',N",N"-Pentamethyl-diethylenetriamine (PMDETA) as ligand under nitrogen atmosphere. The reaction times were varied with the longest time being 150 min. Significant reduction in bovine serum albumin (BSA) and FBG was seen for the modified membranes with the longest polymerization time of 150 min. showing the best results. Hemocompatibility was also evaluated with respect to hemolysis of whole blood, platelet adhesion and clotting time. The coating showed no apparent hemolysis with no adhesion of platelets and slightly prolonged clotting times. In addition, improved cytocompatibility was also found for the grafted membranes through a so called MTT assay. Human embryonic hepatocytes LO-2 cells were shown to be able to proliferate over a six day incubation study. This indicated that the SBMA modified membranes had both excellent antifouling capabilities as well as good cyto and hemocompatibility.
Keefe et al.[42] have likewise used SI-ATRP to introduce a third kind of zwitterion, poly(carboxybetaine methacrylate) (PCBMA), onto PDMS surfaces. An ATRP initiator made from trichlorosilane and 10-undecen-1-yl 2-bromo-2-methylpropionate was attached via an initial treatment of the substrate followed by vapor deposition of the ATRP initiator. Grafting of the CBMA monomer was done using a mixture of Cu(I)Br/Cu(II)Br_2 and 1,1,4,7,10,10-hexamethyltriethylene tetramine (HMTETA) in water under nitrogen and polymerized for up to 48 h. Highest antifouling effect was seen for reaction times of around 18 h. and

reduction in FBG and BSA adhesion was measured to be >98 and 100% respectively. A long term stability study further found that the antifouling properties could be maintained after storage under wet conditions for more than 74 days. This showed that the surface modification was able to overcome the natural hydrophobic regeneration of PDMS, which occurs through the rearrangement of polymer chains[42].
Smith et al.[45] investigated SBMA surface coatings on polyurethane (PU) venous catheters in an extensive study. PU catheters were modified via a free radical polymerization (FRP) technique by first soaking them in a tert-butylperoxy 2-ethylhexyl carbonate (TBEC) solution (initiator) for 2 h. The catheters were then transferred to a monomer solution of SBMA and Fe(II) gluconate and left for 16 h. The modified catheters showed significant reduction of microbial attachment of g(+) Staphylococcus epidermidis (S. epidermidis), g(+) Methicillin-resistant Staphylococcus aureus (MRSA), g(+) S. aureus, g(-) A. baumannii, g(-) E. coli and C. albicans. This was also found to be the case for blood cells and proteins such as human platelets, polymorphonuclear leukocytes, monocytes and lymphocytes. The catheters were further studied *in vivo* using a canine model and had 99% reduced thrombus accumulation. A second study in rabbits gave 50% less inflammation for modified catheters and a lower number of bacteria on site.
Good results was also shown for SBMA modified PDMS urinary catheters when exposed to the conditions experienced in the urethra. Blanco et al.[43] functionalized PDMS using oxygen plasma to generate hydroxyl groups for attachment of (3-Aminopropyl)-triethoxysilan (APTES). The obtained amine surface functionality was then converted to phenolic groups via reaction with gallic acid. The polymerization of SBMA was then conducted for 24 h. by an enzymatically activated FRP using laccase, which generates radicals from phenolic hydroxyl groups. Protein adhesion was evaluated in artificial urine to represent salt concentration and pH. A significant reduction in BSA was found for the modified catheters compared to pristine. Likewise, testing of biofilm formation inhibition for g(+) S. aureus and g(-) P. aeruginosa was also done in artificial urine, where a reduction of only 58 and 65% were seen respectively. A dynamic bladder model was used to evaluate the authentic usage of the catheters and was exposed to the same pathogens under flow conditions for 1 week. S. aureus biofilm was reduced by 90% at the balloon part and P. aeruginosa had 80% less biofilm at the urethra part of the catheter. The tip of the catheters remained more or less similar to that of the unmodified surface, which could be attributed to the more favorable aerobic conditions at the liquid-air interface. Zwitterionic coatings could therefore be promising as part of the solution in creating stronger antifouling coatings. However, most of the coatings are made using ATRP, which require reaction times of several hours and for these to be industrially feasible, they should at least be within minutes.
As a third solution, positively charged surfaces have emerged as a way to induce cell death without the use of an actively released substance. Especially polymeric quaternary ammonium compounds have been readily used in cleaning and as disinfectant in solution, but have also been tethered to surfaces to induce contact active bactericidal properties. Different theories exists on the mechanism behind the antimicrobial properties and some of these are illustrated in **Figure 4**.

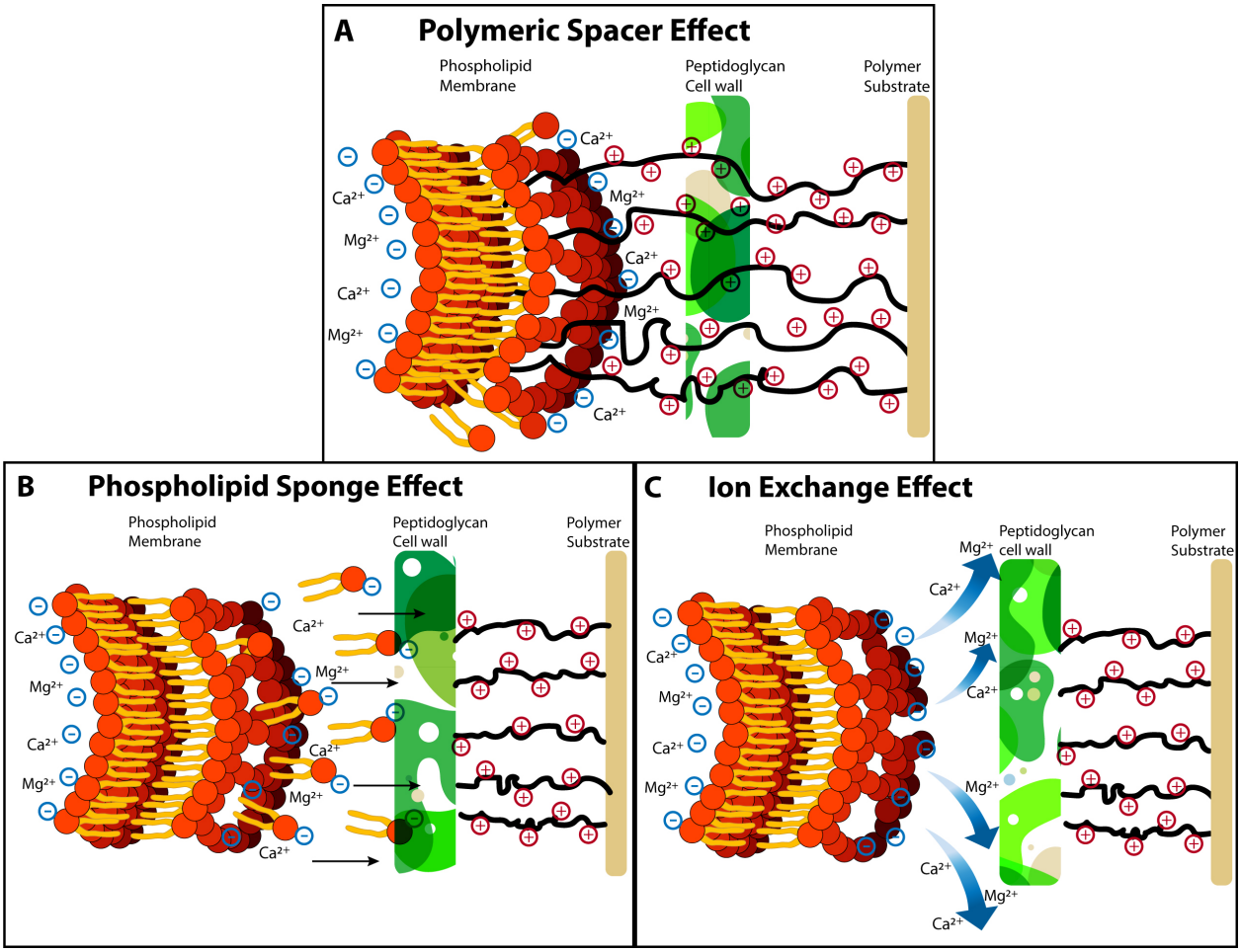

Figure 4 Proposed mechanism for the antimicrobial property of positively charged polymer coatings.

Gram positive bacteria have a phospholipid bilayer membrane and gram negative contains two (an outer and an inner membrane) that possesses an overall negative net charge. It is in general believed that attraction from positive charges on the polymers, provides electrostatic interactions with the cell membrane resulting in cell lysis. The mode of action proposed for what is called the polymeric spacer effect, is based on the cationic polymer having a long enough chain or spacer, which allows for penetration of the peptidoglycan cell wall. The polymer integrates into the cell membrane and destabilizes it, causing disruption and leakage of intracellular constituents[53–55] (**Figure 4, A**). Lewis and Klibanov[56] showed that the length of N-alkylated polyethyleneimine (PEI) immobilized on glass, had significant impact on the antimicrobial properties. They claim that the effect was due to the long chained cationic polymer being able to reach beyond the peptidoglycan cell wall and into the phospholipid membrane. The evidence is on the other hand not conclusive in the sense that other parameters, such as charge density and amphiphilicity of the system, are also changed. They do also mention that other types of quaternary ammonium, which have also been shown to have antimicrobial activity, cannot operate by this mechanism due to their much shorter chain length. The reason for this might be that different mechanisms applies depending on the polymer system.

A second theory explains the activity by the close proximity of positive charges, causing electrostatic interactions strong enough to rip apart the negatively charged phospholipids from the cell membrane, named the phospholipid sponge effect (**Figure 4, B**). Evidence of this effect was investigated by Gao et

al.[57] and was supported by showing, that higher void volume of surface-bound N,N-dodecyl methyl-co-N,N- methylbenzophenone methyl quaternary polyethyleneimine (DMBQPEI), resulted in higher killing efficiency due to having larger uptake capacity of phospholipids.

Another possible mode of action of surface tethered positively charged polymers, is the ion exchange effect (**Figure 4, C**). The stability of the cell membrane depends on divalent cations, such as Ca^{2+} and Mg^{2+}. They are responsible for neutralizing the negatively charged phosphate groups and prevents them from repelling each other, which would otherwise cause disruption. When bacteria come into close association with positive charges the counter ions are displaced to raise the entropy of the system. The loss of these ions results in the disintegration of the membrane and leakage of cell content[54,58,59].

The activity of various surface tethered quaternary ammonium systems have been investigated in relation to their potential as antimicrobial coatings on polymer surfaces. The following section will be reviewing a minor selection of such surfaces, illustrated in **Table 3**, and accessing the applied tethering method as well as antimicrobial activity. A more comprehensive list can be found in the literature survey enlisted in **Appendix 2**.

Table 3 Contact active antimicrobial coatings on polymer substrates.

Polymer substrate	Structure	Bactericidal effect	Comments	Ref.
Cotton	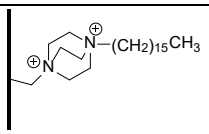	**g(+)** S. aureus: 100%, B. cereus: 100%, M. luteus: 100%. **g(-)** E. coli : 100%, E. aerogenes: 100%, E. cloacae: 100%, P. vulgaris: 100%	Various alkyl lengths were investigated.	60
Cellulose	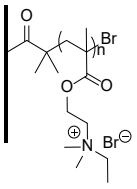	**g(+)** B. subtilis: 52%. **g(-)** E. Coli: 3.5 log		61
	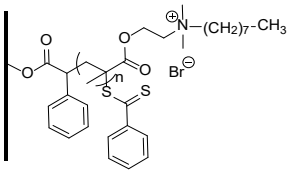	**g(-)** E. coli: 4 log	Various alkyl chain lengths were investigated.	62
PP	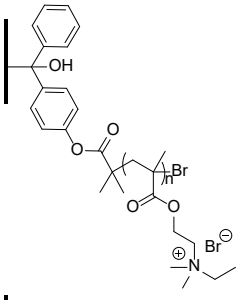	**g(-)** E. Coli: 100%	DMAEMA polymers with higher MW proved more effective with same grafting density.	63
	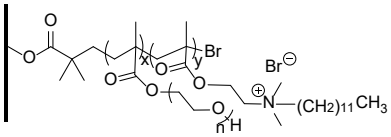	**g(+)** S. aureus: 99.99. **g(-)** E. Coli: 99.2%	Longer ATRP time for DMAEMA increased antibacterial effect due to higher concentration of positive charges. The antibacterial activity was	64

			maintained over 4 repeated bacterial assays.	
PET	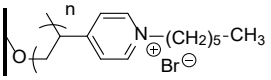	**g(-)** E. coli: 100%	Cellulose filter paper as substrate were also investigated.	65
PE	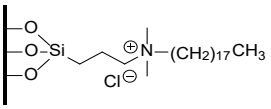	**g(+)** Bacillus subtilis: 2.65. **g(-)** E. coli: 3.1 log, S. enterica: 3.03 log	PS substrate was also investigated.	66
	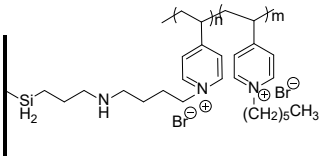	**g(+)** S. aureus: 99 ±1%. **g(-)** E. coli: 98 ±2%.	PP, PET and Nylon surfaces were also tested.	67
PVC	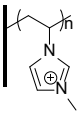	**g(+)** S. aureus: 100%. **g(-)** E. coli: inefficient.	Good hemocompatibility. A vinylimidazole grafting percentage of 20% or higher yielded the best results.	68
	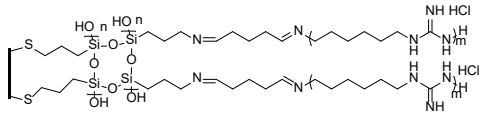	**g(+)** S. aureus: 99.999%, B. subtilis: 99.999%. **g(-)** P. aeruginosa: 99.999%, A. baumannii: 99.956%		69
Membrane	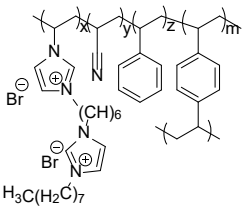	**g(+)** S. aureus: 100%. **g(-)** E. coli: 100%.	Low cytotoxicity. Other derivatives of imidazolium was also evaluated.	70
PVDF	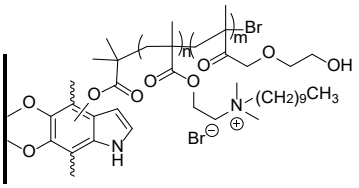	**g(+)** S. aureus: 98.0%		71
	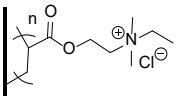	**g(-)** E. coli: few colonies remain		72
	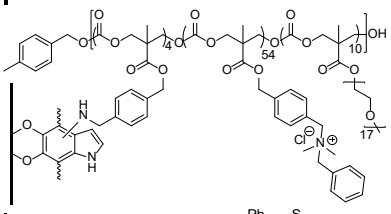	**g(+)** S. aureus: 99.999%. **g(-)** E. coli: 99.999%	Negligible cytotoxicity. Resisted BSA adhesion by 93%.	73
PDMS	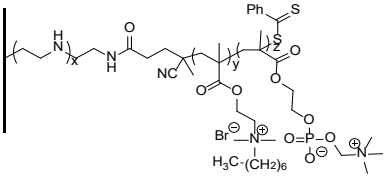	**g(+)** S. aureus: 88%.	Resisted adhesion of S. aureus and BSA by 90 and 70.7% respectively. Low cytotoxicity and good biocompatibility	74

	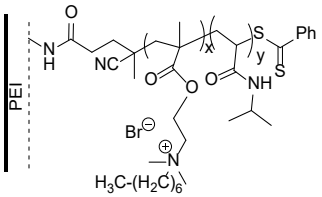	**g(+)** S. aureus: ~3.5. **g(-)** E. coli : ~2 log	Low cytotoxicity.	75
PU	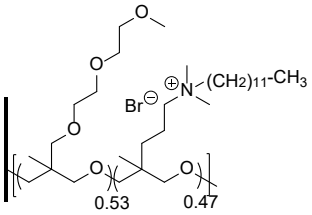	**g(+)** MRSE: 3.7 log, S. aureus: 100%. **g(-)** E. coli: >4 log	Good biocompatibility.	76
PVA	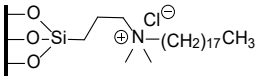	**g(+)** Bacillus cereus: 100%, A. acidoterrestris: 100%. **g(-)** E. coli: ~5 fold reduction	Cellulose surface was also investigated.	77
PCL	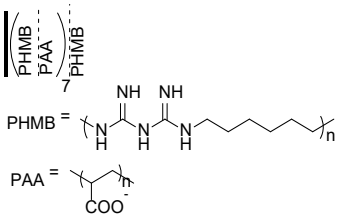	**g(-)** E. coli: 100%	Non-cytotoxic. Was able to eradicate E. coli within 10 min.	78

Introduction of quaternary ammonium into PU blends was done by Wang et al.[76] via a pre-synthesized soft segment. The monomer was made from reaction between 3-((4-bromobutoxy)methyl)-3-methyloxetane (BBOx) and 3-((2-(2-methoxyethoxy)ethoxy)methyl)-3-methyloxetane (ME2Ox), which had also been made by Wang et al. The soft segment was then used to make the corresponding PU by copolymerization with 4,4-methylenebis(cyclohexyl isocyanate) (HMDI), poly(tetramethylene oxide (PTMO) and 1,4-budanediol. The bromine functionality was subsequently N-alkylated by N,N-dimethyl dodecylamine to produce quaternary ammonium with a 12 carbon chain length. Finally a polymer blend of a commercial Tecoflex PU and the antimicrobial PU was made by solvent casting. The polymer effectively killed g(+) methicilin resistant S. epidermidis (MRSE), g(+) S. aureus and g(-) E. coli and reduced the bacterial count by 3.7 log, 100% and 4 log respectively. No cell death or morphological changes were observed for human mesenchymal stem cells (MSC), indicating good biocompatibility.

Poverenov et al.[77] provided a more simple method for obtaining surface bound quaternary ammonium via exploitation of hydroxyl groups in polyvinylalcohol (PVA) substrates. Trimethoxysilylpropyl octadecyldimethyl ammonium chloride was used in a one-step procedure to functionalize the surface with quaternary ammonium. The modified PVA was shown to be highly effective against g(+) Bacillus cereus and g(+) Alicyclobacillus acidoterrestris (A. acidoterrestris) and killed 100% of the bacteria within just 1 h. exposure. It was, however, less effective against g(-) E. coli where a 5 fold reduction was seen.

The same compound was also used to functionalize PE substrate by Fadida et al.[66]. Surface activation was first done by air-ozonolysis to generate carboxylic acid groups. These were then reduced to hydroxyl by sodium borohydride to allow reaction with trimethoxysilylpropyl octadecyldimethyl ammonium chloride. Here a reduction of 2.65 and 3.03 log for g(+) Bacillus subtilis and g(-) Salmonella enterica (S. enterica) were seen, respectively. The modified PE surface also proved to be effective against g(-) E. coli, which were reduced by 3.1 log. This was substantially higher than for that of PVA and suggests that the type of substrate and/or modification method can significantly influence the outcome for the resulting antimicrobial activity.

Huang et al.[63] functionalized polypropylene (PP) substrates with 2-(dimethylamino)ethyl methacrylate (DMAEMA) brushes via SI-ATRP. A benzophenone derivatized with an ATRP initiator was used to covalently bind the initiator via UV-initiation. ATRP of DMAEMA was then conducted using a mixture of $Cu(I)Cl/Cu(II)Cl_2$ and HMTETA at 25 °C and the length of the brush was varied by termination at different reaction times. Subsequent quaternization of the side-chain amine was then done by the use of ethyl bromide. The various lengths of DMAEMA were shown to have different antimicrobial activity. MW of 9.800, 21.300 and 35.100 g/mol killed essentially all g(-) E. coli but chains of 1.500 g/mol only killed 85%. A threshold for the charge density could be estimated from the MW of the polymer and grafting density on the substrate. It was found that complete kill was achieved above 14 quaternary ammonium units/nm^2. A threshold for positive charge density in relation to contact active antimicrobial surfaces have been discussed on several occasions and is an important parameter to consider to achieve potent bactericidal effect[79–81].

Yao et al.[64] modified PP membranes by SI-ATRP to make block copolymers of poly(ethylene glycol) methyl ether methacrylate (M_n = 360 g/mol) (MPEGMA 360) and DMAEMA, which elicited simultaneous bactericidal and repellent properties. An ATRP initiator was likewise attached to the surface, but this time via first ozone treatment to create carboxylic acid groups, which then was reduced by sodium iodide to hydroxyl groups. The OH functionality then allowed for anchoring of 2-bromoisobutyryl bromide initiator. Initially, MPEGMA 360 was grafted using $Cu(I)Br/Cu(II)Br_2$ and PMDETA in tetrahydrofuran (THF) for 2 h. at 45 °C. Chain extension by DMAEMA was then done in a similar fashion with reaction times between 2-6 h. and subsequently quaternized using 1-bromodecane. The longer DMAEMA brushes at 6 h. polymerization time showed the best antimicrobial activity against both g(+) S. aureus and g(-) E. coli reducing bacterial count by 99.99% and 99.2% respectively. The same level of activity was even maintained after four repeated cycles of bacterial exposure. From scanning electron microscopy (SEM) images the adhesion of bacteria on the surface was also proven to be minimal. From this, the implementation of quaternary ammonium into a hydrophilic urinary catheter coatings could potentially be used directly in the prevention of UTI.

As high charge density is critical for the antimicrobial effect a way to increase this is by the use of divalent cationic molecules. Abelet al.[60] modified cotton textiles with 1,4-diazabicyclo[2.2.2]octane (DABCO) by activating the 6-postion of the carbohydrate structure through tosylation with *p*-toluenesulfonyl chloride. The second tertiary amine of the attached DABCO was then used to gain a second positive charge by alkylation. Various alkyl chain lengths as well as DABCO end-capped alkylation agents were investigated. It was found that an alkyl chain length of C16 was able to kill all of g(+) S. aureus, g(+) Bacillus cereus (B. cereus), g(+) Micrococcus luteus (M. luteus), g(-) E. coli, g(-) Enterobacter aerogenes (E. aerogenes), g(-) Enterobacter cloacae (E. cloacae) and g(-) Proteus vulgaris (P. vulgaris). A surprising finding was that the highest effect did not originate from the surface with the potentially highest charge density. Rather than that, the amphiphilicity and correct alkyl chain length played a vital role in the antimicrobial effect to create proper interaction with the bacterial cells.

Another type of quaternary ammonium was investigated by Meléndez-Ortiz et al.[68], who grafted 1-vinylimidazole (VI) onto polyvinylchloride (PVC) via a fast and simple one step FRP procedure using ^{60}Co-gamma irradiation. Quaternization of the 3 position of VI was then done using iodomethane. The modified polymer substrates killed 100% of g(+) S. aureus but was ineffective against E. coli.

In a separate study by Zheng et al.[70], various quaternized VI monomers were copolymerized with acrylonitrile, styrene and divinylbenzene to form polymeric membranes. The pre-synthesized monomer was both made as a monovalent cation with alkyl chain length of C4, C8 or C12 or as a divalent cation as

bis-imidazolium with a 6 carbon spacer between the two imidazole groups. Membranes synthesized with bis-imidazolium and having a C8 quaternization at the second imidazole group was able to clear all g(+) S. aureus and g(-) E. coli, again showing the importance of charge density and amphiphilicity. The membrane also showed good biocompatibility against human dermal fibroblast cells as well as low hemolytic activity towards human red blood cells.

A last example of positively charged polymers, is polyhexamethylene biguanide (PHMB), which have also been used as an effective disinfectant and antiseptic. Tang et al.[78] used a layer-by-layer (LbL) technique to create alternating layers of PHMB and poly(acrylic acid) (PAA) onto polycaprolactone (PCL). PCL was first hydrolyzed by sodium hydroxide to introduce carboxylic acid functionalities. Thereafter layers of first PHMB and subsequently PAA was dip coated onto the surface and finished with a final layer of PHMB. Different numbers of $(PHMB/PAA)_n$/PHMB layers were investigated for n being either 0, 1, 3, 5 or 7. The antimicrobial effect was evaluated against g(-) E. coli and with just 3 layers, the surface was shown to completely eradicate the pathogen and within just 10 min. of contact for 7 layered coatings. The binding of the layers relies on electrostatic interaction of the oppositely charged surface and such relatively weak association could possibly cause leakage of the active PHMB. To prove the stability of the coating, modified substrates was submerged in PBS buffer for 24 h. and trails of released compounds was analyzed by UV-vis spectroscopy. Absorption peaks from PHMB was almost undetectable and concentrations were as low as 0.0005% (w/v). The modified PCL was also shown to have good biocompatibility and allowed proliferation of rat dermal fibroblast cells.

A related polymer of PHMB is poly(hexamethylenediamine guanidinium chloride) (PHMG) and was covalently attached to PVC urinary catheters by Villanueva et al.[69]. The chloride functionalities of PVC was utilized for thiol substitution with mercaptopropyltrimethoxysilane (MPTMS). Amine groups were then introduced by reaction with APTES, which was converted to aldehyde by reaction with glutaraldehyde and finally, PHMG was attached by reaction with the aldehyde groups. The functionalized surface showed excellent antimicrobial activity towards g(+) S. aureus, g(+) B. subtilis, g(-) P. aeruginosa and g(-) A. baumannii and reduced bacterial count by 4.9, 5.4, 6.4 and 3.7 log respectively. In addition, the coating also proved to reduce bacterial attachment as well as being able to maintain its activity for at least 60 days.

In summary, release based antimicrobial coatings, despite their high efficacy, are prone to lead to antimicrobial-resistance in bacteria when used repeatedly and are also considered a pollutant for the environment. As such, these types of systems are not a long term viable strategy to apply in urinary catheter coatings to combat CAUTI. Repellent coatings are efficient in avoiding fouling and have in general good biocompatibility and low cytotoxicity. Their effect alone may, however, not be sufficient since variations of these coatings are already used as smooth coatings for catheters and the risk of contracting CAUTI is still prominent. Contact active systems based on quaternary ammonium have been shown to elicit antimicrobial activity against a broad range of bacteria and their non-leaching ability avoids the risk of developing resistance in pathogens. Effective coatings does, on the other hand, depend on the setting that they are used in. Optimal charge density, mobility and amphiphilicity must be optimized for each unique application to obtain the best possible effect. Feasibility with respect to processing times of the coatings should also be considered, in order to be industrially applicable. A coating containing a combination of both repellent and antimicrobial contact active properties from quaternary ammonium can perhaps be a feasibly way to gain optimal protection against pathogens from CAUTI. In general, information from *in vivo* experiments are lacking for most of the investigated systems, which would be required to evaluate their true potential as antimicrobial coatings.

3. Screening Platform for Modification of Polymer Surfaces

Based on the previous chapter, various techniques and compounds have been identified to obtain non-leaching antimicrobial surface properties. However, foreseeing the precise outcome when conducting surface modifications is difficult, if not impossible, even through a rational design approach. Especially, when trying to predict complex biological interactions of bacteria with the surrounding environment that may have many known and unknown factors with potential major influence. Finding the best antimicrobial candidates inevitably requires investigations of an almost endless number of structural and chemical combinations. Applying these to catheters or larger substrates by regular trial and error methods is tedious and time consuming. A way to overcome this, is by using high throughput screening platforms to fast and reliably explore large libraries of different surface chemistries for suitable candidates. Much research have focused on automated picoliter scale synthesis of polymer libraries conducted on standard microscope glass slides[82]. Through this approach, only little material is needed to make hundreds of formulations that all can be run simultaneously on a single slide. The disadvantage of this method is that such small volumes exclusively run in bulk. This only permits investigations of different ratios of monomers and not the effect of e.g. solvent or concentration. Furthermore, the base substrate is glass, which is a non-ideal representation of the final application, which can have significant impact on e.g. biological studies, as discussed in **Chapter 2**. In this chapter, the possibility of developing a screening platform able to conduct surface modifications under normal atmosphere directly onto a flexible PU substrate for combinatorial investigations of both homo and copolymer systems was investigated (see **Figure 5**). To further enable testing of solvents and monomer concentrations, the design had to comprise chemical and heat resistant parts and with reaction vessel dimensions of at least microliter volume. This resulted in a publication in ACS Applied Polymer Materials[83], which can be found in **Appendix 1.1**.

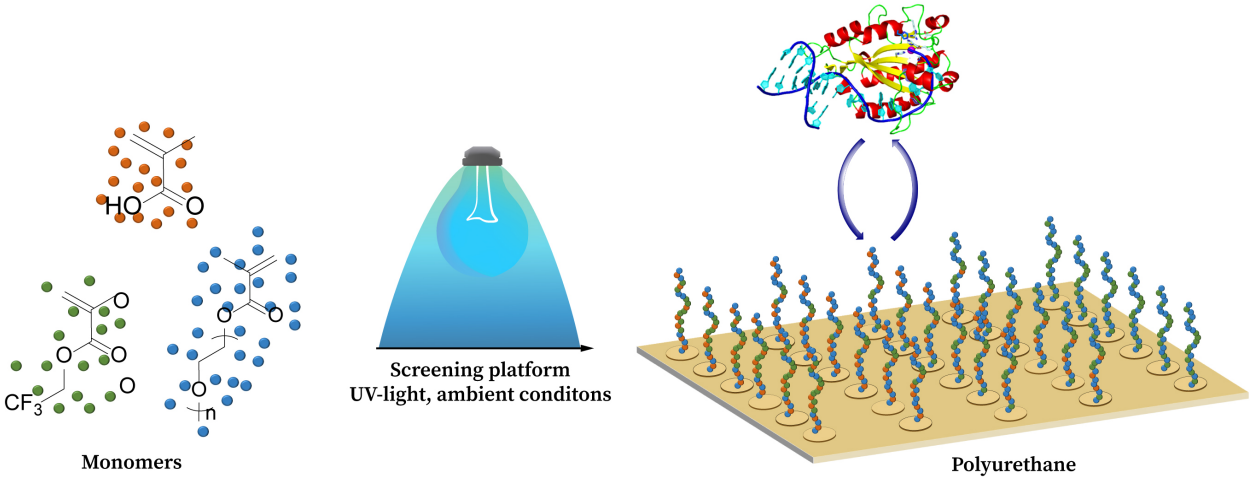

Figure 5 Illustration of grafting of amphiphilic terpolymer systems and their application as antifouling surface modifications.

3.1. Screening platform

To enable testing of different polymerization conditions, an inert holder that would allow parallelization of experiments in separate vessels, was required. As an additional restraint, the intended platform was required to be able to handle a broad range of solvents as well as to be suitable for semicrystalline plastics

such as polyurethanes with melting points above 150 °C. The design of the platform was based on a standard 96 well microtiter plate and was divided into three separate parts as can be seen in **Figure 6**.

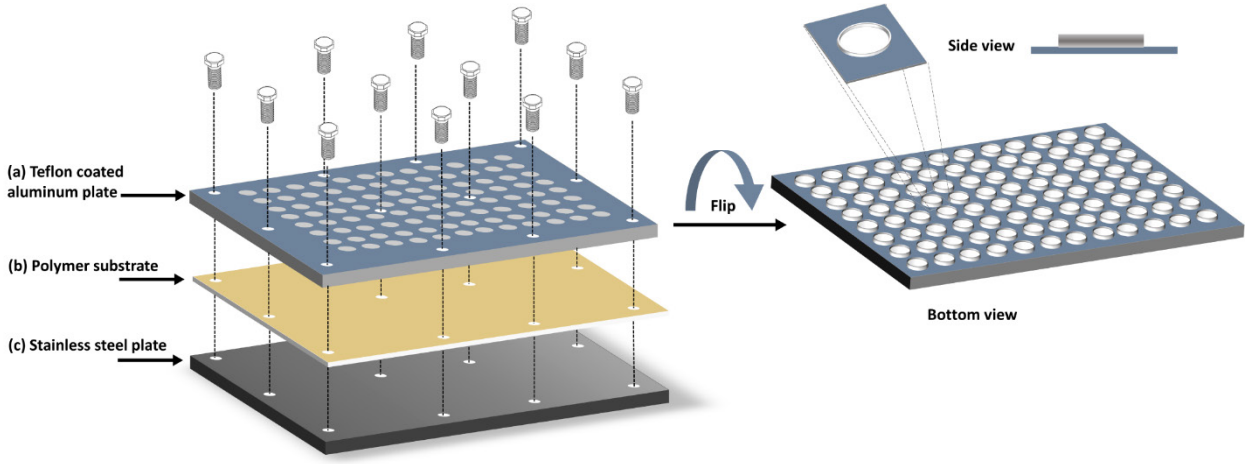

Figure 6 Schematic representation of screening platform (left) and bottom view of well plate, showing milled edges around the wells (right), where (a) is the well plate, (b) is the polymer substrate and (c) is a supporting stainless steel plate.

The top plate (a) were made from aluminum and comprises 96 wells with an inner diameter of 6.1 mm and a height of 7.0 mm giving a well volume of approximately 200 µl. The well size in this platform permits microliter scale experiments, opening the possibility to investigate the influence of solvents as well as monomer concentrations. A Teflon coating was applied to plate (a) to provide a non-stick surface, allowing it to be detached after polymerization without compromising the grafted surface and to access the samples for analysis. The coating also makes for an easy-to-clean surface, permitting it to be re-used after each experiment. When assembling the setup, the polymer substrate (b) was placed in-between plate (a) and the steel support (c) and held together by screws. Having the polymer as a separate part makes switching between substrates a simple process within one platform, making it possible to test the same conditions on various materials. The only requirement being that the substrate can be made into a film or sheet. To prevent leakage and potential mixing of contents, a tight seal between polymer and plate (a) was secured with a thin metal rim around each well on the bottom side of plate (a) (see **Figure 6, right**). During the thermal treatment, the setup is heated to 160 °C, just below the melting point of the polymer, which in this case is a PU (T_m = 166 °C). This softens the substrate and in combination with pressure from the screws, allows the metal rims to submerge into the polymer film, effectively sealing off each chamber. The high temperature treatment additionally also straightened out any unevenness in the film resulting from processing and ensured a good adhesion of the polymer film to the stainless steel support. Such unevenness in film thickness commonly results from release of internal stress after processing, which is critical to remove to ensure an efficient sealing across the entire surface. Therefore, the heat treatment was important with respect to both sealing the system and to obtain a flat homogeneous surface.

3.2. Activation of and Grafting onto Polyurethane

Most polymer surfaces are inert by nature and require activation through implementation of functional groups or initiating species to facilitate modification by polymerization. This can be done through a

stepwise activation and subsequent polymerization as is commonly done by use of controlled radical methods, such as surface initiated atom transfer radical polymerization[84–86], which provides high control for modification of surfaces[87–89]. Such processes typically requires inert conditions, which is not always possible in an industrial setting. In this case, we have evaluated the use of direct grafting using photo initiators under ambient conditions using the screening platform. Such systems have been applied for modification of polymer surfaces[90,91]. Some monomers are more tolerant to oxygen during polymerization, and identification of such systems would be of significant industrial interest for coating applications of thin surface coatings. Therefore, the polymer surface was activated for polymerization by embedding a photoinitiator, Irgacure 2959, into the polymer surface by solution casting, as shown in **Figure 7**.

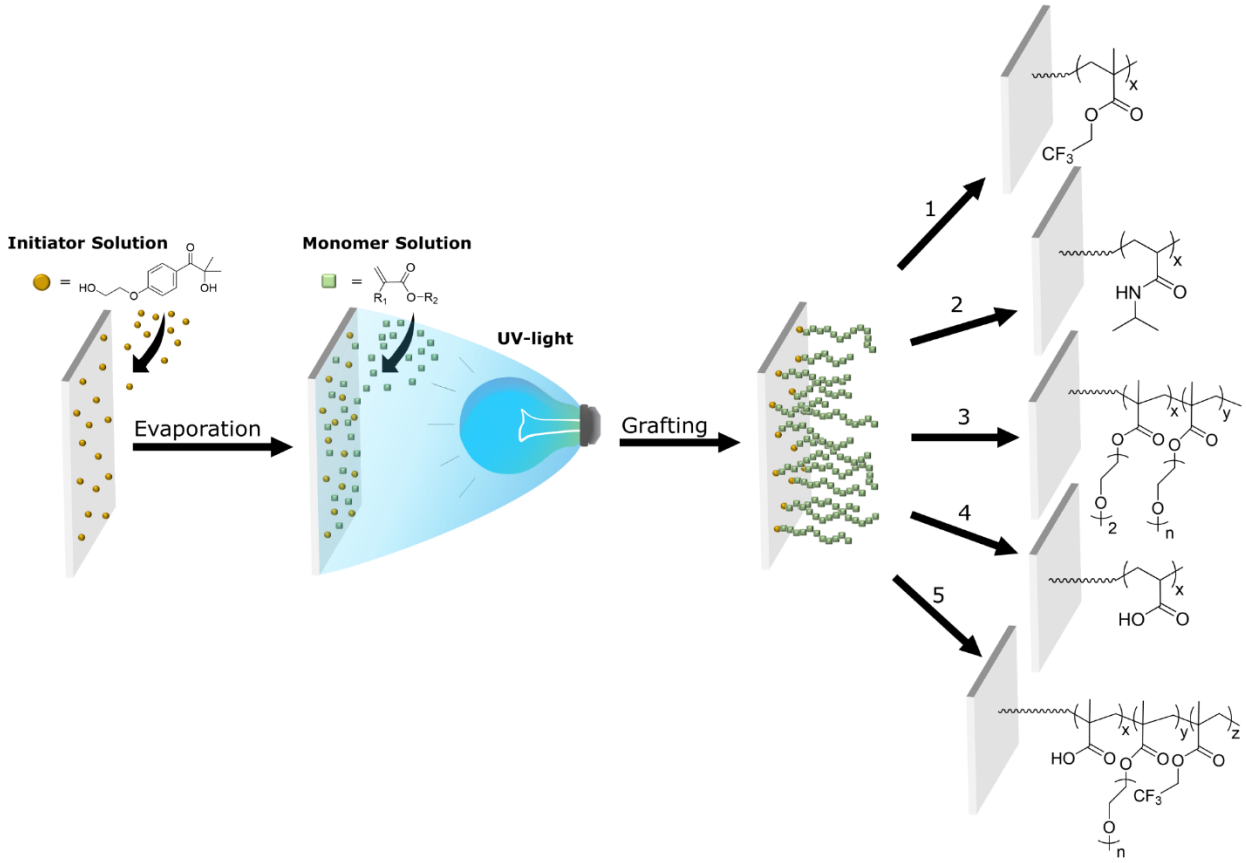

Figure 7 Schematic representation of embedding of photo initiator into polymer substrate followed by grafting of monomer through UV-activation. The illustrated surface modifications are 1) 2,2,2-trifluoroethyl methacrylate (TrFEMA), 2) N-isopropyl acrylamide (NIPAAm), 3) Diethylene glycol methyl ether methacrylate-co-poly(ethylene glycol) methyl ether methacrylate, M_n=500 (MDEGMA-co-MPEGMA 500), 4) Acrylic acid (AA), 5) MAA-co-MPEGMA 500-co-TrFEMA.

The initiator was dissolved in a mixture of THF/MeOH (1:4, v:v), where THF serves the purpose of slightly dissolving the PU substrate, while MeOH swells it. Due to this combination of solvents, solution casting of the photoinitiator solution onto the PU surface, results in embedment of the photo initiator into the outer layers of the surface. Subsequently, it can be functionalized through photoinitiated free radical polymerization with various monomer solutions. By exposing the entire system to UV-light, grafting of monomers from and into the polymer surface takes place, resulting in formation of thin layers of surface

grafted polymers as illustrated in **Figure 7**. Through this method, the formation of radicals are mainly occurring in close proximity to the surface of the substrate. This therefore limits the formation of non-grafted homopolymer compared to having the initiator added as a reagent in solution. This was also confirmed by analysis of the polymerization solutions after grafting, which contained no detectable amounts of free polymer (by SEC and NMR). After completed surface grafting, the detachable top plate (a) can be removed, enabling the surface to be analyzed by various classical analytical tools for surface analysis, such as WCA measurements, XPS as well as fluorescence intensity spectroscopy and UV-Vis spectroscopy. Since the top-plate is only mechanically bonded, it is possible to disassemble the structure without risking polluting the surface with polymer fragments originating from adhesives or other types of sealants, as is commonly used in other applications.

To investigate the possibilities of grafting commonly used acrylic and methacrylic monomers onto surfaces under ambient conditions, a range of different monomers were attempted grafted to the PU surface using UV initiated free radical polymerization. Initially, acrylic acid (AA) was grafted to the PU using a series of AA feed concentrations in an attempt to create a hydrophilic surface by introduction of carboxylic acid functionalities. Investigations of the effect of feed concentration with respect to hydrophilicity and elemental surface composition were done through WCA and XPS analysis, which can be seen in **Figure 8 A** and **D**, respectively. The WCAs obtained for the grafted surfaces ranged between 89-40°, which is substantially lower than that of the pristine polyurethane surface (104°). The lowest WCA of 40° was observed at 1.31 M, reflecting a clear shift from a hydrophobic to a hydrophilic surface, and at the same time illustrating the importance of testing different concentrations of monomers for surface grafting reactions. The grafting was further confirmed by XPS (**Figure 8 D**), showing higher oxygen content and no nitrogen atoms in the surface, corresponding to the structure of a surface grafted layer of poly(AA). This was further corroborated by FT-IR measurements of the grafted polymers (**Appendix 1.2, Figure S2**). The presence of surface grafted AA was confirmed by a broad OH stretch for all samples (2300-3600 cm-1), as well as a characteristic change to the carbonyl stretch resulting from the carbonyl in AA (1700 cm-1). In addition, also the effect of increasing the AA concentration in the feed, was reflected in an increasing strength of the bands assigned to the poly(AA). WCA measurements (**Figure 8 A**) also showed a trend of decreasing contact angle with increasing monomer concentration, suggesting a higher degree of polymerization at higher monomer concentrations (as expected). ANOVA analysis revealed significant differences not only between the pristine and modified surface but also between individual monomer concentrations, which distribute into three separate groups. Concentrations from 0.19 to 0.56 M group together in category A along with the pristine surface, showing that these concentrations only led to a minor change in surface hydrophilicity. Experiments conducted at concentrations of 0.75 M to 0.91 M, showed some impact on the WCA and were grouped together in the intermediate category BC. At high concentrations of 1.31, 1.69 and 2.06 M a clear impact of grafting was observed by significantly reduced contact angles, and these group together in group E, CDE and DE respectively.

Coatings containing poly(ethylene glycol) (PEG) have been of great interest in the field of biomedical devices both due to their ability to create low friction surfaces but also their biocompatibility and being FDA approved[50]. Through parallelization in the screening platform, copolymers of diethylene glycol methyl ether methacrylate (MDEGMA) and poly(ethylene glycol) methyl ether methacrylate (MPEGMA 500) were therefore prepared at various feed ratios of the two monomers. The relation between feed composition and WCA was investigated along with XPS analysis as shown in **Figure 8 B** and **E**, respectively. A decrease

in WCA was observed as MDEGMA was replaced with increasing amounts of MPEGMA 500 throughout the series. This was expected due to the longer PEG side chain in MPEGMA, resulting in a more hydrophilic monomer. However, only a minor decrease in contact angle from 104° for the pristine surface to 101° at 100 mol% MDEGMA was seen, which reduced to 66° for the 6.25/93.75 mol% MDEGMA/MPEGMA copolymer. In general, one would expect a much lower contact angle for these hydrophilic monomers. Similarly, the XPS data (see **Figure 8 E**) only showed a minor increase in oxygen, while the nitrogen peak from the PU substrate was still visible. In combination, this indicates that only a very thin coating of the hydrophilic monomers was formed on the PU. This was also corroborated in the FT-IR data (**Appendix 1.2, Figure S4**), where no significant differences were observed, though the similarity in composition of the monomers and the PU substrate makes small differences difficult to confirm. The statistical analysis of the WCAs, showing that no significant difference can be found between the pristine and modified surfaces, which all belongs within group A with the exception of 6.25 mol% MDEGMA, even though a general trend of decreasing WCA was observed across the series. Grafting under ambient conditions can therefore only be concluded to result in a very thin layer of poly(MPEGMA) or poly(MDEGMA), though this is sufficient to change the immediate surface chemistry (WCA measurements).

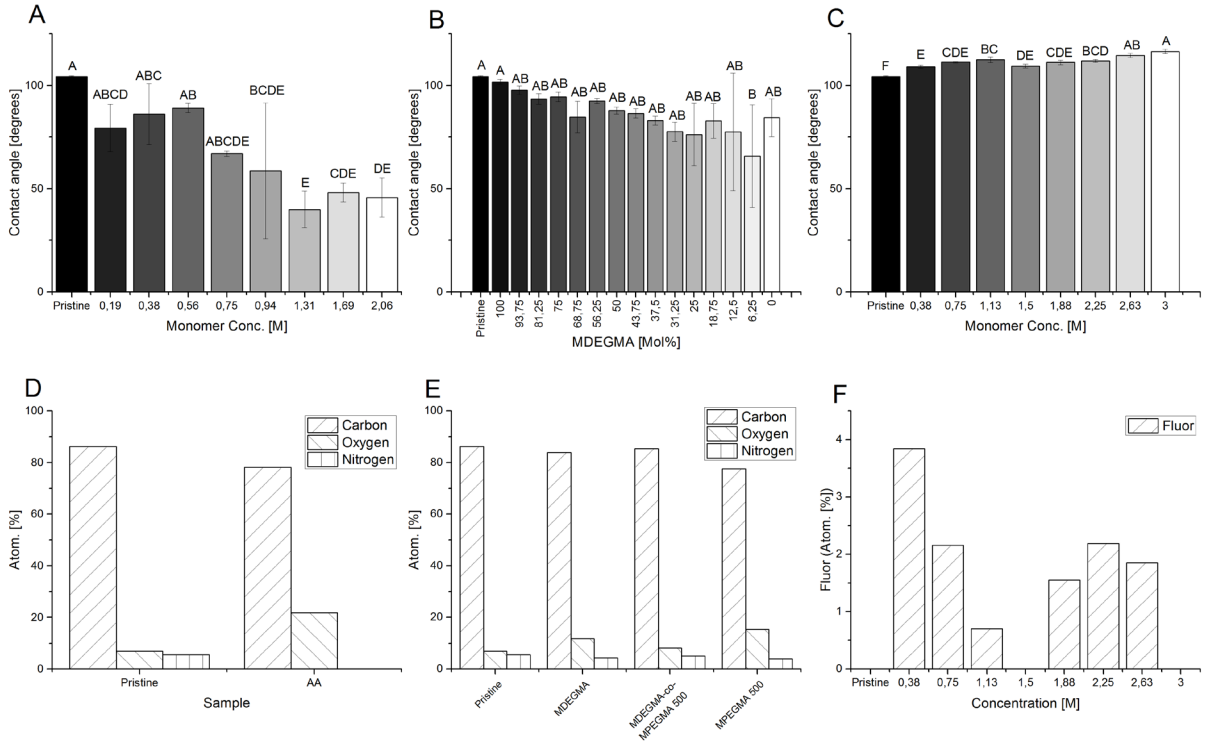

Figure 8 WCA and XPS data of PU surface modified with AA (A and D), MDEGMA-co-MPEGMA 500 (B and E) and TrFEMA (C and F) respectively.

Conversely, hydrophobic surfaces can be prepared through grafting of fluoride containing monomers. As an example of a fluorinated monomer, 2,2,2-trifluoroethyl methacrylate (TrFEMA) was grafted at various monomer feed concentrations to create a low energy surface. The WCA and the atomic fluor composition of the surface were measured and the results can be seen in **Figure 8 C** and **F**, respectively. The contact

angle increased with increasing monomer concentration from 109° at 0.38 M to 116° at 3 M. The pristine surface was assigned by ANOVA analysis to group F, which does not appear at any of the data points obtained, indicating that all modified surfaces were significantly different from the pristine surface. Even at low concentration of 0.38 M, the contact angle was significantly different to that of the pristine surface. The trend shown for the WCA measurements, indicates an increasing hydrophobicity of the surface, which would be expected to correlate with an increasing fluorine content. However, XPS analyses of the surfaces showed that this was not the case (**Figure 8 F**). Fluorine is seen for most of the samples, though the concentration does not appear to follow a trend. Optical microscopy images of the samples (**Figure 9**) reveal that this is due to an uneven coverage of polymer on the surface. The grafting conducted on the surface was incomplete and formed aggregates, which are seen as black dots in **Figure 9**.

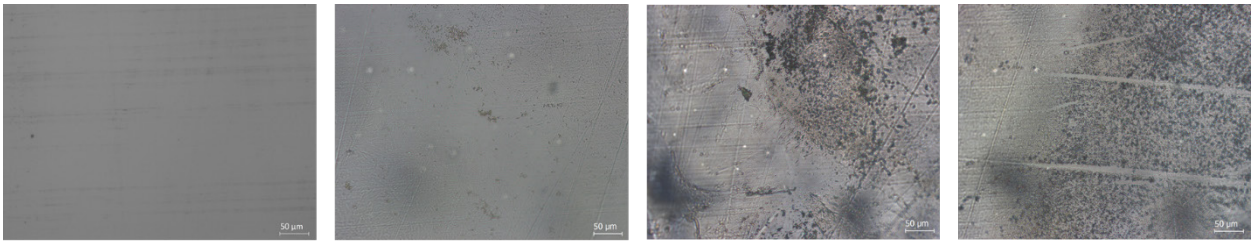

Figure 9 Microscopy images of TrFEMA modified PU at monomer feed concentrations of 0, 0.75, 2.25 and 3.00 M.

The aggregates increases in size and become more dominant with increasing monomer concentration, explaining the increase in WCAs. Analyzing the surfaces by FT-IR only showed insignificant changes in the spectra with increasing concentration, reflecting the incomplete reaction of the monomer. In conclusion, the fluorine monomer cannot be grafted in a homogeneous layer under ambient conditions even though the polymerization does results in a minor increase in the WCA.

A similarly often used monomer is N-isopropylacryl amide (NIPAAm), which, in addition to changing hydrophilicity upon thermal stimuli in solution, have been shown to have great potential for controlled drug delivery systems and nanofiltration membranes[92,93]. The polymer in solution have a lower critical solution temperature (LCST) of 31-33°C, resulting in hydrophobic properties above this point and hydrophilic properties below. The transition is caused by a rearrangement of the polymer chains starting as a linear conformation at low temperature, where amide groups are able to form hydrogen bonds to water. Increasing the temperature creates inter and intramolecular hydrogen bonds, forcing the polymer into a coiled structure, leaving only the hydrophobic backbone exposed. Grafting of the monomer was similarly conducted in a series of monomer feed concentrations with subsequent WCA and XPS analysis as presented in **Figure 10 A** and **B** respectively. To show that the thermoresponsive properties can be transferred to the polymer surface, the WCA of the NIPAAm modified PU was also measured both above and below the LCST (see **Figure 10 C**).

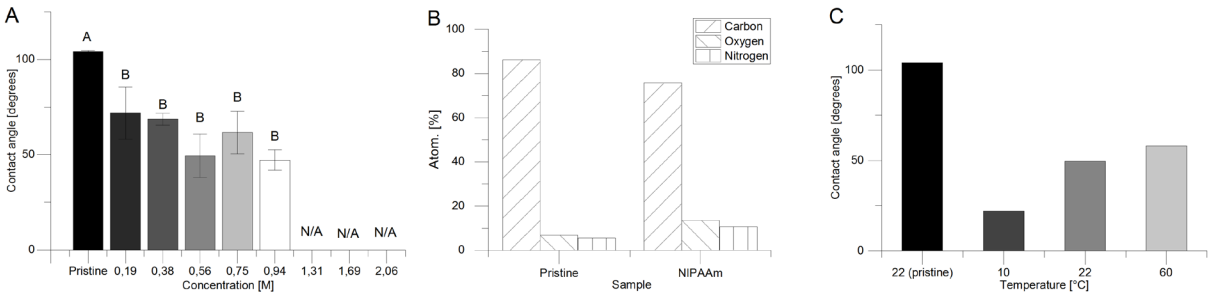

Figure 10 WCA of NIPAAm modified PU at various monomer feed concentration (A), XPS data (B) and WCA at various temperatures (C).

NIPAAm concentrations were varied within the range of 0 - 2.06 M in the feed and from this experiment, an important limitation concerning monomer concentration was observed. When the NIPAAm concentration was increased above 1 M, crosslinking occurred, resulting in large gel formations on the surface (see **Appendix 1.2, Figure S1**). The gels did not adhere well to the substrate and had poor mechanical stability. This demonstrates that the monomer concentration is an important parameter to consider and has great influence for the outcome of the polymer coating. Due to this crosslinking at high monomer concentrations, the XPS analysis was therefore carried out at 0.56 M, below the gel point. From **Figure 10 B**, the ratio between oxygen and carbon (O/C) and nitrogen and carbon (N/C) can be calculated to 0.15 and 0.12 respectively. This corresponds to that of NIPAAm, which have an O/C and N/C ratio of 0.14. This was also corroborated by FT-IR (**Appendix 1.2, Figure S5**), where a clear NH stretch (3300 cm-1) was seen for all concentrations below the gelation point. The thermoresponsive properties were observed by WCA measurements for one of the surfaces (NIPAAm, 0.56 M). At high temperature (60°C), the modified surface showed a WCA of 59°, which was reduced to only 22° at 10°C (**Figure 10 C**). This clearly show that the surface is thermoresponsive, though the transition appear at lower temperatures, compared to the typically observed LCST for NIPAAm. LCSTs have been seen to vary according to molecular weight and structure of the polymer, and it is hypothesized that this may be the reason for the observed deviation.

Overall, it can be concluded that some monomers (AA, NIPAAm) effectively can be grafted in homopolymerization to the PU surface under ambient conditions, while others are less efficient (MPEGMA, MDEGMA and TrFEMA).

3.3. Antifouling Amphiphilic Surface

Screening platforms are ideal for creating large libraries of complex systems in combination with parallelized analysis. To illustrate the possibility to do combinatorial studies, three monomers were tested as surface coating, methacrylic acid (MAA), TrFEMA and MPEGMA 500. The selection was based on the fact that polymer coatings comprising both hydrophobic and hydrophilic segments have proven to be effective in preventing fouling from e.g. marine life[94–96]. The intention of this study was therefore to investigate the optimal formulation to prevent fouling against a fluorescein labeled bovine serum albumin protein (BSA). For each monomer, stock solutions of 1 M concentration in EtOH were made and the ratio of monomers were systematically varied throughout three sets of terpolymer systems named A, B and C (see **Figure 11 A, B** and **C**). The sets all contained different base levels of MPEGMA 500 at 12.5, 25.0 and

37.5 mol% for A, B and C respectively. Tuning the hydrophobicity was done by adding MAA and TrFEMA in various ratios to give nine formulations for each set, providing a total of 27 formulations. The obtained WCA and fluor content from XPS of each formulation for A, B and C can be viewed in **Figure 11, D-F** and **G-I**, respectively.

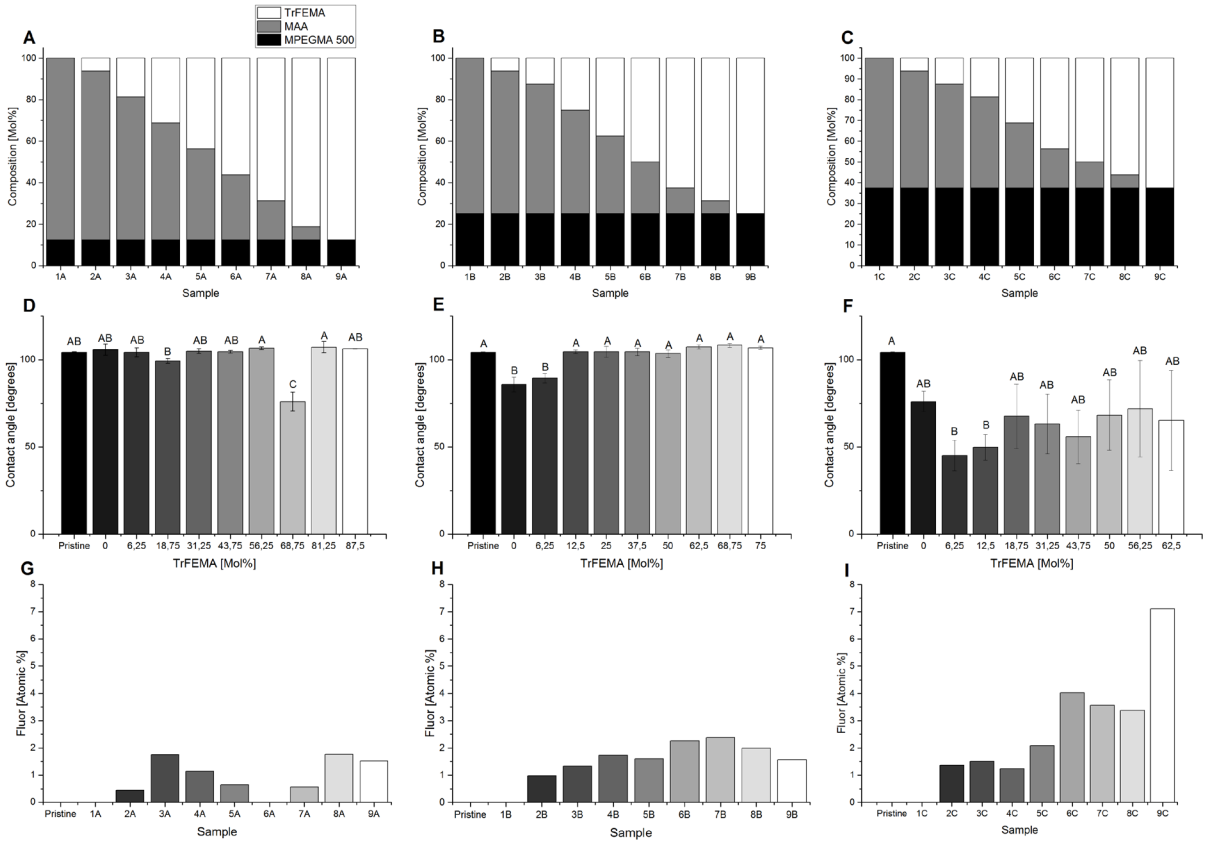

Figure 11 Composition of terpolymer set A, B and C, black: MPEGMA 500, grey: MAA and white: TrFEMA (A, B and C) and their respective WCA (D, E and F) and XPS data on fluor content (G, H, I).

The outcome of the WCA of terpolymer set A and B was heavily influenced by the presence of hydrophobic TrFEMA, even at small feed concentrations (see **Figure 11 D** and **E**). The contact angle of the samples barely deviated from that of the pristine surface, which was also seen from the ANOVA analysis. This was an unexpected result, considering that both MAA and MPEGMA 500 are both hydrophilic and present in high concentrations and a lower contact angle should be observed. A minor exception to this was the samples at 0 and 6.25 mol% TrFEMA in **Figure 11 E**, which obtained a WCA of 85 and 90° respectively. The ANOVA analysis shows that the contact angles are significantly different to that of the pristine surface, but quickly rises to above 100° at 12.5 mol% TrFEMA (see **Figure 11 E**).

For terpolymer C, however, the higher MPEGMA 500 content of 37.5 mol% was enough to counteract the hydrophobic effects of TrFEMA, resulting in a substantial drop in WCA (see **Figure 11 F**). The high content of MPEGMA 500 additionally increased the observed hysteresis of the systems illustrating the amphiphilicity of the surface. Therefore, no significant difference between the modified and the pristine

surface was found from the ANOVA analysis, with the exception at 6.25 and 12.5 mol% TrFEMA (see **Figure 11 F**).

Figure 11 G, **H** and **I**, illustrates the level of fluor in each sample for terpolymer set A, B and C, respectively. A linear trend with a steady increase in fluor with respect to increasing mol% of TrFEMA was expected for all terpolymer systems, but only terpolymer C showed this trend clearly. In **Figure 11 G**, the fluor content is very low and the grafting appears to be sporadic, whereas for **Figure 11 H**, a trend was initially seen but with the last two samples slightly decreasing. Terpolymer set C obtained a gradual increase in fluor with a maximum of 7.1 atom%. This is attributed to TrFEMA copolymerizing better with MPEGMA 500 than MAA. Between the three sets of surfaces, a higher content of fluor is therefore seen for higher contents of MPEGMA 500.

To test the antifouling properties, the modified surfaces were exposed to a 0.04 mg/ml fluorescein labeled BSA protein phosphate-buffer saline (PBS) solution. The mean value of the resulting intensity for terpolymer set A, B and C can be seen in **Figure 12 A, B** and **C** respectively.

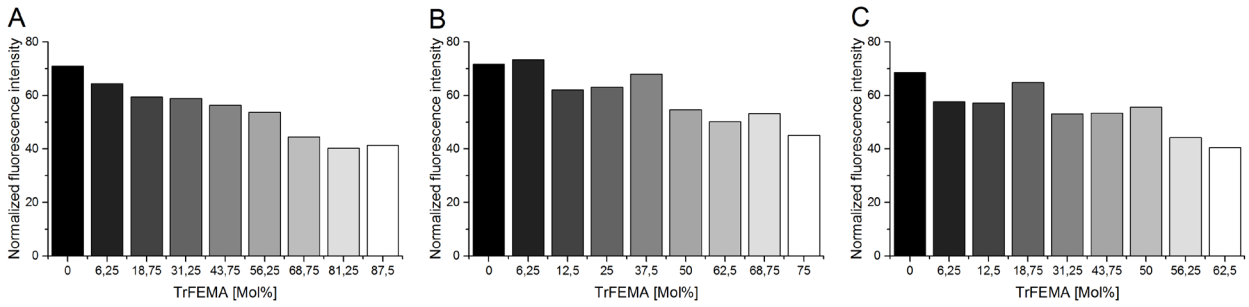

Figure 12 Fluorescence intensity of adsorbed fluorescein labeled BSA of terpolymer set A, B and C (A, B and C respectively) after 2 h. exposure to a 0.04 mg/ml PBS solution.

Comparing the analytical data and the obtained antifouling study showed that copolymers purely of MPEGMA 500 and TrFEMA gave in general the best fouling resistance for all terpolymer systems. The lower the feed concentration of MAA was, the better the fouling resistance became. An intuitive explanation would be that MAA was able to create either hydrogen bonds or electrostatic interaction with the protein through carboxylic acid groups (COO-/COOH). Thereby, even small contents of MAA would create binding sites for the protein to adhere.

3.4. Concluding remarks

The objective for this chapter was to develop a platform capable of screening PU surface modifications. In conclusion, the metal based platform was able to withstand both harsh solvents and elevated temperature, which enabled proper fitting of the PU substrate. The subsequent embedding of a UV initiator into the PU surface, proved as a simple and effective method to conduct FRP of various acrylate and methacrylate monomers, both as homo and copolymer systems. Surface modification through the introduction of both hydrophilic, hydrophobic and amphiphilic polymer systems, could be analyzed via classical characterization and analysis methods such as WCA, FT-IR and XPS. Investigations of reaction conditions with respect to monomer concentration, oxygen tolerance under ambient conditions as well as combinations of monomers were possible. Here it was shown that concentrations of NIPAAm above 1 M resulted in heavy crosslinking and that homopolymerization of TrFEMA was not able to form a homogenous layers. It was, however, possible to incorporate the fluor-containing monomer through

copolymerization with MAA and MPEGMA 500. These results provide valuable information in identifying suitable monomers for surface modification. Furthermore, evaluation of antifouling properties could be conducted using fluorescent labeled BSA using UV-vis spectroscopy. The platform thereby presents the opportunity to screen polymer surface modifications, bio-interactions and conditions through the use of an industrially relevant process.

4. Screening of Antimicrobial Activity of PU Substrates

In literature, many examples of surfaces containing quaternary ammonium groups have been shown to destabilize the membrane integrity of bacterial cells. Based on this, the screening platform described above were used to create various surface modifications having quaternary amine functionalities on PU (see **Figure 13**). Evaluation of the antimicrobial activity of the synthesized polymer surface modifications, were conducted in close collaboration with biologists and test facilities at Coloplast A/S. High antimicrobial activity of the modified surface against relevant pathogens is of paramount importance in order to be able to prevent or reduce the formation of UTIs. The mode of action for contact killing surfaces is not a standard way of introducing bactericidal properties and therefore no standard test method currently exists. Careful selection of test must therefore be made in order to reassure scientifically appropriate results. This chapter discusses the data from the bacteriological studies and serves the purpose of establishing a correct methodology for bacteriological screening. Investigation of a wide range of biological test methods with each having their individual strengths and drawbacks were considered.

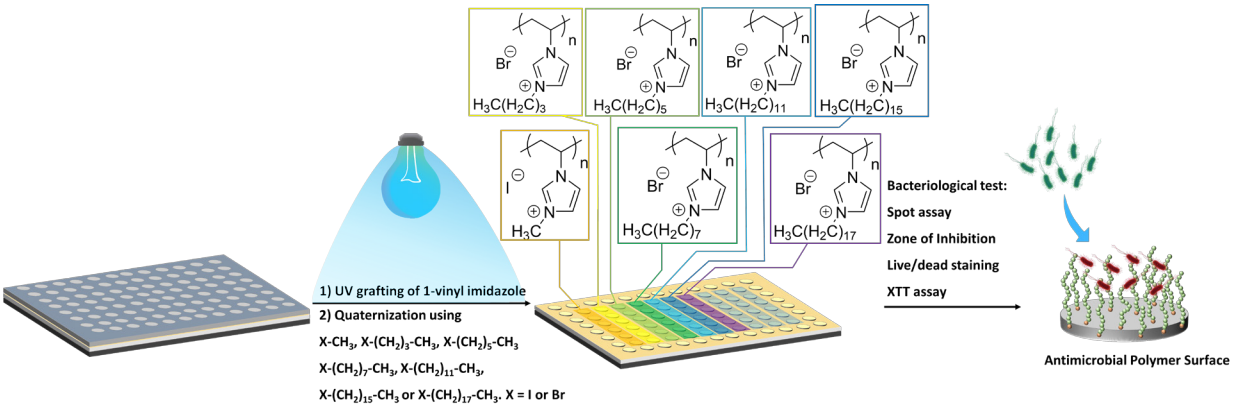

Figure 13 Illustration of screening platform used for grafting of VI onto PU and subsequent quaternization to create antimicrobial polymer surface modifications.

4.1. Spot Assay

A couple of promising candidates were selected based on **Chapter 2** and 1-vinylimidazole was chosen for initial investigations of the antimicrobial potential of quaternized ammonium compounds. Relatively few papers existed at the time on the antibacterial properties of quaternized VI but had shown promising results. Therefore, VI presented itself as a window of opportunity for further exploration.

VI was grafted onto a PU substrate using the screening platform and procedure described in **Chapter 3**. The grafted polymer was subsequently quaternized with a series of alkylation agents with increasing carbon chain length ranging from C1 to C18. This particular study was supplemented with part of Thea Louise Hansen's bachelor project "Preparation of antibacterial polymer surfaces", which was co-supervised by Christian Andersen in connection with this PhD.

Choice of test method should be considered with respect to both the type of material and antimicrobial mechanism used in the system. Some tests are specifically tailored for textiles, while others are made for porous or non-porous surfaces and evaluates activity based on repellency, bactericidal and/or bacteriostatic effect. Bacteriological testing is often the bottle neck in the process due to being time-

consuming, since visualization of antimicrobial effect is predominantly based on bacterial growth in either liquid medium or on agar plates, which usually requires at least 24 h. Therefore, choosing the correct method to apply for a specific system is critical in order to obtain the right information and avoid false positives or negatives. As a first option, the spot method offered a cheap, fast and easy method of screening for antimicrobial activity. The principle of the test is simple and does not require any specialized equipment to carry out. An illustration of the procedure can be seen in **Figure 14**.

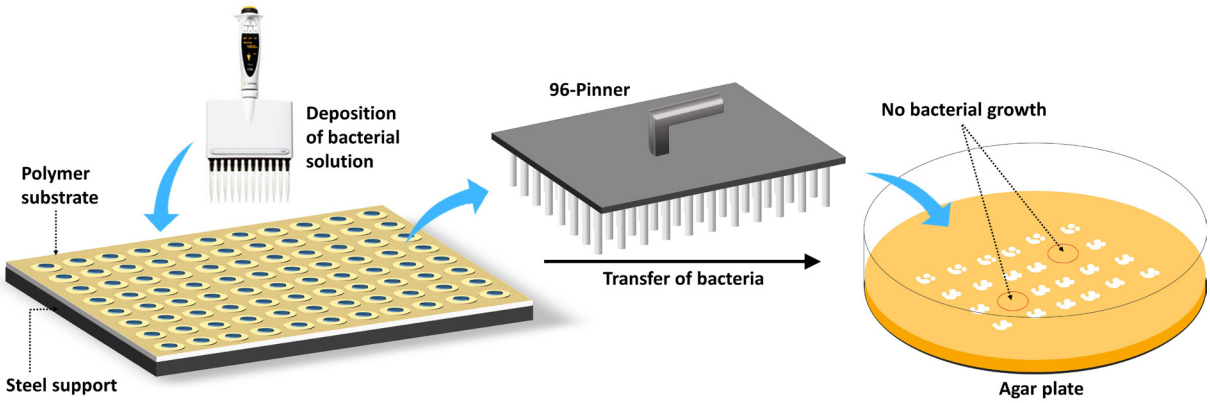

Figure 14 Schematic representation of the spot assay. A bacterial solution is deposited onto modified sample spots on the polymer substrate and incubated for a preset amount of time. Thereafter, bacteria is sampled using the piston and imprints with attached bacteria is transferred onto an agar plate. The plate is then incubated at 37 °C for 24 hours and the level of growth of the bacteria is then determined.

A bacterial solution is placed on top of the modified surface areas, which can be done both with and without the well plate attached depending on the volume of the applied solution. After a certain contact time, samples from each well area are collected by the use of a 96-pinner. The end of the rods from the pinner is put into contact with the substrate and is immediately transferred and imprinted onto an agar plate used for cultivation of bacteria. Viable bacteria is then visualized by incubating the plate overnight allowing the bacteria to grow colonies on the agar. The results are only semi-quantifiable meaning that the extent of bacterial growth can be roughly correlated to the number of surviving bacteria, but was in this context mainly meant to assess complete kill or no killing of bacteria. Using the spot assay, the surface modifications were exposed to a urinary tract E. coli#84 strain with a concentration of 7.7 x 10^3 colony forming units (CFU)/ml and was sampled at 0, 3, 5 and 24 h. and the results can be viewed in **Figure 15**.

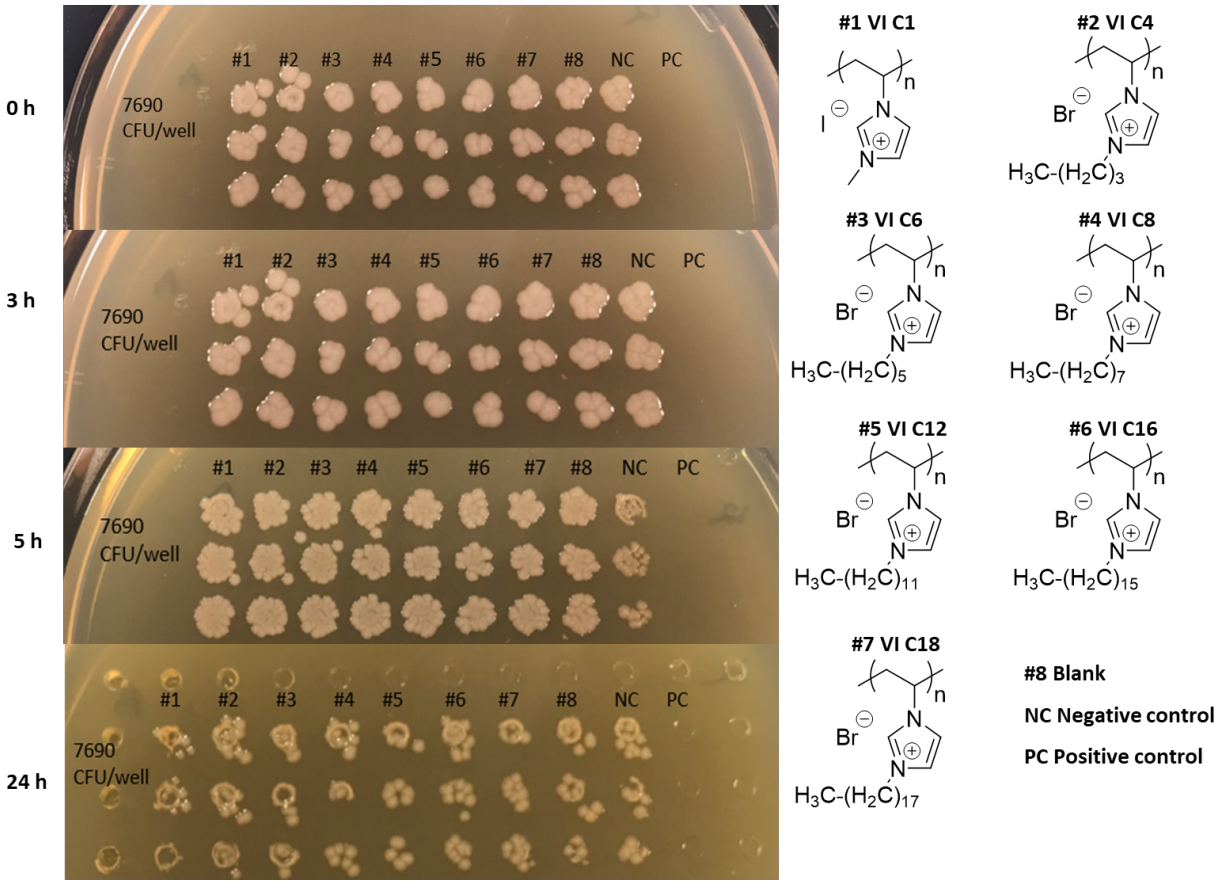

Figure 15 Spot assay of quaternized VI modified PU exposed to E. coli#84 at 7.7 x 10^3 CFU/ml for 0, 3, 5 and 24 h. Positive controls were made by addition of a amphenicol B (Amp B) (250 µg/ml) solution.

Large visible colonies were present in all of the modified well areas at both 0, 3 and 5 h. exposure time. However, at 24 h. the size of the colonies declined but no significant differences between samples and negative controls were seen. A possible explanation for this might be due to poor contact between the surface and bacteria. If the bacterial solution is not properly absorbed into the coating, bacteria residing above the surface-liquid interface remain untouched by the grafted quaternary ammonium, thus resulting in a false negative. The contact active mechanism is therefore inefficient at dealing with bacteria that do not come into close contact. The spot assay method has, in this case, a serious limitation when investigating contact active antimicrobial surfaces and requires the surface to be hydrophilic enough to absorb the administered bacterial solution. This limits the scope with respect to the grafted chemical structure and composition and is ideally best suited for hydrogels.

In an effort to work around this limitation, a second study using combinations of quaternized DMAEMA and MPEGMA 500 (Mn = 500 g/mol) to make hydrophilic networks were made. This type of surface modification is also relevant for catheter application, since a water absorbent surface is important for providing low friction to ease insertion. DMAEMA was chosen instead of VI, since the antibacterial properties for this compound had been reported at several occasions in the literature and would therefore, be better suited as a model compound. The DMAEMA was grafted onto PU substrates as both

homopolymer and as a DMAEMA-co-MPEGMA 500 copolymer in a 3:1 mol:mol ratio respectively. Quaternization of DMAEMA was carried out using 1-bromobutane (C4), 1-bromooctane (C8) and 1-bromohexadecane (C16) and were exposed to a 6.4 x 10^3 CFU/ml E. coli#84 solution. Samples were collected after 1, 3 and 24 h and the results can be viewed in **Figure 16**.

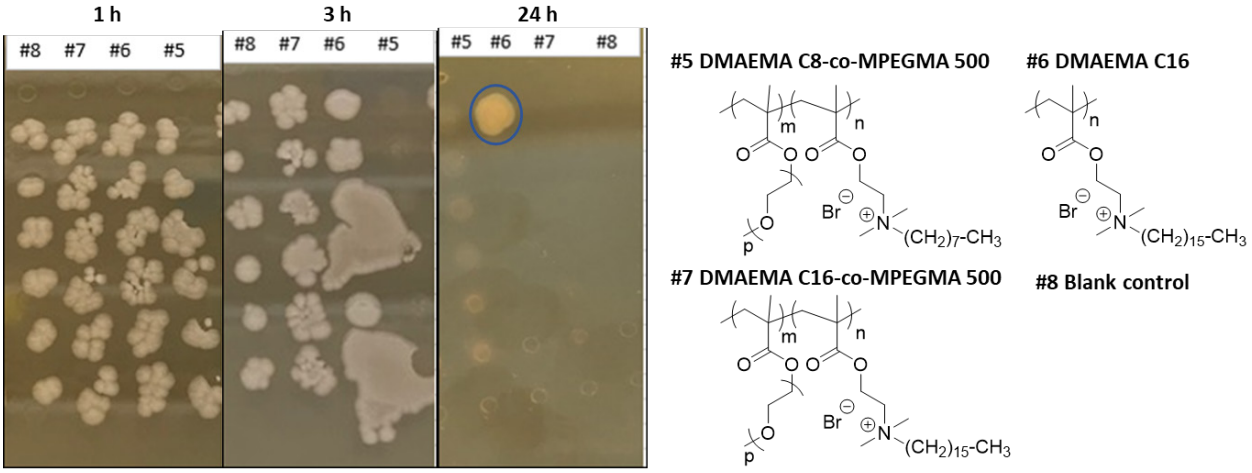

Figure 16 Spot assay of quaternized DMAEMA and DMAEMA-co-MPEGMA (Mn=500 g/mol) grafted PU exposed to 6.4 x 10^3 CFU/ml E. coli#84 for 1, 3 and 24 h. Blue ring indicates bacterial contamination of the agar and does not originate from E. coli#84. Note that column order is reversed for 1 and 3 h. compared to 24 h.

Due to a mistake during bacteriological testing parts of the results from this study were missing. Data from DMAEMA C4, DMAEMA C4-co-MPEGMA 500 and DMAEMA C8 along with positive and negative control samples were therefore lost during testing.

Bacterial growth was found for all samples after both 1 and 3 h. of exposure with the exception of DMAEMA C8-co-MPEGMA 500 (column #5) at 3 h. The bacteria were also observed to be swimming (see **Figure 16**, 3 h., column #6), meaning that they were able to float around on top of the agar and contaminate nearby samples. This is caused when the agar is too wet and the wetness can vary from batch to batch and is unavoidable. After 24 h. there were no visible colonies formed on the agar with the exception of a single colony circled in blue, which was due to contamination and did not originate from the E. coli#84 strain. It was surprising that the non-modified surface showed activity and was also seen for the PU substrate in the previous study after 24 h. This was an early indication that release of an active compound from the polymer matrix itself, could be responsible for lack of bacterial growth. Since it is a processed polymer, additives are often used during manufacturing and are not always possible to remove, despite initial washing and cleaning. A second option could also be stress induced cell death, since no nutrients were provided in the bacterial solution and no conclusion regarding release of additives could be made.

The spot assay was concluded to have too many variables that could influence the outcome of the test e.g. overloading of bacteria, proper contact between substrate and pathogen and transfer of bacterial samples. The contact active mechanism of positively charged surfaces rely on having sufficient charge density available to produce damaging electrostatic interaction with the cell membrane. Having too high concentration of bacteria could result in overloading of the surface. This could create a monolayer of dead

cells that would be shielding new bacteria entering the surface from the electrostatic effect allowing them to survive. Secondly, as discussed previously, the bacterial solution must be completely absorbed to be able to achieve complete eradication of the pathogen, which limits screening to gels or very hydrophilic surfaces. Finally, having a highly swellable gel comprised of positive charges could, hypothetically, be able to attract bacteria without necessarily killing them. Again, overloading could cause death in a certain portion of the bacterial population while the rest would be ionically bound, but without causing cell death. This would create a "sponge" that potentially could absorb the bacteria and hold it in the network, which would be unable to be transferred via the pinner, due to higher affinity for the gel. The biological result would therefore be a false positive, since the cells would still be alive. The spot assay was therefore deemed as a non-compatible method for evaluation of antimicrobial contact active systems.

4.2. Zone of Inhibition Assay

A method that offers better contact between the substrate and bacteria is the zone of inhibition (ZOI) assay and was implemented as the next step in the bacteriological investigation. In this test, a bacterial solution is spread across an agar plate before placing samples on top with the active side face down and is left to incubate overnight. If the samples possess antimicrobial activity, growth inhibition zones can be seen underneath the samples after removal (see **Figure 17**).

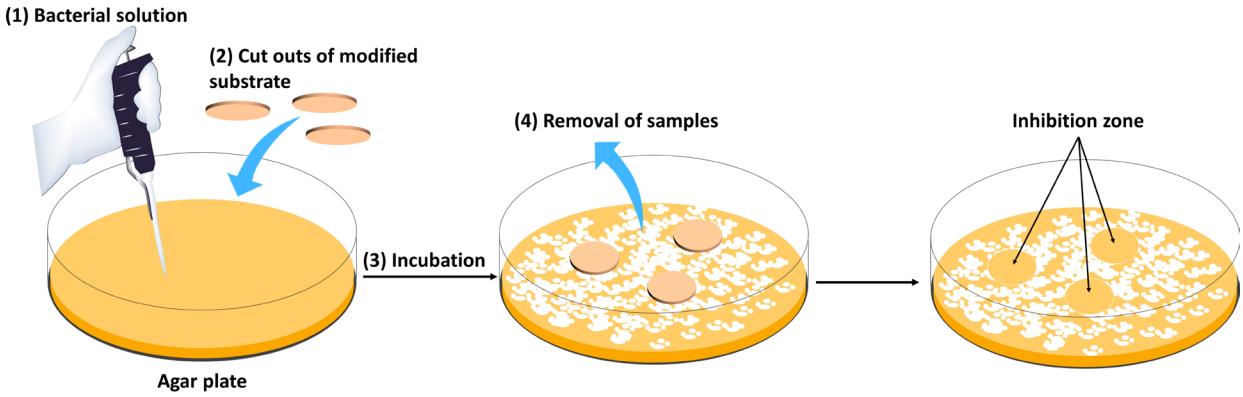

Figure 17 Schematic representation of the Zone of Inhibition test. (1) A bacterial solution is spread across an agar plate. (2) Samples are placed on top of the agar having the modified side face down. (3) The plate is incubated for a predetermined period. (4) Removal of samples to reveal zones of growth inhibition.

The test is normally used to qualitatively assess susceptibility of bacteria to antimicrobial compounds, typically leachables that diffuse from a given matrix. However, several studies have used this method to evaluate quaternary ammonium systems as a way of proving the contact active mechanism[97–100]. The samples provides a clear ZOI directly under the substrates but does not diffuse or create a zone larger than the diameter/area of sample. However, it is difficult entirely to distinguish subtle effects from leaching and surface contact since inhibition zones can be very small. Nonetheless, it can still be used to give an early indication of antimicrobial activity.

For this type of assay, smaller sample size was needed to avoid creating oxygen deficient areas beneath the polymer substrate that would potentially result in killing the bacteria. Therefore, a punch-out tool was used to create oblates of the modified PU. The surface modifications investigated was VI, VI C4, VI C16, DMAEMA, DMAEMA C4 and DMAEMA C8 and the results can be seen in **Figure 18**.

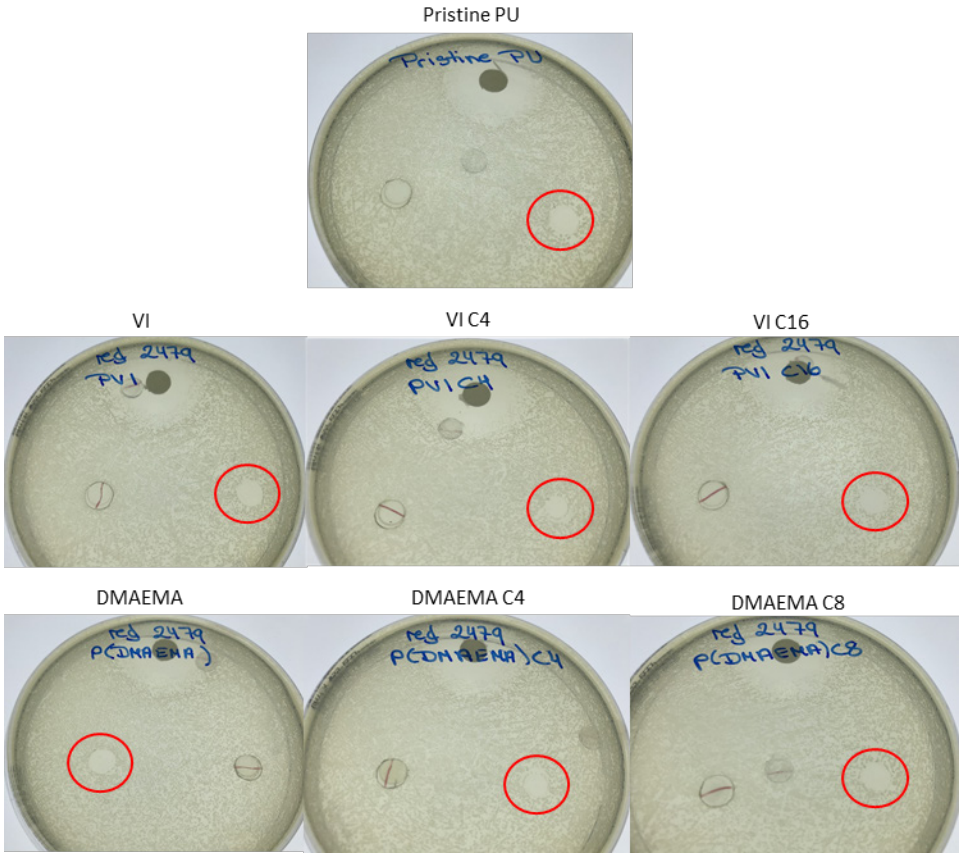

Figure 18 ZOI assay of quaternized VI and DMAEMA grafted PU substrate exposed to E. coli#84 for 24 h. Red circles indicates zones of bacterial growth inhibition and positive controls were made from 10 µl solution mixture of penicillin, streptomycin and amphenicol B dispensed on filters and were placed at the top of the agar plates.

ZOI was observed for all samples including the pristine PU. Despite bacterial growth only being inhibited directly underneath the area of the sample, these results still indicate the presence of a potential leachable in the PU since no antimicrobial activity was to be expected from the base material. FT-IR analysis of liquid extractions from the polymer further revealed the presence of a process aid. The spectra pointed towards being an aliphatic esters, which are often used as a release agents in production of polymers such as PU[101]. This study further demonstrates as to why the ZOI assay should not mistakenly be used as a tool to rule out leachables from presumably contact active coatings and is a common misconception conducted in practice for many papers.

Release of the presumed aliphatic ester proved to have greatly influenced bacteriological data due to its high antimicrobial activity. The processed PU could therefore no longer be directly included in further bacteriological studies. In an attempt to avoid the release of these compounds a secondary option is presented below.

4.3. Thermoplastic PU with covalently attached photoinitiator

As a new approach to utilize the platform and to avoid process additives, a PU having a benzophenone (photoinitiator) covalently attached to the backbone of the polymer were supplied by Coloplast. The polymer contained no additives and consisted of a large hydrophilic soft segment and a minor hard segment. Having the initiator already anchored on the surface removes the need for applying previously

described activation step. Since radicals will only be formed close to the surface with no chance of initiator solubilizing into solution, this should further improve the grafting capabilities of the system and reduce homopolymer formation. The polymer was supplied in pellet form and had to be melt pressed into a suitable shape to fit the platform. A PU plate was placed underneath during the melt press process to bind the two layers thermally together (see **Figure 19**).

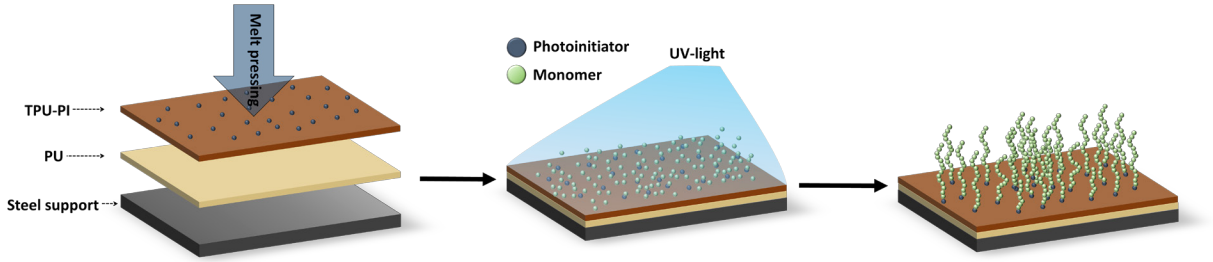

Figure 19 Illustration of the preparation procedure for PU/TPU-PI substrates and subsequent application for surface modification via UV-grafting of monomer.

The PU helped significantly to keep the film straight and provided a suitable support for the TPU-PI and will be referred to as PU/TPU-PI and was implemented for grafting of VI and DMAEMA. N-alkylation of VI was done with carbon chain lengths of 4 (VI C4) and 16 (VI C16) while carbon chain lengths of 4 (DMAEMA C4) and 8 (DMAEMA C8) were used for DMAEMA. Antimicrobial activity was evaluated for samples using the ZOI test and were exposed to E. coli#84 for 24 h. The results can be viewed in **Figure 20**.

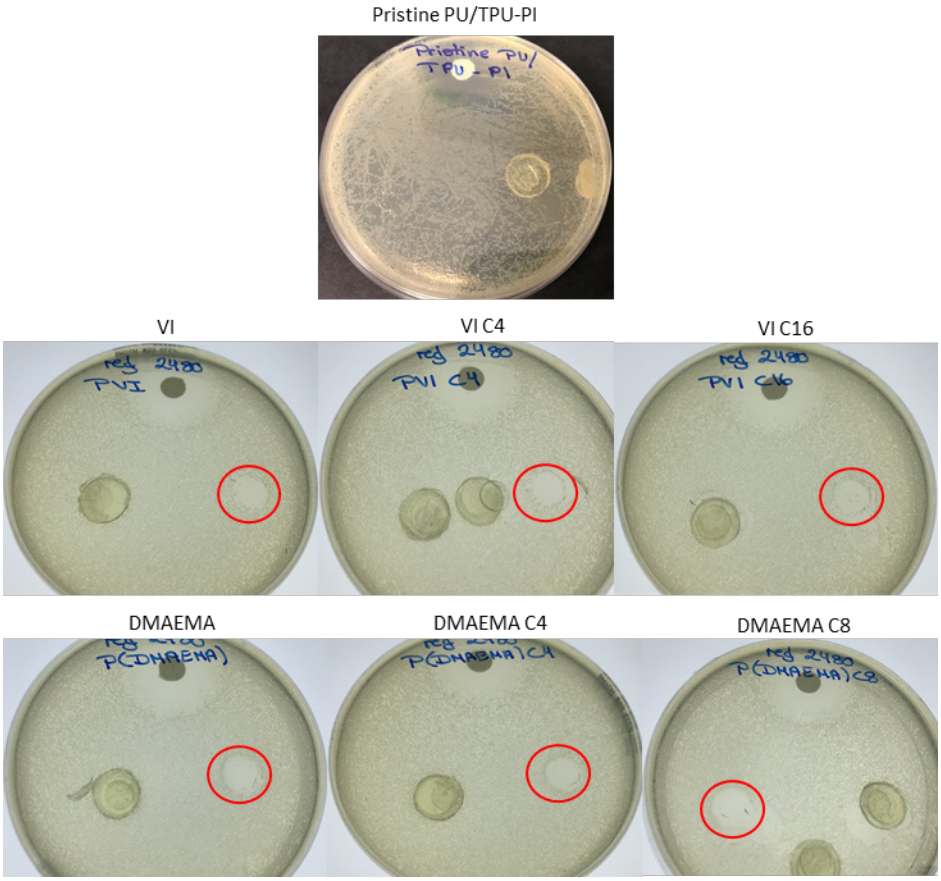

Figure 20 ZOI assay of quaternized VI and DMAEMA grafted PU/TPU-PI exposed to E. coli#84 for 24 h. Red circles indicates zones of bacterial growth inhibition and positive controls were made from 10 µl solution mixtures of penicillin, streptomycin and amphenicol B dispensed onto filters and were placed at the top of the agar plates.

The PU/TPU-PI did not produce any ZOI showing that the TPU-PI layer was capable of blocking diffusion of additives from the underlying PU, while the remaining samples did all have visible ZOI. This was surprising since no antimicrobial properties were expected for the non-quaternized surfaces of VI and DMAEMA. To ensure that this was not an artifact originating from the grafting procedure, e.g. residues of toxic monomers, liquid extraction of a series of samples were collected and analyzed by high performance liquid chromatography (HPLC). The surface modifications investigated were VI, VI C4 and 2-hydroxyethyl methacrylate (HEMA) grafted PU/TPU-PI.

Another factor to consider in the testing of these materials is sterilization, which is a common practice during the production of catheters. Therefore, in addition, a set of samples were sterilized using E-beam, which is the current method of choice for sterilization of catheters at Coloplast. In the case of having monomer present during this type sterilization, the high energy electron beam would induce vinyl bonds to form radicals that either forms homopolymers or binds to the substrate. Through this process, any potential residues from monomers would therefore be eliminated.

No detectable residues could be identified from the HPLC data with the exception of non-sterilized HEMA samples. The peaks did, however, disappear after having undergone E-beam sterilization showing that any potential monomers present after washing of the surface will be removed during this treatment. The ZOI assay were further used to evaluate the antimicrobial activity of both sterilized (S) and non-sterilized (NS) samples against E. coli#84 and the results can be seen in **Figure 21**.

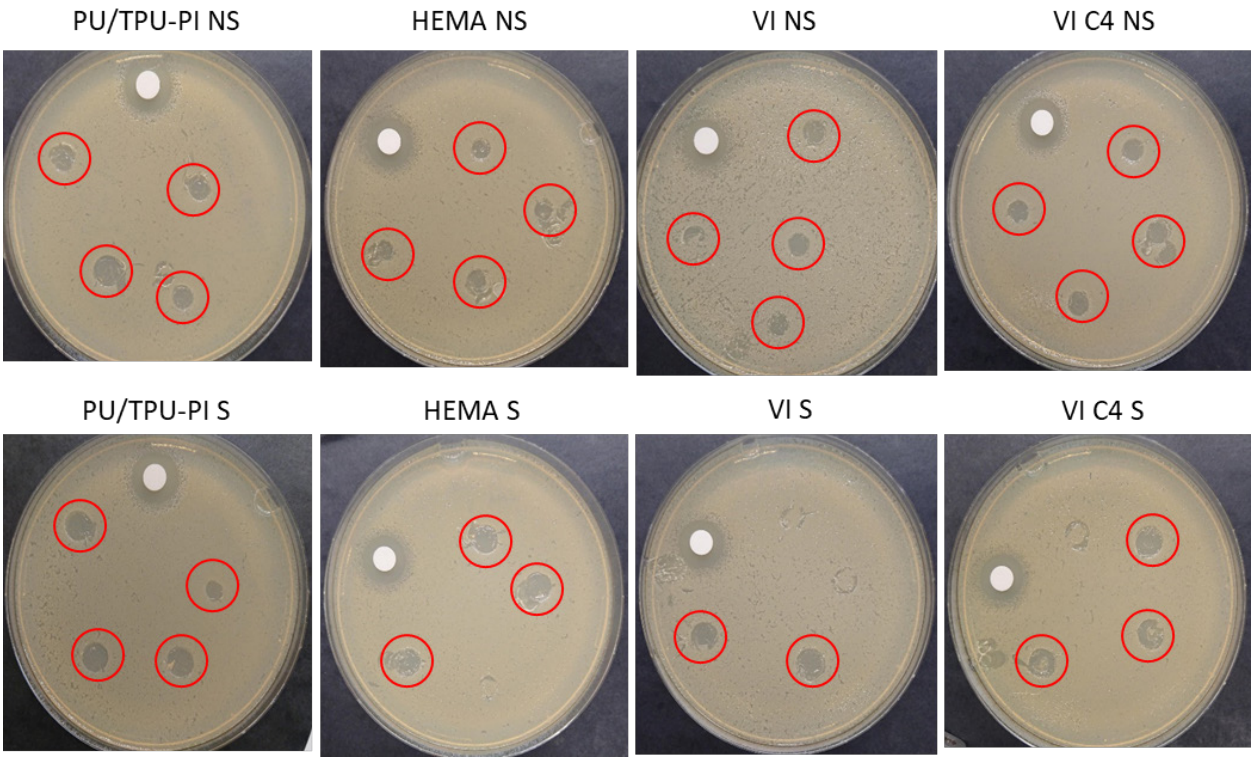

Figure 21 ZOI assay of both sterilized (S) and non-sterilized (NS) HEMA, VI and VI C4 grafted PU/TPI-PI. The samples were exposed to E. coli#84 for 24 h. Red circles indicates zones of bacterial growth inhibition and positive controls were made from 10 µl solution mixtures of penicillin, streptomycin and amphenicol B dispensed onto filters and were placed at the top of the agar plate.

In contrast to previous findings, the S PU/TPU-PI and NS PU/TPU-PI surface had clear visible ZOI and was in general found for all samples. The zones could not originate from any leachables as was proven by HPLC data. It was in fact discovered that the hydrophilic segment of the TPU-PI rendered the material able to absorb large amounts of water from the moist agar. This made the polymer swell significantly and made it sink into the agar that in turn, created an apparent ZOI. The TPU-PI polymer can therefore not be used in relation to the ZOI assay as the presence of false positive results were a significant drawback.

Other well-established bacteriological methods such as live/dead staining and XTT assay were investigated as alternative solutions.
Live/dead staining evaluates living vs dead bacteria and is able to distinguish and quantify these through the use of dyes that binds to specific targets within bacterial cells. It utilizes a combination of two different dyes where one is able to penetrate intact cell membranes and typically produces a green fluorescent signal. The second dye is only able to enter bacteria, which have a compromised membrane and provides a red fluorescent color representing dead cells. Measurement of fluorescence intensity from the two dyes can then tell how many living and dead cells are present. However, when tested a high background signal was observed, which was due to PU being autofluorescent. This prevented quantification of the dyes in the assay and can in addition also be observed for PEG-based substrates.
XTT assay is another attractive method and works through an extracellular reduction of a tetrazolium salt e.g. 2,3-bis-(2-methoxy-4-nitro-5-sulfophenyl)-2H-tetrazolium-5-carboxanilide (XTT) to formazan. The reduced product forms an orange water soluble dye that can be measured colorimetrically and can be correlated directly to the number of viable bacterial cells. The test was investigated for the PU/TPU-PI

substrate but the dye was absorbed by the very hydrophilic TPU-PI and could not be used for quantification of the antimicrobial activity.
Finding a method that both allowed proper testing of contact active antimicrobial systems as well as avoiding interference from the underlying material proved to be a great challenge. Having PU as a base substrate continued to be one of the major complications for the bacteriological investigations.

4.4. Concluding Remarks

In this study, investigations of bacteriological test methods were done to establish a procedure for the evaluation of antimicrobial activity for surface modified PU substrates having quaternary ammonium groups. The spot assay proved to have critical limitations, especially to ensure sufficient contact between bacteria and surface. Inconclusive results along with uncertainties regarding proper sampling of bacteria, lead to the conclusion that the spot assay was not suitable for determining antimicrobial activity for this type of system. To resolve this issue, the ZOI assay was used as an alternative option. However, here it was found that the PU contained additives, which diffused from the polymer matrix during bacteriological testing. The processed polymer possibly contained residues originating from a release agent and proved to have antimicrobial activity that heavily influenced experimental data. To avoid release of additives, a TPU-PI polymer was applied as a melt pressed layer on top of the processed PU. Although this blocked diffusion of the release agent, the large hydrophilic segment of the TPU-PI was able to swell and sink into the moist agar. Bacterial growth was thereby inhibited leaving behind a ZOI, giving a false positive result. Despite repeated efforts to obtain scientifically reliable results, the complicated nature of having PU as base material continued to interfere with the bacteriological outcome of these studies.

5. Model Study of Antimicrobial Coatings Through the use of SI-SARA-ATRP

Although the screening platform was initially intended for FRP of monomers, which mimics industrial processing, the system lacks control over both molecular weight and architecture of the obtained polymer systems. Greater freedom to tailor-make complex molecular structures are achieved through the use of controlled radical polymerization (CRP) techniques and permits to further investigate the structure-property relationship of the antimicrobial activity of the coatings. Due to the complication of having PU as substrate, PDMS was considered as an alternative material, since this is also a widely applied polymer for catheter production. PDMS further provides a more inert surface that would ease chemical surface analysis and characterization. In this chapter, a model system made by attachment of an ATRP initiator onto PDMS substrates was used to conduct surface initiated supplemental activation reducing agent atom transfer radical polymerization (SI-SARA-ATRP), as illustrated in **Figure 22**. The method was utilized for grafting of DMAEMA and the effect of brush length as well as alkylation agents with respect to antimicrobial activity were investigated. The experimental data can be found in **Chapter 9**.

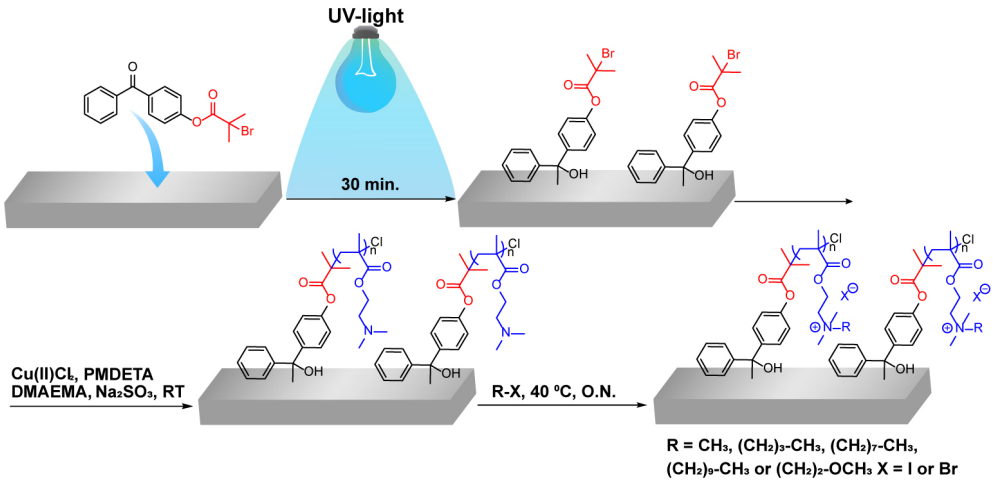

Figure 22 Schematic representation of surface activation, grafting procedure and quaternization of DMAEMA modified PDMS by SI-SARA-ATRP

5.1. Investigation of ATRP Mechanism and Conditions

SI-ATRP have become a widely used method for producing advanced surface functionalizations for high end applications within the biomedical field as e.g. biosensors or antifouling[102–106]. Modification of surfaces is commonly done by anchoring of an alkyl halide specie serving as the initiator. Grafting of monomer then proceeds via a metal complex mediated reaction, which is often copper based with a polydentate nitrogen ligand, creating well defined polymer brushes on the surface (see **Figure 23, top**).

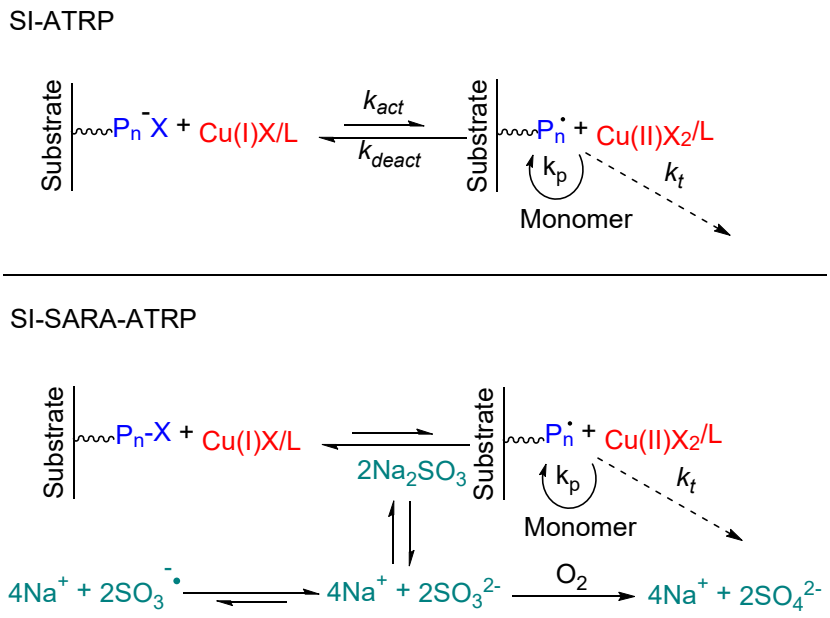

Figure 23 Schematic illustration of typical Cu mediated SI-ATRP mechanism (top) and Cu mediated SI-SARA-ATRP mechanism using sodium sulfite as reducing agent (bottom). Cu = metal catalyst, L = ligand, X = halide, P_n = polymer chain end, Na_2SO_3 = reducing agent, k_{act} = activation rate constant, k_{deact} = deactivation rate constant, k_t = termination rate constant and k_p = propagation rate constant.

The high control over MW and dispersity (*Đ)* originates from the equilibrium between the inactive halogenated polymer chain end (P_n-X) and the active radical ($P_n^{\bullet}$). Activation of chains happens through a reversible one electron transfer redox reaction mediated by the metal-ligand complex that switches between the reduced state (Cu(I)X) and the oxidized state ($Cu(II)X_2$)[107]. The equilibrium is deliberately shifted towards the dormant P_n-X, which reduces the number of radicals during reaction and thereby lowers reaction rate and minimizes unwanted termination. However, some disadvantages for this type of CRP is for example the need for relatively high catalyst concentration and poor stability of Cu(I), which sometimes require purification before addition. Low tolerance towards oxygen leads to accumulation of oxidized Cu(II), which forces the equilibrium towards the dormant state. Freeze-pump-thaw cycles of the reaction vessel is then required for removal of residual oxygen[108]. Advances within ATRP have led to strategies able to circumvent some of these limitations as for instance SARA-ATRP (see **Figure 23, bottom**). This method greatly reduces the amount of catalyst needed and is also applied in its more stable oxidized form. The addition of a reducing agent subsequently converts $Cu(II)X_2$ to Cu(I)X that allows for initiation of polymerization. Excess reducing agent is, in addition, able to react with oxygen in the solution and protects the catalyst against unwanted oxidation and thereby significantly improves oxygen tolerance.

Here, a simple method of attaching a benzophenone derivatized with an ATRP initiator (Br-BPh) onto PDMS was applied, which then permitted grafting of DMAEMA through SI-SARA-ATRP as illustrated in **Figure 22**. The reactions were conducted with low amounts of catalyst (1.3 mM) and moderate concentration of both reducing agent (5 mM) and monomer (1.4 M). Having sodium sulfite as a novel reducing agent allowed parallelized polymerization under ambient conditions, with no use of degassing procedures. The low concentration of reagents simplified subsequent purification and removal of Cu, to ensure a non-leaching material. A distinctive feature for CRP reactions is that MW develops in a linear

fashion with respect to time. To confirm the controlled nature of the reaction an initial study of the propagation of brush thickness with respect to time on silicon wafers was conducted (see **Figure 24, left**).

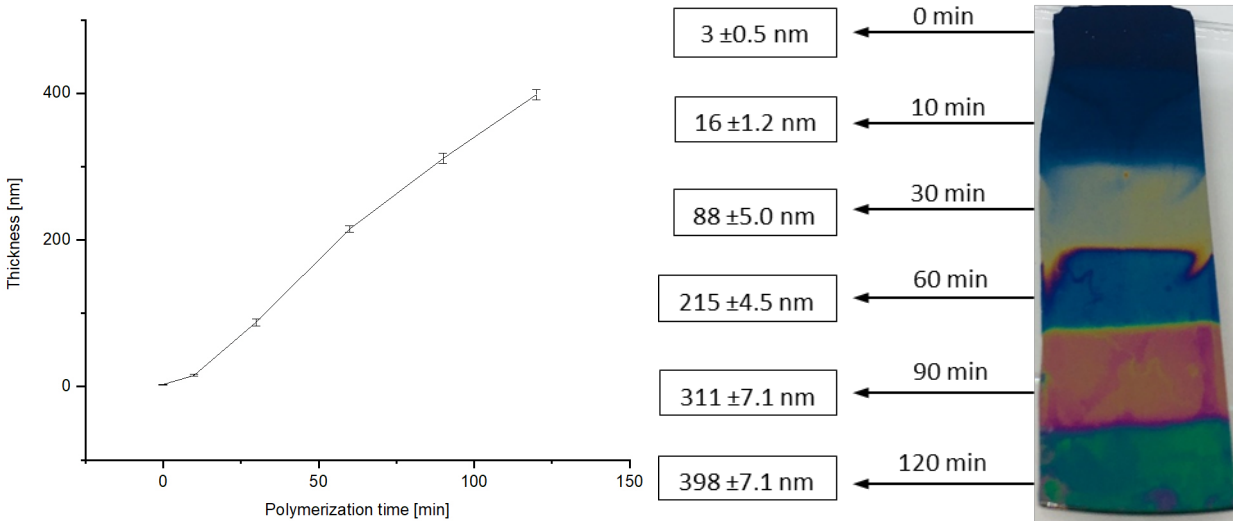

Figure 24 Time development of brush thickness of DMAEMA by SI-SARA-ATRP on silicon wafer using Na_2SO_3 as reducing agent (left) and silicon wafer after grafting showing a shift in coloration at various brush lengths (right).

This study took place in collaboration with PhD student Koosha Ehtiati, who conducted ellipsometry analysis of the wafers. From this data, a good linear tendency was observed between brush thickness and reaction time. Polymerization of nitrogen containing monomers have previously been proved to be challenging due to competing complexation with the ligand, which may lead to an inefficient catalyst[109]. This was not the case using these conditions and the reaction showed that long DMAEMA brushes could be achieved within very short reaction times and reached a maximum length of 398 ±7.1 nm after only 120 min. Another interesting result from this experiment was that individual sampling times could be observed as visual changes in coloration directly on the silicon wafer, as shown in **Figure 24 (right)**.

In this type of polymerization, as the name also implies, supplemental activation of monomer occurs as a result of radical formation from the reducing agent. Sodium sulfite is able to disproportionate into SO_3^{2-}, which can convert into radicals in the form of $SO_3^{-\bullet}$. These are able to take part in a FRP of monomers in the surrounding solution alongside the ATRP reaction. Fortunately, these polymer chains are not bonded to the surface and can easily be washed off and do not interfere with the architecture or dispersity of the grafted chains. However, the free polymer chains contributes significantly to increased viscosity of the reaction mixture and limits the timespan of which the reaction can proceed. Another common method to increase oxygen tolerance is activators regenerated by electron transfer atom transfer radical polymerization (ARGET-ATRP). Here a reducing agent is also applied, often sodium ascorbate or ascorbic acid[110–114], to regenerate the catalyst, but avoids the supplemental activation. However, this method was observed to be significantly slower and reached only a brush thickness of 34 ±0.49 nm after a reaction time of 120 min. (see **Figure 25**).

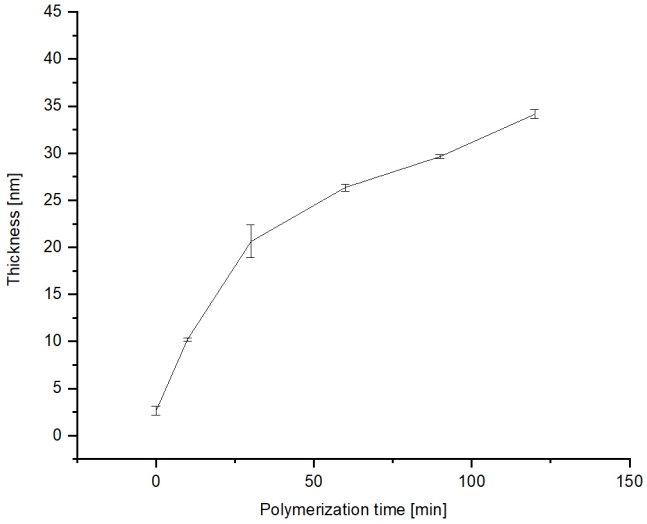

Figure 25 Time development of brush thickness of DMAEMA by SI-SARA-ATRP on silicon wafer using sodium ascorbate as reducing agent

Additionally, the evolution in thickness was a less than an ideal linear curve and the SARA-ATRP system therefore proved to be able to rapidly produce a broad range of thicknesses within short polymerization times. The long brushes achieved through SARA-ATRP also permits shorter reaction times to sufficiently functionalize the surface, which reduces the impact of the polymers formed by supplemental activation.

5.2. Screening Platform for Parallelized Synthesis of DMAEMA by SI-SARA-ATRP

Conducting ATRP in parallel is in general challenging even for most ARGET and SARA systems since they, despite their oxygen tolerance, are still conducted under limited amounts of air in sealed containers or atmosphere boxes. By use of the screening platform it was possible to conduct SARA-ATRP under completely ambient conditions, which was utilized for grafting of a series of DMAEMA brushes with varying lengths and quaternization (see **Figure 26**).

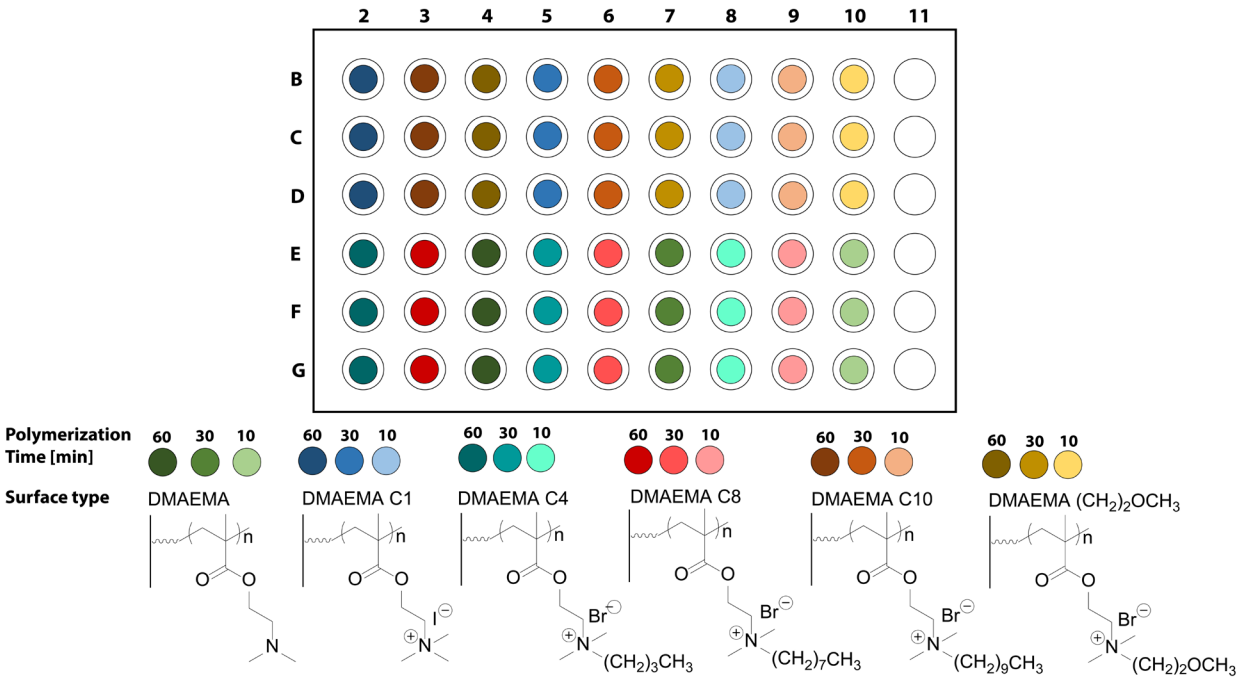

Figure 26 Well layout of screening platform for DMAEMA surface modifications on PDMS substrate.

The brush length was varied by removing the reaction mixture from the well and replacing it with solvent, terminating the reaction. In this way DMAEMA brushes after 10, 30 and 60 min. reaction time were obtained, which based on kinetic studies of silicon wafers, corresponds to app. 33, 100 and 200 nm, respectively. Post modification through alkylation of the side chain nitrogen were conducted using iodomethane (DMAEMA C1), 1-bromobutane (DMAEMA C4), 1-bromooctane (DMAEMA C8), 1-bromodecane (DMAEMA C10) and 2-bromoethyl methyl ether (DMAEMA $(CH_2)_2OCH_3$).

5.3. Biofilm Inhibition

Prior to investigating the antimicrobial activity of the acquired DMAEMA surface modifications, an initial study of a wide range of organisms and their ability to create biofilm on PDMS were conducted in collaboration with DTU National Food Institute. Biofilm formation were in this case visualized through the use of crystal violet staining. Crystal violet is a dye, which is able to bind to sugar containing molecules such as peptidoglycans in the cell wall of bacteria. The dye can then be either measured colorimetrically directly or re-solubilized and transferred to a microtiter well to avoid potential background noise. The absorbance directly correlate to the number of viable cells and is therefore an indirect method for quantification of biofilm. Pristine PDMS samples were subjected to the crystal violet assay and the results can be seen in **Figure 27**.

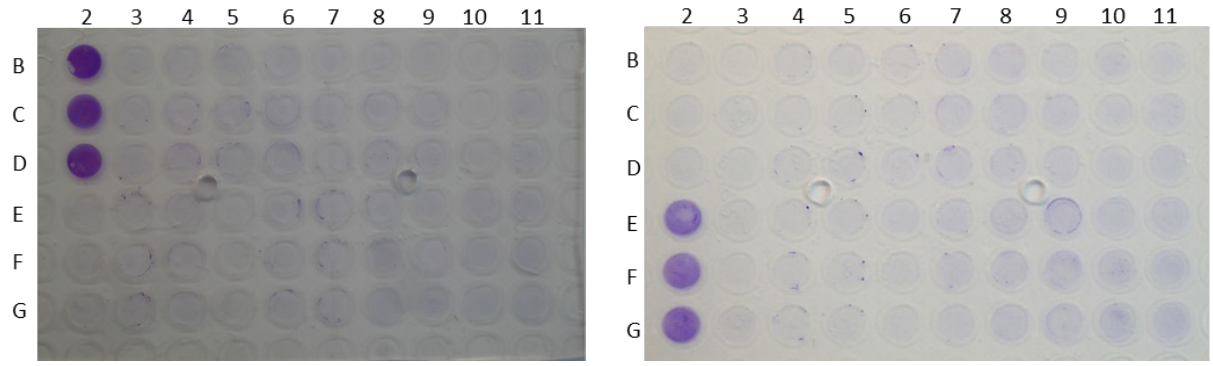

Figure 27 Investigation of biofilm forming pathogens incubated for 24 h. on non-modified PDMS. Biofilm formation was visualized by crystal violet staining. n = 3.

A total of 31 pathogens of different species and strains, being both gram positive (S. aureus, S. epidermidis, Ent. faecalis and Ent. faecium) gram negative (E. coli, P. aeruginosa, P. vulgaris, P. mirabilis and Klebsiella) and fungi (C. albicans and C. glibrata) were analyzed. From this study, most organisms showed little to no biofilm formation. Only two species, (g-) Proteus mirabilis (**Figure 27** column 2 row E-G, right) and (g-) P. aeruginosa (**Figure 27** column 2 row B-D, left), had clear biofilm formation on the PDMS substrate. P. aeruginosa was previously described in **Chapter 2 Figure 3** as to constitute part of the biofilm colonies found in incidences of UTI. The pathogen was therefore chosen for further investigation in prevention of biofilm formation. P. aeruginosa was exposed to the DMAEMA modified PDMS substrates over a 24 h. period. Staining was done using crystal violet and subsequently re-solubilized and transferred to a microtiter plate to quantify biofilm formation. The absorbance of the dye was for each sample measured at 550 nm and the results can be viewed in **Figure 28**.

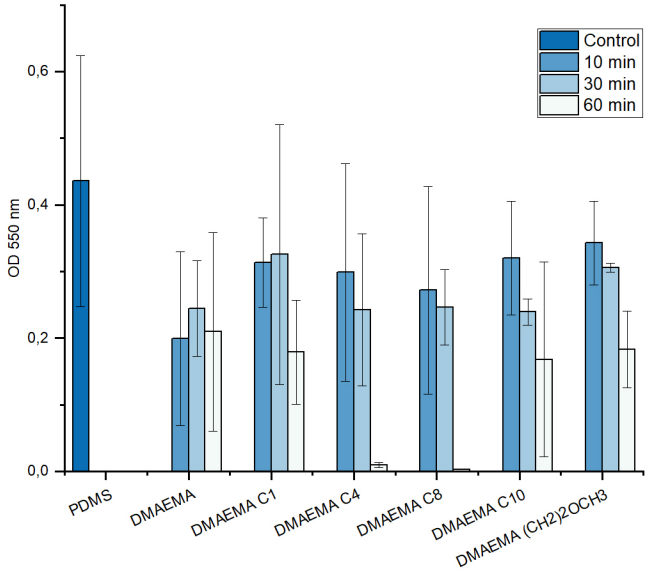

Figure 28 Quantification of crystal violet stain via optical density measurements for surface modified PDMS, control PDMS (dark blue), 10 min. polymerization time (blue), 30 min. polymerization time (light blue) and 60 min. polymerization time (white). n = 3.

Most of the analyzed surfaces showed only little reduction in biofilm, with the exception of DMAEMA C4 and DMAEMA C8 at 60 min. polymerization time. Here a significant difference in optical density (OD)

reading compared to that of the pristine PDMS was observed, showing almost no absorbance. The antimicrobial effect quickly diminishes with the use of longer or shorter carbon chains for quaternization outside this range. This shows that change in amphiphilicity of the polymer system plays a pivotal role in acquiring proper interaction with the cell membrane to induce damaging effect. Furthermore, increasing polymerization time also in general provided a higher effect for most surfaces with the exception of DMAEMA. An explanation could be that the longer polymer chains provided additional sites for quaternization. This would result in increased charge density of the surface, which previously have also been shown to be a big factor in obtaining effective contact active quaternary ammonium surfaces[79,81,115]. Higher mobility of the longer chains may also add to this phenomenon by providing the chains with the ability to better aggregate on the cell, giving better contact. The high standard deviation of the data, however, makes it difficult to reliably point out these kinds of tendencies.

5.4. Concluding Remarks

The scope of this study, were to develop and implement a CRP technique with the previously described screening platform to investigate the structure-property relationship of surface modifications in relation to their antimicrobial activity. Here, DMAEMA brushes were grafted onto PDMS using SI-SARA-ATRP and utilizing Na_2SO_3 as a novel reducing agent. The reaction provided extraordinarily long polymer brushes of almost 400 nm within short reaction times of ≤ 2 h. Additionally, the system showed high oxygen tolerance and the screening platform enabled parallelized synthesis in a completely open system under ambient conditions. Variation in brush length could be obtained through termination of reactions at different times. Post functionalization of the side-chain amine of DMAEMA brushes were evaluated for their ability to prevent biofilm formation of P. aeruginosa via a crystal violet staining assay. A clear trend between brush length and choice of alkylation agent with respect to antimicrobial activity could be observed. Significantly lower level of biofilm formation were found for DMAEMA C4 and C8 at 60 min. polymerization time. This indicates that longer polymer chains can possibly provide better mobility and charge density to interact with the cell membrane along with having the correct amphiphilicity of the system and plays a crucial role in obtaining highly effective antimicrobial surfaces. The platform thereby presents itself as a versatile method of not only screening various types of surface chemistries for antimicrobial properties but can also be applied with different polymerization techniques as well as polymer substrates.

6. Industrial Application of Coatings

Based on the previous chapters, grafting of monomers having quaternary ammonium functionalities on polymer surfaces have been shown as a feasible way of obtaining antimicrobial properties without the release of additives. As one of the final objectives in this project, an attempt to produce smooth antimicrobial catheter coatings through the combination of previously acquired knowledge with currently used coating procedures for Coloplast catheters were made. Several aspects had to be taken into consideration and adjustments to align with the industrial process with respect to e.g. the use of non-toxic solvents in formulations, replacement of monomers with polymer systems, chemical stability towards E-beam sterilization and coating application method were needed. Due to confidentiality, parts of the procedure as well as formulation recipes and chemical structures have intentionally been excluded from this chapter.

6.1. Investigation of Commercial Polymers

High demands and regulations are set for the safety and health impact of biomedical devices. This also applies to the use of toxic chemicals during production where no significant traces, if at all, of such compounds must be detected in the final product. Therefore, employing a monomer based system for coating of catheters compared to a polymeric version requires detailed proof of either conversion or removal of the substance and is thereby less likely to receive the final approval for distribution. To avoid the complication of using monomers, although previous experiments had proved that leaching could be avoided (see **Chapter 4**), a pre-synthesized polymer was used instead. Since the current coatings are PVP based the prerequisites for the choice of polymer was that it must contain some level of PVP and preferably have a MW above 100.000 g/mol, to afford good binding/integration in the current base-coating of the catheters. It should also comprise some level of tertiary amines either as part of the side-chain or backbone able to undergo quaternization to afford antimicrobial properties. Conveniently, commercial polymers were available that fitted the criteria. Initially, three commercial copolymers P1 and P2 consisting of poly(1-vinyl-2-pyrrolidone)-co-poly(1-vinylimidazole) (PVP-co-PVI) and P3 made from poly(1-vinyl-2-pyrrolidone)-co-poly(2-(dimethylamine)ethyl methacrylate) (PVP-co-P(DMAEMA)), were purchased and investigated as candidates for application in catheter coating formulations (see **Figure 29**).

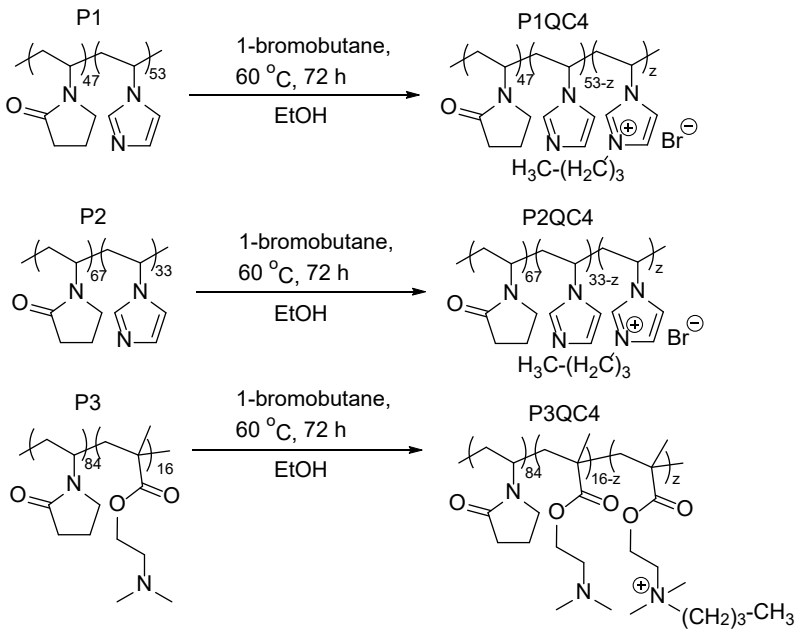

Figure 29 Alkylation of tertiary amines of commercial polymers with 1-bromobutane to produce quaternary positively charged amine groups.

The MW of the polymers was not given by the manufacture accept for P1, which had a MW of approximately 70.000 g/mol. Investigation by size exclusion chromatography (SEC) was attempted but high affinity of the polymers to the column material, rendered this method impossible on our systems. All polymers contained PVP and the second part were either VI or DMAEMA, which can undergo quaternization to afford antimicrobial quaternary ammonium. An advantage of these polymers were their solubility in EtOH and/or water and thereby allowed preparation of coating formulations in non-toxic dispersive media. The composition of the copolymers were estimated by ^{1}H-NMR analysis and **Figure 29** shows the mol% of each unit.

To obtain effective antimicrobial activity of the polymer coatings, high charge density is needed to induce damaging electrostatic interaction with the bacterial membrane. Achieving this, requires a high number of amine groups available to produce the positive charges as well as sufficient conversion of these. P1 had the highest amount of amine functionalities with 53 mol% imidazole groups, followed by P2 with 33 mol% and P3 with 16 mol% DMAEMA. An initial screening of antimicrobial activity was investigated through the use of a so called “kill test” and was conducted for both the non-modified polymer and a quaternized version. The test was done on polymer solutions and not covalently bonded coatings due to the feasibility of being a fast and easy method, to give an initial indication of bacteriological effect. No quantitative analysis could be made from this, but simply served as a mean to visualize whether bacteria were killed by the presence of the polymer or not. Quaternized polymers were synthesized by the use of 1-bromobutane to functionalize either the 3 position of the imidazole amine or the amine side-chain of DMAEMA. The alkyl chain length was chosen based on both the results obtained in **Chapter 5** and on the work of Zheng et al.[70] as plausible candidates and the quaternized product was named accordingly: P1QC4, P2QC4 and P3QC4 (see **Figure 29** above). The extent of conversion for the quaternization was estimated by ^{1}H-NMR and the results can be seen in **Figure 30**.

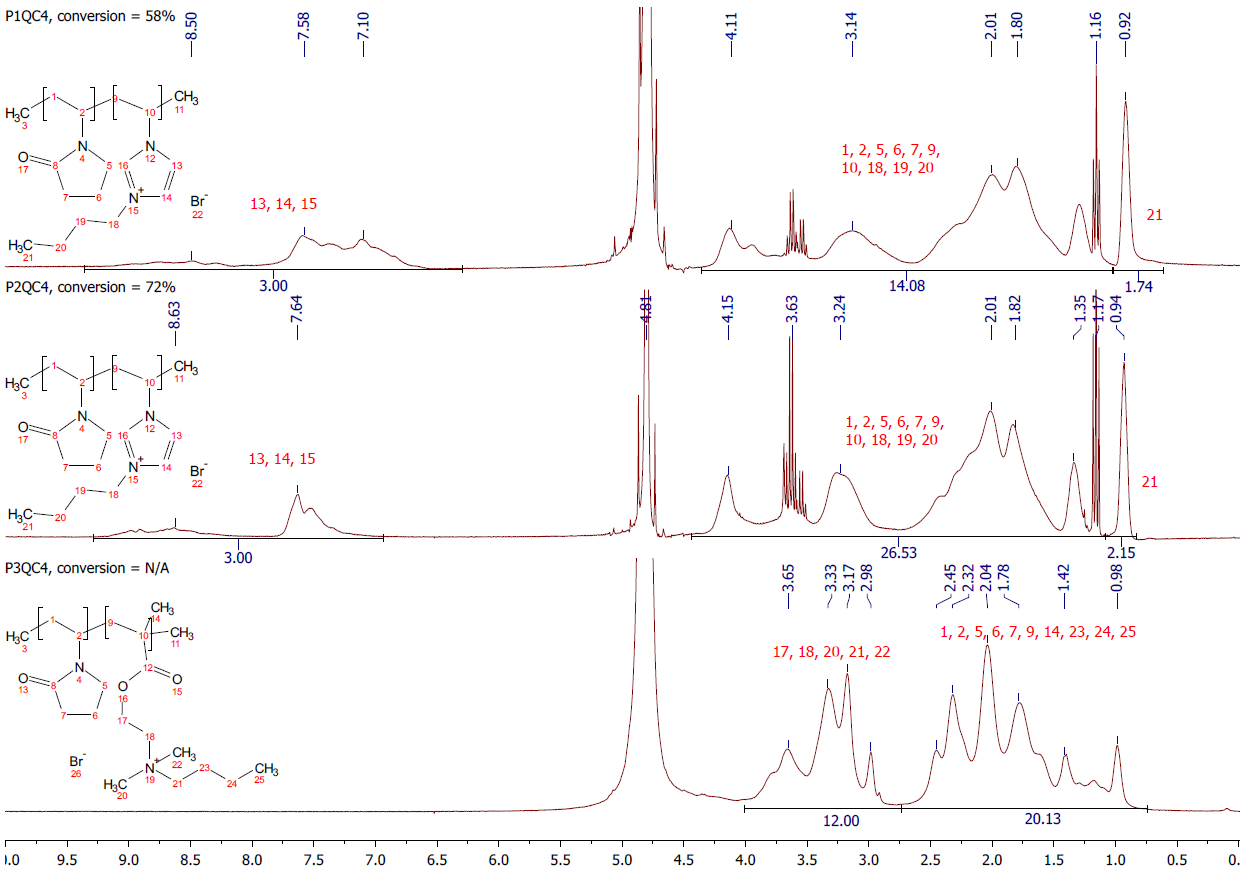

Figure 30 ^{1}H-NMR spectra of commercial polymers quaternized with 1-bromobutane and conversion of amine functionality.

It was not possible to estimate conversion for P3QC4 due to overlapping peaks in the ^{1}H-NMR spectra. However, the product was no longer soluble in $CDCl_3$, showing a drastic characteristic change for the polymer. For simplicity, full conversion was assumed for this reaction. The concentrations of the polymers used in the kill test, were based on the minimum inhibitory concentration (MIC) used by Zheng et al.[70] for the synthesized poly(ionic liquid) C4 (PIL C4). Since both MW and fraction of quaternized amines of the commercial polymers differed from that of PIL C4, compensation in polymer concentration were made. The amount of dissolved polymer were set to give an equal concentration of quaternary amines per ml with respect to the work of Zheng et al.[70] and the concentration is shown in **Figure 31**.

The procedure of the kill test involves the use of a bacterial solution of E. coli#84, which is added to a known volume and concentration of the dissolved polymers and exposure time was in this case set to 24 h. Bacterial growth is then visualized by sampling the liquid onto agar plates and incubated overnight. The samples were sent for bacteriological test at Coloplast and the results can be viewed in **Figure 31**.

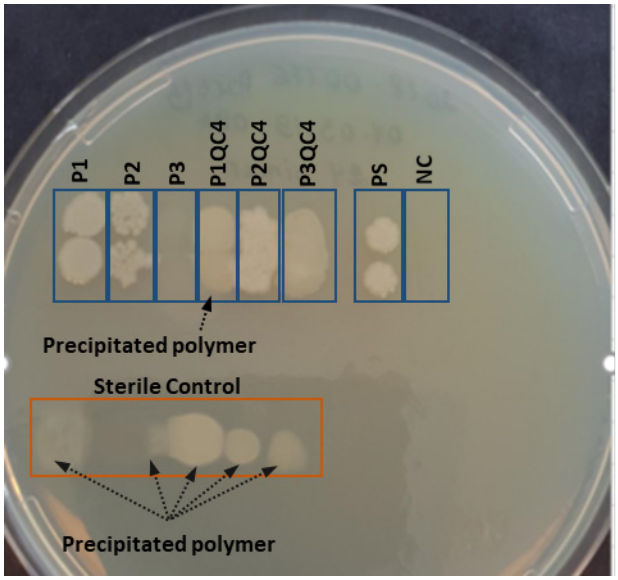

Polymers	Concentration [mg/ml]
P1, P1QC4	315
P2, P2QC4	249
P3, P3QC4	212

Figure 31 Bacteriological results of kill test of both commercial and quaternized polymers exposed to a 10^4 CFU/ml E. coli#84 solution for 24 h (left). Polymer precipitation could be seen on the agar and is indicated by dashed arrows. n = 2. The table shows the concentrations used for the different polymers for the kill test (right).

Antimicrobial activity was only seen for P1QC4 and for P3, which had no bacteria growing on the agar. The cloudy formation for P1QC4 was due to precipitation of the polymer and not bacterial growth. P2QC4 was not able to kill E. coli in solution despite achieving higher quaternization conversion than P1QC4. This might be attributed to an overall lower content of imidazole groups of almost 20% in the polymer composition, making for a lower charge density. Unexpectedly, P3QC4 had no effect against E. coli while P3 showed no sign of surviving bacteria. Although, certain studies have shown that tertiary amines have antibacterial properties[97–99], higher antimicrobial effect is usually seen for quaternary amine systems. The amines of DMAEMA are also able to be protonated and form positive charges depending on pH and along with the different amphiphilicity of the system, due to no carbon chain being present at the amine, could provide better interaction with the cell membrane and possibly explain the difference in antimicrobial activity. From the two antimicrobially active polymers, P1QC4 was chosen as the best suitable candidate for implementation in catheter coatings due to the high percentage of imidazole groups in the polymer composition.

One should consider that running the test in solution is significantly different compared to having the polymer anchored to a surface, as have also been shown by Zheng et al.[70]. This does therefore not give any conclusive results for antimicrobial activity as coatings for the polymer systems investigated. Applying the polymer as a coating could change the mode of action, charge density, mobility and ability to form aggregates, all of which are important parameters that could influence activity.

6.2. Implementation in Coating Formulations

In addition to having antimicrobial activity, catheter coatings should also be sufficiently bonded to the base material, have low surface friction and the ability to endure E-beam sterilization. To allow investigation of these parameters, an altered version of the previously described screening platform were developed by Lavik, H.[116]. The platform was initially made with the purpose of being able to find new

smooth coating formulations and therefore had to be designed to allow for friction measurements of the samples. The design of the two setups were fairly similar, although, an important difference for this system was the well dimension and shape. Here, a rectangular well with a length of 30 mm and a width of 14 mm were found to give the best reproducible results for friction measurements and thereby also producing the most consistent coating layer[116]. Based on this, an aluminum platform containing the optimized well dimensions was made and is illustrated in **Figure 32**.

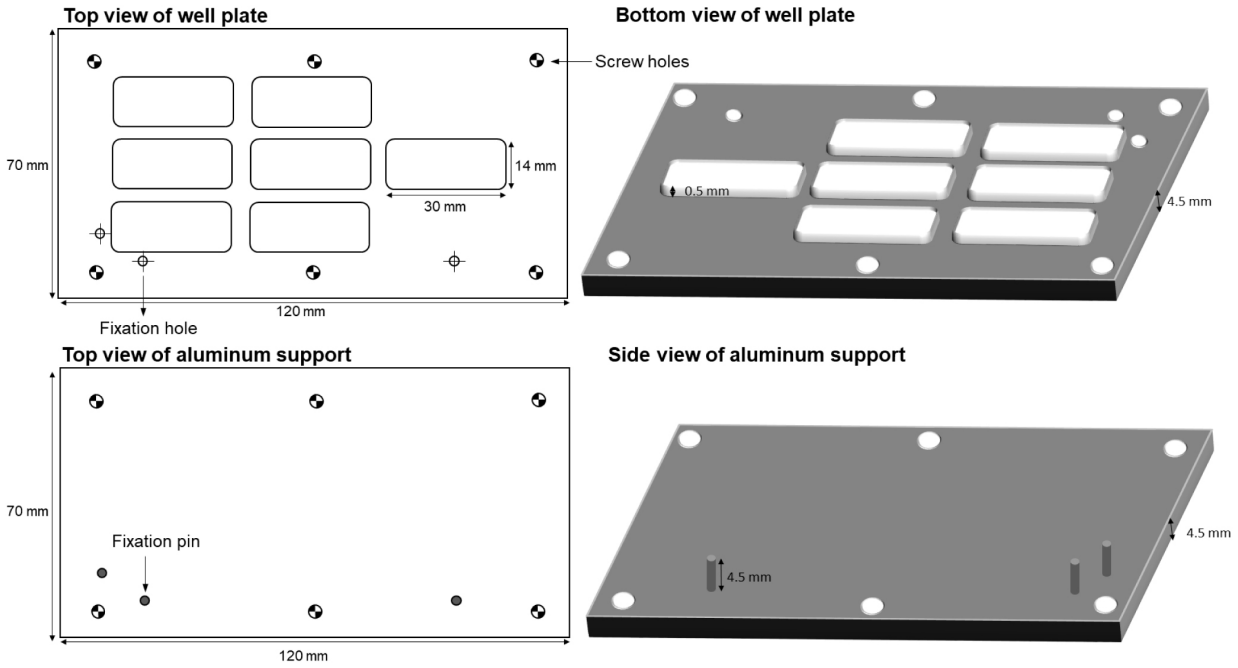

Figure 32 Schematic representation of screening platform used for testing of coating formulation, showing the well plate in both a top and bottom view (top) and the aluminum support shown as top and side view (bottom).

The setup was similarly divided into a well containing top plate and an aluminum support, which could be fitted with a polymer substrate in-between the two. The smaller plate size and use of larger screws (Ø = 5.5 mm) resulted in higher pressure onto the polymer substrate. This combined with having sharper metal rims around the wells at the bottom side of the top plate, made heat treatment unnecessary for proper sealing of the well edges. The larger sample size also allowed for antimicrobial testing using the ISO 22196 Test for Antimicrobial Activity of Plastics, which will be described later in this chapter.

The currently used formulation for catheter coatings contains a number of different components and among those are photoinitiator and PVP and uses EtOH as solvent. The catheters are normally plasma treated before applying the coating in a two-step dip coating procedure. First a pre-coating, which helps ensure binding to the PU substrate and a second coating layer is thereafter placed on top that gives a smooth low friction surface. The target for the implementation of antimicrobial properties therefore lies in the top coating, which is in direct contact with skin. Investigation of antimicrobial activity was done for a series of top coating formulations having 0, 5, 15 and 30 wt% of the PVP content replaced with P1QC4, where 0% corresponds to the reference catheter coating. Substituting PVP with P1QC4 rather than adding extra polymer keeps the solid content in the formulation constant and reduces the influence on other

additives in the mixture. The coatings were cured under UV-light and bacteriological testing was carried out using the ISO 22196 test.

6.3. ISO 22196 Test for Antimicrobial Activity of Plastics

This test method is specially designed to evaluate the antimicrobial properties of plastic surfaces. The sample preparation and procedure is fairly simple and again requires no advanced analysis tools or equipment to conduct. It does, however, require a relatively large surface area of the substrate to give reliable results. The method was therefore not suitable for high throughput screening using the platform first presented in this thesis, but were compatible with the larger surface area of the samples in the second platform developed. A schematic illustration of the procedure can be seen in **Figure 33**

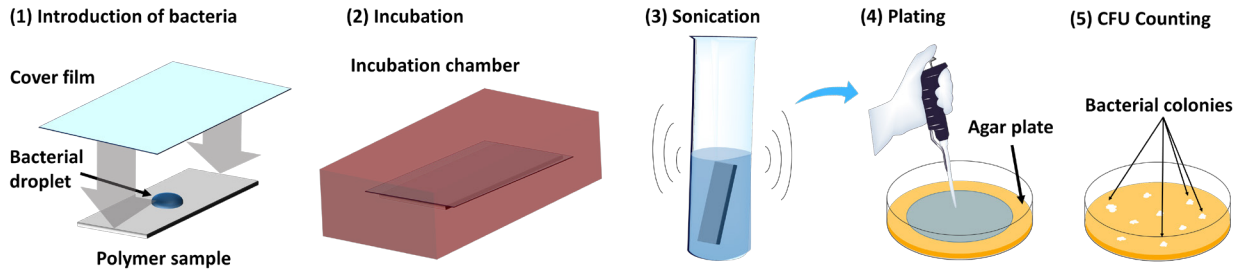

Figure 33 Schematic representation of the ISO 22196 test. (1) A bacterial droplet is placed on the polymer substrate and spread across the surface by the use of a plastic cover film. (2) Substrate is incubated at fixed temperature and humidity for a predetermined period. (3) The substrate is lightly rinsed before being transferred to a vial and sonicated. (4) Samples from the solution is then plated onto agar and incubated. (5) Counting of bacterial colonies to determine antimicrobial activity.

First, a droplet of bacterial solution is added on top of the polymer substrate and spread across the surface using a thin polymer film. The sample is then transferred to an incubation chamber with constant temperature and humidity for a preset exposure time. A brief gentle wash is done before immersing the sample in a vial with DI water and sonicated to release adhered bacteria. Sampling of the liquid is then plated onto agar and incubated to reveal bacterial colonies for CFU count. The P1QC4 coated samples was tested against E. coli#84 for a 24 h. exposure period. A total of six samples were made from each formulation were three of them were used to study the effect of E-beam sterilization and the results can be viewed in **Figure 34**.

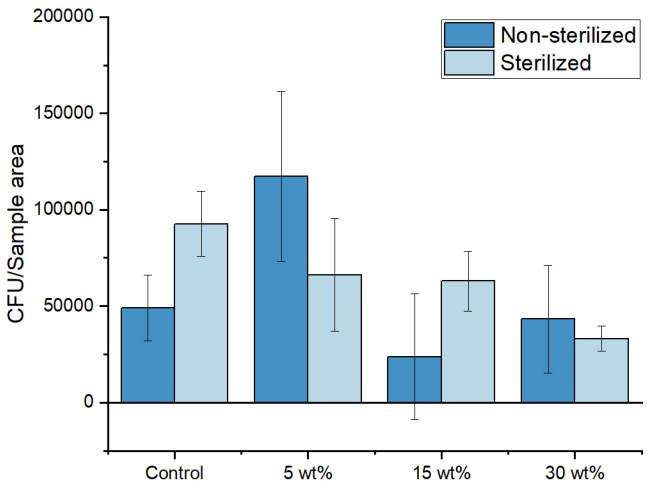

Figure 34 Antimicrobial activity of coated PU having 5, 15 and 30 wt% P1QC4 exposed to E. coli#84 for 24 h.

At 5 wt% both sterilized and non-sterilized samples had either higher or similar number of living bacteria attached to the surface compared to the reference coating (control). This could be explained by the coating having too low charge density to kill bacteria, due to low concentration of quaternized polymer. Since bacterial membranes are overall negatively charged the coating could act as a "magnet", attracting bacteria without the ability to promote cell death. However, a steady decrease in CFU count were observed when increasing the content of quaternized polymer and the coatings with 30 wt% showed the highest activity. Although, at 15 wt% (non-sterilized) a slightly lower bacteria count was seen but here the slightly large standard deviation should also be taken into account. The data also shows that E-beam sterilization did not affect the ability of the coating to express antimicrobial activity. For the PVP control a higher number of bacteria was found for the sterilized samples compared to non-sterilized. This may seem contradicting but prior results from Coloplast have shown the same trend for sterilization (data not shown) although no explanation could be given for this phenomenon.

A general issue regarding the coatings was layer thickness, which was much less compared to regular catheter coatings. Good binding of the coating originates from a combination of high MW polymers and correct amount of photoinitiator to crosslink chains and create a stable network, without having too high crosslinking density. This would otherwise reduce the ability of the coating to swell and absorb water and thereby increase surface friction. Incorporation of P1QC4 would theoretically require an increase in photoinitiator concentration to allow sufficient anchoring of the polymer in the network, due to the lower MW of the polymer. Binding ability of a coating formulation having 30 wt% P1QC4 was evaluated for a series of photoinitiator concentrations having 1, 1.5, 2.0 and 3.0 eq. relative to the original recipe. The resulting coatings were assessed on a qualitative basis with respect to rub-off, which determines how well the coating was attached to the surface on a scale from 0 – 5 with 0 showing no signs in loss of coating and 5 having no coating binding to the surface. Simultaneously, the smoothness of the coating was also assessed on a scale from 0 – 5 with 0 having high friction and 5 being a very smooth coating and the results can be viewed in **Table 4**.

Table 4 Qualitative rub-off and smoothness evaluation of coatings with 30 wt% P1QC4 with various concentration of photoinitiator.

Photoinitiator conc. [eq.]	Rub-off [0 – 5]	Smoothness [0 – 5]	Comments
1.0	3-4	1-2	Poor binding and smoothness
1.5	3	2	Relatively high rub-off and low smoothness
2.0	1	4	Good binding and smoothness
3.0	1	4	Good binding and smoothness

In accordance with the previous study, the current level of photoinitiator was inadequate to provide a coherent coating network on the PU surface, resulting in poor smoothness. With higher content of photoinitiator, improvement of these properties were seen for 1.5 eq. and when increased to 2.0 and 3.0 eq. showed excellent binding and low friction. The 2.0 and 3.0 eq. might be too high when considering crosslinking density and on recommendation from Coloplast supervisor Niels Jørgen Madsen, the 1.5 eq. was deemed as a more suitable adjustment for the photinitiator content, despite being inferior in the evaluation.

6.4. Application of Coatings on Catheters

Having shown that implementation of a quaternized polymer in catheter coatings lead to antimicrobial activity even after sterilization and that proper adjustment of photoinitiator content could be used to obtain acceptable properties with respect to binding and smoothness on a PU substrate, the next step was to apply these coatings to catheters. As an addition to this work, investigation of a second quaternized form of P1 was synthesized. Using formerly described procedure, alkylation with iodomethane was done to produce a one carbon chain on the amine imidazole group and is referred to in this text as P1QC1 (see **Chapter 9**). The extent of quaternization was not possible to determine by ^{1}H-NMR due to overlapping peaks (see **Figure 35**).

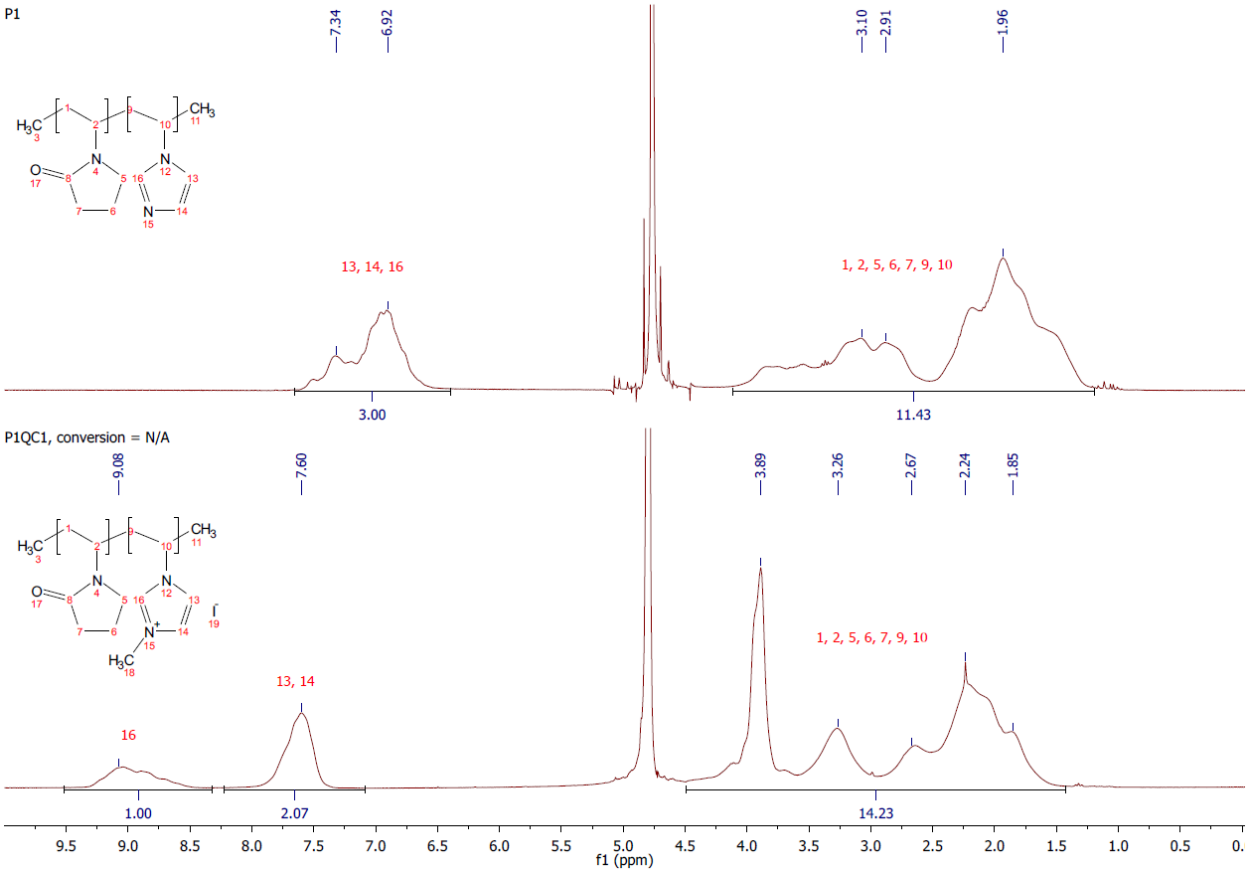

Figure 35 ^{1}H-NMR spectra of P1 (top) and iodomethane quaternized P1QC1 (bottom).

However, a clear shift of the imidazole protons of P1 from 6.92 and 7.34 ppm to 7.60 and 9.08 ppm for P1QC1 as a result of higher de-shielding originating from the positively charged amine, was observed. The solubility of the product also changed drastically, since the product precipitated during reaction in EtOH and only proved soluble in water, water/EtOH mixture or dimethyl sulfoxide (DMSO). Due to these changes in polymer properties full conversion was therefore assumed. Of both P1QC4 and P1QC1 a series of coating formulations having 15, 30 and 50 wt% of the quaternized polymer were applied onto urinary catheters at the test facilities of Coloplast. Due to the fact that P1QC1 was not soluble in pure EtOH, a mixture having 75 vol% EtOH (aq) was used as solvent.

Because of the replacement of the high MW PVP with the lower MW of P1, adjustment for the viscosity had to be made with respect to retraction speed during dip coating and UV dosage. Coatings containing P1QC4 provided in general good binding and very uniformly distributed coating layers. On the contrary, sufficient binding was more difficult to achieve when applying P1QC1 formulations. High rub-off was observed when using similar parameters as for P1QC4, which possibly originates from the presence of water and is a potential challenge when it comes to crosslinking PVP polymers. PVP is a very hydrophilic polymer and water is able to bind strongly to these types of systems, potentially blocking radical crosslinking processes during UV irradiation. In an attempt to remove the water, both increased drying time and UV dosage was investigated but still resulted in little to no binding of the polymer system to the catheter substrate. The P1QC1 formulations was therefore not included in any further studies.

Friction was analyzed by in-house instruments at Coloplast A/S and measured the friction force applied in both a forward and backward motion along the catheter and overall surface friction was given as an average of the two. The friction test was performed as a so called 0 min. test, meaning that catheters were directly measured after having been submerged in DI water for 10 min. The resulting friction of the catheters can be viewed in **Figure 36**.

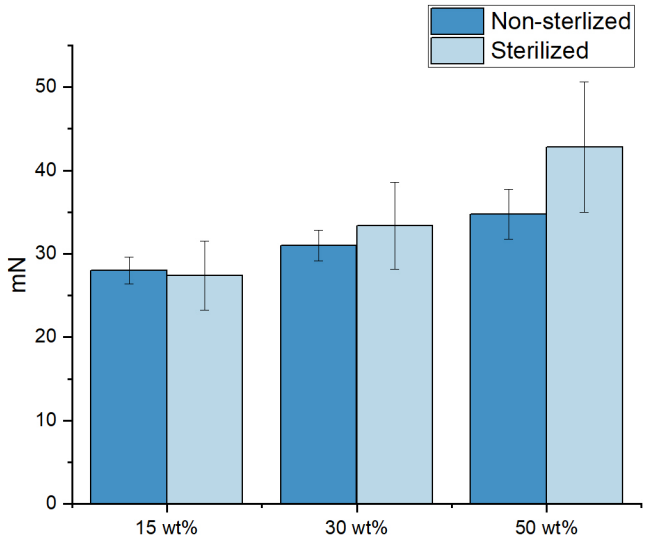

Figure 36 Friction measurement of urinary catheters coated with 15, 30 and 50 wt% P1QC4.

Friction was in general low around 27.4 – 42.8 mN with little difference between sterilized and non-sterilized samples. A slight tendency with increasing friction for higher content of P1QC4 was observed but was still acceptable according to industry standards. Along with uniform coating layers, P1QC4 provided excellent properties for production of smooth catheters.

Coated catheters were cut into samples of ca. 1 cm in length and evaluated for antimicrobial properties using the aforementioned ISO 22196 Test for Antimicrobial Activity of Plastics against E. coli#84 for a 24 h. incubation period. The activity of the catheters were compared to commercial SpeediCath catheters and the data is shown in **Figure 37** below.

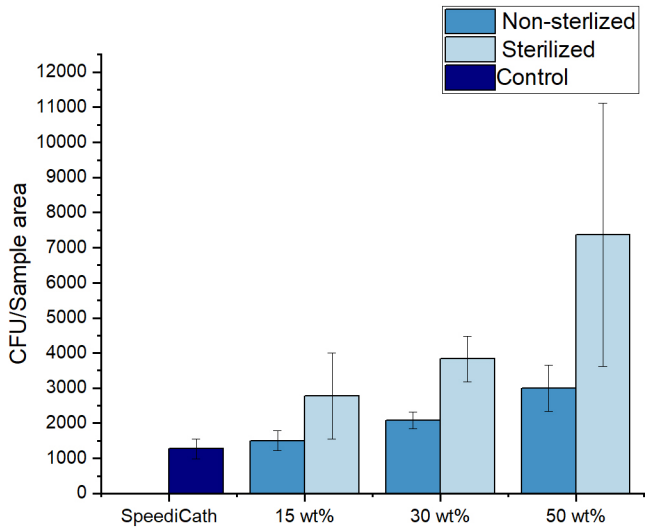

Figure 371 Antimicrobial activity of catheters coated with 15, 30, and 50 wt% P1QC4 against E. coli#84 for 24 h. incubation period.

It was surprisingly found that antimicrobial activity in this case was lower for catheters containing P1QC4 compared to SpeediCath. A steady rise in CFU count was observed for increasing content of the quaternized polymer and samples having underwent sterilization, further increased this number. This was contradicting to the general evidence found from previous investigations and no obvious difference could fully explain this phenomenon. The major difference between the test conducted here and in **Figure 34** was that catheter samples had a larger coating layer on the surface. A possible reason could be that the larger gel layers have a different network structure able to absorb more water and increase swelling. This would increase the distance between cationic charges as the network expands and thereby reduce the concentration of positive charges below the antibacterial threshold. The higher level of bacteria at 50 wt% P1QC4 can then be explained by having a less densely crosslinked network. This would possibly also be more hydrophilic providing a higher degree of swelling, which further increases distance between charges. As the data are only preliminary, further investigations are needed to confirm the lack antimicrobial effect.

6.5. Concluding Remarks

Commercially available polymers, which were post functionalized to have quaternary ammonium groups, were investigated for implementation in urinary catheter coatings. An initial selection of candidates were done based on bacteriological studies of the polymers in solution. Here P1QC4 showed best antimicrobial activity and was therefore chosen for further implementation in catheter coating formulations. A screening platform was used in the optimization of bonding and integration of the polymer in existing coating formulations and to evaluate the antimicrobial effect as well as the chemical stability towards E-beam sterilization. The coated PU samples showed good antimicrobial activity towards E. coli#84 with increasing activity towards higher content of P1QC4. This was the case for both sterilized and non-sterilized samples, proving that activity was retained during sterilization treatment. Application of P1QC4 formulations directly onto urinary catheters gave smooth coatings with low friction and was uniformly distributed along the material. Incorporation of P1QC1 was not possible due to having water as solvent, which blocked radical binding of the coating. Bacteriological studies surprisingly showed opposite tendencies compared to previous findings, having higher CFU count than that of commercially available SpeediCath catheters. Increasing content of P1QC4 increased the number of surviving cells found on the

samples. A possible explanation could be that the gels were more hydrophilic and able to achieve a higher degree of swelling and thereby lowering the positive charge density of the network and reduced its antimicrobial potential.

7. Conclusion

People relying on urinary catheters for voiding of their bladder are, despite repeated efforts, still experiencing an increased risk of contracting UTIs. Antimicrobial contact active quaternary ammonium surfaces have proven to be an effective method able to kill bacteria without the release of an active substance. This provides an alternative to existing release based catheter coatings, which are prone to development of resistant bacteria. However, incorporation of such a system into urinary catheter coatings requires a suitable tethering technique, amphiphilicity, charge density, mobility and chemical stability towards sterilization treatment to obtain the highest antimicrobial activity. Creating a hydrophilic contact active urinary catheter coating to prevent bacterial colonization was therefore the scope of this thesis.

Initially, the development of a screening platform able to conduct grafting onto PU catheter material was done to identify optimal reaction conditions for a series of acrylate and methacrylate based monomers. The platform was able to functionalize the PU substrate with both hydrophilic and hydrophobic monomers and showed that considerations with respect to monomer concentration and combinations of these, plays a vital role for the outcome of the polymerization. The modular design and choice of materials for the platform allowed the use of harsh chemicals, as well as withstanding elevated temperatures, needed for incorporation of the substrate and initiator. This also permitted the use of classical chemical analysis and characterization tools of the modified surface presenting itself as a versatile method for screening of surface modifications of PU substrates.

The platform was then further utilized for bacteriological evaluation of surface bound quaternary ammonium polymer systems to identify relevant antimicrobial candidates. Here, the choice of having a commercial PU proved to be problematic in relation to both Spot and ZOI assay. Process aids were found to be released from the substrate during the test and heavily influenced bacteriological data. In an attempt to circumvent this, thermal attachment of a layer of TPU-PI on top of the PU substrate managed to prevent the release of additives. Another concern regarding release, was the potential presence of residual unreacted monomer. Analysis from liquid extraction of samples having underwent E-beam sterilization proved to be able to eliminate such artifacts. Having TPU-PI as substrate caused, on the other hand, complications for bacteriological evaluation using the ZOI assay due to high hydrophilicity and swelling properties of the system, giving rise to false positive results. Other conventional bacteriological assays, such as live/dead staining and XTT, were similarly shown to be unsuitable in the combination with PU materials.
From this, PDMS was chosen as an alternative catheter material and was used as substrate in the development and investigation of a controlled SI-SARA-ATRP technique. In combination with the platform, the method allowed for grafting of exceptionally long DMAEMA brushes and the kinetic control could be used to vary the length of the polymer chains. A crystal violet assay was utilized for evaluation of the structure-property relationship between brush length and the choice of N-alkylation agent to obtain antimicrobial activity. It was shown that correct amphiphilicity, charge density and mobility was critical for obtaining the right conditions to induce bactericidal effect. Again the platform proved to be a versatile tool for investigating surface modifications of different polymer substrates and compatible with bacteriological assays to determine antimicrobial activity.

For the practical application of quaternary ammonium systems, pre-synthesized PVP-based quaternary ammonium polymers were applied in combination with urinary catheter coating formulations to obtain

hydrophilic antimicrobial surfaces. Initial data obtained from coatings conducted on flat surfaces, showed that addition of such polymer additive improved antimicrobial activity. The activity was further maintained for samples exposed to E-beam sterilization indicating good chemical stability. Applying the same formulation onto urinary catheters gave low friction surfaces as well as an evenly distributed coating layer and showed that quaternary ammonium polymers could be used in an industrial production line. Although, when evaluating their antimicrobial properties, the number of bacteria increased in contrast to previous results. Thicker coating layer, higher hydrophilicity and swelling capacity of the system may be responsible for lowering the charge density and thereby antimicrobial activity. To resolve this issue a better understanding of how quaternary ammonium systems function in highly hydrophilic environment is needed.

8. Outlook

The screening platform has demonstrated its versatile use for surface modification of various polymer substrates with a long range of monomer systems applied using different polymerization techniques. The platform thereby paves the way for a deeper investigation and understanding of important parameters for the antimicrobial activity of quaternary ammonium based polymer system with respect to charge density of cationic groups, grafting density, amphiphilicity through copolymerization and N-alkylation, architecture of polymer chains such as insertion of spacer segments and length of polymer chains etc. From this, general concepts of designing contact active antimicrobial surface could be obtained and help tailor-make optimal efficiency against desired pathogens.

In the interest of conducting high throughput screening of contact active antimicrobial surface modifications on PU substrates, further research is needed to find a bacteriological methodology that is compatible with the functional groups present in such materials. Furthermore, it also has to be reliable for the evaluation of the contact active mechanism and be able to distinguish it from release based antimicrobials, which is currently challenging. Since PU is inherently autofluorescent, methods applying colorimetric analysis directly on these surfaces should be avoided such as OD readings, live/dead staining and XTT assays. Sampling should therefore possibly be transferred and analyzed in separate containers to avoid interference from background noise.

Although, initial screening is good for finding relevant candidates, they often poorly represent the conditions experienced under clinical conditions. A way to optimize the screening to better evaluate its use in relation to a specific application, in this case urinary catheters, several adjustment to experiments run in the platform can be made.
In addition to the chemical stability of quaternary ammonium systems towards E-beam sterilization, another interesting study would be to look into the effect of physiological conditions such as pH and salt concentration. quaternary ammonium may be affected by the presence of salt that can coordinate to the positive charges and non-quaternized amines could be protonated at certain levels of pH, all of which may elicit an impact on antimicrobial effect. Friction of the surface is also important to assess under these conditions, since salts may precipitate and form an encrustation layer that would highly increase resistance of the surface.
Activity against a broad spectrum of gram positive and gram negative bacteria is also required by the coating if to be considered for use as urinary catheter coatings. Combinations of pathogens have been found for many cases of CAUTI and exposure to solutions of mixed bacterial species, should therefore also be assessed.
While the coatings have to be lethal for bacteria it should, on the other hand, not be harmful towards mammalian cells. The integrity and proliferation of relevant human cells should therefore be evaluated to determine the cytotoxicity of the materials.

By implementing the above recommendations and adjustments a more reliable evaluation in determining the applicability of the surface modifications for use in urinary catheter coatings should be obtained.

9. Experimental Section

Materials

Polyurethane (PU), benzophenone derivatized polyurethane (TPU-PI) and photoinitiator Irgacure 2959 was supplied by Coloplast A/S. Iodomethane (C1, 99%), 1-bromobutane (C4, 99%), 1-bromohexane (C6, 98%), 1-bromooctane (C8, 99%), 1-bromododecane (C12, 97%), 1-bromohexadecane (C16, 97%), 1-bromooctadecane (C18, ≥97%), N,N,N′,N′′,N′′-Pentamethyldiethylenetriamine (PMDETA, 99%), copper(II) chloride (99%), methanol (MeOH, ≥99.9), diethyl ether (Et_2O, ≥99.8%), dichloromethane (≥99.8%), (+)-sodium L-ascorbate (98%), 2-bromoethyl methyl ether, 2-bromo-2-methyl-propanoyl bromide (98%), 4-hydroxybenzophenone (98%) and trimethylamine (≥99.5%), Albumin–fluorescein isothiocyanate conjugate bovin (BSA), Acrylic acid (99%), methacrylic acid (MAA, 99%) poly(ethylene glycol) methyl ether methacrylate (MPEGMA 500, M_n = 500), di(ethylene glycol) methyl ether methacrylate (MDEGMA, 95%), N-isopropylacrylamide (NIPAAm, 97%), 2-(Dimethylamino)ethyl methacrylate (DMAEMA, 98%) and 2,2,2-Trifluoroethyl methacrylate (TrFEMA, 99%) were purchased from Sigma-Aldrich. Monomers were passed through a short plug-flow column containing aluminum oxide (Sigma-Aldrich, activated, basic, Brockmann I, standard grade) prior to use for polymerization. Magnesium sulfate was from Fischer Scientific, Ethanol (EtOH, 99.97%) and tetrahydrofuran (THF, ≥99%) from VWR, 1-vinylimidazole (VI, ≥98%) from TCI and polydimethylsiloxane Elastosil RT 625 A/B (PDMS) was from WACKER.

Characterization

Water contact angle measurements was conducted on a Dataphysics Contact Angle System OCA 20. Static contact angles were measured on a droplet of 4 µl Millipore water. X-ray photoelectron spectroscopy (XPS) was performed on a Thermo Fisher Scientific K Alpha (East Grinstead, UK) using monochromatized aluminum KR radiation in a 400 µm spot on the sample. Survey and high-resolution spectra were acquired and analyzed using the manufacturer's Avantage software package. Fluorescence intensity measurements and UV-vis spectroscopy was carried out on a POLARstar Omega from BMG Labtech, where fluorescence measurements were conducted using an excitation filter at 485 nm and an emission filter at 520 nm scanning across the surface in a matrix scan of 10x10. Differential scanning calorimetry (DSC) was performed on a DSCQ1000 from TA Instruments. The thermal analyses were performed at a heating and cooling rate of 10 K/min. The melting temperatures (T_m) are reported as the peak temperatures of the endothermic melting peaks. Glass transition temperatures (T_g) were measured at the inflection point. *One way analysis of variance (ANOVA)* was done in Minitab 18 using the Tukey method with a 95% confidence interval in order to calculate statistically significant differences between a set of obtained values. NMR characterization of polymers was performed on a 7 Tesla Spectrospin-Bruker AC 300 MHz spectrometer. Chemical shifts are given in ppm. Molecular weight and polydispersities were determined using Size Exclusion Chromatography (SEC). SEC was performed in THF on a Viscotek GPCmax autosampler equipped with a Viscotek TriSEC model 302 triple detector array (RI detector, viscometer detector and light scattering detectors measuring at 90° and 7°) and a Knauer K-2501 UV detector on two Polymer Laboratories PLgel MIXED-D columns. The samples were run at a flow rate of 1 ml min^{-1} at 35 °C and molecular weights were determined from a PS calibration.

Preparation of VI and DMAEMA modified PU

Preparation and pretreatment of setup

A PU plate was cut into suitable dimensions and washed with first ethanol and then acetone and left to dry for a few minutes. The PU substrate was then placed between the top and bottom plate and fixed with screws. The setup was heated at 155 °C for 15 min and the screws were tightened before increasing the temperature to 160 °C for another 60 min. The screws were tightened once more and the setup was left to cool to room temperature.

Embedding of photo initiator

To each well 80 µl of a 0.5 M stock solution of Irgacure 2959 in THF/MeOH (1:4, v:v) was added. The solution was left to evaporate overnight in the dark, resulting in solvent casting of the photo initiator in the polymer surface.

General procedure for polymer grafting

A stock solution of 1.0 M vinylimidazole (VI) in MeOH was made and 80 µl of this solution were added in to their respective wells. The plate was left under orbital shaking for 5 min at 200 rpm at 25 °C in a Hettich Benelux Cooling Thermomixer MKR 13. Thereafter the plate was exposed to UV-light (λ=365 nm, 10 mW/cm^2) for 30 min. at 25 °C under continued shaking at 200 rpm. Thereafter, the reaction mixture was removed, and wells were washed excessively with solvent (MeOH). In addition, all wells were refilled with pristine solvent mixture and left shaking at 200 rpm at RT for 15 min. The rinsing procedure was repeated with H_2O, where after the wells were filled with H_2O and shaken at 200 rpm at RT for 15 min to remove any residual solvents. The setup was left to dry in vacuum oven at RT overnight.

General procedure for quaternization

Quaternization of VI was done using 80 µl of a 1.5 M stock solution of the following alkyl halides in their respective solvents: iodomethane (MeOH), 1-bromobutane (MeOH), 1-bromohexane (MeOH), 1-bromooctane (MeOH), 1-bromododecane (Et_2O), 1-bromohexadecane (Et_2O) and 1-bromooctadecane (Et_2O). The platform was left under orbital shaking at 200 rpm at 40 °C for 30 min. Thereafter, the reaction mixture was removed, and wells were washed excessively with solvent (MeOH). In addition, all wells were refilled with pristine solvent mixture and left shaking at 200 rpm at RT for 15 min. The rinsing procedure was repeated with H_2O, where after the wells were filled with H_2O and shaken at 200 rpm at RT for 15 min to remove any residual solvents. The setup was left to dry in vacuum oven at RT overnight.

Sterilization of PU samples

The setup was placed in beaker containing 70 vol% EtOH (aq) and left for 20 min. After sterilization the setup was placed in a plastic container, which was wiped with EtOH prior to use, and dried in vacuum oven at RT overnight.

Preparation of VI and DMAEMA modified PU/TPU-PI

Preparation and pretreatment of setup

A PU plate was cut into suitable dimensions and washed with first ethanol and then acetone and left to dry for a few minutes. The PU substrate was then placed on a steel support with a piece of aluminum foil in between. The PU substrate was made flat by hot pressing at 150 °C for 15 min. Afterwards, a metal frame was placed on top of the PU and filled with granulates of TPU-PI. The TPU-PI was melt pressed onto the PU at 150 °C for ca. 25 min. forming the PU/TPU-PI substrate. The system was fitted with a well plate and fixed with screws. The setup was heated to 40 °C for 15 min. and the screws were tightened and left for another 15 min. before tightening the screws again.

General procedure for polymer grafting

A stock solution of 3.0 M VI in MeOH/H_2O (1:1, v:v) was made and 80 µl of this solution were added in to their respective wells. Thereafter the plate was exposed to UV-light (λ =365 nm, 10 mW/cm^2) for 30 min. at 25 °C under continued shaking at 200 rpm. The reaction mixture was removed and the wells were washed excessively with solvent (MeOH/H_2O (1:1, v:v)). Further washing was done in a similarly fashion described for “Preparation of VI and DMAEMA modified PU”. The setup was left to dry in vacuum oven at RT overnight.

General procedure for quaternization

Quaternization of VI was done using 80 µl of a 3 M stock solution of the following alkyl halides in their respective solvents: 1-bromobutane (EtOH), 1-bromooctane (Et_2O) and 1-bromohexadecane (Et_2O). The platform was left under orbital shaking at 200 rpm at 40 °C for 30 min. Thereafter, the reaction mixture was removed, and wells were washed excessively with solvent (EtOH). Further washing was done in a similarly fashion described for “Preparation of VI and DMAEMA modified PU”. The setup was left to dry in vacuum oven at RT overnight.

Sterilization for ZOI assay

Punched out samples were placed in beaker containing 70 vol% EtOH (aq) and left for 20 min. After sterilization the samples were placed in a sterile microtiter plate and dried in vacuum oven at RT overnight.

Synthesis of BPh SI-ATRP initiator

To a 50 ml round bottomed flask covered with aluminum foil, 4-hydroxybenzophenone (3.00 g, 0.0151 mol), triethylamine (2.40 mL, 0.0172 mol) and dichloromethane (9 ml) was added. The flask was placed in an ice bath under magnetic stirring and dropwise added a solution of 2-bromo-2-methyl-propanoyl bromide (2.10 mL, 0.0170 mol) in dichloromethane (6 ml). The flask was sealed with a septum and left to proceed overnight. The reaction was filtered to remove unwanted precipitate and the solution was extracted with 3 x 25 ml sat. $NaHCO_3$ (aq) and once with 25 ml water containing a few ml of brine. The organic phase was then dried with magnesium sulfate for 10 min. The solution was filtered into a 50 ml round bottomed flask and evaporated in vacuo. The flask was placed in vacuum oven at RT to dry overnight. The product was obtained as an off-white solid (m = 3.38 g, 64% yield). ^{1}H-NMR (300 MHz, $CDCl_3$) δ 7.80 (d, J = 8.6 Hz, 2H), 7.72 (d, J = 7.1 Hz, 2H), 7.52 (t, J = 7.4 Hz, 1H), 7.41 (t, J = 7.5 Hz, 2H), 7.19 (d, J = 8.6 Hz, 2H), 2.01 (s, 6H)

SI-SARA-ATRP on Silicon wafer

To a 40 ml vial 2.6 mg Cu(II)Cl_2, 8.14 ul PMDETA, 3.54 ml DMAEMA and 9.45 ml MeOH/H_2O (1:1, v:v) was added and mixed under magnetic stirring. A metal wire was fixed on a clamp, which was then fastened to the top of the 2-bromoisobutyrylbromide functionalized silicon wafer and transferred to the vial. The vial was sealed with a septum and evacuated and filled with nitrogen three times. In a separate 4 ml vial 9.45 mg of Na_2SO_3 was dissolved in 1 ml H_2O and then added 1 ml MeOH and transferred to the reaction vial via a nitrogen filled syringe to initiate polymerization. The total volume used was 15 ml with a final concentration of Cu(II)Cl_2:1.3 mM, PMDETA: 2.6 mM, Na_2SO_3: 5 mM and DMAEMA: 1.4 M. Sampling of different reaction times to obtain various DMAEMA brush lengths, was controlled by the depth of the wafer in the reaction mixture. After reaction the wafer was briefly washed in pristine solvent (MeOH/H_2O), water and EtOH.

SI-SARA-ATRP on PDMS

Preparation and pretreatment of setup

PDMS films of Elastosil RT 625 were prepared by mixing 12 g part A with 1.33 g part B. The reagents were mixed by speedmixer at 2700 rpm for 3 min. The mixture was poured into a steel support fitted with an aluminum frame and then placed in an oven at 100 °C for 60 min. After curing the setup was left to cool to RT.

Attachment of Initiator

A 10 mg/ml solution in THF/MeOH (1:4, v:v) of the BPh SI-ATRP initiator (synthesized in “Synthesis of BPh SI-ATRP initiator”) was spread across the PDMS surface (ca. 12 ml). The setup was agitated at 200 rpm while exposed to UV-light (λ =365 nm, 10 mW/cm^2) for 30 min. at 25 °C. The surface was then washed with MeOH while agitated at 200 rpm at RT for 15 min. followed by rinsing with MeOH, water and EtOH before being dried under air flow. The metal frame was removed and high standing edges of the PDMS film was removed using a scalpel. The setup was then fitted with a well plate and fixed with screws.

General procedure for SI-SARA-ATRP

To each well was added 40 µl of a 2.8 M DMAEMA in MeOH/H_2O (1:1, v:v), 20 µl solvent (MeOH/H_2O (1:1, v:v)), 10 µl 10.4 mM Cu(II)Cl_2/20.8 mM PMDETA in MeOH/H_2O (1:1, v:v). To initiate polymerization 10 µl of 40 mM Na_2SO_3 in MeOH/H_2O (1:1, v:v) was added. The platform was left under orbital shaking at 200 rpm at 24 °C for a predetermined reaction time. Different brush lengths of DMAEMA was achieved through removal of reaction mixture of the wells at predetermined times and replaced with solvent (MeOH/H_2O (1:1, v:v)). After end polymerization the well were emptied and the wells were washed excessively with solvent (MeOH/H2O (1:1, v:v)). In addition, all wells were refilled with pristine solvent mixture and left shaking at 200 rpm at RT for 15 min. The rinsing procedure was repeated with H_2O, where after the wells were filled with H_2O and shaken at 200 rpm at RT for 15 min to remove any residual solvents. The setup was left to dry in vacuum oven at RT overnight.

General procedure for quaternization of DMAEMA brushes

Quaternization of DMAEMA was done using 80 µl of a 3 M stock solution of the following alkyl halides in their respective solvents: iodomethane (MeOH), 1-bromobutane (MeOH), 1-bromooctane (Et_2O), 1-bromodecane (Et_2O) and 2-bromoethyl methyl ether (MeOH). The platform was covered with parafilm to avoid evaporation and left under orbital shaking at 200 rpm at 40 °C overnight. Thereafter, the reaction mixture was removed, and wells were washed excessively with solvent (MeOH). In addition, all wells were refilled with pristine solvent mixture and left shaking at 200 rpm at RT for 15 min. The rinsing procedure was repeated with H_2O, where after the wells were filled with H_2O and shaken at 200 rpm at RT for 15 min to remove any residual solvents. The setup was left to dry in vacuum oven at RT overnight.

Synthesis of P1QC1

Polymer P1 (80.0 g) and EtOH (300.0 ml) was a added to a 1000 ml round bottomed flask and stirred with a magnetic stir bar at 45 °C until the polymer was dissolved. Iodomethane (35.0 ml) was then added slowly to the mixture and the setup was fitted with a condenser and heated to 60 °C and left under magnetic stirring for 3 days. The reaction was stopped by letting the mixture cool. The supernatant was decanted off and the polymer was dissolved in water (150 ml) while heating the mixture to 60 °C. The mixture was then cooled and subsequently precipitated in a beaker in acetone (ca. 2000 ml). The beaker was left in the freezer for ca. 15 min. to allow full precipitation. The liquid was decanted off and the product was washed with acetone thrice (ca. 150 ml) and dried in vacuum oven at RT for 2 days. The product was obtained as a yellow solid (111.60 g, 81% yield). ^{1}H-NMR (δ, ppm, 300 MHz, D_2O): 9.06 (br s, 1H), 7.60 (br s, 2.07 H), 2.95 (br m, 14.23 H).

Synthesis of P1QC4

Polymer P1 (0.500 g) and EtOH (9.0 ml) was added to a 25 ml round bottomed flask and stirred with a magnetic stir bar at 45 °C until the polymer was dissolved. 1-bromobutane (0.361 ml, 3.35 mmol) was then added to the mixture and the setup was fitted with a condenser and heated to 60 °C for 3 days. The reaction was stopped by letting the mixture cool and most of the solvent was removed by evaporation in vacuo. The mixture was then precipitated in diethyl ether (ca. 150 ml). The beaker was left in freezer for ca. 15 min. to allow full precipitation. The solvent was decanted off and the product was dried in vacuum

oven at RT for 3 days. The product was obtained as an off white solid (0.420 g, 49% yield). ^{1}H-NMR (δ, ppm, 300 MHz, D_2O): 7.82 (br m, 3.00 H), 2.70 (br m, 14.08 H), 0.92 (s, 1.74 H).

Synthesis of P2QC4

Polymer P2QC4 was synthesized in accordance with the procedure of "**Synthesis of P1QC4"** in which P2 (0.500 g), EtOH (2.0 ml), 1-bromobutane (0.223 ml, 2.07 mmol) were used. Off-white solid (0.452 g, 63% yield). ^{1}H-NMR (δ, ppm, 300 MHz, D_2O): 8.12 (br m, 3 H), 2.93 (br m, 26.53 H), 0.94 (s, 2.15 H)

Synthesis of P3QC4

Polymer P3QC4 was synthesized in accordance with the procedure of "**Synthesis of P1QC4"** in which P3 (0.500 g), Acetonitrile (4.0 ml), 1-bromobutane (0.0991 ml, 0.918 mmol) were used. White solid (0.506 g, 85% yield). ^{1}H-NMR (δ, ppm, 300 MHz, D_2O): 3.38 (m, 12.00 H), 1.73 (m, 20.13 H).

10. References

1. Kirdis H. Development of novel methods for microbiological evaluation of urology products. 2011.

2. Fisher LE, Hook AL, Ashraf W, et al. Biomaterial modification of urinary catheters with antimicrobials to give long-term broadspectrum antibiofilm activity. *J Control Release*. 2015;202:57-64. doi:10.1016/j.jconrel.2015.01.037

3. Warren JW. Catheter-associated urinary tract infections. *Int J Antimicrob Agents*. 2001;17(4):299-303. doi:10.1016/S0924-8579(00)00359-9

4. Pickard R, Lam T, MacLennan G, et al. Antimicrobial catheters for reduction of symptomatic urinary tract infection in adults requiring short-term catheterisation in hospital: A multicentre randomised controlled trial. *Lancet*. 2012;380(9857):1927-1935. doi:10.1016/S0140-6736(12)61380-4

5. Nicolle LE. Urinary Catheter-Associated Infections. *Infect Dis Clin NA*. 2012;26(1):13-27. doi:10.1016/j.idc.2011.09.009

6. Cardenas DD, Hooton TM. Urinary tract infection in persons with spinal cord injury. *Arch Phys Med Rehabil*. 1995;76(3):272-280. doi:10.1016/S0003-9993(95)80615-6

7. Burrows LL, Khoury AE. Issues surrounding the prevention and management of device-related infections. *World J Urol*. 1999;17(6):402-409. doi:10.1007/s003450050166

8. Gupta P, Sarkar S, Das B, Bhattacharjee S, Tribedi P. Biofilm, pathogenesis and prevention—a journey to break the wall: a review. *Arch Microbiol*. 2016;198(1):1-15. doi:10.1007/s00203-015-1148-6

9. Stocker R. Reverse and flick: Hybrid locomotion in bacteria. *Proc Natl Acad Sci U S A*. 2011;108(7):2635-2636. doi:10.1073/pnas.1019199108

10. Manson MD, Armitage JP, Hoch JA, Macnab RM. Bacterial locomotion and signal transduction. *J Bacteriol*. 1998;180(5):1009-1022.

11. Garrett TR, Bhakoo M, Zhang Z. Bacterial adhesion and biofilms on surfaces. *Prog Nat Sci*. 2008;18(9):1049-1056. doi:10.1016/j.pnsc.2008.04.001

12. Kumar CG, Anand SK. Significance of microbial biofilms in food industry: A review. *Int J Food Microbiol*. 1998;42(1-2):9-27. doi:10.1016/S0168-1605(98)00060-9

13. Davies DG, Parsek MR, Pearson JP, Iglewski BH, Costerton JW, Greenberg EP. The involvement of cell-to-cell signals in the development of a bacterial biofilm. *Science (80-)*. 1998;280(5361):295-298. doi:10.1126/science.280.5361.295

14. Bjarnsholt T. Introduction to biofilms. *Biofilm Infect*. 2011;11:1-9. doi:10.1007/978-1-

4419-6084-9_1

15. Klausen M, Aaes-Jørgensen A, Molin S, Tolker-Nielsen T. Involvement of bacterial migration in the development of complex multicellular structures in Pseudomonas aeruginosa biofilms. *Mol Microbiol*. 2003;50(1):61-68. doi:10.1046/j.1365-2958.2003.03677.x

16. Kostakioti M, Hadjifrangiskou M, Hultgren SJ. Bacterial biofilms: Development, dispersal, and therapeutic strategies in the dawn of the postantibiotic era. *Cold Spring Harb Perspect Med*. 2013;3(4):1-23. doi:10.1101/cshperspect.a010306

17. Watnick P, Kolter R. Biofilm, city of microbes. *J Bacteriol*. 2000;182(10):2675-2679. doi:10.1128/JB.182.10.2675-2679.2000

18. Leid JG. Bacterial biofilms resist key host defenses. *Microbe*. 2009;4(2):66-70.

19. Hadjesfandiari N, Yu K, Mei Y, Kizhakkedathu JN. Polymer brush-based approaches for the development of infection-resistant surfaces. *J Mater Chem B*. 2014;2(31):4968-4978. doi:10.1039/c4tb00550c

20. Tambe SM, Sampath L, Modak SM. In vitro evaluation of the risk of developing bacterial resistance to antiseptics and antibiotics used in medical devices. *J Antimicrob Chemother*. 2001;47(5):589-598. doi:10.1093/jac/47.5.589

21. Hetrick EM, Schoenfisch MH. Reducing implant-related infections: active release strategies. *Chem Soc Rev*. 2006;35:780-789. doi:10.1039/b515219b

22. Falsetta ML, Klein MI, Colonne PM, et al. Symbiotic relationship between Streptococcus mutans and Candida albicans synergizes virulence of plaque biofilms in vivo. *Infect Immun*. 2014;82(5):1968-1981. doi:10.1128/IAI.00087-14

23. López D, Vlamakis H, Kolter R. Biofilms. *Cold Spring Harb Perspect Biol*. 2010;2(7):1-12. doi:10.1101/cshperspect.a000398

24. Saha S, Nayak S, Bhattacharyya I, et al. Understanding the patterns of antibiotic susceptibility of bacteria causing urinary tract infection in West Bengal, India. *Front Microbiol*. 2014;5(SEP):1-7. doi:10.3389/fmicb.2014.00463

25. Podschun R, Ullmann U. Klebsiella spp. as Nosocomial Pathogens: Epidemiology, Taxonomy, Typing Methods, and Pathogenicity Factors. *Am Soc Microbiol*. 1998;11(4):589-603. doi:10.1128/CMR.11.4.589

26. Edokpolo L, Stavris K, Foster H. Intermittent catheterization and recurrent urinary tract infection in spinal cord injury. *Top Spinal Cord Inj Rehabil*. 2012;18(2):187-192. doi:10.1310/sci1802-187

27. Schierholz JM, Steinhauser H, Rump AFE, Berkels R, Pulverer G. Controlled release of antibiotics from biomedical polyurethanes: Morphological and structural features.

Biomaterials. 1997;18(12):839-844. doi:10.1016/S0142-9612(96)00199-8

28. Johnson JR, Johnston BD, Kuskowski MA, Pitout J. In vitro activity of available antimicrobial coated foley catheters against escherichia coli, including strains resistant to extended spectrum cephalosporins. *J Urol*. 2010;184(6):2572-2577. doi:10.1016/j.juro.2010.07.032

29. Singha P, Locklin J, Handa H. A review of the recent advances in antimicrobial coatings for urinary catheters. *Acta Biomater*. 2017;50:20-40. doi:10.1016/j.actbio.2016.11.070

30. Crabtree JH, Burchette RJ, Siddiqi RA, Huen IT, Hadnott LL, Fishman A. The efficacy of silver-ion implanted catheters in reducing peritoneal dialysis-related infections. *Perit Dial Int*. 2003;23(4):368-374.

31. Samuel U, Guggenbichler JP. Prevention of catheter-related infections: The potential of a new nano-silver impregnated catheter. *Int J Antimicrob Agents*. 2004;23(SUPPL. 1):75-78. doi:10.1016/j.ijantimicag.2003.12.004

32. Srinivasan A, Karchmer T, Richards A, Song X, Perl TM. A Prospective Trial of a Novel, Silicone-Based, Silver-Coated Foley Catheter for the Prevention of Nosocomial Urinary Tract Infections. *Infect Control Hosp Epidemiol*. 2006;27(1):38-43. doi:10.1086/499998

33. Brar SK, Verma M, Tyagi RD, Surampalli RY. Engineered nanoparticles in wastewater and wastewater sludge - Evidence and impacts. *Waste Manag*. 2010;30(3):504-520. doi:10.1016/j.wasman.2009.10.012

34. Hirota K, Murakami K, Nemoto K, Miyake Y. Coating of a surface with 2-methacryloyloxyethyl phosphorylcholine (MPC) co-polymer significantly reduces retention of human pathogenic microorganisms. *FEMS Microbiol Lett*. 2005;248(1):37-45. doi:10.1016/j.femsle.2005.05.019

35. Dong B, Manolache S, Wong ACL, Denes FS. Antifouling ability of polyethylene glycol of different molecular weights grafted onto polyester surfaces by cold plasma. *Polym Bull*. 2011;66(4):517-528. doi:10.1007/s00289-010-0358-y

36. Chang Y, Shih YJ, Ko CY, Jhong JF, Liu YL, Wei TC. Hemocompatibility of poly(vinylidene fluoride) membrane grafted with network-like and brush-like antifouling layer controlled via plasma-induced surface pegylation. *Langmuir*. 2011;27(9):5445-5455. doi:10.1021/la1048369

37. Li Q, Bi QY, Zhou B, Wang XL. Zwitterionic sulfobetaine-grafted poly(vinylidene fluoride) membrane surface with stably anti-protein-fouling performance via a two-step surface polymerization. *Appl Surf Sci*. 2012;258(10):4707-4717. doi:10.1016/j.apsusc.2012.01.064

38. Yue WW, Li HJ, Xiang T, Qin H, Sun SD, Zhao CS. Grafting of zwitterion from polysulfone membrane via surface-initiated ATRP with enhanced antifouling property and biocompatibility. *J Memb Sci*. 2013;446:79-91. doi:10.1016/j.memsci.2013.06.029

39. Li M, Neoh KG, Xu LQ, et al. Surface modification of silicone for biomedical applications requiring long-term antibacterial, antifouling, and hemocompatible properties. *Langmuir*. 2012;28(47):16408-16422. doi:10.1021/la303438t

40. Chen H, Brook MA, Chen Y, Sheardown H. Surface properties of PEO-silicone composites: Reducing protein adsorption. *J Biomater Sci Polym Ed*. 2005;16(4):531-548. doi:10.1163/1568562053700183

41. Tugulu T, Klok HA. Surface modification of polydimethylsiloxane substrates with nonfouling poly(poly(ethylene glycol)methacrylate) brushes. *Macromol Symp*. 2009;279(1):103-109. doi:10.1002/masy.200950516

42. Keefe AJ, Brault ND, Jiang S. Suppressing surface reconstruction of superhydrophobic PDMS using a superhydrophilic zwitterionic polymer. *Biomacromolecules*. 2012;13(5):1683-1687. doi:10.1021/bm300399s

43. Diaz Blanco C, Ortner A, Dimitrov R, Navarro A, Mendoza E, Tzanov T. Building an antifouling zwitterionic coating on urinary catheters using an enzymatically triggered bottom-up approach. *ACS Appl Mater Interfaces*. 2014;6(14):11385-11393. doi:10.1021/am501961b

44. Venkateswaran S, Wu M, Gwynne PJ, et al. Bacteria repelling poly(methylmethacrylate-co-dimethylacrylamide) coatings for biomedical devices. *J Mater Chem B*. 2014;2(39):6723-6729. doi:10.1039/c4tb01129e

45. Smith RS, Zhang Z, Bouchard M, et al. Vascular Catheters with a Nonleaching Poly-Sulfobetaine Surface Modification Reduce Thrombus Formation and Microbial Attachment. *Sci Transl Med*. 2012;4(153). doi:10.1126/scitranslmed.3004120

46. Yu K, Lo JCY, Yan M, et al. Anti-adhesive antimicrobial peptide coating prevents catheter associated infection in a mouse urinary infection model. *Biomaterials*. 2017;116:69-81. doi:10.1016/j.biomaterials.2016.11.047

47. Zheng J, Li L, Tsao HK, Sheng YJ, Chen S, Jiang S. Strong repulsive forces between protein and oligo (ethylene glycol) self-assembled monolayers: A molecular simulation study. *Biophys J*. 2005;89(1):158-166. doi:10.1529/biophysj.105.059428

48. Chen S, Li L, Zhao C, Zheng J. Surface hydration: Principles and applications toward low-fouling/nonfouling biomaterials. *Polymer (Guildf)*. 2010;51(23):5283-5293. doi:10.1016/j.polymer.2010.08.022

49. Chen S, Yu F, Yu Q, He Y, Jiang S. Strong resistance of a thin crystalline layer of balanced charged groups to protein adsorption. *Langmuir*. 2006;22(19):8186-8191. doi:10.1021/la061012m

50. Hutanu D. Recent Applications of Polyethylene Glycols (PEGs) and PEG Derivatives. *Mod Chem Appl*. 2014;02(02):2-7. doi:10.4172/2329-6798.1000132

51. Zhu Z, Wang Z, Li S, Yuan X. Antimicrobial strategies for urinary catheters. *J Biomed Mater Res - Part A*. 2019;107(2):445-467. doi:10.1002/jbm.a.36561

52. Kuo PL, Chuang TF, Wang HL. Surface-fragmenting, self-polishing, tin-free antifouling coatings. *J Coatings Technol*. 1999;71(893):77-83. doi:10.1007/bf02697909

53. Petersen S, Gattermayer M, Biesalski M. *Bioactive Surfaces*. Vol 240. (Börner HG, Lutz J-F, eds.).; 2010. doi:10.1007/12_2010_77

54. Timofeeva L, Kleshcheva N. Antimicrobial polymers: Mechanism of action, factors of activity, and applications. *Appl Microbiol Biotechnol*. 2011;89(3):475-492. doi:10.1007/s00253-010-2920-9

55. Bieser AM, Tiller JC. Mechanistic Considerations on Contact-Active Antimicrobial Surfaces with Controlled Functional Group Densities. *Macromol Biosci*. 2011;11(4):526-534. doi:10.1002/mabi.201000398

56. Lewis K, Klibanov AM. Surpassing nature: Rational design of sterile-surface materials. *Trends Biotechnol*. 2005;23(7):343-348. doi:10.1016/j.tibtech.2005.05.004

57. Gao J, White EM, Liu Q, Locklin J. Evidence for the Phospholipid Sponge Effect as the Biocidal Mechanism in Surface-Bound Polyquaternary Ammonium Coatings with Variable Cross-Linking Density. *ACS Appl Mater Interfaces*. 2017;9(8):7745-7751. doi:10.1021/acsami.6b14940

58. Chen A, Peng H, Blakey I, Whittaker AK. Biocidal Polymers: A Mechanistic Overview. *Polym Rev*. 2017;57(2):276-310. doi:10.1080/15583724.2016.1223131

59. Ferreira L, Zumbuehl A. Non-leaching surfaces capable of killing microorganisms on contact. *J Mater Chem*. 2009;19(42):7796-7806. doi:10.1039/b905668h

60. Abel T, Cohen JLI, Engel R, Filshtinskaya M, Melkonian A, Melkonian K. Preparation and investigation of antibacterial carbohydrate-based surfaces. *Carbohydr Res*. 2002;337(24):2495-2499. doi:10.1016/S0008-6215(02)00316-6

61. Lee SB, Koepsel RR, Morley SW, Matyjaszewski K, Sun Y, Russell AJ. Permanent, nonleaching antibacterial surfaces, 1. Synthesis by atom transfer radical polymerization. *Biomacromolecules*. 2004;5(3):877-882. doi:10.1021/bm034352k

62. Roy D, Knapp JS, Guthrie JT, Perrier S. Antibacterial cellulose fiber via RAFT surface graft polymerization. *Biomacromolecules*. 2008;9(1):91-99. doi:10.1021/bm700849j

63. Huang J, Murata H, Koepsel RR, Russell AJ, Matyjaszewski K. Antibacterial polypropylene via surface-initiated atom transfer radical polymerization. *Biomacromolecules*. 2007;8(5):1396-1399. doi:10.1021/bm061236j

64. Yao F, Fu GD, Zhao J, Kang ET, Neoh KG. Antibacterial effect of surface-functionalized polypropylene hollow fiber membrane from surface-initiated atom transfer radical

polymerization. *J Memb Sci*. 2008;319(1-2):149-157. doi:10.1016/j.memsci.2008.03.049

65. Cen L, Neoh KG, Kang ET. Surface Functionalization Technique for Conferring Antibacterial Properties to Polymeric and Cellulosic Surfaces. *Langmuir*. 2003;19(24):10295-10303. doi:10.1021/la035104c

66. Fadida T, Kroupitski Y, Peiper UM, Bendikov T, Sela Saldinger S, Poverenov E. Air-ozonolysis to generate contact active antimicrobial surfaces: Activation of polyethylene and polystyrene followed by covalent graft of quaternary ammonium salts. *Colloids Surfaces B Biointerfaces*. 2014;122:294-300. doi:10.1016/j.colsurfb.2014.07.003

67. Tiller JC, Lee SB, Lewis K, Klibanov AM. Polymer surfaces derivatized with poly(vinyl-N-hexylpyridinium) kill airborne and waterborne bacteria. *Biotechnol Bioeng*. 2002;79(4):465-471. doi:10.1002/bit.10299

68. Meléndez-Ortiz HI, Alvarez-Lorenzo C, Concheiro A, Jiménez-Páez VM, Bucio E. Modification of medical grade PVC with N-vinylimidazole to obtain bactericidal surface. *Radiat Phys Chem*. 2016;119:37-43. doi:10.1016/j.radphyschem.2015.09.014

69. Villanueva ME, González JA, Rodríguez-Castellón E, Teves S, Copello GJ. Antimicrobial surface functionalization of PVC by a guanidine based antimicrobial polymer. *Mater Sci Eng C*. 2016;67:214-220. doi:10.1016/j.msec.2016.05.052

70. Zheng Z, Xu Q, Guo J, et al. Structure-Antibacterial Activity Relationships of Imidazolium-Type Ionic Liquid Monomers, Poly(ionic liquids) and Poly(ionic liquid) Membranes: Effect of Alkyl Chain Length and Cations. *ACS Appl Mater Interfaces*. 2016;8(20):12684-12692. doi:10.1021/acsami.6b03391

71. Sui Y, Gao X, Wang Z, Gao C. Antifouling and antibacterial improvement of surface-functionalized poly(vinylidene fluoride) membrane prepared via dihydroxyphenylalanine-initiated atom transfer radical graft polymerizations. *J Memb Sci*. 2012;394-395:107-119. doi:10.1016/j.memsci.2011.12.038

72. Hilal N, Kochkodan V, Al-Khatib L, Levadna T. Surface modified polymeric membranes to reduce (bio)fouling: A microbiological study using E. coli. *Desalination*. 2004;167(1-3):293-300. doi:10.1016/j.desal.2004.06.138

73. Yang C, Ding X, Ono RJ, et al. Brush-Like Polycarbonates Containing Dopamine, Cations, and PEG Providing a Broad-Spectrum, Antibacterial, and Antifouling Surface via One-Step Coating. *Adv Mater*. 2014;26(43):7346-7351. doi:10.1002/adma.201402059

74. Wang B, Ye Z, Tang Y, et al. Fabrication of nonfouling, bactericidal, and bacteria corpse release multifunctional surface through surface-initiated RAFT polymerization. *Int J Nanomedicine*. 2017;12:111-125. doi:10.2147/IJN.S107472

75. Wang B, Xu Q, Ye Z, et al. Copolymer Brushes with Temperature-Triggered, Reversibly Switchable Bactericidal and Antifouling Properties for Biomaterial Surfaces. *ACS Appl Mater Interfaces*. 2016;8(40):27207-27217. doi:10.1021/acsami.6b08893

76. Wang C, Zolotarskaya O, Ashraf KM, et al. Surface Characterization, Antimicrobial Effectiveness, and Human Cell Response for a Biomedical Grade Polyurethane Blended with a Mixed Soft Block PTMO-Quat/PEG Copolyoxetane Polyurethane. *ACS Appl Mater Interfaces*. 2019;11:20699-20714. doi:10.1021/acsami.9b04697

77. Poverenov E, Shemesh M, Gulino A, et al. Durable contact active antimicrobial materials formed by a one-step covalent modification of polyvinyl alcohol, cellulose and glass surfaces. *Colloids Surfaces B Biointerfaces*. 2013;112:356-361. doi:10.1016/j.colsurfb.2013.07.032

78. Tang Y, Zhao Y, Wang H, et al. Layer-by-layer assembly of antibacterial coating on interbonded 3D fibrous scaffolds and its cytocompatibility assessment. *J Biomed Mater Res - Part A*. 2012;100 A(8):2071-2078. doi:10.1002/jbm.a.34116

79. Huang J, Koepsel RR, Murata H, et al. Nonleaching antibacterial glass surfaces via "grafting onto": The effect of the number of quaternary ammonium groups on biocidal activity. *Langmuir*. 2008;24(13):6785-6795. doi:10.1021/la8003933

80. Murata H, Koepsel RR, Matyjaszewski K, Russell AJ. Permanent, non-leaching antibacterial surfaces-2: How high density cationic surfaces kill bacterial cells. *Biomaterials*. 2007;28(32):4870-4879. doi:10.1016/j.biomaterials.2007.06.012

81. Kügler R, Bouloussa O, Rondelez F. Evidence of a charge-density threshold for optimum efficiency of biocidal cationic surfaces. *Microbiology*. 2005;151(5):1341-1348. doi:10.1099/mic.0.27526-0

82. Urquhart AJ, Anderson DG, Taylor M, Alexander MR, Langer R, Davies MC. High throughput surface characterisation of a combinatorial material library. *Adv Mater*. 2007;19(18):2486-2491. doi:10.1002/adma.200700949

83. Andersen C, Madsen NJ, Daugaard AE. Screening Platform for Identification of Suitable Monomer Mixtures Able To Form Thin-Film Coatings on Polyurethanes by UV-Initiated Free Radical Polymerization. *ACS Appl Polym Mater*. 2020. doi:10.1021/acsapm.9b00744

84. Fristrup CJ, Jankova K, Hvilsted S. Surface-initiated atom transfer radical polymerization — a technique to develop biofunctional coatings. *Soft Matter*. 2009;5:4623-4634. doi:10.1039/b821815c

85. Zoppe JO, Ataman NC, Mocny P, Wang J, Moraes J, Klok HA. Surface-Initiated Controlled Radical Polymerization: State-of-the-Art, Opportunities, and Challenges in Surface and Interface Engineering with Polymer Brushes. *Chem Rev*. 2017;117(3):1105-1318. doi:10.1021/acs.chemrev.6b00314

86. Barbey R, Lavanant L, Paripovic D, et al. Polymer brushes via surface-initiated controlled radical polymerization: synthesis, characterization, properties, and applications. *Chem Rev*. 2009;109(11):5437-5527. doi:10.1021/cr900045a

87. Hoffmann C, Silau H, Pinelo M, Woodley JM, Daugaard AE. Surface modification of

polysulfone membranes applied for a membrane reactor with immobilized alcohol dehydrogenase. *Mater Today Commun*. 2018;14:160-168. doi:10.1016/j.mtcomm.2017.12.019

88. Daugaard AE, Jankova K, Hvilsted S. Poly(lauryl acrylate) and poly(stearyl acrylate) grafted multiwalled carbon nanotubes for polypropylene composites. *Polymer (Guildf)*. 2014;55(2):481-487. doi:10.1016/j.polymer.2013.12.031

89. Daugaard AE, Jankova K, Bøgelund J, Nielsen JK, Hvilsted S. Novel UV initiator for functionalization of multiwalled carbon nanotubes by atom transfer radical polymerization applied on two different grades of nanotubes. *J Polym Sci Part A Polym Chem*. 2010;48(20):4594-4601. doi:10.1002/pola.24257

90. Wang H, Brown HR. UV grafting of methacrylic acid and acrylic acid on high-density polyethylene in different solvents and the wettability of grafted high-density polyethylene. II. Wettability. *J Polym Sci Part A Polym Chem*. 2004;42(2):263-270. doi:10.1002/pola.11010

91. Ditizio V, DiCosmo F. Method of making anti-microbial polymeric surfaces. US 8,840,927 B2. 2014.

92. Nykänen A, Nuopponen M, Laukkanen A, et al. Phase behavior and temperature-responsive molecular filters based on self-assembly of polystyrene-block-poly(N-isopropylacrylamide)-block-polystyrene. *Macromolecules*. 2007;40(16):5827-5834. doi:10.1021/ma070378i

93. Okano T, Bae YH, Jacobs H, Kim SW. Thermally on-off switching polymers for drug permeation and release. *J Control Release*. 1990;11(1-3):255-265. doi:10.1016/0168-3659(90)90138-J

94. Van Zoelen W, Buss HG, Ellebracht NC, et al. Sequence of hydrophobic and hydrophilic residues in Amphiphilic polymer coatings affects surface structure and marine antifouling/fouling release properties. *ACS Macro Lett*. 2014;3(4):364-368. doi:10.1021/mz500090n

95. Krishnan S, Ayothi R, Hexemer A, et al. Anti-biofouling properties of comblike block copolymers with amphiphilic side chains. *Langmuir*. 2006;22(11):5075-5086. doi:10.1021/la0529781

96. Zhou Z, Callow JA, Ober CK, et al. A General Approach to Controlling the Surface Composition of Poly(ethylene oxide)-Based Block Copolymers for Antifouling Coatings. *Langmuir*. 2011;27(22):13762-13772. doi:10.1021/la202509m

97. Chung MG, Kim HW, Kim BR, Kim YB, Rhee YH. Biocompatibility and antimicrobial activity of poly(3-hydroxyoctanoate) grafted with vinylimidazole. *Int J Biol Macromol*. 2012;50(2):310-316. doi:10.1016/j.ijbiomac.2011.12.007

98. Ye Y, Song Q, Mao Y. Solventless hybrid grafting of antimicrobial polymers for self-

sterilizing surfaces. *J Mater Chem*. 2011;21(35):13188-13194. doi:10.1039/c1jm12050f

99. Meléndez-Ortiz HI, Alvarez-Lorenzo C, Burillo G, Magariños B, Concheiro A, Bucio E. Radiation-grafting of N-vinylimidazole onto silicone rubber for antimicrobial properties. *Radiat Phys Chem*. 2015;110:59-66. doi:10.1016/j.radphyschem.2015.01.025

100. Martin TP, Kooi SE, Chang SH, Sedransk KL, Gleason KK. Initiated chemical vapor deposition of antimicrobial polymer coatings. *Biomaterials*. 2007;28(6):909-915. doi:10.1016/j.biomaterials.2006.10.009

101. Briscoe BJ, Panesar SS. Aliphatic esters as mould release agents for polyurethanes; the role of interface morphology. *J Phys D Appl Phys*. 1986;19(5):841-856.

102. Fan X, Lin L, Messersmith PB. Cell fouling resistance of polymer brushes grafted from Ti substrates by surface-initiated polymerization: Effect of ethylene glycol side chain length. *Biomacromolecules*. 2006;7(8):2443-2448. doi:10.1021/bm060276k

103. Xu FJ, Wang ZH, Yang WT. Surface functionalization of polycaprolactone films via surface-initiated atom transfer radical polymerization for covalently coupling cell-adhesive biomolecules. *Biomaterials*. 2010;31(12):3139-3147. doi:10.1016/j.biomaterials.2010.01.032

104. Xu FJ, Zhao JP, Kang ET, Neoh KG, Li J. Functionalization of nylon membranes via surface-initiated atom-transfer radical polymerization. *Langmuir*. 2007;23(16):8585-8592. doi:10.1021/la7011342

105. Ma H, Hyun J, Stiller P, Chilkoti A. "Non-Fouling" Oligo(ethylene glycol)-Functionalized Polymer Brushes Synthesized by Surface-Initiated Atom Transfer Radical Polymerization. *Adv Mater*. 2004;16(4):338-341. doi:10.1002/adma.200305830

106. Yuan L, Wu Y, Shi H, Liu S. Surface-initiated atom-transfer radical polymerization of 4-acetoxystyrene for immunosensing. *Chem - A Eur J*. 2011;17(3):976-983. doi:10.1002/chem.201001271

107. Matyjaszewski K. Atom Transfer Radical Polymerization (ATRP): Current status and future perspectives. *Macromolecules*. 2012;45(10):4015-4039. doi:10.1021/ma3001719

108. Maaz M, Elzein T, Bejjani A, et al. Surface initiated supplemental activator and reducing agent atom transfer radical polymerization (SI-SARA-ATRP) of 4-vinylpyridine on poly(ethylene terephthalate). *J Colloid Interface Sci*. 2017;500:69-78. doi:10.1016/j.jcis.2017.03.115

109. Tsarevsky N V., Braunecker WA, Brooks SJ, Matyjaszewski K. Rational selection of initiating/catalytic systems for the copper-mediated atom transfer radical polymerization of basic monomers in protic media: ATRP of 4-vinylpyridine. *Macromolecules*. 2006;39(20):6817-6824. doi:10.1021/ma0609937

110. Holthausen D, Vasani RB, McInnes SJP, Ellis A V., Voelcker NH. Polymerization-

amplified optical DNA detection on porous silicon templates. *ACS Macro Lett*. 2012;1(7):919-921. doi:10.1021/mz300064k

111. Wischerhoff E, Glatzel S, Uhlig K, Lankenau A, Lutz JF, Laschewsky A. Tuning the thickness of polymer brushes grafted from nonlinearly growing multilayer assemblies. *Langmuir*. 2009;25(10):5949-5956. doi:10.1021/la804197j

112. Yuan J, Meng JQ, Kang YL, Du QY, Zhang YF. Facile surface glycosylation of PVDF microporous membrane via direct surface-initiated AGET ATRP and improvement of antifouling property and biocompatibility. *Appl Surf Sci*. 2012;258(7):2856-2863. doi:10.1016/j.apsusc.2011.10.148

113. Yamagami T, Kitayama Y, Okubo M. Preparation of stimuli-responsive “mushroom-like” janus polymer particles as particulate surfactant by site-selective surface-initiated AGET ATRP in aqueous dispersed systems. *Langmuir*. 2014;30(26):7823-7832. doi:10.1021/la501266t

114. Willott JD, Murdoch TJ, Humphreys BA, Edmondson S, Webber GB, Wanless EJ. Critical salt effects in the swelling behavior of a weak polybasic brush. *Langmuir*. 2014;30(7):1827-1836. doi:10.1021/la4047275

115. Waschinski CJ, Zimmermann J, Salz U, Hutzier R, Sadowski G, Tiller JC. Design of contact-active antimicrobial acrylate-based materials using biocidal macromers. *Adv Mater*. 2008;20(1):104-108. doi:10.1002/adma.200701095

116. Lavik HE, Hansen MH, Daugaard AE. Development of new screening assay, for coating process optimisation and testing. 2019.

Appendix 1

Screening Platform for Identification of Suitable Monomer Mixtures Able To Form Thin-Film Coatings on Polyurethanes by UV-Initiated Free Radical Polymerization

Christian Andersen, Niels Jørgen Madsen, and Anders E. Daugaard

Published in ACS Applied Polymer Chemistry, 2020, DOI: 10.1021/acsapm.9b00744

Appendix 1.1 Publication

ACS APPLIED POLYMER MATERIALS

Article

Cite This: ACS Appl. Polym. Mater. XXXX, XXX, XXX−XXX

pubs.acs.org/acsapm

Screening Platform for Identification of Suitable Monomer Mixtures Able To Form Thin-Film Coatings on Polyurethanes by UV-Initiated Free Radical Polymerization

Christian Andersen,[†] Niels Jørgen Madsen,[‡] and Anders E. Daugaard*[,†]

[†]Danish Polymer Centre, Department of Chemical and Biochemical Engineering, Technical University of Denmark, Lyngby DK-2800, Denmark

[‡]Coloplast A/S, Humlebæk DK-3050, Denmark

Supporting Information

ABSTRACT: Screening platforms have become a valuable tool for exploring large libraries of surface chemistries helping the discovery of new materials for especially biological applications. Methods applied in these platforms, however, are mainly based on inert bulk synthesis at picoliter scale, resulting in noncovalently attached molecules on stiff glass substrates. This is a poor representation of a potential final product from an industrial perspective. To overcome this, we have developed a screening platform capable of conducting UV-initiated free radical polymerization (FRP) directly onto a flexible polyurethane under ambient conditions. The platform allows for the study of solvent and monomer effects under industrially relevant conditions and was used to graft a series of homo- and copolymer systems (2,2,2-trifluoroethyl methacrylate (TrFEMA), *N*-isopropylacrylamide (NIPAAm), diethylene glycol methyl ether methacrylate-*co*-poly(ethylene glycol) methyl ether methacrylate, (MDEGMA-*co*-MPEGMA), and acrylic acid (AA)), which was confirmed by both water contact angle (WCA) and X-ray photoelectron spectroscopy (XPS) analysis. The versatility of the system was further demonstrated through investigation of terpolymer systems and direct evaluation of their antifouling properties using a fluorescein-labeled bovine serum albumin (BSA).

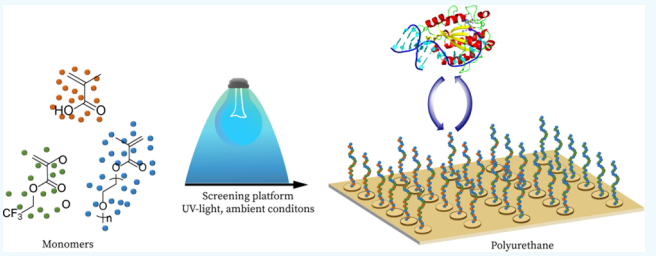

KEYWORDS: *screening, surface-initiated polymerization, water contact angle, XPS, UV-grafting, free radical grafting*

INTRODUCTION

A determining factor for a material's potential application is its surface physical and chemical properties and being able to tailor these properties allows for a significant expansion of the range of application. Polymers are often used as inexpensive bulk materials with good mechanical properties but do not necessarily comprise the desired surface properties—especially when used in biological environments, where there are specific requirements to surface chemistry and topology in order for the material to be compatible with the surroundings or promote certain interactions.[1−4] The complexity of these systems makes discovery of novel materials a tedious and time-consuming process that requires testing of hundreds if not thousands of different formulations to find suitable candidates even through a rational design approach. To accelerate development and to illuminate nonintuitive structure−property relationships, the use of screening platforms has become a popular method of choice either for determination of interactions with cells and proteins[5,6] as well as enzymes[7] or for determination of surface properties of polymers.[8−10] Large chemical libraries can be obtained through systematic and combinatorial mixing of compounds. For polymer grafting, such platforms are often based on automated picoliter scale synthesis conducted on glass slides under inert atmosphere.[10−14] The small scale allows for hundreds of samples to be placed on a single glass slide with minimum use of material. The small volume, however, imposes the limitation that polymerizations are run under bulk conditions without the use of solvents. Such methods are therefore restricted to investigate monomer ratios and not effects of polymerization conditions such as concentrations and solvents. The inert conditions used during polymerization are also difficult to obtain at an industrial scale, and therefore to better simulate the final product, polymerizations should be conducted under an ambient atmosphere. In addition, glass as a substrate cannot directly be compared to surface modification of polymer substrates, and such systems will therefore only be model systems. This is especially important when working with cell scaffolds where the flexibility of the matrix and substrate is very important for e.g. cell proliferation.[15,16]

The aim of this work was therefore to develop a screening platform along with a suitable method able to conduct surface

Received: August 9, 2019
Accepted: October 29, 2019
Published: October 29, 2019

DOI: 10.1021/acsapm.9b00744
ACS Appl. Polym. Mater. XXXX, XXX, XXX−XXX

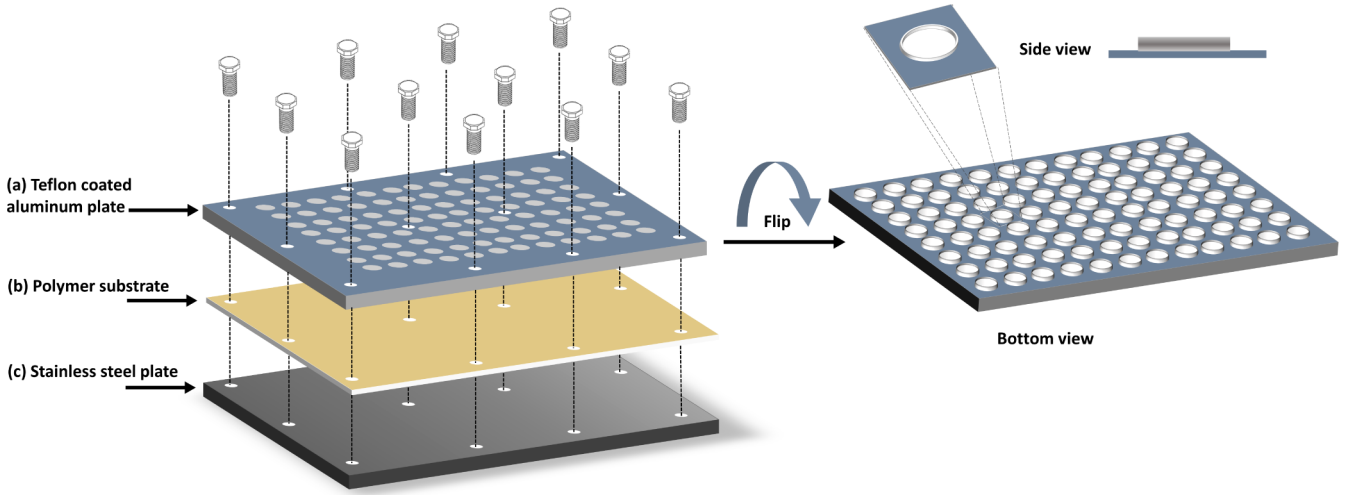

Figure 1. Schematic representation of screening platform (left) and bottom view showing milled edges around the wells (right), where a is the well plate, b is the polymer substrate, and c is a supporting stainless steel plate.

modifications under normal atmosphere directly onto a flexible polymer substrate for combinatorial investigations of both homo- and copolymer systems. To further enable testing of solvents and monomer concentrations on a flexible substrate, the design had to comprise chemical and heat resistant parts and with reaction vessel dimensions of at least microliter volume. The platform thereby presents the opportunity to screen polymer surface modifications and conditions through the use of an industrially relevant process.

EXPERIMENTAL SECTION

Materials. All chemicals and solvents were of analytical grade and were used without further purification as obtained from commercial suppliers, unless stated otherwise. Inhibitors were removed from the monomers prior to use by passing them through a short plug flow column of basic alumina.

Characterization. Water contact angle measurements was conducted on a Dataphysics Contact Angle System OCA 20. Static contact angles were measured on a droplet of 4 μL Millipore water. X-ray photoelectron spectroscopy (XPS) was performed on a Thermo Fisher Scientific K Alpha (East Grinstead, UK) using monochromatized aluminum KR radiation in a 400 μm spot on the sample. Survey and high-resolution spectra were acquired and analyzed using the manufacturer's Avantage software package. Fluorescence intensity measurements and UV−vis spectroscopy were performed on a POLARstar Omega from BMG Labtech, where fluorescence measurements were conducted using an excitation filter at 485 nm and an emission filter at 520 nm scanning across the surface in a matrix scan of 10 × 10. Differential scanning calorimetry (DSC) was performed on a DSCQ1000 from TA Instruments. The thermal analyses were performed at a heating and cooling rate of 10 K/min. The melting temperatures (T_m) are reported as the peak temperatures of the endothermic melting peaks. Glass transition temperatures (T_g) were measured at the inflection point.

One way analysis of variance (ANOVA) was done in Minitab 18 using the Tukey method with a 95% confidence interval to calculate statistically significant differences between a set of obtained values.

Preparation of the Screening Platform. The screening platform consists of two individual metal plates: a top plate (a) and a bottom plate (c) (see Figure 1). The top plate was made from aluminum with dimensions 127.7 × 85.5 × 7.0 mm^3 and contains 96 wells with a diameter of 6.1 mm and 12 holes for screws with a diameter of 3.3 mm. On the bottom side of the top plate, metal rings around each well were milled in a height of 0.5 mm. Furthermore, the top plate was coated with an Accofal 2G54 Teflon coating from ACCOAT a/s. The bottom plate was made from stainless steel with dimensions of 127.7 × 85.5 × 3.0 mm^3.

Preparation and Pretreatment of Setup. A PU plate was cut into suitable dimensions and washed with first ethanol and then acetone and left to dry for a few minutes. The PU substrate was then placed between the top and bottom plate and fixed with screws. The setup was heated at 155 °C for 15 min, and the screws were tightened before increasing the temperature to 160 °C for another 60 min. The screws were tightened once more, and the setup was left to cool to room temperature.

Embedding of Photoinitiator. To each well 80 μL of a 0.5 M stock solution of Irgacure 2959 in THF/MeOH (1:4, v:v) was added. The solution was left to evaporate overnight in the dark, resulting in solvent casting of the photoinitiator in the polymer surface.

General Procedure for Polymer Grafting. A stock solution of 3.0 M acrylic acid in H_2O/MeOH (1:1, v:v) was made and 0−55 μL of this solution were added in to their respective wells. The solution was diluted with H_2O/MeOH (1:1, v:v) to give a total volume of 80 μL. The plate was left under orbital shaking for 5 min at 200 rpm at 25 °C in a Hettich Benelux Cooling Thermomixer MKR 13. Thereafter, the plate was exposed to UV-light (λ = 365 nm, 10 mW/cm^2) for 30 min at 25 °C under continued shaking at 200 rpm. Thereafter, the reaction mixture was removed, and wells were washed excessively with solvent (H_2O/MeOH (1:1, v:v)). In addition, all wells were refilled with pristine solvent mixture and left shaking at 200 rpm at RT for 15 min The rinsing procedure was repeated with H_2O, where after the wells were filled with H_2O and shaken at 200 rpm at RT for 15 min to remove any residual solvents. The top plate was removed and replaced with an aluminum frame, which was fixed with screws and covered with aluminum foil. The setup was left to dry in a vacuum oven at RT overnight. All samples were conducted in triplicates. Different solvents were used for specific monomers as follows: AA: H_2O/MeOH (1:1, v:v); NIPAAm: H_2O/MeOH (1:1, v:v); MDEGMA-*co*-MPEGMA 500: H_2O/MeOH (1:1, v:v); TrFEMA-*co*-MAA-*co*-MPEGMA 500: EtOH.

Antifouling Test. A surface was exposed to a solution of 0.04 mg/mL fluorescein-labeled BSA in PBS buffer and left for 2 h at RT. The plate was covered with aluminum foil to reduce evaporation and to prevent the solution from drying out. The sample was then washed excessively with PBS buffer and dried in air. The fluorescence intensity was measured by using an excitation wavelength of 485 nm and an emission wavelength of 520 nm.

RESULTS AND DISCUSSION

To enable testing of different polymerization conditions, an inert holder that would allow parallelization of experiments in

DOI: 10.1021/acsapm.9b00744
ACS Appl. Polym. Mater. XXXX, XXX, XXX−XXX

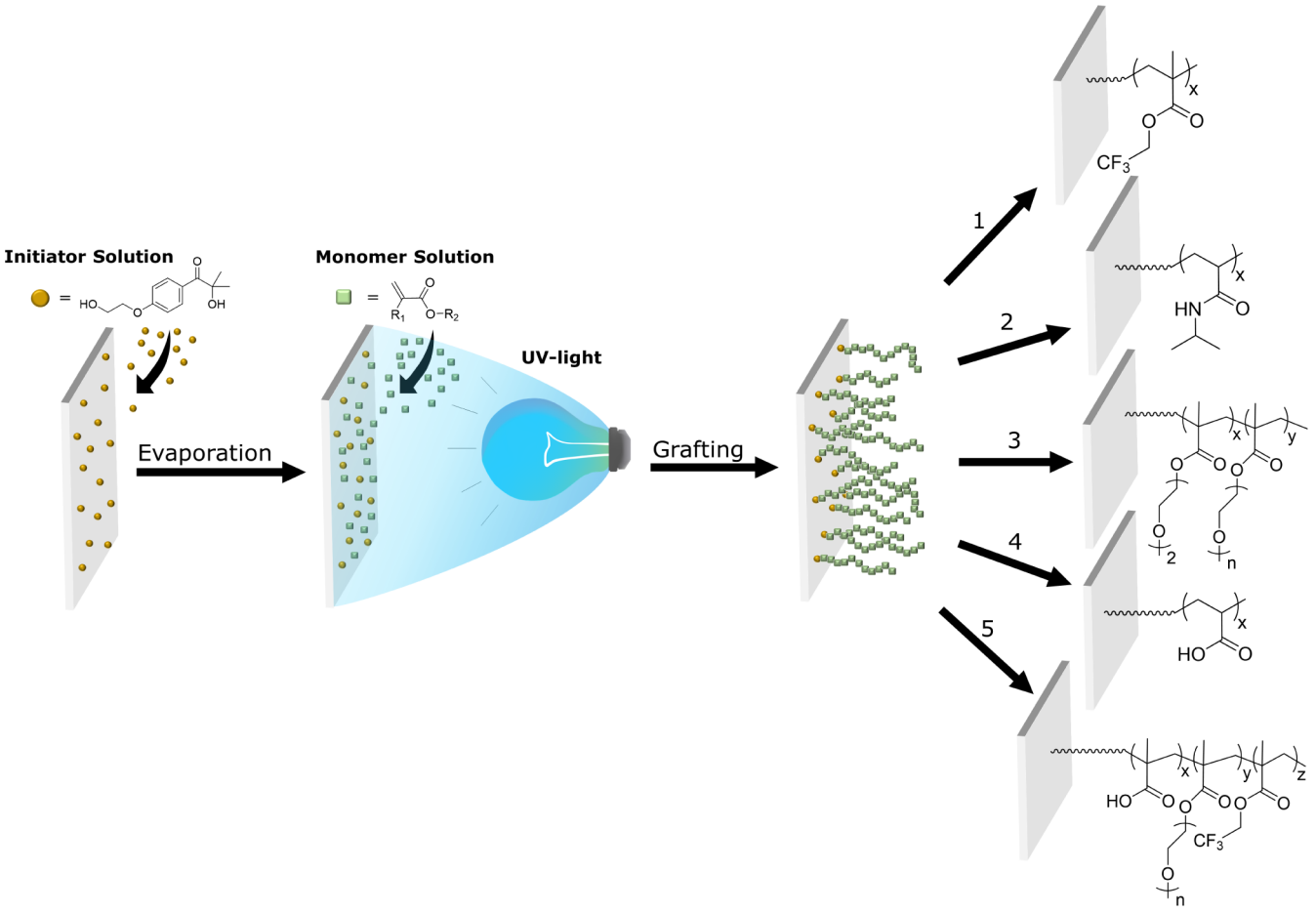

Figure 2. Schematic representation of embedding of photoinitiator into polymer substrate followed by grafting of monomer through UV activation. The illustrated surface modifications are (1) 2,2,2-trifluoroethyl methacrylate (TrFEMA), (2) *N*-isopropylacrylamide (NIPAAm), (3) diethylene glycol methyl ether methacrylate-*co*-poly(ethylene glycol) methyl ether methacrylate, M_n = 500 (MDEGMA-*co*-MPEGMA 500), (4) acrylic acid (AA), and (5) MAA-*co*-MPEGMA 500-*co*-TrFEMA.

separate vessels was required. As an additional restraint, the intended platform was required to be able to handle a broad range of solvents as well as to be suitable for semicrystalline plastics such as polyurethanes with melting points above 150 °C. The design of the platform was based on a standard 96-well microtiter plate and was divided into three separate parts as can be seen in Figure 1.

The top plate (a) was made from aluminum and comprises 96 wells with an inner diameter of 6.1 mm and a height of 7.0 mm, giving a well volume of ∼200 μL. The well size in this platform permits microliter scale experiments, opening the possibility to investigate the influence of solvents as well as monomer concentrations. A Teflon coating was applied to plate (a) to provide a nonstick surface, allowing it to be detached after polymerization without compromising the grafted surface and to access the samples for analysis. The coating also makes for an easy-to-clean surface, permitting it to be reused after each experiment. When assembling the setup, the polymer substrate (b) was placed in-between plate (a) and the steel support (c) and held together by screws. Having the polymer as a separate part makes switching between substrates a simple process within one platform, making it possible to test the same conditions on various materials—the only requirement being that the substrate can be made into a film or sheet. To prevent leakage and potential mixing of contents, a tight seal between polymer and plate (a) was secured with a thin metal rim around each well on the bottom side of plate (a) (see Figure 1, right). During the thermal treatment, the setup is heated to 160 °C, just below the melting point of the polymer, which in this case is a PU (T_m = 166 °C). This softens the substrate and, in combination with pressure from the screws, allows the metal rims to submerge into the polymer film, effectively sealing off each chamber. The high-temperature treatment additionally also straightened out any unevenness in the film resulting from processing ensured a good adhesion of the polymer film to the stainless steel support. Such unevenness in film thickness commonly result from release of internal stress after processing, which it is critical to remove to ensure an efficient sealing across the entire surface. Therefore, the heat treatment was important with respect to both sealing the system and to obtain a flat homogeneous surface.

Activation of and Grafting onto Polyurethane. Most polymer surfaces are inert by nature and require activation through implementation of functional groups or initiating species to facilitate modification by polymerization. This can be done through a stepwise activation and subsequent polymerization as is commonly done by use of controlled radical methods such as surface-initiated atom transfer radical polymerization,[17−19] which provides high control for modification of surfaces.[20−22] Such processes typically require inert conditions, which is not always possible in an industrial setting.

DOI: 10.1021/acsapm.9b00744
ACS Appl. Polym. Mater. XXXX, XXX, XXX−XXX

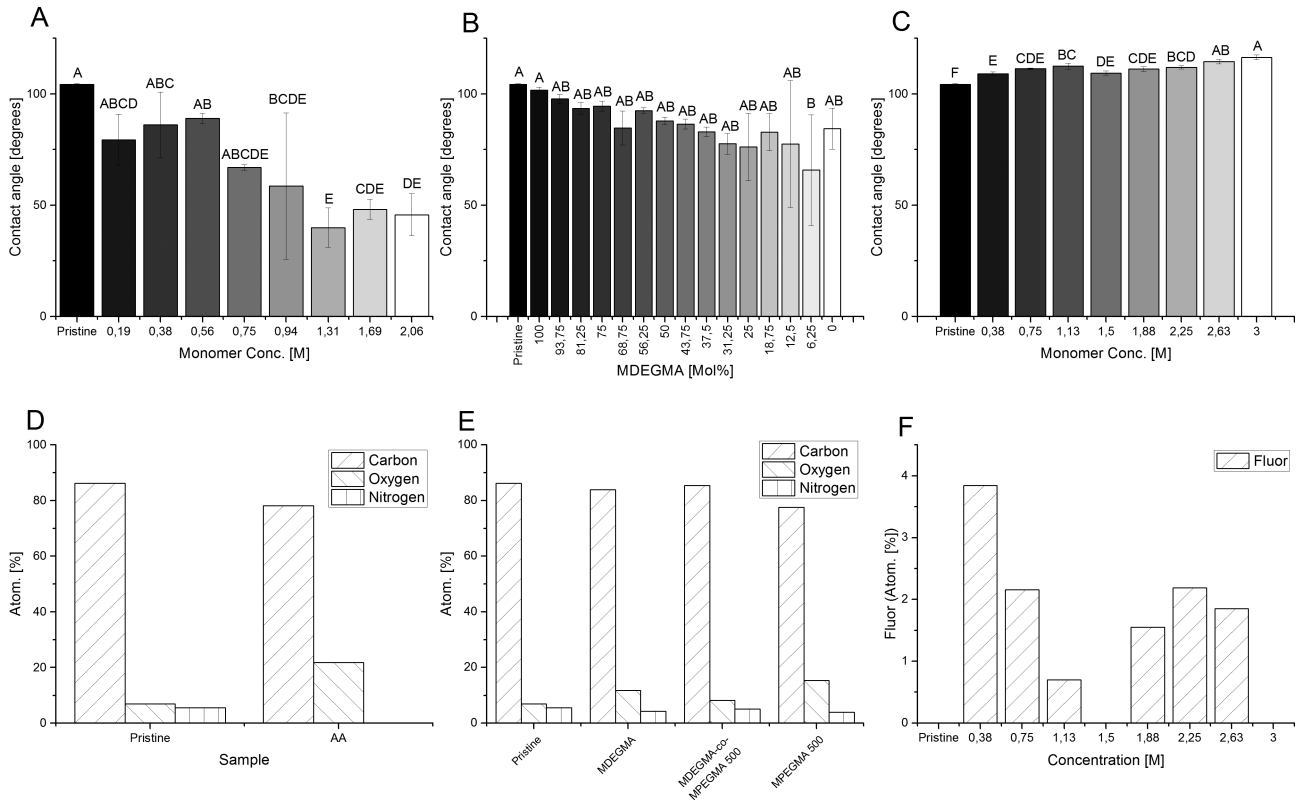

Figure 3. WCA and XPS data of PU surface modified with AA (A, D), MDEGMA-*co*-MPEGMA 500 (B, E), and TrFEMA (C, F).

In this case, we have evaluated the use of direct grafting using photoinitiators under ambient conditions using the screening platform. Such systems have been applied for modification of polymer surfaces.[23,24] Some monomers are more tolerant to oxygen during polymerization, and identification of such systems would be of significant industrial interest for coating applications of thin surface coatings. Therefore, the polymer surface was activated for polymerization by embedding a photoinitiator, Irgacure 2959, into the polymer surface by solution casting, as shown in Figure 2.

The initiator was dissolved in a mixture of THF/MeOH (1:4, v:v), where THF serves the purpose of slightly dissolving the PU substrate, while MeOH swells it. Because of this combination of solvents, solution casting of the photoinitiator solution onto the PU surface, results in embedment of the photoinitiator into the outer layers of the surface. Subsequently, it can be functionalized through photoinitiated free radical polymerization with various monomer solutions. By exposure of the entire system to UV light, grafting of monomers from and into the polymer surface takes place, resulting in formation of thin layers of surface grafted polymers as illustrated in Figure 2. Through this method, the formation of radicals is mainly occurring in close proximity to the surface of the substrate. This therefore limits the formation of nongrafted homopolymer compared to having the initiator added as a reagent in solution. This was also confirmed by analysis of the polymerization solutions after grafting, which contained no detectable amounts of free polymer (by SEC and NMR). After completed surface grafting, the detachable top plate (a) can be removed, enabling the surface to be analyzed by various classical analytical tools for surface analysis, such as WCA measurements, XPS, fluorescence intensity spectroscopy, and UV−vis spectroscopy. Because the top plate is only mechanically bonded, it is possible to disassemble the structure without risking polluting the surface with polymer fragments originating from adhesives or other types of sealants as is commonly used in other applications.

To investigate the possibilities of grafting commonly used acrylic and methacrylic monomers onto surfaces under ambient conditions, a range of different monomers were attempted grafted to the PU surface by using UV-initiated free radical polymerization. Initially, acrylic acid (AA) was grafted to the PU using a series of AA feed concentrations in an attempt to create a hydrophilic surface by introduction of carboxylic acid functionalities. Investigations of the effect of feed concentration with respect to hydrophilicity and elemental surface composition were done through WCA and XPS analysis, which can be seen in Figures 3A and 3D, respectively. The WCAs obtained for the grafted surfaces ranged between 89° and 40°, which is substantially lower than that of the pristine polyurethane surface (104°). The lowest WCA of 40° was observed at 1.31 M, reflecting a clear shift from a hydrophobic to a hydrophilic surface and at the same time illustrating the importance of testing of different concentrations of monomers for surface grafting reactions. The grafting was further confirmed by XPS (Figure 3D), showing higher oxygen content and no nitrogen atoms in the surface, corresponding to the structure of a surface grafted layer of poly(AA). This was further corroborated by FT-IR measurements of the grafted polymers (Figure S2). The presence of surface grafted AA was confirmed by a broad OH stretch for all samples (2300−3600 cm^{-1}) as well as a characteristic change to the carbonyl stretch resulting from the carbonyl in AA (1700 cm^{-1}). In addition, also the effect of increasing the AA concentration in the feed was reflected in an increasing strength of the bands assigned to the PAA. In

DOI: 10.1021/acsapm.9b00744
ACS Appl. Polym. Mater. XXXX, XXX, XXX−XXX

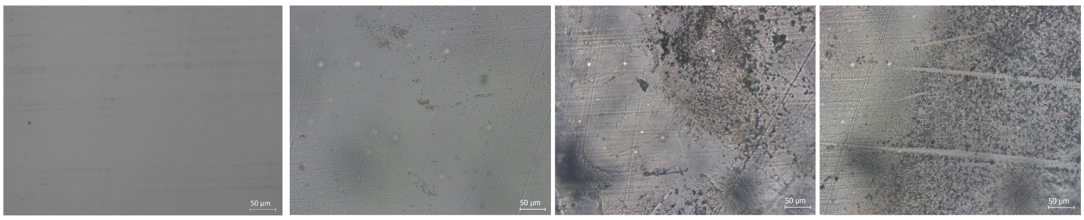

Figure 4. Microscopy images of TrFEMA modified PU at monomer feed concentrations of 0, 0.75, 2.25, and 3.00 M.

addition, WCA measurements (Figure 3A) show a trend of decreasing contact angle with increasing monomer concentration, suggesting a higher degree of polymerization at higher monomer concentrations (as expected). ANOVA analysis revealed significant differences not only between the pristine and modified surface but also between individual monomer concentrations, which distribute into three separate groups. Concentrations from 0.19 to 0.56 M group together in category A along with the pristine surface, showing that these concentrations only led to a minor change in surface hydrophilicity. Experiments conducted at concentrations of 0.75−0.91 M showed some impact on the WCA and were grouped together in the intermediate category BC. At high concentrations of 1.31, 1.69, and 2.06 M a clear impact of grafting was observed by significantly reduced contact angles, and these group together in groups E, CDE, and DE, respectively.

Coatings containing poly(ethylene glycol) (PEG) have been of great interest in the field of biomedical devices due to not only their ability to create low friction surfaces but also their biocompatibility and being FDA approved.[25] Through parallelization in the screening platform, copolymers of diethylene glycol methyl ether methacrylate (MDEGMA) and poly(ethylene glycol) methyl ether methacrylate (MPEGMA 500) were therefore prepared at various feed ratios of the two monomers. The relation between feed composition and WCA was investigated along with XPS analysis as shown in Figures 3B and 3E, respectively. A decrease in WCA was observed as MDEGMA was replaced with increasing amounts of MPEGMA (M_n = 500 g/mol) throughout the series. This was expected due to the longer PEG side chain in MPEGMA, resulting in a more hydrophilic monomer. However, only a minor decrease in contact angle from 104° for the pristine surface to 101° at 100 mol % MDEGMA was seen, which reduced to 66° for the 6.25/93.75 mol % MDEGMA/MPEGMA copolymer. In general, one would expect a much lower contact angle for these hydrophilic monomers. Similarly, the XPS data (see Figure 3E) only showed a minor increase in oxygen, while the nitrogen peak from the PU substrate was still visible. In combination, this indicates that only a very thin coating of the hydrophilic monomers was formed on the PU. This was also corroborated in the FT-IR data (Figure S4), where no significant differences were observed, though the similarity in composition of the monomers and the PU substrate makes small differences difficult to confirm. The statistical analysis of the WCAs showed that no significant difference can be found between the pristine and modified surfaces, which all belongs within group A with the exception of 6.25 mol % MDEGMA, even though a general trend of decreasing WCA was observed across the series. Grafting under ambient conditions can therefore only be concluded to result in a very thin layer of poly(PEGMA) or poly(MDEGMA), though this is sufficient to change the immediate surface chemistry (WCA measurements).

Conversely, hydrophobic surfaces can be prepared through grafting of fluoride containing monomers. As an example of a fluorinated monomer, 2,2,2-trifluoroethyl methacrylate (TrFEMA) was grafted at various monomer feed concentrations to create a low energy surface. The WCA and the atomic fluor composition of the surface were measured, and the results can be seen in Figures 3C and 3F, respectively. The contact angle increased with increasing monomer concentration from 109° at 0.38 M to 116° at 3 M. The pristine surface was assigned by ANOVA analysis to group F, which does not appear at any of the data points obtained, indicating that all modified surfaces were significantly different from the pristine surface. Even at low concentration of 0.38 M, the contact angle was significantly different from that of the pristine surface. The trend shown for the WCA measurements indicates an increasing hydrophobicity of the surface, which would be expected to correlate with an increasing fluorine content. However, XPS analyses of the surfaces showed that this was not the case (Figure 3F). Fluorine is seen for most of the samples, though the concentration does not appear to follow a trend. Optical microscopy images of the samples (Figure 4) reveal that this is due to an uneven coverage of polymer on the surface. The grafting conducted on the surface was incomplete and formed aggregates, which are seen as black dots in Figure 4.

The aggregates increases in size and become more dominant with increasing monomer concentration, explaining the increase in WCAs. Analyzing the surfaces by FT-IR only showed insignificant changes in the spectra with increasing concentration, reflecting the incomplete reaction of the monomer. In conclusion, the fluorine monomer cannot be grafted in a homogeneous layer under ambient conditions even though the polymerization does result in a minor increase in the WCA.

A similar often-used monomer is *N*-isopropylacrylamide (NIPAAm), which, in addition to changing hydrophilicity upon thermal stimuli in solution, has been shown to have great potential for controlled drug delivery systems and nanofiltration membranes.[26,27] The polymer in solution has a lower critical solution temperature (LCST) of 31−33 °C, resulting in hydrophobic properties above this point and hydrophilic properties below. The transition is caused by a rearrangement of the polymer chains starting as a linear conformation at low temperature, where amide groups can form hydrogen bonds to water. Increasing the temperature creates inter- and intramolecular hydrogen bonds, forcing the polymer into a coiled structure, leaving only the hydrophobic backbone exposed. Grafting of the monomer was similarly conducted in a series of monomer feed concentrations with subsequent WCA and XPS analysis as presented in Figures 5A and 5B, respectively. To

DOI: 10.1021/acsapm.9b00744
ACS Appl. Polym. Mater. XXXX, XXX, XXX−XXX

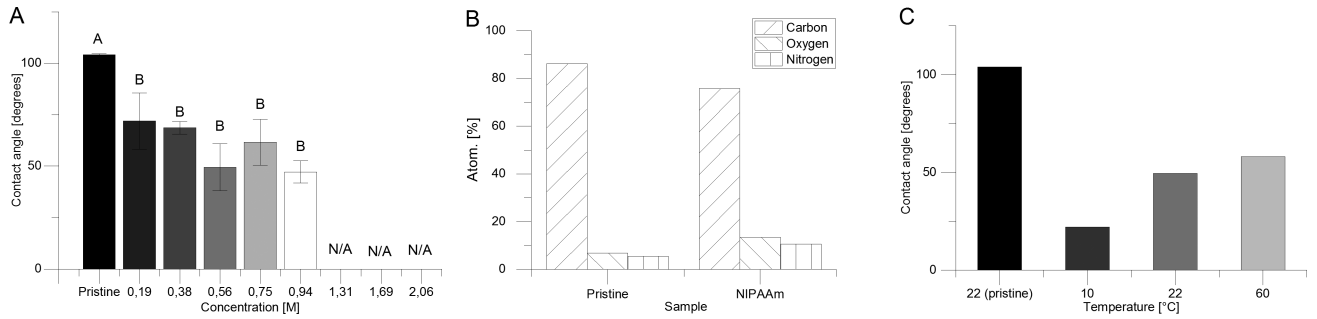

Figure 5. WCA of NIPAAm modified PU at various monomer feed concentrations (A), XPS data (B), and WCA at various temperatures (C).

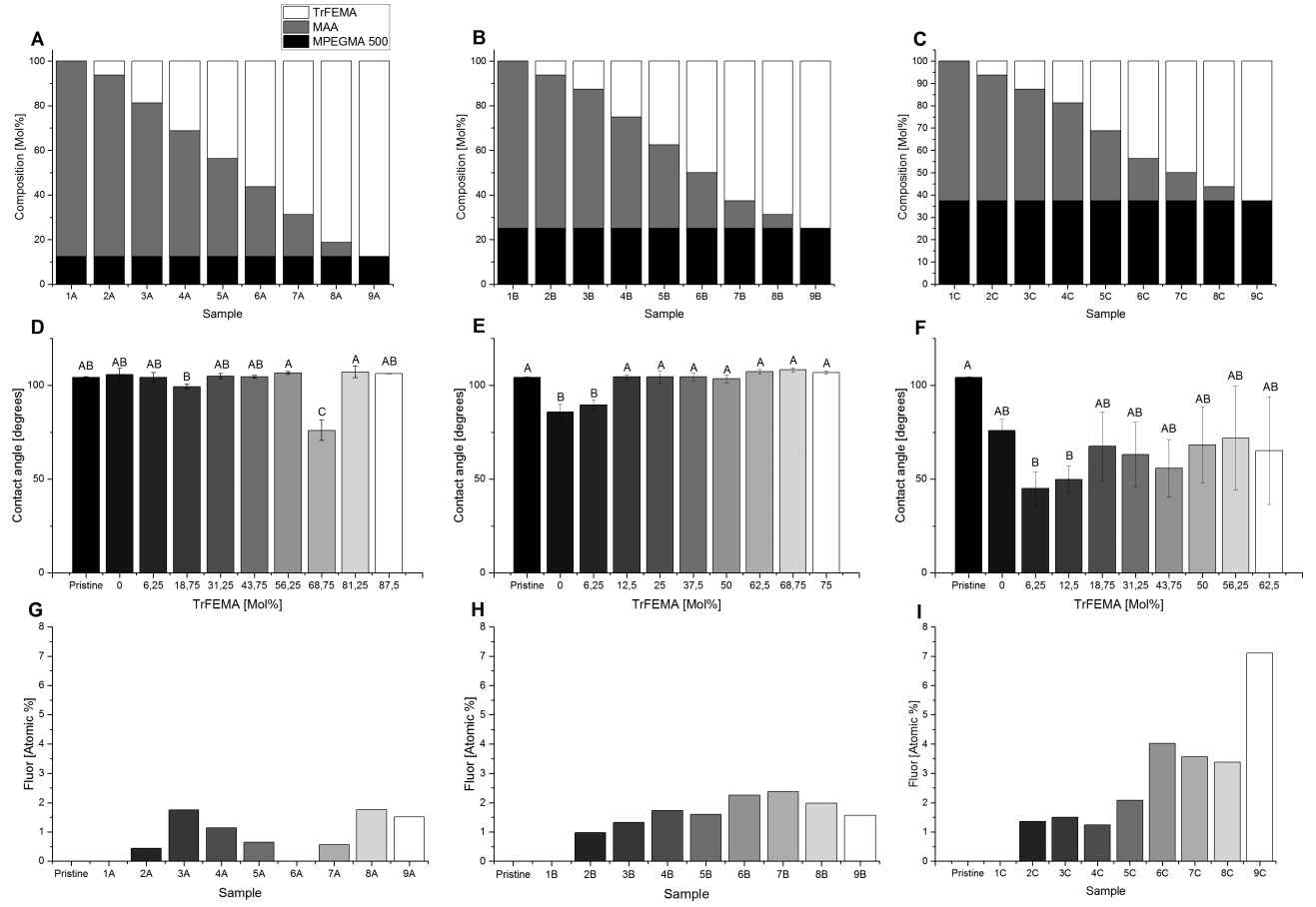

Figure 6. Composition of terpolymer set A, B, and C, black: MPEGMA 500; gray: MAA; and white: TrFEMA (A, B, and C) and their respective WCA (D, E, and F) and XPS data on fluor content (G, H, and I).

show that the thermoresponsive properties can be transferred to the polymer surface, the WCA of the NIPAAm modified PU was also measured both above and below the LCST (see Figure 5C).

NIPAAm concentrations were varied within the range 0–2.06 M in the feed, and from this experiment, an important limitation concerning monomer concentration was observed. When the NIPAAm concentration was increased above 1 M, cross-linking occurred, resulting in large gel formations on the surface (see Figure S1). The gels did not adhere well to the substrate and had poor mechanical stability. This demonstrates that the monomer concentration is an important parameter to consider and has great influence for the outcome of the polymer coating. Because of this cross-linking at high monomer concentrations, the XPS analysis was therefore performed at 0.56 M, below the gel point. From Figure 5B, the ratio between oxygen and carbon (O/C) and nitrogen and carbon (N/C) can be calculated to 0.15 and 0.12, respectively. This corresponds to that of NIPAAm, which have an O/C and N/C ratio of 0.14. This was also corroborated by FT-IR (Figure S5), where a clear NH stretch (3300 cm^{-1}) was seen for all concentrations below the gelation point. The thermoresponsive properties were observed by WCA measurements for one of the surfaces (NIPAAm, 0.56 M). At high temperature (60 °C), the modified surface showed a WCA of 59°, which was reduced to only 22° at 10 °C (Figure 5C). This clearly shows that the surface is thermoresponsive, though the transition appear at lower temperatures, compared to the typically observed LCST for NIPAAm. LCSTs have been seen to vary according to molecular weight and structure of the

DOI: 10.1021/acsapm.9b00744
ACS Appl. Polym. Mater. XXXX, XXX, XXX−XXX

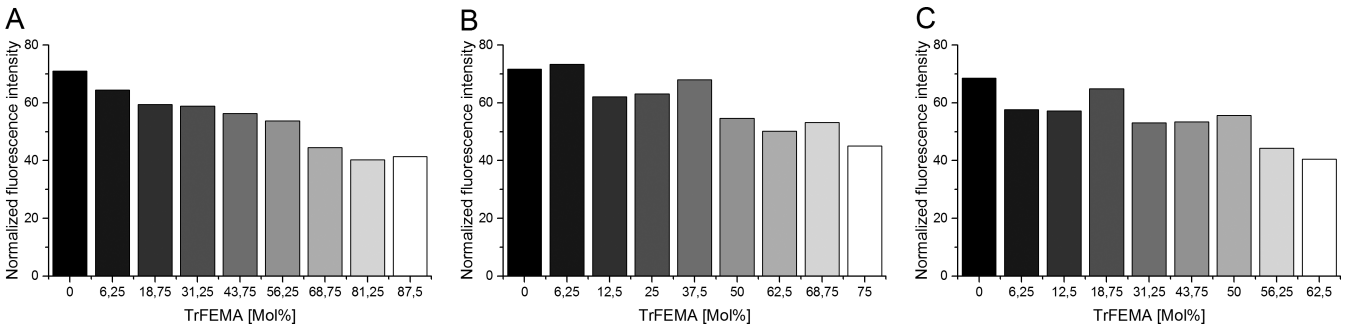

Figure 7. Fluorescence intensity of adsorbed fluorescein labeled BSA of terpolymer sets A, B, and C (A, B, and C respectively) after 2 h exposure to a 0.04 mg/mL PBS solution.

polymer, and it is hypothesized that this may be the reason for the observed deviation.

Overall, it can be concluded that some monomers (AA, NIPAAm) effectively can be grafted in homopolymerization to the PU surface under ambient conditions, while others are less efficient (PEGMA, MDEGMA, and TrFEMA).

Antifouling Amphiphilic Surface. Screening platforms are ideal for creating large libraries of complex systems in combination with parallelized analysis. To illustrate the possibility to do combinatorial studies, three monomers were tested a surface coating: methacrylic acid (MAA), 2,2,2-trifluoroethyl methacrylate (TrFEMA), and MPEGMA 500. The selection was based on the fact that polymer coatings comprising both hydrophobic and hydrophilic segments have proven to be effective in preventing fouling from e.g. marine life.[28−30] The intention of this study was therefore to investigate the optimal formulation to prevent fouling against a fluorescein labeled bovine serum albumin protein (BSA). For each monomer, stock solutions of 1 M concentration in EtOH were made, and the ratios of monomers were systematically varied throughout three sets of terpolymer systems named A, B, and C (see Figure 6A− C). The sets all contained different base levels of MPEGMA 500 at 12.5, 25.0, and 37.5 mol % for A, B, and C, respectively. Tuning the hydrophobicity was done by adding MAA and TrFEMA in various ratios to give nine formulations for each set, providing a total of 27 formulations. The obtained WCA and fluor content from XPS of each formulation for A, B, and C can be viewed in Figures 6D−F and 6G−I, respectively.

The outcome of the WCA of terpolymer sets A and B was heavily influenced by the presence of hydrophobic TrFEMA, even at small feed concentrations (see Figure 6D,E). The contact angle of the samples barely deviated from that of the pristine surface, which was also seen from the ANOVA analysis. This was an unexpected result, considering that both MAA and MPEGMA 500 are both hydrophilic and present in high concentrations, and a lower contact angle should be observed. A minor exception to this was the samples at 0 and 6.25 mol % TrFEMA in Figure 6E, which obtained a WCA of 85° and 90°, respectively. The ANOVA analysis shows that the contact angles are significantly different from that of the pristine surface but quickly rises to above 100° at 12.5 mol % TrFEMA (see Figure 6E).

For terpolymer C, however, the higher MPEGMA 500 content of 37.5 mol % was enough to counteract the hydrophobic effects of TrFEMA, resulting in a substantial drop in WCA (see Figure 6F). The high content of MPEGMA 500 additionally increased the observed hysteresis of the systems illustrating the amphiphilicity of the surface. Therefore, no significant difference between the modified and the pristine surface was found from the ANOVA analysis, with the exception at 6.25 and 12.5 mol % TrFEMA (see Figure 6F).

Figures 6G, 6H and 6I illustrate the level of fluor in each sample for terpolymer set A, B, and C, respectively. A linear trend with a steady increase in fluor with respect to increasing mol % of TrFEMA was expected for all terpolymer systems, but only terpolymer C showed this trend clearly. In Figure 6G, the fluor content is very low, and the grafting appears to be sporadic, whereas for Figure 6H, a trend was initially seen but with the last two samples slightly decreasing. Terpolymer set C obtained a gradual increase in fluor with a maximum of 7.1 atom %. This is attributed to TrFEMA copolymerizing better with MPEGMA 500 than MAA. Between the three sets of surfaces, a higher content of fluor is therefore seen for higher contents of MPEGMA 500.

To test the antifouling properties, the modified surfaces were exposed to a 0.04 mg/mL fluorescein labeled BSA protein phosphate-buffered saline (PBS) solution. The mean value of the resulting intensity for terpolymer sets A, B, and C can be seen in Figures 7A, 7B, and 7C, respectively.

Comparing the analytical data and the obtained antifouling study showed that copolymers purely of MPEGMA 500 and TrFEMA gave in general the best fouling resistance for all terpolymer systems. The lower the feed concentration of MAA was, the better the fouling resistance became. An intuitive explanation would be that MAA was able to create either hydrogen bonds or electrostatic interaction with the protein through carboxylic acid groups (COO^-/COOH). Thereby, even small contents of MAA would create binding sites for the protein to adhere.

CONCLUSION

A new screening platform capable of modifying a thermoplastic polyurethane via UV-initiated FRP under ambient conditions was developed. The setup comprises 96 reaction wells and was demonstrated with a series of acrylate and methacrylate monomers using WCA, FT-IR, and XPS data to validate the outcome of the polymerizations. The system allowed for investigations of the influence of feed concentration in relation to surface wettability. Through ANOVA, a clear correlation between WCA and feed concentration/composition were found for AA, MDEGMA-*co*-MPEGMA 500, and TrFEMA. However, XPS showed that grafting of MDEGMA-*co*-MPEGMA 500 and TrFEMA was found to be inefficient, leading to aggregates on the surface in the case of TrFEMA. Additionally, for NIPAAm systems, it was found that

DOI: 10.1021/acsapm.9b00744
ACS Appl. Polym. Mater. XXXX, XXX, XXX−XXX

concentrations above 0.94 M resulted in cross-linking and proved to be an important factor for optimal grafting for this type of monomer, underlining the importance of screening polymerization conditions. Finally, a combinatorial screening of amphiphilic terpolymer systems comprising TrFEMA-*co*-MAA-*co*-MPEGMA 500 was conducted, illustrating how combining monomers can beneficially improve the outcome of the polymerizations under ambient conditions. For the terpolymers, compositions containing MAA had higher protein adhesion compared to those consisting only of TrFEMA-*co*-MPEGMA 500. This was attributed to hydrogen bonding/ionic interactions through the carboxylic moiety of the MAA.

The platform can be adapted to fit different polymer substrates and is resistant to both heat and chemicals and represents a new and useful tool in the discovery of novel surface modifications for polymeric materials in an industrially relevant setting.

■ ASSOCIATED CONTENT

Supporting Information

The Supporting Information is available free of charge on the ACS Publications website at DOI: 10.1021/acsapm.9b00744.

Picture of gelled NIPAAm polymerization (Figure S1); FT-IR spectra of grafted surfaces (Figures S2–S6) (PDF)

■ AUTHOR INFORMATION

Corresponding Author

*E-mail adt@kt.dtu.dk.

ORCID

Anders E. Daugaard: 0000-0002-0627-6310

Notes

The authors declare no competing financial interest.

■ ACKNOWLEDGMENTS

Innovation Fund Denmark and Coloplast A/S is acknowledged for financial support.

■ REFERENCES

(1) Anderson, D. G.; Levenberg, S.; Langer, R. Nanoliter-Scale Synthesis of Arrayed Biomaterials and Application to Human Embryonic Stem Cells. *Nat. Biotechnol.* **2004**, *22* (7), 863–866.

(2) Taylor, M.; Urquhart, A. J.; Anderson, D. G.; Williams, P. M.; Langer, R.; Alexander, M. R.; Davies, M. C. A Methodology for Investigating Protein Adhesion and Adsorption to Microarrayed Combinatorial Polymers. *Macromol. Rapid Commun.* **2008**, *29* (15), 1298–1302.

(3) Hook, A. L.; Chang, C.-Y.; Yang, J.; Luckett, J.; Cockayne, A.; Atkinson, S.; Mei, Y.; Bayston, R.; Irvine, D. J.; Langer, R.; Anderson, D. G.; Williams, P.; Davies, M. C.; Alexander, M. R. Combinatorial Discovery of Polymers Resistant to Bacterial Attachment. *Nat. Biotechnol.* **2012**, *30* (9), 868–875.

(4) Caliari, S. R.; Gonnerman, E. A.; Grier, W. K.; Weisgerber, D. W.; Banks, J. M.; Alsop, A. J.; Lee, J.-S.; Bailey, R. C.; Harley, B. A. C. Collagen Scaffold Arrays for Combinatorial Screening of Biophysical and Biochemical Regulators of Cell Behavior. *Adv. Healthcare Mater.* **2015**, *4* (1), 58–64.

(5) Gupta, N.; Lin, B. F.; Campos, L. M.; Dimitriou, M. D.; Hikita, S. T.; Treat, N. D.; Tirrell, M. V.; Clegg, D. O.; Kramer, E. J.; Hawker, C. J. A Versatile Approach to High-Throughput Microarrays Using Thiol-Ene Chemistry. *Nat. Chem.* **2010**, *2* (2), 138–145.

(6) Duffy, C.; Venturato, A.; Callanan, A.; Lilienkampf, A.; Bradley, M. Arrays of 3D Double-Network Hydrogels for the High-Throughput Discovery of Materials with Enhanced Physical and Biological Properties. *Acta Biomater.* **2016**, *34*, 104–112.

(7) Hoffmann, C.; Pinelo, M.; Woodley, J. M.; Daugaard, A. E. Development of a Thiol-Ene Based Screening Platform for Enzyme Immobilization Demonstrated Using Horseradish Peroxidase. *Biotechnol. Prog.* **2017**, *33*, 1267–1277.

(8) Urquhart, A. J.; Anderson, D. G.; Taylor, M.; Alexander, M. R.; Langer, R.; Davies, M. C. High Throughput Surface Characterisation of a Combinatorial Material Library. *Adv. Mater.* **2007**, *19* (18), 2486–2491.

(9) Urquhart, A. J.; Taylor, M.; Anderson, D. G.; Langer, R.; Davies, M. C.; Alexander, M. R. TOF-SIMS Analysis of a 576 Micropatterned Copolymer Array to Reveal Surface Moieties That Control Wettability. *Anal. Chem.* **2008**, *80* (1), 135–142.

(10) Celiz, A. D.; Hook, A. L.; Scurr, D. J.; Anderson, D. G.; Langer, R.; Davies, M. C.; Alexander, M. R. ToF-SIMS Imaging of a Polymer Microarray Prepared Using Ink-Jet Printing of Acrylate Monomers. *Surf. Interface Anal.* **2013**, *45* (1), 202–205.

(11) Hook, A. L.; Scurr, D. J.; Anderson, D. G.; Langer, R.; Williams, P.; Davies, M.; Alexander, M. High Throughput Discovery of Thermo-Responsive Materials Using Water Contact Angle Measurements and Time-of-Flight Secondary Ion Mass Spectrometry. *Surf. Interface Anal.* **2013**, *45* (1), 181–184.

(12) Hook, A. L.; Williams, P. M.; Alexander, M. R.; Scurr, D. J. Multivariate ToF-SIMS Image Analysis of Polymer Microarrays and Protein Adsorption. *Biointerphases* **2015**, *10* (1), 019005.

(13) Hook, A. L.; Chang, C. Y.; Yang, J.; Atkinson, S.; Langer, R.; Anderson, D. G.; Davies, M. C.; Williams, P.; Alexander, M. R. Discovery of Novel Materials with Broad Resistance to Bacterial Attachment Using Combinatorial Polymer Microarrays. *Adv. Mater.* **2013**, *25* (18), 2542–2547.

(14) Celiz, A. D.; Smith, J. G. W.; Patel, A. K.; Langer, R.; Anderson, D. G.; Barrett, D. A.; Young, L. E.; Davies, M. C.; Denning, C.; Alexander, M. R. Chemically Diverse Polymer Microarrays and High Throughput Surface Characterisation: A Method for Discovery of Materials for Stem Cell Culture. *Biomater. Sci.* **2014**, *2* (11), 1604–1611.

(15) Hohn, H. P.; Steih, U.; Denker, H. W. A Novel Artificial Substrate for Cell Culture: Effects of Substrate Flexibility/Malleability on Cell Growth and Morphology. *In Vitro Cell. Dev. Biol.: Anim.* **1995**, *31* (1), 37–44.

(16) Provenzano, P. P.; Keely, P. J. Mechanical Signaling through the Cytoskeleton Regulates Cell Proliferation by Coordinated Focal Adhesion and Rho GTPase Signaling. *J. Cell Sci.* **2011**, *124* (8), 1195–1205.

(17) Fristrup, C. J.; Jankova, K.; Hvilsted, S. Surface-Initiated Atom Transfer Radical Polymerization — a Technique to Develop Biofunctional Coatings. *Soft Matter* **2009**, *5*, 4623–4634.

(18) Zoppe, J. O.; Ataman, N. C.; Mocny, P.; Wang, J.; Moraes, J.; Klok, H. A. Surface-Initiated Controlled Radical Polymerization: State-of-the-Art, Opportunities, and Challenges in Surface and Interface Engineering with Polymer Brushes. *Chem. Rev.* **2017**, *117* (3), 1105–1318.

(19) Barbey, R.; Lavanant, L.; Paripovic, D.; Schüwer, N.; Sugnaux, C.; Tugulu, S.; Klok, H.-A. Polymer Brushes via Surface-Initiated Controlled Radical Polymerization: Synthesis, Characterization, Properties, and Applications. *Chem. Rev.* **2009**, *109* (11), 5437–5527.

(20) Hoffmann, C.; Silau, H.; Pinelo, M.; Woodley, J. M.; Daugaard, A. E. Surface Modification of Polysulfone Membranes Applied for a Membrane Reactor with Immobilized Alcohol Dehydrogenase. *Mater. Today Commun.* **2018**, *14*, 160–168.

(21) Daugaard, A. E.; Jankova, K.; Hvilsted, S. Poly(Lauryl Acrylate) and Poly(Stearyl Acrylate) Grafted Multiwalled Carbon Nanotubes for Polypropylene Composites. *Polymer* **2014**, *55* (2), 481–487.

(22) Daugaard, A. E.; Jankova, K.; Bøgelund, J.; Nielsen, J. K.; Hvilsted, S. Novel UV Initiator for Functionalization of Multiwalled Carbon Nanotubes by Atom Transfer Radical Polymerization Applied on Two Different Grades of Nanotubes. *J. Polym. Sci., Part A: Polym. Chem.* **2010**, *48* (20), 4594–4601.

DOI: 10.1021/acsapm.9b00744
ACS Appl. Polym. Mater. XXXX, XXX, XXX–XXX

(23) Wang, H.; Brown, H. R. UV Grafting of Methacrylic Acid and Acrylic Acid on High-Density Polyethylene in Different Solvents and the Wettability of Grafted High-Density Polyethylene. II. Wettability. *J. Polym. Sci., Part A: Polym. Chem.* **2004**, *42* (2), 263−270.
(24) DiTrizio, V.; DiCosmo, F. Method of Making Anti-Microbial Polymeric Surfaces, U.S. Patent 8,840,927 B2, 2014 .
(25) Hutanu, D. Recent Applications of Polyethylene Glycols (PEGs) and PEG Derivatives. *Mod. Chem. Appl.* **2014**, *02* (02), 2−7.
(26) Nykänen, A.; Nuopponen, M.; Laukkanen, A.; Hirvonen, S. P.; Rytelä, M.; Turunen, O.; Tenhu, H.; Mezzenga, R.; Ikkala, O.; Ruokolainen, J. Phase Behavior and Temperature-Responsive Molecular Filters Based on Self-Assembly of Polystyrene-Block-Poly(N-Isopropylacrylamide)-Block-Polystyrene. *Macromolecules* **2007**, *40* (16), 5827−5834.
(27) Okano, T.; Bae, Y. H.; Jacobs, H.; Kim, S. W. Thermally On-off Switching Polymers for Drug Permeation and Release. *J. Controlled Release* **1990**, *11* (1−3), 255−265.
(28) Van Zoelen, W.; Buss, H. G.; Ellebracht, N. C.; Lynd, N. A.; Fischer, D. A.; Finlay, J.; Hill, S.; Callow, M. E.; Callow, J. A.; Kramer, E. J.; Zuckermann, R. N.; Segalman, R. A. Sequence of Hydrophobic and Hydrophilic Residues in Amphiphilic Polymer Coatings Affects Surface Structure and Marine Antifouling/Fouling Release Properties. *ACS Macro Lett.* **2014**, *3* (4), 364−368.
(29) Krishnan, S.; Ayothi, R.; Hexemer, A.; Finlay, J. A.; Sohn, K. E.; Perry, R.; Ober, C. K.; Kramer, E. J.; Callow, M. E.; Callow, J. A.; Fischer, D. A. Anti-Biofouling Properties of Comblike Block Copolymers with Amphiphilic Side Chains. *Langmuir* **2006**, *22* (11), 5075−5086.
(30) Dimitriou, M. D.; Zhou, Z.; Yoo, H. S.; Killops, K. L.; Finlay, J. A.; Cone, G.; Sundaram, H. S.; Lynd, N. A.; Barteau, K. P.; Campos, L. M.; Fischer, D. A.; Callow, M. E.; Callow, J. A.; Ober, C. K.; Hawker, C. J.; Kramer, E. J. A General Approach to Controlling the Surface Composition of Poly(Ethylene Oxide)-Based Block Copolymers for Antifouling Coatings. *Langmuir* **2011**, *27* (22), 13762−13772.

DOI: 10.1021/acsapm.9b00744
ACS Appl. Polym. Mater. XXXX, XXX, XXX−XXX

Appendix 1.2 Supporting Information

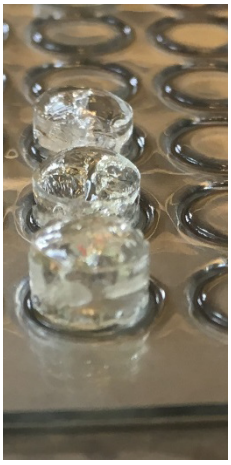

Figure S1 PU surface modified with NIPAAm showing gelation at high monomer feed concentration.

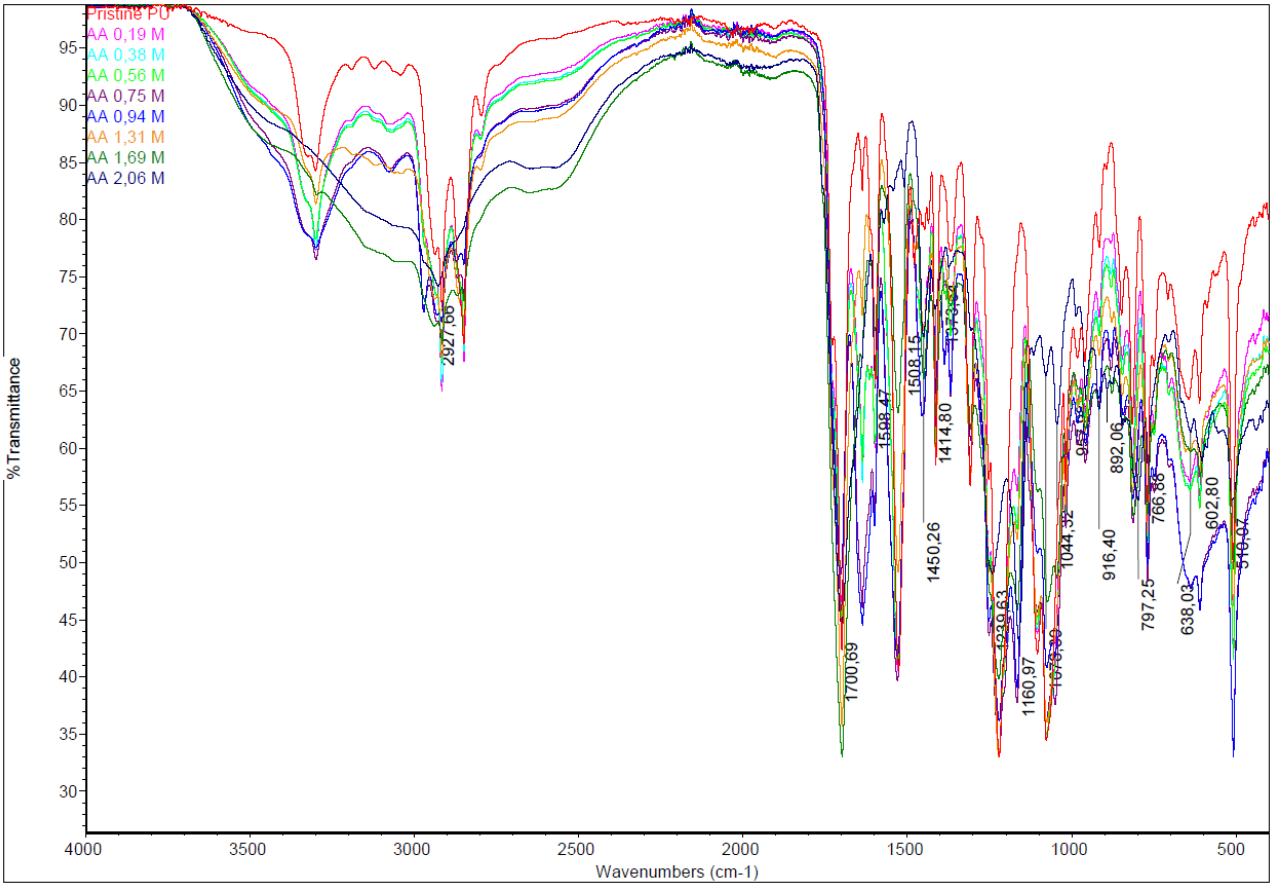

Figure S2 FT-IR spectra of AA modified PU at concentration ranging from 0.19 to 2.06 M.

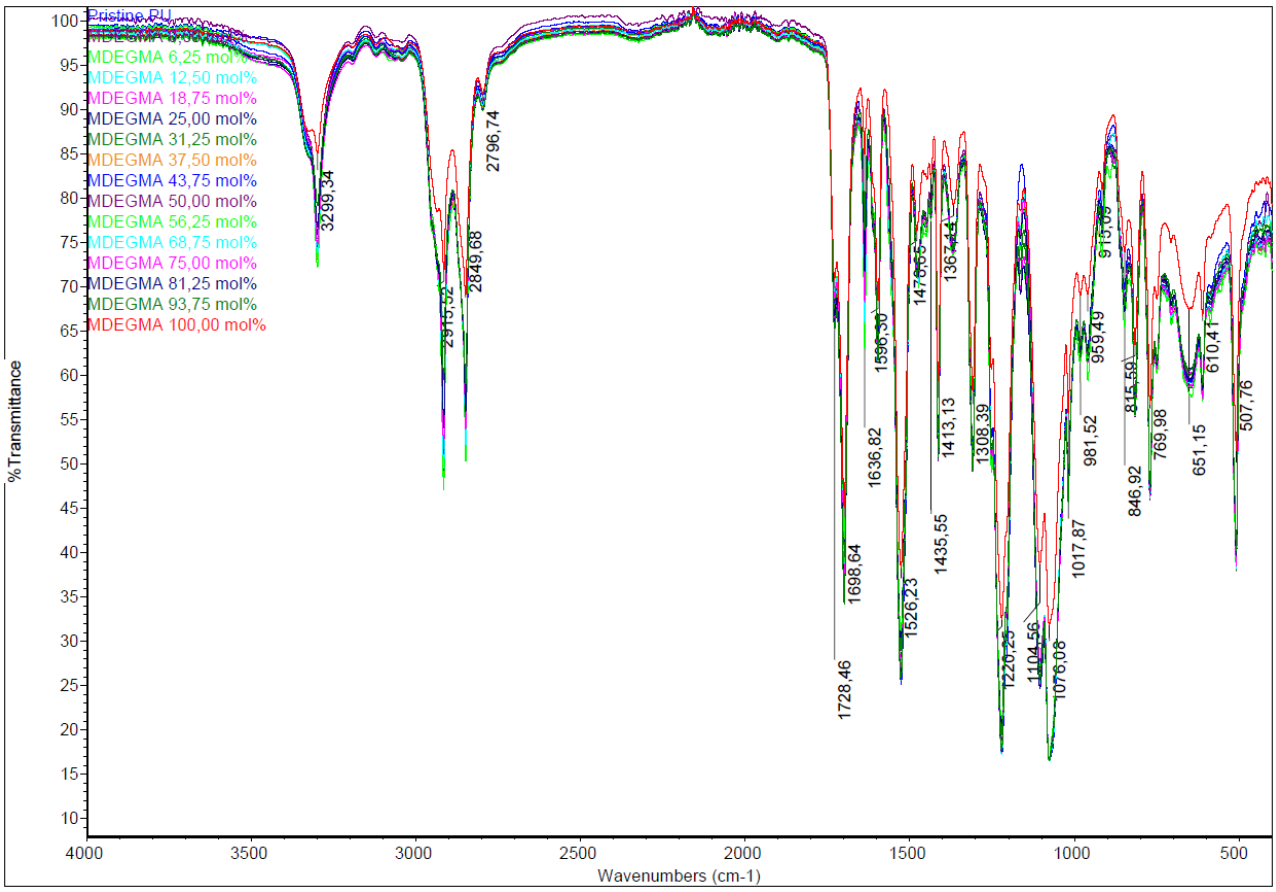

Figure S3 FT-IR spectra of MDEGMA-co-MPEGMA 500 modified PU at ratios ranging from 0 to 100% MDEGMA.

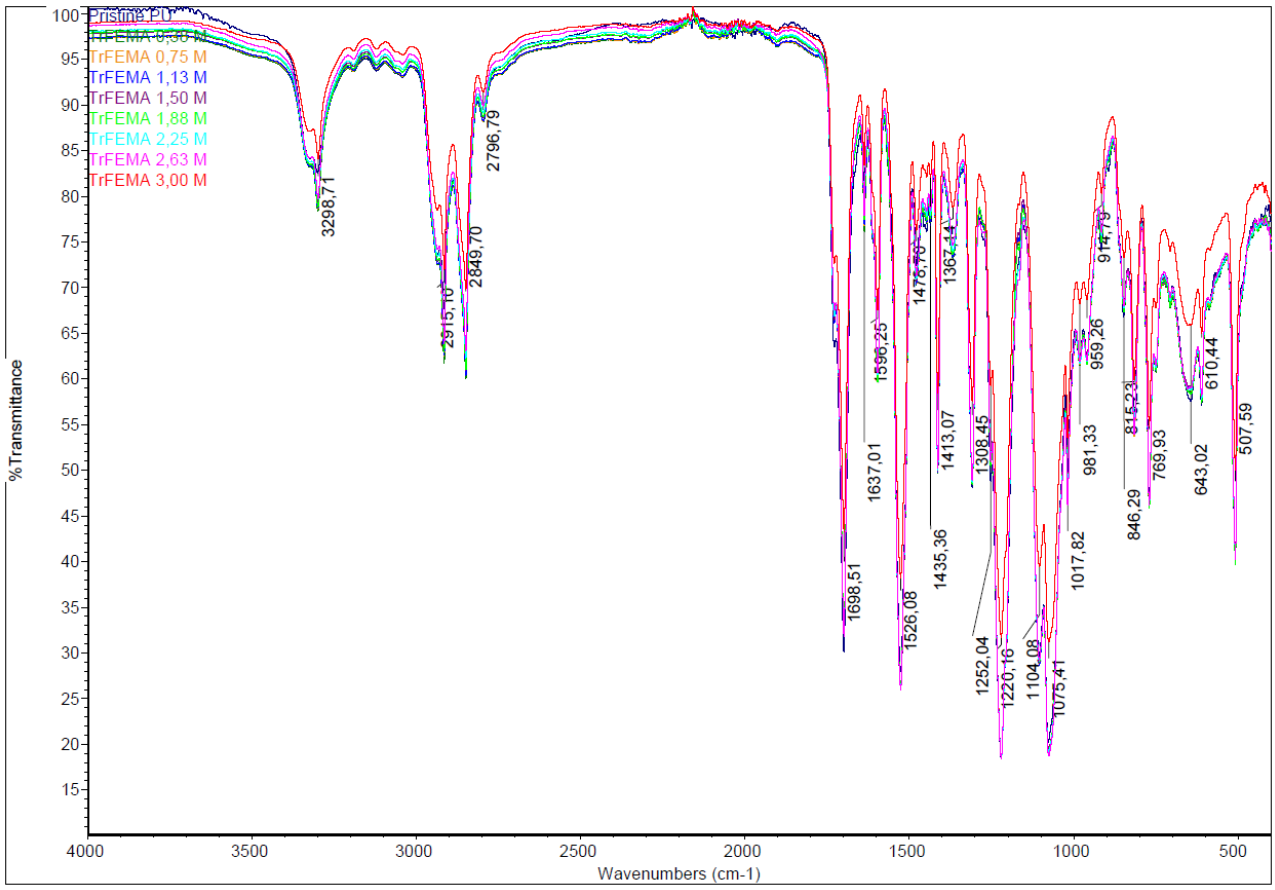

Figure S4 FT-IR spectra of TrFEMA modified PU at concentration ranging from 0.38 to 3.00 M.

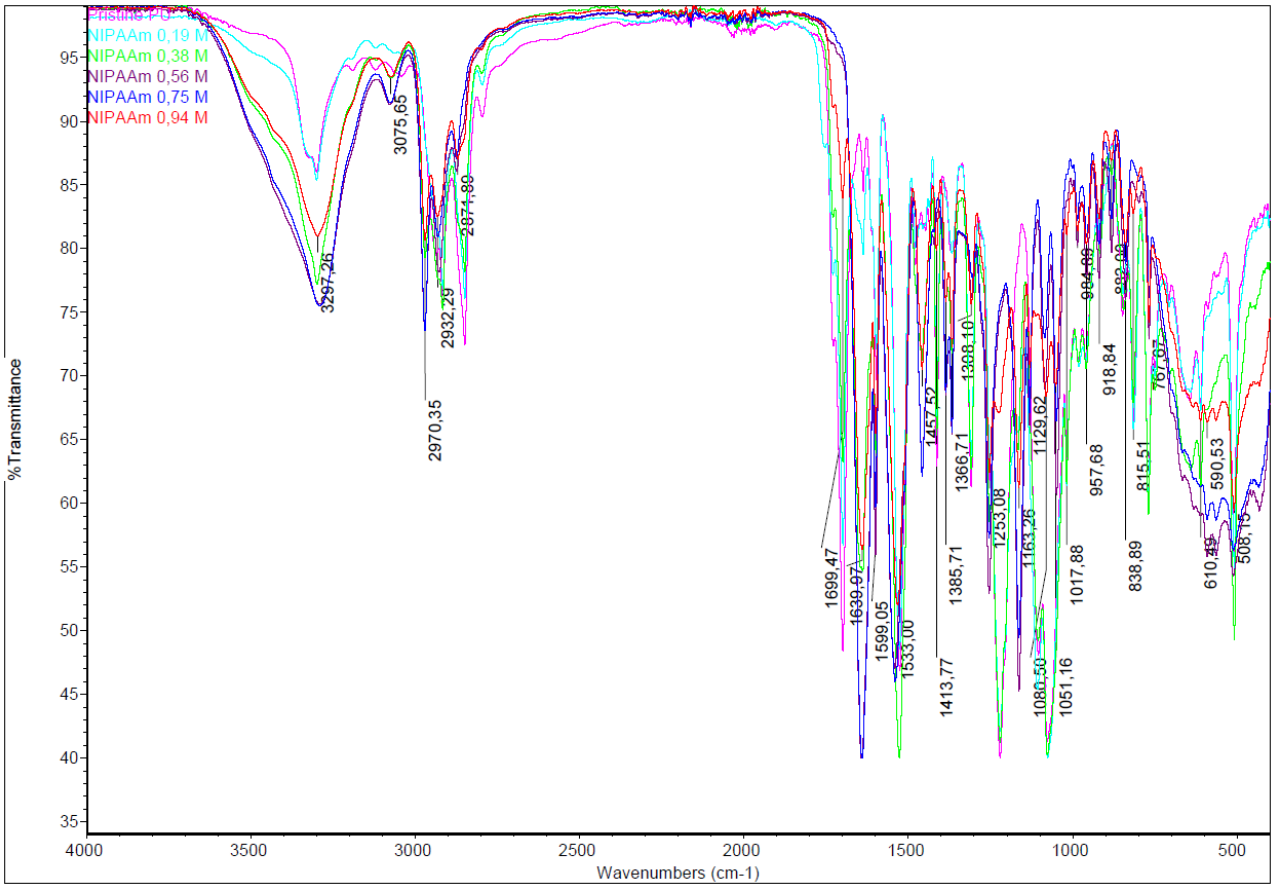

Figure S5 FT-IR spectra of NIPAAm modified PU at concentration ranging from 0.19 to 0.94 M.

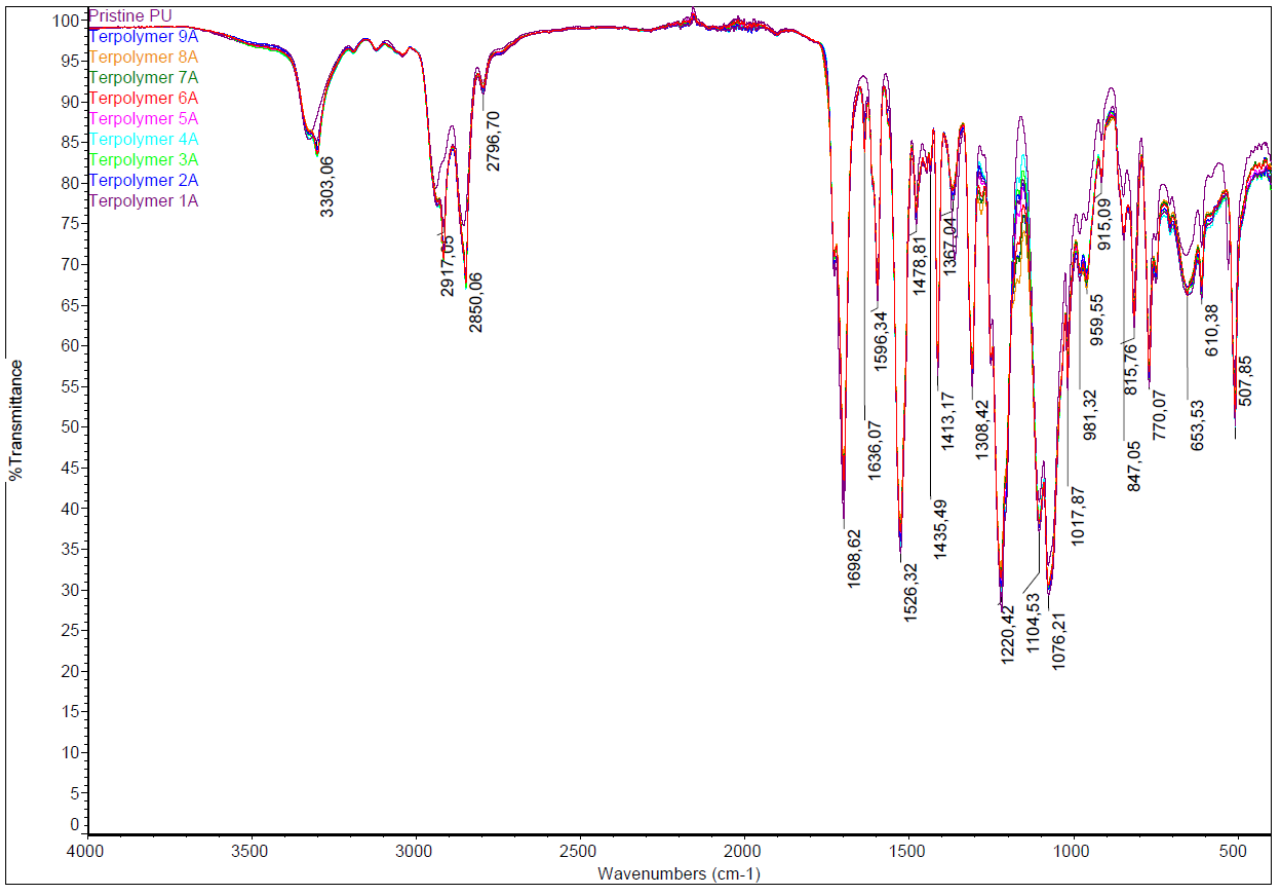

Figure S6 FT-IR spectra of TrFEMA-co-AA-MPEGMA 500 modified PU.

Appendix 2

Appendix 2.1 Literature Survey

Appendix 2

Appendix 2.1 Literature Survey

Non leaching Antimicrobial Polymer Surfaces

Reading guide

This literature survey is meant to give an overview of the current state of the art of antimicrobial surface modifications to polymer surfaces. The tables are categorized according to polymer substrate so that e.g. all PDMS substrates are collected in one table and so forth. Surfaces with less than six references are collected under miscellaneous. The scope comprises surface modifications, which are non-leaching and have been biologically tested either *in vitro* and/or *in vivo*. Cytotoxicity and biocompatibility is stated if addressed in the publications. The antimicrobial properties have been divided into *in vitro* results of bactericidal activity and adhesion reduction and *in vivo* studies. A brief summary of the surface modification method applied and an illustration of the final chemical structure is provided. It should be noted that patents have generally not been included in this literature study.

Abbreviations

AG	Agarose
AGE	Allyl glycidyl ether
AIBN	2,2’-Azobis(2-methylpropionitrile)
AMP	Antimicrobial peptide
AMPS	2-Acrylamido-2-methyl-1-propanesulfonic acid
APC	Aminated polycarboantes
ARGET–ATRP	Activators regenerated by electron transfer atom transfer radical polymerization
ATRP	Atom transfer radical polymerization
BBC	4-Bromobutyrylchloride
BFG	Bovine serum fibrinogen
BIBB	2-Bromoisobutyryl bromide
BisGMA	Bisphenol A diglycidyl methacrylate
BP	Benzophenone
BPBriBu	2-Benzophenonyl bromoisobutyrate
BSA	Bovine serum albumin
CBMA	Carboxy betaine methacrylate
CCTP	Catalytic chain transfer polymerization
CDIP	Chlorodimethylisopropylsilane
CFU	Colony-forming units
CHI	Chitosan
CMBC	4-(Chloromethyl)benzoyl chloride
DA	Dopamine
DHP	5-Methylene-1-(prop-2-enoyl)-4-(2-fluorophenyl)-dihydropyrrol-2-one
DMAm	Dimethylacrylamide
DNase I	Deoxyribonuclease
DOPA	Dopamine
ED	Ethylene diamine
ePTFE	Expanded poly(tetrafluoroethylene)
FBG	Bovine plasma fibrinogen
FG	Fibrinogen
FRP	Free radical polymerization

HEA-Cl	2-(Methyl-2'-chloropropionato) ethyl acrylate
HEMA	2-Hydroxyethylmethacrylate
HMDI	Hexamethylene diisocyanate
IgG	Immunoglobulin G
LbL	Layer-by-layer
MA	Maleic anhydride
MPEGMA	Poly(ethylene glycol) methyl ether methacrylate
MPEGAm	Methoxypolyethyleneglycol acrylamide
MRSA	Methicillin-resistant Staphylococcus aureus
MW	Molecular weight
NH2MA	2-Aminoethyl methacrylate hydro-chloride
OD	Optical density
ODDMAC	Octadecyldimethyl(3-trimethoxysilylpropyl)ammonium chloride
OX	Oxazoline
PAA	Poly(acrylic acid)
PAN	Poly(acrylonitrile)
PBA	Poly(butylene adipate)
PBS	Phosphate buffered saline
PBSu	Poly(butylene succinate)
PCL	Poly(ε-caprolactone)
PDA	Poly(dopamine)
PDMAEMA	Poly(2-(dimethylamino)ethyl methacrylate)
P(DMAPS)	poly((2-(methacryloyloxy)ethyl)dimethyl-(3-sulfopropyl)ammonium hydroxide)
PDMS	Poly(dimethyl siloxane)
PE	Poly(ethylene)
PEG	Poly(ethylene glycol)
PEGDA	Poly(ethylene glycol) diacrylate
PEI	Poly(ethyleneimine)
PEN	Penicillin
PES	Poly(ether sulfone)
PET	Poly(ethylene terephthalate)
PHA	Poly(hydroxyalkanoate)

PHB-HV	Poly(3-hydroxybutyrate-co-3-hydroxyvalerate)
PHMG	Poly(hexamethylenediamine guanidine hydrochloride
PHMB	Poly(hexamethylene biguanide)
PHO	Poly(hydroxyoctanoate)
PI	Poly(isoprene)
PIB	Poly(isobutylene)
PLL	Poly(L-lysine)
PMMA	Poly(methyl methacrylate)
PMOXA	Poly(2-methyl-2-oxazoline)
PP	Poly(propylene)
PPI	Poly(propyleneimine)
PRP	Platelet rich plasma
PS	Poly(styrene)
PTFE	Poly(tetrafluroethylene)
PTL	Phase-Transited Lysozyme
PU	Poly(urethane)
PVA	Poly(vinyl alcohol)
PVC	Poly(vinyl chloride)
PVF	Poly(vinyl fluoride)
PVDF	Poly(vinylidene fluoride)
PVP	Poly(vinyl pyrollidone)
P(3HB-4HB)	Poly(3-hydroxybutyrate-co-4- hydroxybutyrate)
QAS	Quaternary ammonium siloxanes
QCS	Quaternized chitosan
RAFT	Reversible addition-fragmentation chain-transfer polymerization
SBMA	Sulfobetaine methacrylate
SI-ATRP	Surface initiated atom transfer radical polymerization
SMPS	Surface-modified polystyrene
St	Styrene
StBP	Styryl bisphosphonate
TBEC	Tert-butylperoxy 2-ethylhexyl carbonate
tBu	Tertbutyl

TBP	Tert-butyl peroxide
TFA	Trifluoroacetic acid
TPGDA	Tripropylenglycol diacrylate
TPP	Tripolyphosphate
TsCl	p-Toluenesulfonyl chlroide
UV	Ultra violet
XPS	X-ray photoelectron spectrosco

Contents

Figures and symbols

Substrate surface	Interface between chemical layers of X and Y	A bilayer comprised of X and Y applied to a substrate Z times.	A wavy line defines a non-covalent attachment of X.	Beads or particles
	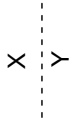	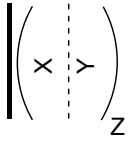	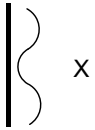	

Table 1 Miscellaneous coatings

Structure	Tethering Method	In vitro results		In vivo results	Cytotox., biocomp. and remarks	Ref.
		Bactericidal activity	Adhesion reduction			
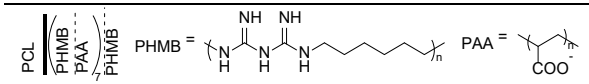	1) NaOH 2) LbL deposition	**g(-)** E. coli: 100%	-	-	Non-cytotoxic Was able to eradicate E. coli within 10 min	1
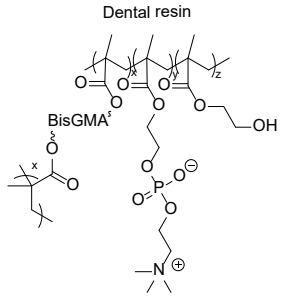	Photo polymerization of resin formulation	-	**g(+)** S. aureus: 90%, Bacteria from saliva: Greatly reduced **Protein** BSA: 20 fold	-	-	2
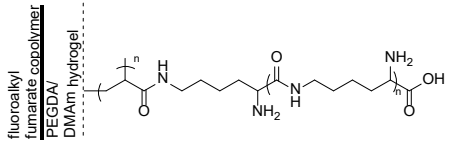	Argon plasma-UV induced surface grafting	**g(+)** S. aureus: 2.6 log **g(-)** E. coli: 3.0 log, P. aeruginosa: 2.1 log, S. marcescence: 3.1 log **Yeast** C. albicans: 0.9 log **Fungi** F. solani: 1.0 log	-	-	Good biocompatibility	3
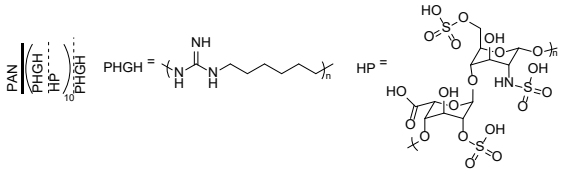	1) NaOH 2) LbL deposition	**g(+)** S. aureus: 100% **g(-)** E. coli: 100%	-	-	Able to eradicate S. aureus after only 30 min.	4
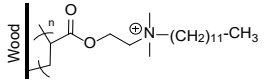	Dip coating	**Fungi** A. niger: 100%	-	-	Quaternization with C6 was also investigated but leached from the surfaces due to solubility in water.	5

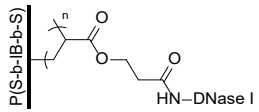	1) Initiator BP 2) UV initiated FRP of CA 3) Peptide coupling	-	**g(+)** S. aureus: 97.4% **g(-)** E. coli: 99.7% **Protein** BFG: ~1.6 μg/cm^2	-	Non-cytotoxic Good biocompatibility	6
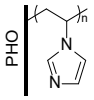	1) FRP (bezoylperoxide) 2) Solvent cast	**g(+)** S. aureus: >90% **g(-)** E. coli: >90% **Yeast** C. Albicans: >90%	**Protein** Albumin: significant FG: significant	-	Non-cytotoxic Good biocompatibility	7
	N_2 plasma treatment	-	**g(+)** S. aureus: 91.41% **g(-)** E. coli: 90.34%	-	Non-cytotoxic	8
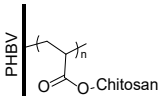	1) Ozone 2) AA polymerization 3) Grafting of chitosan via esterification	**g(+)** S. aureus: >99%, MRSA: >99% **g(-)** E. coli: >99%, P. aeruginosa: >99%	-	-	-	9
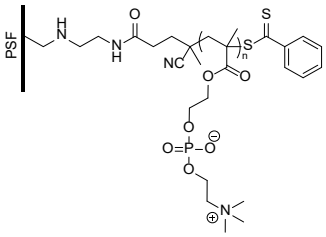	1) Chloromethylation 2)Amination 3) Immobil. Of RAFT agent 4) RAFT polymerization, grafting from	-	**Protein** Human platelet: complete suppression of platelet adhesion, BSA: 0.03 μg/cm^2 (roughly 80% reduction), FG: 0.28 μg/cm^2 (roughly 60% reduction)	-	Non-cytotoxic Good biocompatibility	10
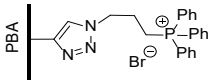	Azide-alkyne “click” reaction	**g(-)** E. Coli: >3.95 log	-	-	-	11
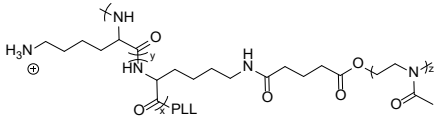	1) Polymerization 2) End group conversion 3) Peptide coupling, grafting to	-	**g(-)** E. Coli: >99%	-	-	12
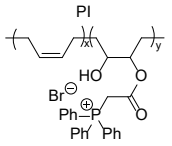	1) Ring opening of epoxides (bromoacetic acid) 2) Nucleophilic reaction	**g(+)** S. aureus: 83% **g(-)** E.coli: 99.5%	-	-	-	13

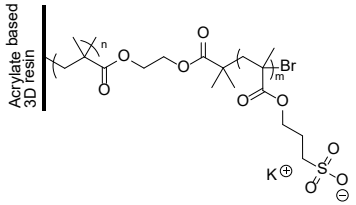	Grafting from, SI-ATRP	**g(+)** Bacillus cereus: No visible colony forming units **g(-)** Escherichia coli: No visible colony forming units	**g(+)** Bacillus cereus: <50 bacteria per mm^2 **g(-)** Escherichia coli: <50 bacteria per mm^2	-	-	[14]
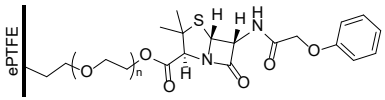	1) Microwave plasma treatment with MA 2) PEGylation 3) Esterification	**g(+)** S. aureus: 100%	-	-	Ester bond prone to hydrolysis resulted in 32% loss of PEN.	[15]
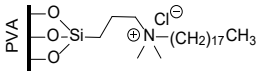	Silane coupling	**g(+)** Bacillus cereus: 100%, A. acidoterrestris: 100% **g(-)** E. coli: ~5 fold reduction	-	-	Cellulose surface was also investigated.	[16]
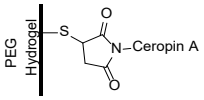	Thiol-ene	**g(-)** E. Coli: 99 ±1%	-	-	-	[17]
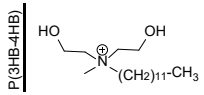	Electrospinning of polymer blend	**g(+)** S. aureus: 100% **g(-)** E. Coli: 100%	-	-	Able to kill all bacteria within 5 min.	[18]
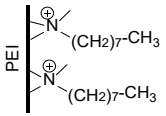	Alkylation	**g(+)** S. aureus: >6 log **g(-)** P. aeruginosa: >6 log	-	-	Tendency to leach depending on cross-linking degree. More cross-linking reduced antibacterial activity. Various alkyl chain lengths were investigated.	[19]
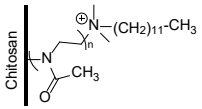	1) Argon plasma treatment 2) OX polymerization 3) Quaternization	**g(+)** S aureus: 99.999% **g(-)** Escherichia coli: 99.999%	**Protein** BSA: 80%	-	Antibacterial results achieved after only 3 min of contact.	[20]

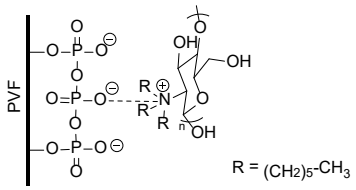 Cross-linked	1) Oxygen plasma 2) TPP anchoring 3) QCS cross-linking	**g(+)** S. aureus: 95% **g(-)** P. aeruginosa: 91%	-	-	-	[21]
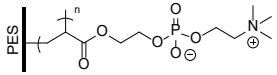	1) BP 2) UV photo grafting, grafting from	-	**g(-)** P. putida: No bacteria found **Protein** BSA: Remarkably reduced, Lysozyme: Remarkably reduced	-	-	[22]
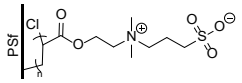	1) Chloromethylation 2) SI-ATRP, grafting from	-	**Protein** BSA: Significant, FG: Significant, Platelet: 100%	-	Non-cytotoxic Good biocompatibility	[23]
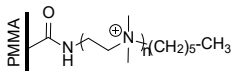	1) NaOH 2) Peptide coupling of PEI 3) Alkylation	-	**g(+)** S. aureus: >99%	-	Non-cytotoxic	[24]
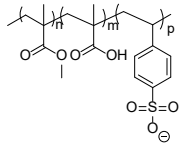	Copolymerization, FRP	-	**g(+)** S. aureus: 98%	-	-	[26]
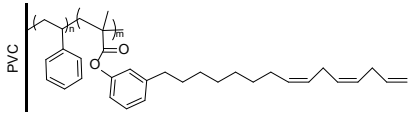	1) Polymer synthesis 2) FRP (AIBN), grafting to	-	**g(+)** S. epidermidis: no significant biofilm formation **g(-)** P. aeruginosa: no significant biofilm formation **Fungi** A. niger: no significant biofilm formation	-	Modest toxicity level	[27]

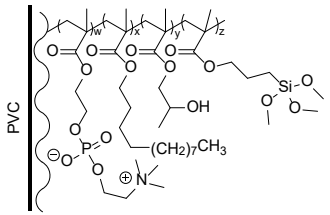 Crosslinked	1) Polymer synthesis, FRP (AIBN) 2) Dip coating	-	**g(-)** E. coli: ca. 85%	-	Latex and silicone surfaces were also tested.	[28]
	Thiocyanation	-	**g(+)** S. epidermidis: ~90%, S. aureus. ~90%	-	Non-cytotoxic	[29]
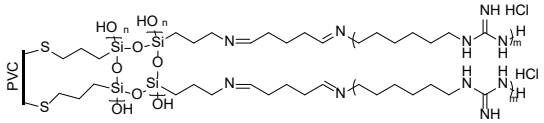	1) Silane treatment 2) Glutaraldehyde 3) PHMG	**g(+)** S. aureus: 99.999%, B. subtilis: 99.999% **g(-)** P. aeruginosa: 99.999%, A. baumannii: 99.956%	-	-	-	[30]

Table 2 Poly(dimethyl siloxane) coatings

Structure	Tethering Method	In vitro results		In vivo results	Cytotox., biocomp. and remarks	Ref.
		Bactericidal activity	**Adhesion reduction**			
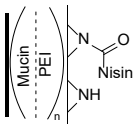	1) LbL deposition 2) Peptide coupling	**g(+)** S. aureus: 95.2%	**Protein** BSA: 50% adhesion reduction	Rabbits: **g(+)** S. aureus: significantly lower infection rate	Non-cytotoxicity Good biocompatibility	[31]
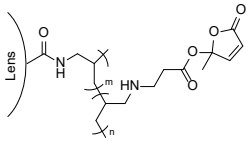	1) Gas plasma glow discharge of propanal 2) Reductive amination 3) Michael-type addition	-	**g(+)** S. aureus: 92% **g(-)** P.aeruginosa: 67%, S. marcescens: 87% **Cells** Acanthamoeba sp.: 70%	Human: No significant difference. Only two animals had infiltration in control but not in coated lens. In vivo human study: No significant differences in redness after 6 h.	Non-cytotoxic	[32]
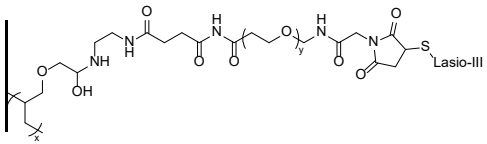	1) Argon plasma 2) FRP of AGE 3) Amination 4) Peptide coupling 5) Thiol-ene	**g(+)** E. faecalis: 99% **g(-)** E. coli: 99%	-	-	Low cytotoxicity Good biocompatibility PS substrate was also investigated	[33]
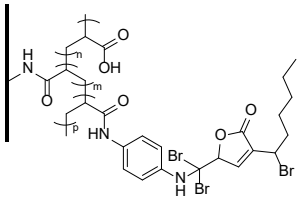	1) Plasma-activated CVD of heptylamine 2) Peptide coupling of PAA 3) Peptide coupling of 4-azidoaniline 4) Radical grafting	-	**g(+)** S. epidermidis: 78%	Sheep: Was able to effectively control infection for up to 65 days.	After sacrifice at 84 days no bromine signal was detected using XPS on explants.	[34]
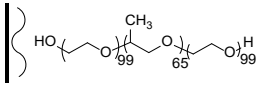	Dip coating	-	**g(+)** S. aureus:29 ±9%, S. epidermidis: 40 ±33% **g(-)** P. aeruginosa: 76%	-	P. aeruginosa was inhibited by 76% for both pristine and coated silicone.	[35]
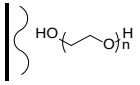	Dip coating	-	-	Mice: **g(+)** S. aureus: None of the polymer brush-coated discs after	Antibiotics might work better on loosely adhered S. aureus on coated	[36]

				antibiotic treatment appeared colonized by staphylococci	discs compared to firm attachment to pristine silicone.	
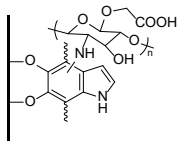	1) PDA 2) Michael addition and Schiff-base reaction	-	**g(-)** E. coli: 90%, P. mirabilis: 93%	-	No significant cytotoxicity Stable in PBS buffer for 21 days and autoclaving at 121 °C for 20 min.	37
Crosslinked						
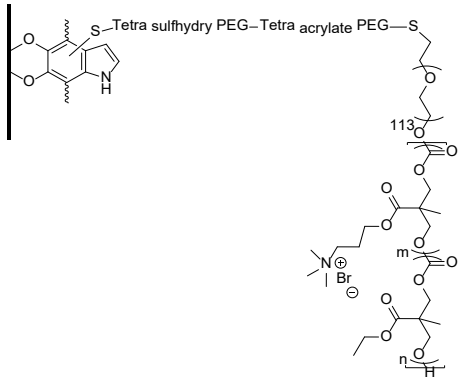	1) PDA 2) Tetra sulfhydryl PEG 3) Thiol-ene with APC conjugated tetra acrylate PEG	**g(+)** S. aureus: 100% **g(-)** E. coli: 100%	-	-	Negligible cytotoxicity The hydrogel before attachment to PDMS was able to kill 99.9-100% of MRSA, VRE, A. baumannii, C. albicans and C. neoformans.	38
Network						
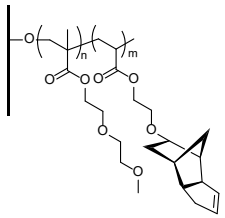	1) Oxygen plasma 2) Dip coating followed by UV curing	-	-	Mice: **g(+)** S. aureus: Nearly 2-fold reduction compared to uncoated catheter.	No cytotoxicity Good biocompatibility Part of screening library involving 22 acrylates combined to give 576 formulations.	39
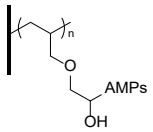	1) Argon plasma 2) UV grafting of AGE 3) Peptide coupling	**g(+)** S. aureus: 78±6% **g(-)** E. coli: 98±1% **Yeast** C. Albicans: 31±3%	-	-	No cytotoxicity	40
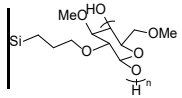	1) Silane coupling	-	**g(+)** S. aureus: ca. 7 log **g(-)** P. aeruginosa: ca. 7 log	Totally implantable venous access ports in rats: **g(+)** S. aureus: 4-5 log reduction **g(-)** P. aeruginosa: 4-5 log	Not evaluated but generally considered non-cytotoxic. The substrate contained both	41

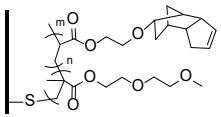	1) Silane coupling of 3-mercaptopropyl)-trimethoxysilane 2) Thiol-ene, grafting to	-	**g(-)** P. aeruginosa: >99%, Pr. Mirabilis: >99%	-	PDMS and titanium parts. -	42
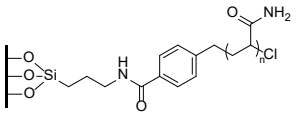	1) Surface hydrophilization 2) Aminosilation 3) CMBC 4) ATRP	-	**g(+)** S. aureus: 58%, S. salivarius: 52% **Yeast** C. albicans. 77%	-	-	43
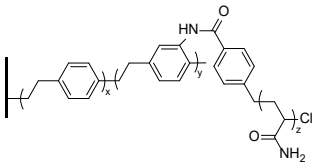	1) Amination by CVC 2) CMBC 3) ATRP	-	**g(+)** S. aureus: 93% **g(-)** E. coli: 99% reduction	-	-	44
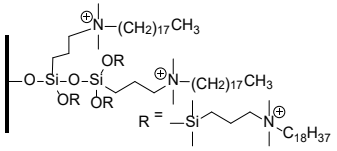	1) Argon plasma 2) Silane coupling	**g(+)** S. epidermidis: 99.7 ±0.4% **g(-)** E. coli: 74 ±17%, P. aeruginosa: 81 ±4%	-	Rats: **g(+)** S. aureus: 0/4 samples had infections with no viable bacteria detected.	Silanization increased adherence of **cells** slightly but significantly reduced viability	45
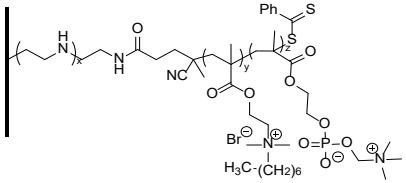	1) PEI 2) Peptide coupling of RAFT agent 3) RAFT 4) Alkylation	**g(+)** S. aureus: 88% (after 24 h.)	**g(+)** S. aureus: ca. 90% (after 24 h.) **Protein** BSA: 70.7% (after 24 h.)	-	Low cytotoxicity Good biocompatibility	46
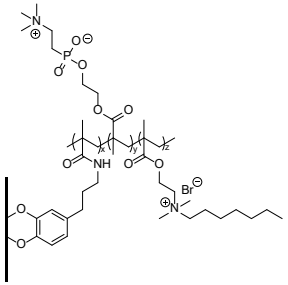	1) Polymer synthesis, FRP (AIBN) 2) Dip coating 3) Alkylation	**g(+)** S. aureus: 72.2%	**g(+)** S. aureus: almost no bacteria adhered **g(-)** E. coli: almost no bacteria adhered **Protein** BSA: 32%	-	Low cytotoxicity	47

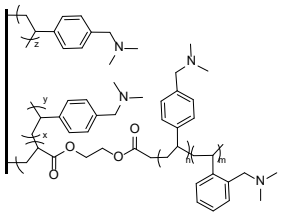	CVD by di-tert-amylperoxide	**g(-)** E. coli: >99.9%	-	-	-	48
Network						
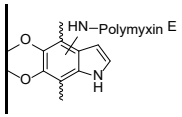	Dip coating	**g(-)** P. aeruginosa: good antimicrobial activity	**g(-)** P. aeruginosa: bacterial attachment was decreased to the same levels as the ones achieved by PDA coating alone	-	Low cytotoxicity	49
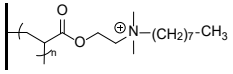	1) BP 2) UV initiated FRP 3) Alkylation		**Yeast** C. albicans: 92.1%		Various alkyl agents was investigated. C1 was most effective after 1 h but C8 showed better results after 24 h.	50
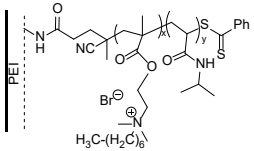	1) PEI 2) Peptide coupling of RAFT agent 3) RAFT	**g(+)** S. aureus: ~3.5 log **g(-)** E. coli : ~2 log	**Protein** BSA: Readily adsorbed	-	Low cytotoxicity	51
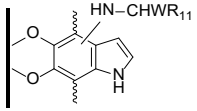	1) DPA 2) Peptide coupling	**g(+)** S. aureus: Complete growth inhibition **g(-)** E. Coli: Complete growth inhibition, P. aeruginosa: Complete growth inhibition	**g(+)** S. aureus: significant **g(-)** E. Coli: significant, P. aeruginosa: significant.		Non- cytotoxic. Highly compatible Maintained activity for over a period of 21 days with no apparent leaching of peptide	52
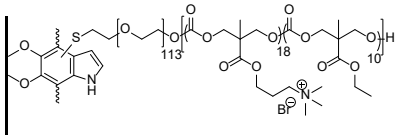	1) Polymer synthesis 2) PDA 3) Thiol-ene	**g(+)** S. aureus: 100%, MRSA: 100%	**g(+)** S. aureus: 100%, MR S. aureus: 99.94% **Protein** Platelet: 100%, BSA: no significant adsorption	-	Non-cytotoxic The coating prevented biofilm formation for 7 days.	53

	Irradiation by ^{60}Co γ	-	**g(+)** S. aureus: ineffective **g(-)** P. aeruginosa: 42.9%	-	-	54
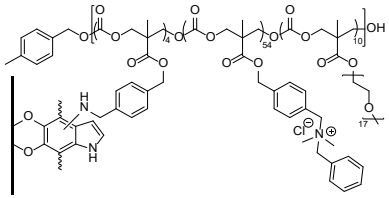	1) Polymer synthesis 2) PDA modification of polymer 3) Quaternization 4) Dip coating	**g(+)** S. aureus: 99.999% **g(-)** E. coli: 99.999%	**Protein** BSA: 93%	-	Negligible cytotoxicity	55
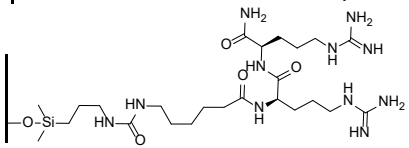	1) Ppetide synthesis 2) Oxygen plasma 3) Silane coupling	**g(+)** S. aureus: 75% **g(-)** P. aeruginosa: 75%, E. Coli: 75%	-	-	Non-cytotoxic	56
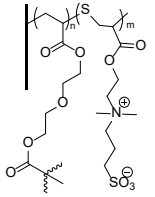	1) Ozone 2) UV grafting of PEGDMA 3) Thiol-ene of P(DMAPS)	-	**g(+)** S. aureus: ca. 93%, S. epidermidis: >90% **g(-)** E. coli: >99% **Cells** 3T3 fibroblast cells:>90% **Protein** FBG: 92%, BSA: 90%	-	Negligible cytotoxicity	57
Crosslinked						
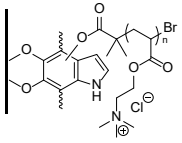	1) DPA 2) ATRP agent 3) ARGET–ATRP	-	**g(-)** P. aeruginosa: 90%, E. Coli: 50%	-	Non-cytotoxic	58

Table 3 Poly(vinylidene fluoride) Coatings

Structure	Tethering Method	In vitro results		In vivo results	Cytotox., biocomp. and remarks	Ref.
		Bactericidal activity	Adhesion reduction			
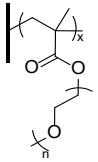	1) Dip coating 2) Argon plasma	-	**Protein** BSA: >80%, γ-globulin: >80%, FG: >80%	-	Good biocompatibility	[59]
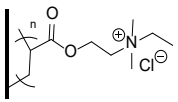	1) BP 2) UV initiated FRP	**g(-)** E. coli: few colonies remain	-	-	Attachment of PEI and was AMPS also investigated with good results.	[60]
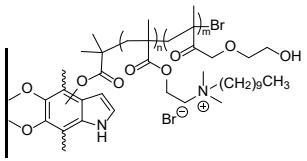	1) PDA 2) ATRP agent 3) SI-ATRP 4) Alkylation	**g(+)** S. aureus: 98.0%	-	-	-	[61]
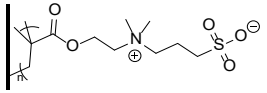	1) AIBN 2) FRP	-	**Protein** BSA: 77%	-	-	[62]
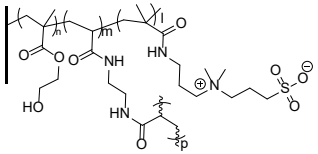	1) ATRP of HEMA 2) ARGET-ATRP (Co(IV))	-	**Protein** BSA: 100%, Lysozyme: 100%	-	-	[63]
Crosslinked						

Table 4 Poly(ethylene) Coatings

Structure	Tethering Method	In vitro results		In vivo results	Cytotox., biocomp. and remarks	Ref.
		Bactericidal activity	Adhesion reduction			
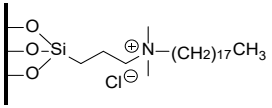	1) Ozonolysis 2) Reduction 3) Silane coupling, grafting to	**g(+)** Bacillus subtilis: 2.65 log **g(-)** E. coli: 3.1 log, S. enterica: 3.03 log	-	-	PS substrate was also investigated.	64
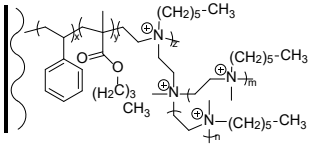	1) Polymer synthesis 2) Dip coating	**g(+)** S. aureus: 100% **g(-)** E. coli: 100%	-	-	-	65
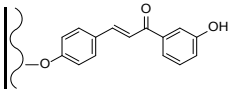	Adsorption	-	**g(+)** S. aureus: 47% **g(-)** E. coli: 15%, P. aeruginosa: 14%	-	PP and PU substrates were also investigated.	66
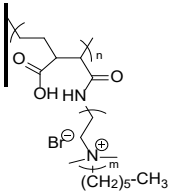	1) FRP (AIBN) of Maleic anhydride 2) PEI 3) quaternization	**g(+)** S. aureus: 98 ±1%, S. epidermidis: 97 ±1% **g(-)** E. coli : 99 ±1%, P. aeruginosa: 99 ±1% **Yeast** C. albicans: 81 ±3%	-	-	PP and cotton substrates were also investigated.	67
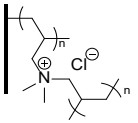	1) Helium plasma 2) FRP	**g(+)** M. luteus: 10^5-10^6 CFU reduction **g(-)** E. Coli: 10^5-10^6 CFU reduction	-	-	Bacterial adhesion analysis by SEM	68
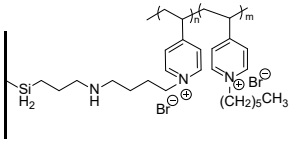	1) Silylation 2) Amination with 1,4-dibromobutane 3) Alkylation 3) PVP, Grafting to	**g(+)** S. aureus: 99 ±1% **g(-)** E. coli: 98 ±2% killed	-	-	PP, PET and Nylon surfaces were also tested. Optical bacterial assessment.	69
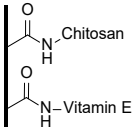	1) Corona activation 2) Peptide coupling via electrospraying of chitosan and vitamin E formulation.	**g(+)** Listeria monocytogenes: ~85% **g(-)** Salmonella Typhimurium: ~80% E. Coli: ~84%	-	-	-	70
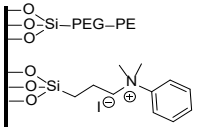	Spin coating of sol-gel mixture Structure not correct PE-PEG-SI, TEOS and QAS-Si	**g(+)** S. aureus: 99.1% **g(-)** E. Coli: 96.4%	-	-	Due to the removal of QAS moieties by the nucleophilic attack of water, the antibacterial activity	71

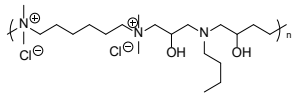	Melt reactive blending	**g(-)** E. coli: 99.9%	-	-	after 24 h was strongly reduced. -	[72]

Table 5 Polyethylene Terephthalate Coatings

Structure	Tethering Method	In vitro results		In vivo results	Cytotox., biocomp. and remarks	Ref.
		Bactericidal activity	Adhesion reduction			
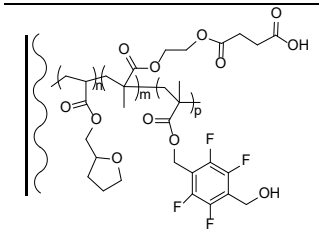	1) Polymer synthesis 2) Solvent cast onto PET	**g(+)** B. subtilis: 100% **g(-)** E. Coli: 100%	-	-	-	[73]
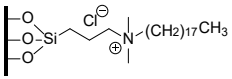	Sol-gel polymerization	**g(-)** E. coli: >99.5%	-	-	Even at low concentration antimicrobial activity of >99.5% was still maintained	[74]
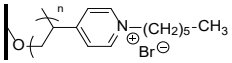	1) Argon plasma 2) Air 3) UV copolymerization, grafting from 4) Alkylation	**g(-)** E. coli: 100%	-	-	Cellulose filter paper as substrate were also investigated	[75]
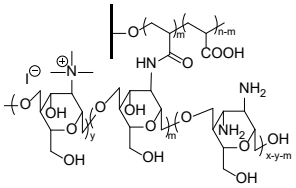	1) Oxygen plasma 2) Air 3) Acrylic acid, Na 4) Chitosan, grafting from	**g(+)** S. aureus : 83%	-	-	Able to maintain antimicrobial activity after laundering at 58%.	[76]
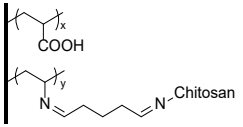	1) Irradiation by ^{60}Co γ-rays 2) Acrylic acid + vinyl formamide 3) Hydrolysis 4) Glutaraldehyde 5) Chitosan, grafting from	**g(+)** MRSA: ~6 log, S. aureus: ~6 log **g(-)** P. aeruginosa: ~6 log, E. coli: ~7 log	-	-	-	[77]

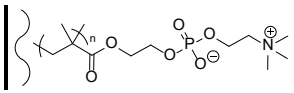	Solvent cast	-	**g(+)** S. aureus: significant, S. mutans: significant **g(-)** P. aeruginosa: significant **Yeast** C. albicans: significant	-	-	[78]
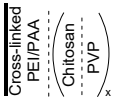	1) Crosslinking through peptide coupling of PEI and AA 2) LbL of CHI and PVP	**g(+)** S. aureus: 100% **g(-)** E. coli: 80%	-	-	Non-cytotoxic Good biocompatibility S. aureus had 0% viable cells after just 10 min.	[79]
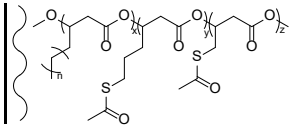	Solvent cast	**g(+)** S. aureus: 10-fold, S. epidermidis: 1-fold, M. smegmatis: 2-fold, Bacillus subtilis: less than 1-fold, S. pyogenes: ineffective, S. dysgalactiae: ineffective **g(-)** P. aeruginosa: ineffective, E. Coli: ineffective	**g(+)** S. aureus: 50% **g(-)** P. aeruginosa: ineffective	In vivo mice study **g(+)** S. aureus: No significant differences among sterile PHA and PHO implants and the sham control. This result indicates minimal inflammation associated with these polymers.	Non-cytotoxic Various strains of S. aureus were used and all were more or less susceptible to PHACOS	[80]
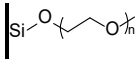	1) $SiCl_4$ plasma 2) PEG, grafting to	-	**g(+)** L. monocytogenes: 96.1%, S. enterica: 99.8%	-	Various MW of PEG brush was analyzed but 2000 MW gave the best results.	[81]
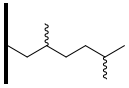 Crosslinked	acetylene plasma immersion ion implantation-deposition	-	**g(+)** S. aureus: 65%, S. epidermidis: 86%	-	-	[82]

Table 6 Poly(propylene) coatings

Structure	Tethering Method	In vitro results		In vivo results	Cytotox., biocomp. and remarks	Ref.
		Bactericidal activity	Adhesion reduction			
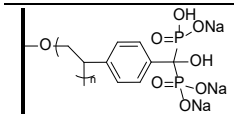	1) Oxygen plasma 2) FRP of StBp grafting from	-	**g(+)** S. epidermidis: 55%, S. aureus: 80% **g(-)** E. coli : 35%	-	-	[83]
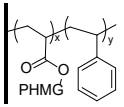	Melt grafting in supercritical CO_2	**g(+)** S. aureus: 100% (PP pellets 10 min.) **g(-)** E. coli: 100% (PP pellets 10 min.), P. aeruginosa: >99% (PP fabric 10 min.)	-	-	Evaluation of skin irritation on rabbits. No skin irritation was observed after 48 h. on a total of 6 rabbits. Killed almost all bacteria in only 10 min.	[84]
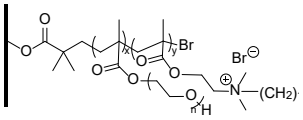	1) Ozone 2) ATRP init. 3) ATRP of PEGMA and DMAEMA 4) Alkylation	**g(+)** S. aureus: 99.99% **g(-)** E. Coli: 99.2%	-	-	Chain length of brushes could be varied with reaction time of ATRP. Longer brushes equalled higher bactericidal efficiency.	[85]
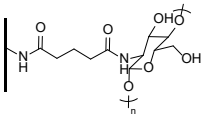	1) Plasma activation with CO_2 2) Dip coating, grafting to	**g(+)** B. subtilis: ca. 4 log **g(-)** E. Coli:> 2 log	-	-	-	[86]
Crosslinked 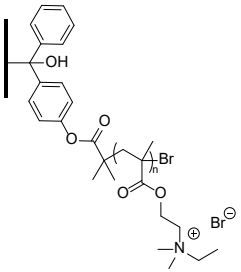	1) BPBriBU 2) ATRP 3) Alkylation	**g(-)** E. Coli: 100%	-	-	PDMAEMA polymers with higher MW proved more effective with same grafting density.	[87]
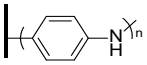	1) Polymer synthesis 2) Oxygen plasma 3) Dip coating	**g(+)** B. subtillis: 100%, S. aureus: 100% **g(-)** E. coli: 100%	-	-	-	[88]

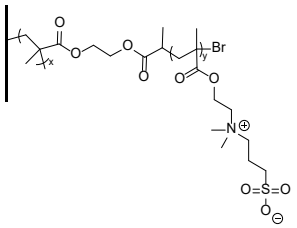	1) BP 2) UV polymerization of HEMA 3) ATRP init. 4) ATRP of SBMA	-	**Protein** BSA: 45.1% higher flux compared to control	-	The antifouling ability was tested via flux recovery of PP membrane	[89]

Table 7 Polystyrene Coatings

Structure	Tethering Method	In vitro results Bactericidal activity	Adhesion reduction	In vivo results	Cytotox., biocomp. and remarks	Ref.
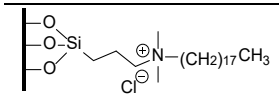	1) Ozonolysis 2) Reduction 3) Silane coupling, grafting to	**g(+)** Bacillus subtilis: 3.37 log **g(-)** E. coli: 6.58 log, S. enterica: 2.55 log	-	-	-	64
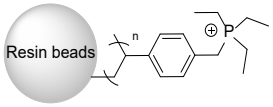	Phosphination	**g(+)** S. aureus: 38.81% **g(-)** E. coli: 30.28%, P. aeruginosa: 36.81%	-	-	Stable after 5 cycles of washing and sterilization at 100 ° for 24.	90
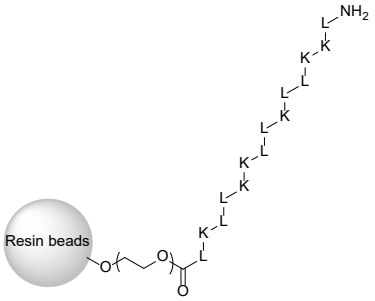	1) anionic polymerization of ethylene oxide 2) Peptide coupling	**g(+)** S. aureus: almost 4 log, B. subtilis: >6 log, L. monocytogenes: >6 log **g(-)** E. coli: >6 log, S. liquefasciens: >4 log, S. typhimurium: >6 log, K. marxianus: >3 log, P. Fluorescence: >6 log	-	-	SMPS buffer was bactericidal suggesting leaching of peptide.	91
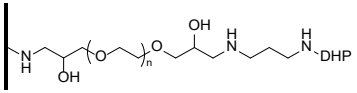	1) Allylamine plasma 2) Diaminopropane, PEGDGE 3) Michael addition of DHP	-	**g(+)** S. aureus: 88% **g(-)** P. aeruginosa: 80% **Protein** fibroblast: 97%	-	Non-cytotoxic The agent act as a quorum sensing inhibitor.	92
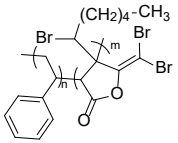	1) Copolymerization of St and furanone 2) Disc by melt moulding	-	**g(+)** S. epidermidis: 89%	-	-	34
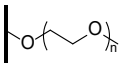	1) Atmospheric plasma 2) Dip coating	-	**Protein** BSA: complete	-	PMMA substrates gave similar results. PEG with MW of 2000	93

	3) Atmospheric plasma		resistance of protein adsorption		g/mol gave the best result.	
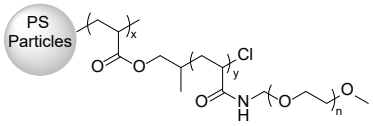	1) Suspension polymerization of St and HEA-Cl 2) SI-ATRP of MPEGAm	-	**Protein** Human whole blood plasma: >90%	-	Reduced adsorption of protein was seen for higher graft density of PEG.	94

Table 8 Polyurethane Coatings

Structure	Tethering Method	In vitro results		In vivo results	Cytotox., biocomp. and remarks	Ref.
		Bactericidal activity	Adhesion reduction			
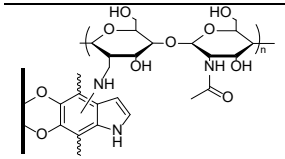	1)DPA 2) Michael addition of chitosan, grafting to	**g(+)** S. aureus: 48.78% **g(-)** E. Coli: 35.44%	-	-	Low cytotoxicity	[95]
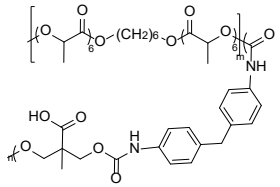	1) Copolymerization 2) Solvent cast	-	**g(+)** S. epidermidis: No bacterial colonies	-	-	[96]
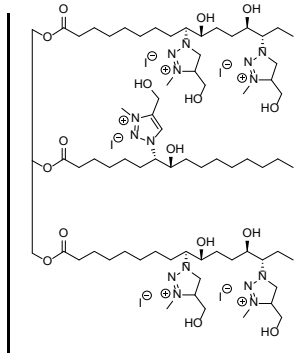	1) Copolymerization 2) Solvent casting	**g(+)** S. aureus: 100% **g(-)** P. aeruginosa: 100% **Yeast** C. albicans: 100%	-	-	Non-cytotoxic	[97]
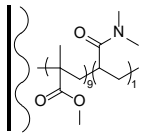	1) Polymer synthesis 2) Dip coating	-	**g(+)** S. saprophyticus: 96-98%, S. aureus: 96-98%, S. mutans: ≥ 98% **g(-)** K. pneumonia: ≥ 96%, E. faecalis: ≥ 98%	-	Part of screening library of 381 polyacrylate/acrylamides. Mixtures of bacteria was used instead of homogenous culture.	[98]
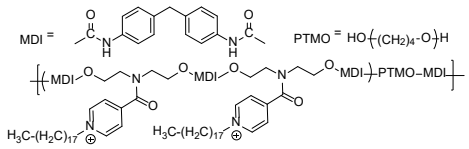	Copolymerization	**g(+)** S. aureus: 95% **g(-)** E. Coli: 10%	-	-	-	[99]

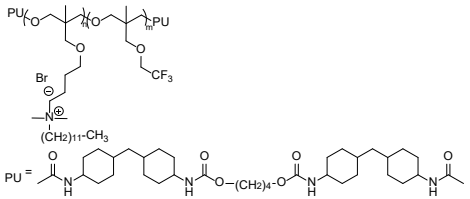	1) Copolymerization 2) Spin coating	**g(+)** S. aureus: 3.57 log **g(-)** E. Coli: 4.38 log, P. aeruginosa: 4.33	-	-	-	100
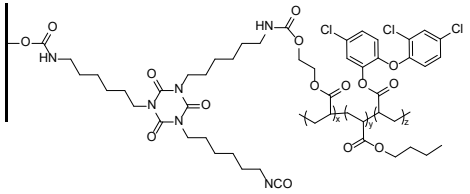	1) Polymer synthesis 2) Copolymerization	-	**g(+)** S. epidermis:>90% **g(-)** C. lytica: ineffective, E. Coli: ineffective **Diatom Algae** N. incerta: ineffective	-	-	101
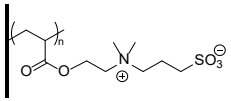	1) TBEC 2) Redox polymerization, grafting from	-	**g(+)** S. epidermidis: 97-99.9%, MRSA: 97-99.9%, S. aureus: 97-99.9% **g(-)** A. baumannii: 97-99.9%, E. Coli: 97-99.9% **Yeast** Candida albicans: 97-99.9% **Cells** human platelets: >98%, polymorphonuclear leukocytes: >98% monocytes: >98%, lymphocytes: >98%	-	-	102
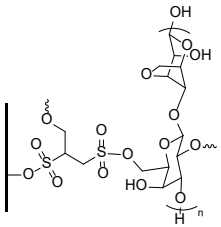 Crosslinked	1) Oxygen plasma 2) UV spin coating of dimercaprol and agarose	-	**g(+)** S. aureus: 2.3 log **g(-)** P. aeruginosa: 2.3 log	-	Non-cytotoxic	103

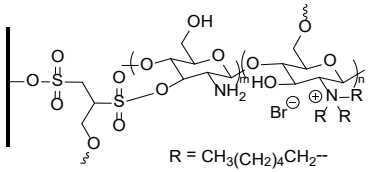 Crosslinked	1) Oxygen plasma 2) UV spin coating of dimercaprol and QCS	**g(+)** S. aureus: >95% **g(-)** P. aeruginosa: >95%	-	-	Non-cytotoxic	103
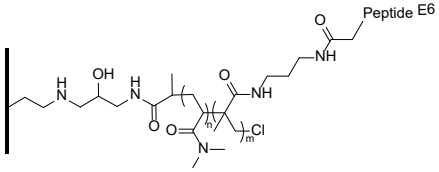	1) Allylamine plasma 2) ATRP agent 3) SI-ATRP 4) Iodoacetic acid N-hydroxysuccinimide ester modification 5) Tiolether substitution	-	**g(+)** S. aureus: 98.4%, S. saprophyticus: 96.6% **g(-)** P. aeruginosa: 93.2%	Mice: **g(-)** P. aeruginosa: 99.7%	Non-cytotoxic Good biocompatibility S. aureus was also tested in vivo but mice have natural resistance against this pathogen and cleared the bacteria on its own.	104
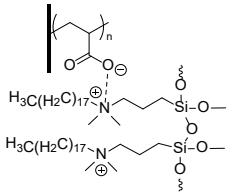	1) Argon plasma 2) Vapour phase polymerization of AA 3) Dip coating	**g(-)** E. Coli: 100%	-	-	-	105
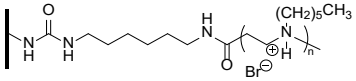	1) HMDI 2) PEI 3) Alkylation	-	**g(-)** E. Coli: 2 orders of magnitude, K. pneumonia: 2 orders of magnitude, P. mirabilis: 2 orders of magnitude	-	Non-cytotoxic	106
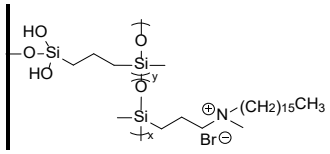	1) Condensation curing 2) Solvent cast	**g(-)** E. coli: 77%	-	-	Stable for 30 days in water	107
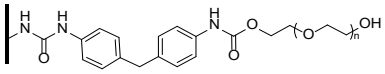	1) MDI 2) PEO, grafting to	-	**Protein** FG: 80%	-	-	108

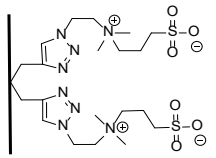	1) Alkyne PU 2) Azide-alkyne click reaction	-	**Protein** BSA: 92.4%	-	-	109
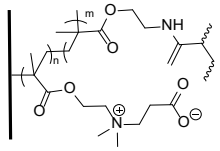 Crosslinked	1) Synthesis of CBMA-tBu monomer 2) FRP of CBMA-tBu and NH_2MA 2) Side-chain functionalization of NH_2MA with acryloyl chloride 3) Deprotection of tBu with TFA 4) Grafting from by redox polymerization using TBEC (initiator),	-	**g(-)** E. coli: Almost zero bacteria **Protein** FG: Low protein binding	-	Was able to maintain antimicrobial activity after 7 days.	110
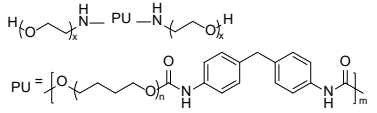	Polymer blend	-	**Protein** FG: 96%, Platelet: 99%	-	Lower MW PEO had better antiadhesive properties	111
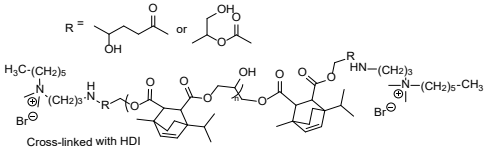	1) Polymer synthesis 2) Solvent cast	**g(+)** S. aureus 55.0% **g(-)** E. Coli: 45.2%	-	-	Various alkyl lengths were investigated.	112

Table 9 Textile Coatings

Structure	Tethering Method	In vitro results		In vivo results	Cytotox., biocomp. and remarks	Ref.
		Bactericidal activity	Adhesion reduction			
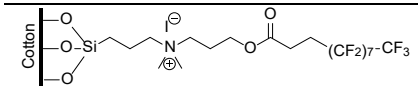	Pad-dry-cure method	**Gram positive** S. aureus: 97.3%	-	-	Maintains a 95.6% reduction of S. aureus even after 10 laundering cycles	113
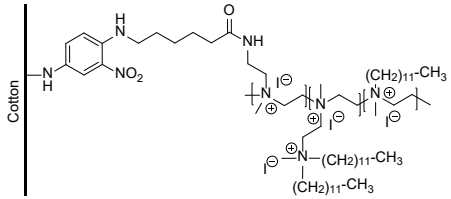	1) Dip coating 2) UV-curing	**Gram positive** S. aureus: 100% **Gram negative** E. Coli: No viable bacteria detected	-	-	-	114
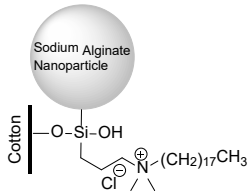	pad-dry-cure method	**Gram positive** S. aureus: >99.99 **Gram negative** E. Coli: >99.99	-	-	The antimicrobial activity was preserved even after 30 washing cycles	115
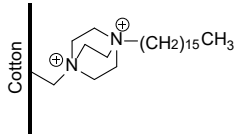	1) Tosylation 2) Surface modification	**Gram positive** S. aureus: 100%, B. cereus: 100%, M. luteus: 100% **Gram negative** E. coli : 100%, E. aerogenes: 100%, E. cloacae: 100%, P. vulgaris: 100%	-	-	Various alkyl lengths were investigated	116
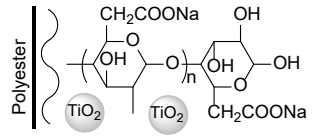	pad-dry-cure method	**Gram negative** E. Coli: 99.9%	-	-	Was able to maintain antimicrobial activity even after 5 washing cycles	117
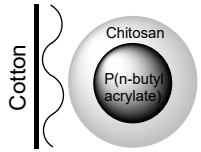	pad-dry-cure method	**Gram positive** S. aureus: >99%	-	-	-	118

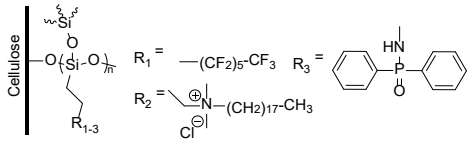	Sol-gel process	-	**Gram positive** S. aureus: 100% **Gram negative** E. Coli: 81%	-	After repeated washing, the antimicrobial activity of the coating gradually decreased against E. coli.	119
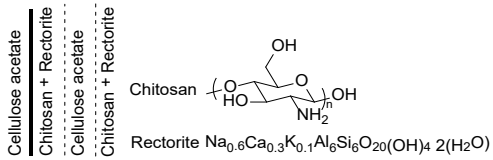	LbL deposition	**Gram positive** S. aureus: 94.7% **Gram negative** E. coli: 95.0%	-	-	Hypotoxic Good biocompatibility	120
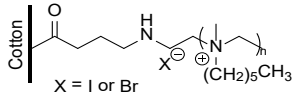	1) Acylation with BBC 2) Alkylation of PEI 3) Alkylation with bromohexane 4) Alkylation with Iodomethane	**Gram positive** S. aureus: 98 ± 1%, S. epidermidis: 97 ± 1% **Gram negative** E. coli: 99 ± 1%, P. aeruginosa: 98 ± 1% **Yeast** S. cerevisiae: 97 ± 1%, C. albicans: 96 ± 1%	-	-	Wool, nylon, PE and PET surfaces were also tested.	121
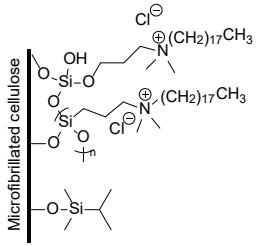	1) Silane coupling with ODDMAC 2) Silane coupling CDIP	**Gram positive** S. aureus: >99% **Gram negative** E. Coli: >99%	-	-	-	122
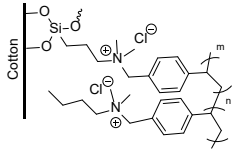	1) Polymer modification 2) Silane coupling	**Gram negative** E. Coli: 100%	-	-	-	123
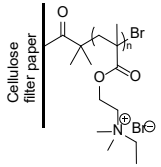	1) BIBB 2) ATRP, DMAEMA	**Gram positive** B. subtilis: 4.0 log **Gram negative** E. Coli: 3.5 log	-	-	-	124
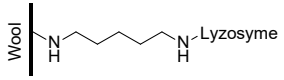 Crosslinked	1) Glutaraldehyde 2) Lysozyme	**Gram positive** S. aureus: 80.95%	-	-	Able to withhold 43% activity after 5 washing cycles	125

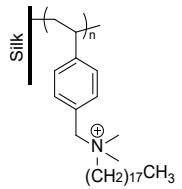	1) FRP of QA styrene monomers 2) Pad-dry-cure method	**Gram positive** S. aureus: 6.27 log **Gram negative** E. Coli: 6.12 log	-	-	Various alkyl lengths were investigated	126
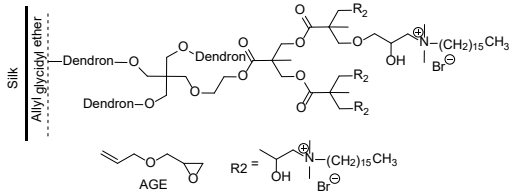	1) Dendrimer synthesis 2) AGE and QA coupling of dendrimer	**Gram positive** S. aureus: 98.24% **Gram negative** E. Coli: 99.06%	-	-	The antimicrobial activity were reduced for S. aureus and E. coli to 71.76% and 70.09% after 15 wash treatments respectively.	127
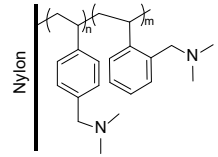	Grafting from, Initiated chemical vapour deposition	**Gram positive** B. subtilis: >6 log **Gram negative** E. Coli: >6 log	-	-	E. coli was reduced by 4 log in only 2 min.	128
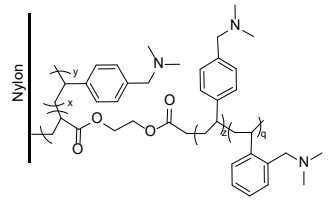	1) CVD of DMAMS and EGDA using TBP as initiator 2) Grafting to by CVD of DMAMS	**Gram positive** B. subtilis: >99%	-	-	-	48
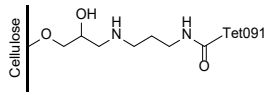	Peptide coupling	**Gram negative** P. aeruginosa: 98 ± 1%	-	-	Low cytotoxicity The result is part of a screening library comprising 122 peptides.	129
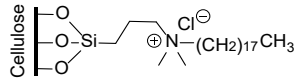	QA Silane coupling	**Gram positive** Bacillus cereus: ~90%, A. acidoterrestris: ~60% **Gram negative** E. coli: ca. 95%	-	-	-	16
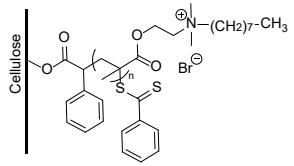	1) Coupling of RAFT agent to surface 2) RAFT, DMAEMA 3) Alkylation	**Gram negative** E. coli: 4 log	-	-	Various alkyl chain lengths were investigated	130

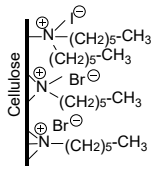	1) ED plasma 2) Alkylation	**Gram positive** S. aureus: 98.7% **Gram negative** K. pneumonia: 96.8%	-	-	-	131
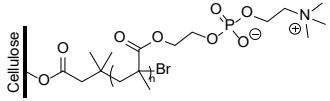	1) BIBB 2) SI-ATRP, grafting from	- Perhaps delete	**Protein** human PRP: Almost no platelet adhesion	-	-	132

References

1. Tang Y, Zhao Y, Wang H, et al. Layer-by-layer assembly of antibacterial coating on interbonded 3D fibrous scaffolds and its cytocompatibility assessment. *J Biomed Mater Res - Part A*. 2012;100 A(8):2071-2078. doi:10.1002/jbm.a.34116

2. Zhang N, Melo MAS, Bai Y, Xu HHK. Novel protein-repellent dental adhesive containing 2-methacryloyloxyethyl phosphorylcholine. *J Dent*. 2014;42(10):1284-1291. doi:10.1016/j.jdent.2014.07.016

3. Zhou C, Li P, Qi X, et al. A photopolymerized antimicrobial hydrogel coating derived from epsilon-poly-l-lysine. *Biomaterials*. 2011;32(11):2704-2712. doi:10.1016/j.biomaterials.2010.12.040

4. Mei Y, Yao C, Li X. A simple approach to constructing antibacterial and anti-biofouling nanofibrous membranes. *Biofouling*. 2014;30(3):313-322. doi:10.1080/08927014.2013.871540

5. Ravikumar T, Murata H, Koepsel RR, Russell AJ. Surface-active antifungal polyquaternary amine. *Biomacromolecules*. 2006;7(10):2762-2769. doi:10.1021/bm060476w

6. Yuan S, Zhao J, Luan S, Yan S, Zheng W, Yin J. Nuclease-functionalized poly(styrene-b-isobutylene-b-styrene) surface with anti-infection and tissue integration bifunctions. *ACS Appl Mater Interfaces*. 2014;6(20):18078-18086. doi:10.1021/am504955g

7. Gyu M, Woo H, Ra B, Baek Y, Ha Y. Biocompatibility and antimicrobial activity of poly(3-hydroxyoctanoate) grafted with vinylimidazole. *Int J Biol Macromol*. 2012;50(2):310-316. doi:10.1016/j.ijbiomac.2011.12.007

8. Wang H, Ji J, Zhang W, et al. Rat calvaria osteoblast behavior and antibacterial properties of O2 and N2 plasma-implanted biodegradable poly(butylene succinate). *Acta Biomater*. 2010;6(1):154-159. doi:10.1016/j.actbio.2009.07.026

9. Hu SG, Jou CH, Yang MC. Antibacterial and biodegradable properties of polyhydroxyalkanoates grafted with chitosan and chitooligosaccharides via ozone treatment. *J Appl Polym Sci*. 2003;88(12):2797-2803. doi:10.1002/app.12055

10. Ma Q, Zhang H, Zhao J, Gong YK. Fabrication of cell outer membrane mimetic polymer brush on polysulfone surface via RAFT technique. *Appl Surf Sci*. 2012;258(24):9711-9717. doi:10.1016/j.apsusc.2012.06.017

11. Anthierens T, Billiet L, Devlieghere F, Du Prez F. Poly(butylene adipate) functionalized with quaternary phosphonium groups as potential antimicrobial packaging material. *Innov Food Sci Emerg Technol*. 2012;15:81-85. doi:10.1016/j.ifset.2012.02.010

12. Pidhatika B, Möller J, Vogel V, Konradi R. Nonfouling Surface Coatings Based on Poly(2-methyl-2-oxazoline). *Chim Int J Chem*. 2008;62(4):264-269. doi:10.2533/chimia.2008.264

13. Li C, Liu Y, Zeng QY, Ao NJ. Preparation and antimicrobial activity of quaternary phosphonium modified epoxidized natural rubber. *Mater Lett*. 2013;93:145-148. doi:10.1016/j.matlet.2012.11.045

14. Guo Q, Cai X, Wang X, Yang J. "Paintable" 3D printed structures via a post-ATRP process with antimicrobial function for biomedical applications. *J Mater Chem B*. 2013;1(48):6644-6649. doi:10.1039/c3tb21415j

15. Aumsuwan N, Heinhorst S, Urban MW. The Effectiveness of Antibiotic Activity of Penicillin Attached to Expanded Poly (tetrafluoroethylene) (ePTFE) Surfaces : A Quantitative Assessment. *Biomacromolecules*. 2007;8:3525-3530.

16. Poverenov E, Shemesh M, Gulino A, et al. Durable contact active antimicrobial materials formed by a one-step covalent modification of polyvinyl alcohol, cellulose and glass surfaces. *Colloids Surfaces B Biointerfaces*. 2013;112:356-361. doi:10.1016/j.colsurfb.2013.07.032

17. Cole MA, Scott TF, Mello CM. Bactericidal Hydrogels via Surface Functionalization with Cecropin A. *ACS Biomater Sci Eng*. 2016;2(11):1894-1904. doi:10.1021/acsbiomaterials.6b00266

18. Fan X, Yin M, Jiang Z, Pan N, Ren X, Huang TS. Antibacterial poly(3-hydroxybutyrate-co-4-hydroxybutyrate) fibrous membranes containing quaternary ammonium salts. *Polym Adv Technol*. 2016;27(12):1617-1624. doi:10.1002/pat.3839

19. Nuzhdina A V., Morozov AS, Kopitsyna MN, et al. Simple and versatile method for creation of non-leaching antimicrobial surfaces based on cross-linked alkylated polyethyleneimine derivatives. *Mater Sci Eng C*. 2017;70:788-795. doi:10.1016/j.msec.2016.09.033

20. Correia VG, Ferraria AM, Pinho MG, Aguiar-Ricardo A. Antimicrobial Contact-Active Oligo(2-oxazoline)s-Grafted Surfaces for Fast Water Disinfection at the Point-of-Use. *Biomacromolecules*. 2015;16(12):3904-3915. doi:10.1021/acs.biomac.5b01243

21. Mitra D, Li M, Wang R, Tang Z, Kang ET, Neoh KG. Scalable Aqueous-Based Process for Coating Polymer and Metal Substrates with Stable Quaternized Chitosan Antibacterial Coatings. *Ind Eng Chem Res*. 2016;55(36):9603-9613. doi:10.1021/acs.iecr.6b02201

22. Razi F, Sawada I, Ohmukai Y, Maruyama T, Matsuyama H. The improvement of antibiofouling efficiency of polyethersulfone membrane by functionalization with zwitterionic monomers. *J Memb Sci*. 2012;401-402:292-299. doi:10.1016/j.memsci.2012.02.020

23. Yue WW, Li HJ, Xiang T, Qin H, Sun SD, Zhao CS. Grafting of zwitterion from polysulfone membrane via surface-initiated ATRP with enhanced antifouling property and biocompatibility. *J Memb Sci*. 2013;446:79-91. doi:10.1016/j.memsci.2013.06.029

24. Behlau I, Mukherjee K, Todani A, et al. Biocompatibility and biofilm inhibition of N,N-hexyl,methyl-polyethylenimine bonded to Boston Keratoprosthesis materials. *Biomaterials*. 2011;32(34):8783-8796. doi:10.1016/j.biomaterials.2011.08.010

25. West SL, Salvage JP, Lobb EJ, et al. The biocompatibility of crosslinkable copolymer coatings containing sulfobetaines and phosphobetaines. *Biomaterials*. 2004;25(7-8):1195-1204. doi:10.1016/j.biomaterials.2003.08.010

26. Anagnostou F, Debet A, Pavon-Djavid G, Goudaby Z, Hélary G, Migonney V. Osteoblast functions on functionalized PMMA-based

polymers exhibiting Staphylococcus aureus adhesion inhibition. *Biomaterials*. 2006;27(21):3912-3919. doi:10.1016/j.biomaterials.2006.03.004

27. Mahata D, Nag A, Mandal SM, Nando GB. Antibacterial coating on in-line suction respiratory catheter to inhibit the bacterial biofilm formation using renewable cardanyl methacrylate copolymer. *J Biomater Sci Polym Ed*. 2017;28(4):365-379. doi:10.1080/09205063.2016.1277623

28. Lewis AL, Cumming ZL, Goreish HH, Kirkwood LC, Tolhurst LA, Stratford PW. Crosslinkable coatings from phosphorylcholine-based polymers. *Biomaterials*. 2001;22(2):99-111. doi:10.1016/S0142-9612(00)00083-1

29. James NR, Jayakrishnan A. Surface thiocyanation of plasticized poly(vinyl chloride) and its effect on bacterial adhesion. *Biomaterials*. 2003;24(13):2205-2212. doi:10.1016/S0142-9612(03)00022-X

30. Villanueva ME, González JA, Rodríguez-Castellón E, Teves S, Copello GJ. Antimicrobial surface functionalization of PVC by a guanidine based antimicrobial polymer. *Mater Sci Eng C*. 2016;67:214-220. doi:10.1016/j.msec.2016.05.052

31. Xu X, Jin T, Zhang B, et al. In vitro and in vivo evaluation of the antibacterial properties of a nisin-grafted hydrated mucin multilayer film. *Polym Test*. 2017;57:270-280. doi:10.1016/j.polymertesting.2016.12.006

32. Zhu H, Kumar A, Ozkan J, et al. Fimbrolide-coated antimicrobial lenses: Their in vitro and in vivo effects. *Optom Vis Sci*. 2008;85(5):292-300. doi:10.1097/OPX.0b013e31816bea0f

33. Mishra B, Basu A, Chua RRY, et al. Site specific immobilization of a potent antimicrobial peptide onto silicone catheters: Evaluation against urinary tract infection pathogens. *J Mater Chem B*. 2014;2(12):1706-1716. doi:10.1039/c3tb21300e

34. Hume EBH, Baveja J, Muir B, Schubert TL, Kumar N. The control of Staphylococcus epidermidis biofilm formation and in vivo infection rates by covalently bound furanones. *Biomaterials*. 2004;25:5023-5030. doi:10.1016/j.biomaterials.2004.01.048

35. Nejadnik MR, van der Mei HC, Norde W, Busscher HJ. Bacterial adhesion and growth on a polymer brush-coating. *Biomaterials*. 2008;29(30):4117-4121. doi:10.1016/j.biomaterials.2008.07.014

36. Nejadnik MR, Engelsman AF, Saldarriaga Fernandez IC, Busscher HJ, Norde W, van der Mei HC. Bacterial colonization of polymer brush-coated and pristine silicone rubber implanted in infected pockets in mice. *J Antimicrob Chemother*. 2008;62(6):1323-1325. doi:10.1093/jac/dkn395

37. Wang R, Neoh KG, Shi Z, Kang ET, Tambyah PA, Chiong E. Inhibition of escherichia coli and proteus mirabilis adhesion and biofilm formation on medical grade silicone surface. *Biotechnol Bioeng*. 2012;109(2):336-345. doi:10.1002/bit.23342

38. Liu SQ, Yang C, Huang Y, et al. Antimicrobial and antifouling hydrogels formed in situ from polycarbonate and poly(ethylene glycol) via

Michael addition. *Adv Mater*. 2012;24(48):6484-6489. doi:10.1002/adma.201202225

39. Hook AL, Chang CY, Yang J, et al. Combinatorial discovery of polymers resistant to bacterial attachment. *Nat Biotechnol*. 2012;30(9):868-875. doi:10.1038/nbt.2316

40. Li X, Li P, Saravanan R, et al. Antimicrobial functionalization of silicone surfaces with engineered short peptides having broad spectrum antimicrobial and salt-resistant properties. *Acta Biomater*. 2014;10(1):258-266. doi:10.1016/j.actbio.2013.09.009

41. Chauhan A, Bernardin A, Mussard W, et al. Preventing biofilm formation and associated occlusion by biomimetic glycocalyxlike polymer in central venous catheters. *J Infect Dis*. 2014;210(9):1347-1356. doi:10.1093/infdis/jiu249

42. Magennis EP, Hook AL, Williams P, Alexander MR. Making silicone rubber highly resistant to bacterial attachment using thiol-ene grafting. *ACS Appl Mater Interfaces*. 2016;8(45):30780-30787. doi:10.1021/acsami.6b10986

43. Fundeanu I, van der Mei HC, Schouten AJ, Busscher HJ. Polyacrylamide brush coatings preventing microbial adhesion to silicone rubber. *Colloids Surfaces B Biointerfaces*. 2008;64(2):297-301. doi:10.1016/j.colsurfb.2008.02.005

44. Fundeanu I, Klee D, Schouten AJ, Busscher HJ, Van Der Mei HC. Solvent-free functionalization of silicone rubber and efficacy of PAAm brushes grafted from an amino-PPX layer against bacterial adhesion. *Acta Biomater*. 2010;6(11):4271-4276. doi:10.1016/j.actbio.2010.06.010

45. Gottenbos B, van der Mei HC, Klatter F, Nieuwenhuis P, Busscher HJ. In vitro and in vivo antimicrobial activity of covalently coupled quaternary ammonium silane coatings on silicone rubber. *Biomaterials*. 2002;23(6):1417-1423. http://www.ncbi.nlm.nih.gov/pubmed/11829437.

46. Wang B, Ye Z, Tang Y, et al. Fabrication of nonfouling, bactericidal, and bacteria corpse release multifunctional surface through surface-initiated RAFT polymerization. *Int J Nanomedicine*. 2017;12:111-125. doi:10.2147/IJN.S107472

47. Wang BL, Jin TW, Han YM, et al. Bio-inspired terpolymers containing dopamine, cations and MPC: a versatile platform to construct a recycle antibacterial and antifouling surface. *J Mater Chem B*. 2015;3(27):5501-5510. doi:10.1039/c5tb00597c

48. Ye YM, Song Q, Mao Y. Solventless hybrid grafting of antimicrobial polymers for self-sterilizing surfaces. *J Mater Chem*. 2011;21(35):13188-13194. doi:Doi 10.1039/C1jm12050f

49. Alves D, Pereira MO. Bio-Inspired Coating Strategies for the Immobilization of Polymyxins to Generate Contact-Killing Surfaces. *Macromol Biosci*. 2016;16:1450-1460. doi:10.1002/mabi.201600122

50. de Prijck K, de Smet N, Coenye T, Schacht E, Nelis HJ. Prevention of Candida albicans Biofilm Formation by Covalently Bound Dimethylaminoethylmethacrylate and Polyethylenimine. *Mycopathologia*. 2010;170(4):213-221. doi:10.1007/s11046-010-9316-3

51. Wang B, Xu Q, Ye Z, et al. Copolymer Brushes with Temperature-Triggered, Reversibly Switchable Bactericidal and Antifouling Properties for Biomaterial Surfaces. *ACS Appl Mater Interfaces*. 2016;8(40):27207-27217. doi:10.1021/acsami.6b08893

52. Lim K, Chua RRY, Ho B, Tambyah PA, Hadinoto K, Leong SSJ. Development of a catheter functionalized by a polydopamine peptide coating with antimicrobial and antibiofilm properties. *Acta Biomater*. 2015;15:127-138. doi:10.1016/j.actbio.2014.12.015

53. Ding X, Yang C, Lim TP, et al. Antibacterial and antifouling catheter coatings using surface grafted PEG-b-cationic polycarbonate diblock copolymers. *Biomaterials*. 2012;33(28):6593-6603. doi:10.1016/j.biomaterials.2012.06.001

54. Meléndez-Ortiz HI, Alvarez-Lorenzo C, Burillo G, Magariños B, Concheiro A, Bucio E. Radiation-grafting of N-vinylimidazole onto silicone rubber for antimicrobial properties. *Radiat Phys Chem*. 2015;110:59-66. doi:10.1016/j.radphyschem.2015.01.025

55. Yang C, Ding X, Ono RJ, et al. Brush-Like Polycarbonates Containing Dopamine, Cations, and PEG Providing a Broad-Spectrum, Antibacterial, and Antifouling Surface via One-Step Coating. *Adv Mater*. 2014;26(43):7346-7351. doi:10.1002/adma.201402059

56. Pinese C, Jebors S, Echalier C, et al. Simple and Specific Grafting of Antibacterial Peptides on Silicone Catheters. *Adv Healthc Mater*. 2016;5(23):3067-3073. doi:10.1002/adhm.201600757

57. Li M, Neoh KG, Xu LQ, et al. Surface modification of silicone for biomedical applications requiring long-term antibacterial, antifouling, and hemocompatible properties. *Langmuir*. 2012;28(47):16408-16422. doi:10.1021/la303438t

58. Thompson VC, Adamson PJ, Dilag J, et al. Biocompatible anti-microbial coatings for urinary catheters. *RSC Adv*. 2016;6(58):53303-53309. doi:10.1039/c6ra07678e

59. Chang Y, Shih YJ, Ko CY, Jhong JF, Liu YL, Wei TC. Hemocompatibility of poly(vinylidene fluoride) membrane grafted with network-like and brush-like antifouling layer controlled via plasma-induced surface pegylation. *Langmuir*. 2011;27(9):5445-5455. doi:10.1021/la1048369

60. Hilal N, Kochkodan V, A-khatib L, Levadna T. Surface modified polymeric membranes to reduce (bio) fouling : a microbiological study using E . coli. *Desalination*. 2004;167:293-300.

61. Sui Y, Gao X, Wang Z, Gao C. Antifouling and antibacterial improvement of surface-functionalized poly(vinylidene fluoride) membrane prepared via dihydroxyphenylalanine-initiated atom transfer radical graft polymerizations. *J Memb Sci*. 2012;394-395:107-119. doi:10.1016/j.memsci.2011.12.038

62. Li MZ, Li JH, Shao XS, et al. Grafting zwitterionic brush on the surface of PVDF membrane using physisorbed free radical grafting technique. *J Memb Sci*. 2012;405-406:141-148. doi:10.1016/j.memsci.2012.02.062

63. Li Q, Bi QY, Zhou B, Wang XL. Zwitterionic sulfobetaine-grafted poly(vinylidene fluoride) membrane surface with stably anti-protein-fouling performance via a two-step surface polymerization. *Appl Surf Sci*. 2012;258(10):4707-4717. doi:10.1016/j.apsusc.2012.01.064

64. Fadida T, Kroupitski Y, Peiper UM, Bendikov T, Sela Saldinger S, Poverenov E. Air-ozonolysis to generate contact active antimicrobial surfaces: Activation of polyethylene and polystyrene followed by covalent graft of quaternary ammonium salts. *Colloids Surfaces B Biointerfaces*. 2014;122:294-300. doi:10.1016/j.colsurfb.2014.07.003

65. Park D, Wang J, Klibanov AM. One-step, painting-like coating procedures to make surfaces highly and permanently bactericidal. *Biotechnol Prog*. 2006;22(2):584-589. doi:10.1021/bp0503383

66. Sivakumar PM, Iyer G, Natesan L, Doble M. 3'-Hydroxy-4-methoxychalcone as a potential antibacterial coating on polymeric biomaterials. *Appl Surf Sci*. 2010;256(20):6018-6024. doi:10.1016/j.apsusc.2010.03.112

67. Lin J, Murthy SK, Olsen BD, Gleason KK, Klibanov AM. Making thin polymeric materials, including fabrics, microbicidal and also water-repellent. *Biotechnol Lett*. 2003;25(19):1661-1665. doi:10.1023/A:1025613814588

68. Thome J, Hollander A, Jaeger W, Trick I, Oehr C. Ultrathin antibacterial polyammonium coatings on polymer surfaces. *Surf Coatings Technol*. 2003;174-175:584-587. doi:10.1016/S0257-8972

69. Tiller JC, Lee SB, Lewis K, Klibanov AM. Polymer surfaces derivatized with poly(vinyl-N-hexylpyridinium) kill airborne and waterborne bacteria. *Biotechnol Bioeng*. 2002;79(4):465-471. doi:10.1002/bit.10299

70. Stoleru E, Munteanu SB, Dumitriu RP, et al. Polyethylene materials with multifunctional surface properties by electrospraying chitosan/vitamin E formulation destined to biomedical and food packaging applications. *Iran Polym J (English Ed*. 2016;25(4):295-307. doi:10.1007/s13726-016-0421-0

71. Marini M, Bondi M, Iseppi R, Toselli M, Pilati F. Preparation and antibacterial activity of hybrid materials containing quaternary ammonium salts via sol-gel process. *Eur Polym J*. 2007;43(8):3621-3628. doi:10.1016/j.eurpolymj.2007.06.002

72. Zheng A, Xu X, Xiao H, Guan Y, Li S, Wei D. Preparation of antistatic and antimicrobial polyethylene by incorporating of comb-like ionenes. *J Mater Sci*. 2012;47(20):7201-7209. doi:10.1007/s10853-012-6666-x

73. Bao Q, Nishimura N, Kamata H, et al. Antibacterial and anti-biofilm efficacy of fluoropolymer coating by a 2,3,5,6-tetrafluoro-p-phenylenedimethanol structure. *Colloids Surfaces B Biointerfaces*. 2017;151:363-371. doi:10.1016/j.colsurfb.2016.12.020

74. Abo El Ola SM, Kotek R, White WC, Reeve JA, Hauser P, Kim JH. Unusual polymerization of 3-(trimethoxysilyl)-propyldimethyloctadecyl ammonium chloride on PET substrates. *Polymer (Guildf)*. 2004;45(10):3215-3225. doi:10.1016/j.polymer.2004.02.041

75. Cen L, Neoh KG, Kang ET. Surface Functionalization Technique for Conferring Antibacterial Properties to Polymeric and Cellulosic Surfaces. *Langmuir*. 2003;19(24):10295-10303. doi:10.1021/la035104c

76. Huh MANWOO, Kang I, Lee DUH, Kim WOOSIK, Lee DHO, Park LEES. Surface Characterization and Antibacterial Activity of Chitosan-

Grafted Poly(ethylene terephthalate) Prepared by Plasma Glow Discharge. *J Appl Polym Sci*. 2001;81:2769-2778.

77. Hu S, Jou C, Yang M. Surface Grafting of Polyester Fiber with Chitosan and the Antibacterial Activity of Pathogenic Bacteria. *J Appl Polym Sci*. 2002;86:2977-2983. doi:10.1002/app.11261

78. Hirota K, Murakami K, Nemoto K, Miyake Y. Coating of a surface with 2-methacryloyloxyethyl phosphorylcholine (MPC) co-polymer significantly reduces retention of human pathogenic microorganisms. *FEMS Microbiol Lett*. 2005;248(1):37-45. doi:10.1016/j.femsle.2005.05.019

79. Wang B, Wang J, Li D, Ren K, Ji J. Chitosan/poly(vinyl pyrollidone) coatings improve the antibacterial properties of poly(ethylene terephthalate). *Appl Surf Sci*. 2012;258(20):7801-7808. doi:10.1016/j.apsusc.2012.03.181

80. Dinjaski N, Fernández-Gutiérrez M, Selvam S, et al. PHACOS, a functionalized bacterial polyester with bactericidal activity against methicillin-resistant Staphylococcus aureus. *Biomaterials*. 2014;35(1):14-24. doi:10.1016/j.biomaterials.2013.09.059

81. Dong B, Manolache S, Wong ACL, Denes FS. Antifouling ability of polyethylene glycol of different molecular weights grafted onto polyester surfaces by cold plasma. *Polym Bull*. 2011;66(4):517-528. doi:10.1007/s00289-010-0358-y

82. Wang J, Huang N, Yang P, et al. The effects of amorphous carbon films deposited on polyethylene terephthalate on bacterial adhesion. *Biomaterials*. 2004;25(16):3163-3170. doi:10.1016/j.biomaterials.2003.10.010

83. Steinmetz HP, Rudnick-Glick S, Natan M, Banin E, Margel S. Graft polymerization of styryl bisphosphonate monomer onto polypropylene films for inhibition of biofilm formation. *Colloids Surfaces B Biointerfaces*. 2016;147:300-306. doi:10.1016/j.colsurfb.2016.08.007

84. Li S, Wei D, Guan Y, Zheng A. Preparation and characterization of a permanently antimicrobial polymeric material by covalent bonding. *Eur Polym J*. 2014;51(1):120-129. doi:10.1016/j.eurpolymj.2013.12.004

85. Yao F, Fu G, Zhao J, Kang E, Neoh K. Antibacterial effect of surface-functionalized polypropylene hollow fiber membrane from surface-initiated atom transfer radical polymerization. *J Memb Sci*. 2008;319(1-2):149-157. doi:10.1016/j.memsci.2008.03.049

86. Paulussen S, Vangeneugden D, Vartiainen J, Ratto M, Hurme E. Polymeric Packaging Film. 2009;1(19):1-4. https://www.google.com/patents/US20090011160.

87. Huang J, Murata H, Koepsel RR, Russell AJ, Matyjaszewski K. Antibacterial polypropylene via surface-initiated atom transfer radical polymerization. *Biomacromolecules*. 2007;8(5):1396-1399. doi:10.1021/bm061236j

88. Natarajan TS, Tsai C-H, Huang H-L, Ho K-S, Lin I, Wang Y-F. Fabrication of Polyaniline Coated Plasma Modified Polypropylene Filter for Antibioaerosol Application. *Aerosol Air Qual Res*. 2016;16(8):1911-1921. doi:10.4209/aaqr.2016.04.0167

89. Zhao YH, Wee KH, Bai R. Highly hydrophilic and low-protein-fouling polypropylene membrane prepared by surface modification with

sulfobetaine-based zwitterionic polymer through a combined surface polymerization method. *J Memb Sci*. 2010;362(1-2):326-333. doi:10.1016/j.memsci.2010.06.037

90. Popa A, Davidescu CM, Trif R, Ilia G, Iliescu S, Dehelean G. Study of quaternary “onium” salts grafted on polymers: Antibacterial activity of quaternary phosphonium salts grafted on “gel-type” styrene-divinylbenzene copolymers. *React Funct Polym*. 2003;55(2):151-158. doi:10.1016/S1381-5148(02)00224-9

91. Appendini P, Hotchkiss JH. Surface Modification of Poly(styrene) by the Attachment of an Antimicrobial Peptide. *J Appl Polym Sci*. 2001;81:14-18.

92. Ozcelik B, Ho KKK, Glattauer V, Willcox M, Kumar N, Thissen H. Poly(ethylene glycol)-based coatings combining low-biofouling and quorum-sensing inhibiting properties to reduce bacterial colonization. *ACS Biomater Sci Eng*. 2017;3(1):78-87. doi:10.1021/acsbiomaterials.6b00579

93. D’Sa RA, Meenan BJ. Chemical grafting of poly(ethylene glycol) methyl ether methacrylate onto polymer surfaces by atmospheric pressure plasma processing. *Langmuir*. 2010;26(3):1894-1903. doi:10.1021/la902654y

94. Kizhakkedathu JN, Janzen J, Le Y, Kainthan RK, Brooks DE. Poly(oligo(ethylene glycol)acrylamide) Brushes by surface initiated polymerization: Effect of macromonomer chain length on brush growth and protein adsorption from blood plasma. *Langmuir*. 2009;25(6):3794-3801. doi:10.1021/la803690q

95. Luo C, Liu W, Luo B, et al. Antibacterial activity and cytocompatibility of chitooligosaccharide-modified polyurethane membrane via polydopamine adhesive layer. *Carbohydr Polym*. 2017;156:235-243. doi:10.1016/j.carbpol.2016.09.036

96. Francolini I, Donelli G, Vuotto C, et al. Antifouling polyurethanes to fight device-related staphylococcal infections: Synthesis, characterization, and antibiofilm efficacy. *Pathog Dis*. 2014;70(3):401-407. doi:10.1111/2049-632X.12155

97. Gholami H, Yeganeh H, Burujeny SB, Sorayya M, Shams E. Vegetable Oil Based Polyurethane Containing 1,2,3-Triazolium Functional Groups as Antimicrobial Wound Dressing. *J Polym Environ*. 2018;26(2):462-473. doi:10.1007/s10924-017-0964-y

98. Venkateswaran S, Wu M, Gwynne PJ, et al. Bacteria repelling poly(methylmethacrylate-co-dimethylacrylamide) coatings for biomedical devices. *J Mater Chem B*. 2014;2(39):6723-6729. doi:10.1039/C4TB01129E

99. Grapski JA, Cooper SL. Synthesis and characterization of non-leaching biocidal polyurethanes. *Biomaterials*. 2001;22(16):2239-2246. doi:10.1016/S0142-9612(00)00412-9

100. Kurt P, Wood L, Ohman DE, Wynne KJ. Highly Effective Contact Antimicrobial Surfaces via Polymer Surface Modifiers. *Langmuir*. 2007;23(15):4719-4723. doi:10.1021/la063718m

101. Kugel AJ, Jarabek LE, Daniels JW, et al. Combinatorial materials research applied to the development of new surface coatings XII: Novel, environmentally friendly antimicrobial coatings derived from biocide-functional acrylic polyols and isocyanates. *J Coatings Technol Res*. 2009;6(1):107-121. doi:10.1007/s11998-008-9124-6

102. Catheters V, Surface NP, Smith RS, et al. Vascular Catheters with a Nonleaching Poly-Sulfobetaine Surface Modification Reduce Thrombus Formation and Microbial Attachment. *Sci Transl Med*. 2012;4(153). doi:10.1126/scitranslmed.3004120

103. Li M, Mitra D, Kang E-T, Lau T, Chiong E, Neoh KG. Thiol-Ol Chemistry for Grafting of Natural Polymers to Form Highly Stable and Efficacious Antibacterial Coatings. *ACS Appl Mater Interfaces*. 2016;9:1847-1857. doi:10.1021/acsami.6b10240

104. Yu K, Lo JCY, Yan M, et al. Anti-adhesive antimicrobial peptide coating prevents catheter associated infection in a mouse urinary infection model. *Biomaterials*. 2017;116:69-81. doi:10.1016/j.biomaterials.2016.11.047

105. Zanini S, Polissi A, Maccagni EA, Dell'Orto EC, Liberatore C, Riccardi C. Development of antibacterial quaternary ammonium silane coatings on polyurethane catheters. *J Colloid Interface Sci*. 2015;451:78-84. doi:10.1016/j.jcis.2015.04.007

106. Gultekinoglu M, Tunc Sarisozen Y, Erdogdu C, et al. Designing of dynamic polyethyleneimine (PEI) brushes on polyurethane (PU) ureteral stents to prevent infections. *Acta Biomater*. 2015;21:44-54. doi:10.1016/j.actbio.2015.03.037

107. Hazziza-Laskar J, Helary G, Sauvet G. Biocidal polymers active by contact. IV. Polyurethanes based on polysiloxanes with pendant primary alcohols and quaternary ammonium groups. *J Appl Polym Sci*. 1995;58(1):77-84. doi:10.1002/app.1995.070580108

108. Wu WI, Sask KN, Brash JL, Selvaganapathy PR. Polyurethane-based microfluidic devices for blood contacting applications. *Lab Chip*. 2012;12(5):960-970. doi:10.1039/c2lc21075d

109. Huang J, Gu S, Zhang R, Xia Z, Xu W. Synthesis, spectroscopic, and thermal properties of polyurethanes containing zwitterionic sulfobetaine groups. *J Therm Anal Calorim*. 2013;112(3):1289-1295. doi:10.1007/s10973-012-2715-6

110. Wang W, Lu Y, Xie J, Zhu H, Cao Z. A zwitterionic macro-crosslinker for durable non-fouling coatings. *Chem Commun (Camb)*. 2016;52(25):4671-4674. doi:10.1039/c6cc00109b

111. Tan J, McClung WG, Brash JL. Non-fouling biomaterials based on blends of polyethylene oxide copolymers and polyurethane: Simultaneous measurement of platelet adhesion and fibrinogen adsorption from flowing whole blood. *J Biomater Sci Polym Ed*. 2013;24(4):497-506. doi:10.1080/09205063.2012.690286

112. Liu G, Wu G, Jin C, Kong Z. Preparation and antimicrobial activity of terpene-based polyurethane coatings with carbamate group-containing quaternary ammonium salts. *Prog Org Coatings*. 2015;80:150-155. doi:10.1016/j.porgcoat.2014.12.005

113. Shao H, Meng W, Qing F. Synthesis and surface antimicrobial activity of a novel perfluorooctylated quaternary ammonium silane coupling

agent. *J Fluor Chem*. 2004;125:721-724. doi:10.1016/j.jfluchem.2003.12.008

114. Hsu BB, Klibanov AM. Light-activated covalent coating of cotton with bactericidal hydrophobic polycations. *Biomacromolecules*. 2011;12(1):6-9. doi:10.1021/bm100934c

115. Kim HW, Kim BR, Rhee YH. Imparting durable antimicrobial properties to cotton fabrics using alginate-quaternary ammonium complex nanoparticles. *Carbohydr Polym*. 2010;79(4):1057-1062. doi:10.1016/j.carbpol.2009.10.047

116. Abel T, Cohen JLI, Engel R, Filshtinskaya M, Melkonian A, Melkonian K. Preparation and investigation of antibacterial carbohydrate-based surfaces. *Carbohydr Res*. 2002;337(24):2495-2499. doi:10.1016/S0008-6215(02)00316-6

117. Mihailović D, Šaponjić Z, Radoičić M, et al. Functionalization of polyester fabrics with alginates and TiO2 nanoparticles. *Carbohydr Polym*. 2010;79(3):526-532. doi:10.1016/j.carbpol.2009.08.036

118. Ye W, Leung MF, Xin J, Kwong TL, Lee DKL, Li P. Novel core-shell particles with poly(n-butyl acrylate) cores and chitosan shells as an antibacterial coating for textiles. *Polymer (Guildf)*. 2005;46(23):10538-10543. doi:10.1016/j.polymer.2005.08.019

119. Vasiljević J, Zorko M, Štular D, et al. Structural optimisation of a multifunctional water- and oil-repellent, antibacterial, and flame-retardant sol–gel coating on cellulose fibres. *Cellulose*. 2017;24(3):1511-1528. doi:10.1007/s10570-016-1187-4

120. Wu Y, Li X, Shi X, et al. Production of thick uniform-coating films containing rectorite on nanofibers through the use of an automated coating machine. *Colloids Surfaces B Biointerfaces*. 2017;149:271-279. doi:10.1016/j.colsurfb.2016.10.030

121. Lin J, Qiu S, Lewis K, Klibanov AM. Mechanism of bactericidal and fungicidal activities of textiles covalently modified with alkylated polyethylenimine. *Biotechnol Bioeng*. 2003;83(2):168-172. doi:10.1002/bit.10651

122. Andresen M, Stenstad P, Møretrø T, et al. Nonleaching antimicrobial films prepared from surface-modified microfibrillated cellulose. *Biomacromolecules*. 2007;8(7):2149-2155. doi:10.1021/bm070304e

123. Bouloussa O, Rondelez F, Semetey V. A new, simple approach to confer permanent antimicrobial properties to hydroxylated surfaces by surface functionalization. *Chem Commun*. 2008;(8):951-953. doi:10.1039/b716026g

124. Lee SB, Koepsel RR, Morley SW, Matyjaszewski K, Sun Y, Russell AJ. Permanent, nonleaching antibacterial surfaces, 1. Synthesis by atom transfer radical polymerization. *Biomacromolecules*. 2004;5(3):877-882. doi:10.1021/bm034352k

125. Wang Q, Fan X, Hu Y, Yuan J, Cui L, Wang P. Antibacterial functionalization of wool fabric via immobilizing lysozymes. *Bioprocess Biosyst Eng*. 2009;32(5):633-639. doi:10.1007/s00449-008-0286-5

126. Liu Y, Xiao C, Li X, et al. Antibacterial efficacy of functionalized silk fabrics by radical copolymerization with quaternary ammonium salts. *J Appl Polym Sci*. 2016;133(21):6-11. doi:10.1002/app.43450

127. Chen K, Zhou X, Wang X. Synthesis and application of a hyperbranched polyester quaternary ammonium surfactant. *J Surfactants Deterg*. 2014;17(6):1081-1088. doi:10.1007/s11743-014-1624-z

128. Martin TP, Kooi SE, Chang SH, Sedransk KL, Gleason KK. Initiated chemical vapor deposition of antimicrobial polymer coatings. *Biomaterials*. 2007;28(6):909-915. doi:10.1016/j.biomaterials.2006.10.009

129. Hilpert K, Elliott M, Jenssen H, et al. Screening and Characterization of Surface-Tethered Cationic Peptides for Antimicrobial Activity. *Chem Biol*. 2009;16(1):58-69. doi:10.1016/j.chembiol.2008.11.006

130. Roy D, Knapp JS, Guthrie JT, Perrier S. Antibacterial cellulose fiber via RAFT surface graft polymerization. *Biomacromolecules*. 2008;9(1):91-99. doi:10.1021/bm700849j

131. Jampala SN, Sarmadi M, Somers EB, Wong ACL, Denes FS. Plasma-enhanced synthesis of bactericidal quaternary ammonium thin layers on stainless steel and cellulose surfaces. *Langmuir*. 2008;24(16):8583-8591. doi:10.1021/la800405x

132. Liu PS, Chen Q, Wu SS, Shen J, Lin SC. Surface modification of cellulose membranes with zwitterionic polymers for resistance to protein adsorption and platelet adhesion. *J Memb Sci*. 2010;350(1-2):387-394. doi:10.1016/j.memsci.2010.01.015